**University of Sussex**

Submitted for the degree Doctor of Philosophy

# Analytically Divergence-free Discretization Methods for Darcy's Problem

Daniela Schräder

October 2009

I hereby declare that this thesis has not been and will not be, submitted in whole or in part to another University for the award of any other degree.

Signature:

## Acknowledgements

First of all I would like to thank my supervisor Holger Wendland for all his help and support he has given me throughout the work on my doctorate. He was always very generous with his time and patiently answered all my questions. Moreover, it was at his suggestion to continue my studies at Sussex University. This was one of the best decisions I ever made.

I would like to thank the people who helped me to improve my written English, namely Mel, James and Adrian, as well as Roger Clark. Many thanks to Kerstin for a constructive discussion about the structure of my thesis. Also thanks to the staff of the university, who helped me a lot with all the formalities.

Special thanks to my partner Stefan for listening, cheering me up whenever needed and keeping me sane. Thanks to my parents, who always supported me in my decision to study in the UK. Last, but no means least, I would like to thank my colleagues and house-mates and new friends. You made me enjoy my time in Brighton.

University of Sussex

Submitted for the degree Doctor of Philosophy

# Analytically Divergence-free Discretization Methods for Darcy's Problem

Daniela Schräder

## Abstract

Radial basis functions are well known for their applications in scattered data approximation and interpolation. They can also be applied in collocation methods to solve partial differential equations. We develop and analyse a mesh-free discretization method for Darcy's problem. Our approximation scheme is based upon optimal recovery, which leads to a collocation scheme using divergence-free positive definite kernels. Besides producing analytically incompressible flow fields, our method can be of arbitrary order, works in arbitrary space dimension and for arbitrary geometries. Firstly we establish Darcy's problem. To introduce the scheme we review and study divergence-free and curl-free matrix-valued kernels and their reproducing kernel Hilbert spaces. After developing the scheme, we find the approximation error for smooth target functions and the optimal approximation orders. Furthermore, we develop Sobolev-type error estimates for target functions rougher than the approximating function and show that the approximation properties extend to those functions. To find these error estimates, we apply band-limited approximation. Finally, we illustrate the method with numerical examples.

# Contents


**1. Introduction** **1**

1.1. Numerical Approximation of Partial Differential Equations . . . . . 2

1.2. Outline of the Thesis . . . . . 7

1.3. Technical Details . . . . . 8

**2. Notation and Definitions** **9**

2.1. General Notation . . . . . 9

2.2. Standard Function Spaces . . . . . 10

2.2.1. Lebesgue Spaces . . . . . 11

2.2.2. Sobolev Spaces . . . . . 12

2.3. The Fourier Transform . . . . . 13

2.4. Kernels . . . . . 15

2.4.1. Positive Definite Functions . . . . . 15

2.4.2. Wendland Functions . . . . . 17

2.4.3. Modified Bessel Functions . . . . . 18

2.4.4. Divergence-free Matrix-valued Kernels . . . . . 19

2.4.5. Curl-free Matrix-valued Kernels . . . . . 20

**3. Darcy's Problem** **25**

3.1. Fluid Dynamics in Porous Media . . . . . 25

3.1.1. Porous Media . . . . . 25

3.1.2. Flow in Porous Media . . . . . 27

3.2. The Experimental Law of Darcy . . . . . 28

3.3. The Generalised Darcy's Law . . . . . 29

3.4. Darcy's Problem . . . . . 29

3.5. Existence and Regularity . . . . . 30

3.6. Applications and Restrictions . . . . . 32

**4. Reproducing Kernel Hilbert Spaces** **33**

4.1. Hilbert Spaces with Matrix-valued Reproducing Kernels . . . . . 33

4.1.1. Definition and Properties . . . . . 33

4.1.2. Examples . . . 36
4.2. Native Spaces for Positive Definite Kernels . . . 44
4.2.1. Scalar-valued Native Spaces . . . 44
4.2.2. Matrix-valued Native Spaces . . . 46
4.2.3. Examples . . . 47

**5. Analytically Divergence-free Discretization Methods for Darcy's Problem 52**
5.1. Optimal Recovery to Solve Partial Differential Equations . . . 52
5.2. Native Spaces of Combined Kernels . . . 54
5.3. The Approximation Scheme . . . 56
5.4. The Two Dimensional Scheme . . . 58

**6. Error Analysis 61**
6.1. Extension Operator . . . 61
6.2. Error Estimates . . . 62
6.2.1. Error Estimates Inside the Domain . . . 62
6.2.2. Error Estimates on the Boundary . . . 64
6.2.3. Main Result . . . 66

**7. Error Estimates for Target Functions Outside the Native Space 67**
7.1. Band-limited Functions and Function Spaces . . . 67
7.2. Band-limited Interpolation and Approximation . . . 69
7.3. Error Analysis . . . 82

**8. Numerical Examples 86**
8.1. Implementation of the Method . . . 86
8.2. Numerical Error Estimates . . . 90
8.2.1. Homogeneous Permeability . . . 90
8.2.2. Inhomogeneous Permeability . . . 91
8.3. Numerical Error Estimates for Target Functions Outside the Native Space . 96
8.4. Dependency on the Parameters . . . 101
8.4.1. Dependency on the Basis Function . . . 101
8.4.2. Dependency on the Permeability . . . 102
8.4.3. Dependency on the Data Set . . . 104

**9. Conclusions 106**

**Bibliography 107**

**A. Appendix 112**

# 1. Introduction

Darcy's problem models flow in porous media, i. e. it is important in engineering and science. In particular, it can be applied to describe the creeping flow of a Newtonian fluid in porous media [6]. Moreover, in some projection methods for solving the Navier-Stokes equations, a numerical solution of Darcy's problem is essential [45].

Darcy's law is given by

$$\mathbf{u} = -K\nabla p$$

where $\mathbf{u}$ is the velocity, $p$ the pressure and $K$ describes the porous media and the viscosity of the fluid. The original version of Darcy's law was obtained experimentally. However, in the case of anisotropic homogeneous flow Darcy's law can also be obtained from the Navier-Stokes equations [43]. Darcy's problem is an extension of Darcy's law. It is the partial differential equation given by

$$\begin{aligned} \mathbf{u} + K\nabla p &= \mathbf{f} && \text{in } \Omega, \\ \nabla \cdot \mathbf{u} &= 0 && \text{in } \Omega, \\ \mathbf{u} \cdot \mathbf{n} &= \mathbf{g} \cdot \mathbf{n} && \text{on } \partial\Omega. \end{aligned}$$

Here, $\mathbf{n}$ denotes the outer unit normal vector of the boundary $\partial\Omega \subseteq \mathbb{R}^d$. The right hand sides $\mathbf{f}$ and $\mathbf{g} \cdot \mathbf{n}$ and the permeability tensor $K$ are given. The velocity $\mathbf{u}$ and pressure $p$ are sought.

The goal of this thesis is to find a high-order method to solve Darcy's problem efficiently. This approximation scheme is mesh-free and deals with Darcy's problem directly. It is also of arbitrary order, works in arbitrary space dimension and for arbitrary geometries. The scheme leads to an analytically divergence-free reconstruction of the velocity. The error analysis will be done. Since the standard error analysis is limited to smooth target functions, we present new ideas which extend the ideas from interpolation problems to our collocation method for Darcy's problem. To validate the theoretical results, numerical experiments are carried out.

## 1.1. Numerical Approximation of Partial Differential Equations

Classical numerical techniques for solving partial differential equations such as finite elements or finite volumes require a mesh of the underlying domain. This mesh can be difficult to generate, in particular for complex geometries like aircrafts or in moving frameworks. Furthermore, finite element methods suffer from the fact that the solution is usually not analytically divergence-free. Similar problems appear in other methods like finite differences. Finite element methods for Darcy's problem can be found for example in [5, 8, 10].

Radial basis functions can be applied to solve partial differential equations by collocation, see for example [13, 15, 16]. Our scheme follows the framework presented by Wendland for Stokes problem [55]. The approximation scheme for Darcy's problem, which we present here, is therefore a collocation method, which applies matrix-valued positive definite radial basis functions.

### Radial Basis Functions

Radial basis functions are well-known in scattered data approximation [54], but are also applied in image processing, computer graphics and many other areas. A function $\phi : \mathbb{R}^d \to \mathbb{R}$ is said to be *radial* if a function $\varphi : [0, \infty) \to \mathbb{R}$ exists, such that $\phi(\mathbf{x}) = \varphi(\|\mathbf{x}\|_2)$ for all $\mathbf{x} \in \mathbb{R}^d$. There are many examples of radial basis functions; for instance Gaussians, Hardy's multi-quadrics and thin-plate splines. In 1995, Wendland developed compactly supported, piece-wise polynomial radial basis functions [53]. These positive definite functions are called Wendland functions.

Note that a continuous function $\phi$ is *positive definite* if and only if it is even and for pair-wise distinct $\mathbf{x}_1, \dots, \mathbf{x}_N$ and all non-vanishing $\boldsymbol{\alpha} \in \mathbb{R}^N$ it holds that

$$\sum_{j=1}^{N} \sum_{k=1}^{N} \alpha_j \alpha_k \phi(\mathbf{x}_j - \mathbf{x}_k) > 0.$$

Recently, matrix-valued radial basis functions were developed. Although these matrix-valued kernels are not radial in the sense presented above, they are commonly called radial basis functions, since they are usually constructed from radial basis functions. Of particular importance for the construction of the scheme and its error analysis are the divergence-free and curl-free matrix-valued kernels. The divergence-free kernel has been developed in [38] and further studied in [17, 18, 19, 20, 33, 34]. The curl-free kernel has been studied in [17, 18, 19, 20].

### Reproducing Kernel Hilbert Spaces

Reproducing kernel Hilbert spaces are an important tool in scattered data approximation with radial basis functions. Since most kernels are radial, all relevant positive definite kernels are real-valued. Therefore we will only look at real function spaces.

Let $\Omega \subseteq \mathbb{R}^d$ be a domain which contains at least one point. A real Hilbert space $\mathcal{F}$ of functions $f : \Omega \to \mathbb{R}$ is called a *reproducing kernel Hilbert space* if there exists a function $\phi : \Omega \times \Omega \to \mathbb{R}$, such that

(1) $\phi(\cdot, \mathbf{y}) \in \mathcal{F}$ for all $\mathbf{y} \in \Omega$,

(2) $f(\mathbf{y}) = (f, \phi(\cdot, \mathbf{y}))_{\mathcal{F}}$ for all $f \in \mathcal{F}$ and all $\mathbf{y} \in \Omega$.

The function $\phi$ is uniquely determined and called the *reproducing kernel* of the space $\mathcal{F}$.

A reproducing kernel Hilbert space can be constructed for every positive definite kernel. In particular, radial basis functions are often used as reproducing kernels.

Further information about reproducing kernel Hilbert spaces can be found in [54]. The case when the reproducing function is matrix-valued will be discussed later.

### Native Spaces

Native spaces are of particular importance in the theory of generalised interpolation with radial basis functions. Besides providing the interpolation or approximation space, they are also essential in the error analysis.

Let $\phi : \Omega \times \Omega \to \mathbb{R}$ be a positive definite kernel and $\Omega \subseteq \mathbb{R}^d$. We define the space

$$F_\phi(\Omega) := \left\{ \sum_{j=1}^{N} \alpha_j \phi(\cdot, \mathbf{x}_j) \,:\, \mathbf{x}_j \in \Omega,\, \alpha_j \in \mathbb{R} \right\}$$

equipped with the inner product

$$\left( \sum_{j=1}^{N} \alpha_j \phi(\cdot, \mathbf{x}_j), \sum_{k=1}^{M} \beta_k \phi(\cdot, \mathbf{y}_k) \right)_\phi := \sum_{j=1}^{N} \sum_{k=1}^{M} \alpha_j \beta_k \phi(\mathbf{x}_j, \mathbf{y}_k).$$

The *native space* $\mathcal{N}_\phi(\Omega)$ of the function $\phi$ is the completion of the space $F_\phi(\Omega)$ with respect to the norm associated to the inner product. The native space of a positive definite kernel is a reproducing kernel Hilbert space. Information about native spaces can be found in [54].

Many Sobolev spaces can be characterised as reproducing kernel Hilbert spaces. Certain of these spaces coincide with the native space of Wendland functions [54].

The idea of native spaces can be extended to matrix-valued kernels, which is a recent development, cf. [17, 55].

### Discretizing Partial Differential Equations by Collocation

We aim for a collocation scheme, i. e. the right hand side of the partial differential equation is only prescribed at particular discrete points. Therefore the partial differential equation will be solved by using the information at those points only. Note that the solution of a partial differential equation will often only be approximated, since limited information is given.

We will use functionals to describe our collocation method for solving the partial differential equation. For example, assume that we want to solve the differential equation $Lu = f$ in $\Omega$. For simplicity we will neglect boundary conditions for the time being. Then, we could use discrete data sites $X = \{\mathbf{x}_1, \dots, \mathbf{x}_N\} \subseteq \Omega$, and define the functionals

$$\lambda_j(u) = (Lu)(\mathbf{x}_j),$$

where $1 \leq j \leq N$. The goal is to find an approximating function $s$ which satisfies the collocation conditions

$$\lambda_j(s) = f_j = f(\mathbf{x}_j)$$

for all $1 \leq j \leq N$.

A first approach could be to choose

$$s = \sum_{j=1}^{N} \alpha_j \phi(\cdot - \mathbf{x}_j),$$

like in an interpolation problem. Then the linear system of equations $A\boldsymbol{\alpha} = \mathbf{f}$ has to be solved to determine the $\alpha_j$. The matrix $A$ is defined via $A_{ij} = \lambda_i^{\mathbf{x}}(\phi(\mathbf{x} - \mathbf{x}_j))$, where the functional $\lambda_i$ is only applied to the first or $\mathbf{x}$-argument of the function $\phi$. This method is often referred to as Kansa's method, see [25, 26]. The system of equations is often non-symmetric, since $\lambda_i^{\mathbf{x}}(\phi(\mathbf{x} - \mathbf{x}_j))$ is usually not equal to $\lambda_j^{\mathbf{x}}(\phi(\mathbf{x} - \mathbf{x}_i))$. Moreover, the system could be non-invertible.

The first promising steps to resolve this problem were done by Lorentz et al. and Berentz and Iske, cf. [7, 31]. The idea is to choose the approximating function by the following ansatz

$$s = \sum_{k=1}^{N} \alpha_k \lambda_k^{\mathbf{y}}(\phi(\cdot - \mathbf{y})),$$

which leads to a symmetric collocation matrix

$$A := \begin{pmatrix} \lambda_1^{\mathbf{x}}\lambda_1^{\mathbf{y}} & \dots & \lambda_1^{\mathbf{x}}\lambda_N^{\mathbf{y}} \\ \vdots & \ddots & \vdots \\ \lambda_N^{\mathbf{x}}\lambda_1^{\mathbf{y}} & \dots & \lambda_N^{\mathbf{x}}\lambda_N^{\mathbf{y}} \end{pmatrix} \phi(\mathbf{x}-\mathbf{y}).$$

Furthermore, a unique solution of $A\boldsymbol{\alpha} = \mathbf{f}$ exists if the functionals are linearly independent. Then $A$ is indeed positive definite and $s$ is the unique norm-minimal approximating function in the native space of $\phi$.

This concept can be carried over to matrix-valued kernels. We will apply combined kernels to establish the discretization scheme for Darcy's problem. We will use a divergence-free matrix-valued kernel to model the velocity and a general scalar-valued kernel for the pressure. The idea of using combined kernels together with optimal recovery has been developed by Wendland in [55].

### Error Analysis and Approximation Orders

The error estimates of collocation methods with radial basis functions are usually expressed in terms of the fill distance.

The *fill distance* of a set of points $X = \{\mathbf{x}_1, \dots, \mathbf{x}_N\} \subseteq \Omega$ for a domain $\Omega \subseteq \mathbb{R}^d$ is defined to be

$$h_{X,\Omega} := \sup_{\mathbf{x}\in\Omega} \min_{\mathbf{x}_j \in X} \|\mathbf{x} - \mathbf{x}_j\|_2.$$

It can be interpreted as the radius of the largest open ball in the domain $\Omega$ which does not contain any point from $X$. This means that it is the largest hole in the data set, see figure 1.1 (a).

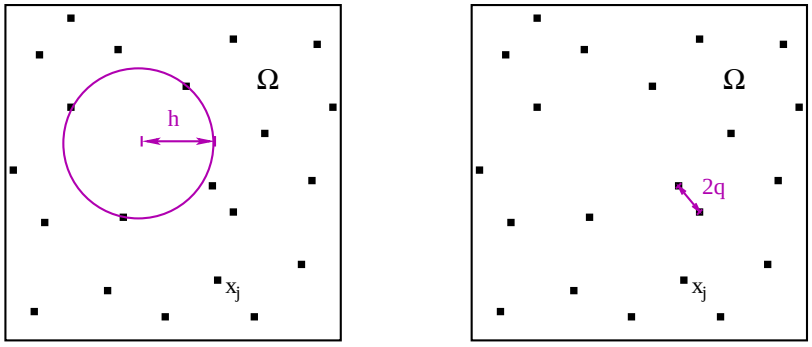


(a) Fill distance (b) Separation radius

Figure 1.1: Measures of the data set.

The other relevant measure is the *separation radius*. For of a discrete set of points

$X = \{\mathbf{x}_1, \ldots, \mathbf{x}_N\}$ it is defined to be

$$q_X := \frac{1}{2} \min_{j \neq k} \|\mathbf{x}_j - \mathbf{x}_k\|_2.$$

The separation radius is therefore half the minimal distance between two points in $X$. An illustration is given in figure 1.1 (b). This means in particular that in the case of an equidistant grid we have that the fill distance is equal to the separation radius, i. e. $h_{X,\Omega} = q_X$.

Error estimates express the worst variation of the approximating function $s_f$ from the true solution $f$. They are often of the form

$$\|f - s_f\|_X \leq ch^\tau \|f\|_Y.$$

Here, $\tau$ is the approximation or convergence order and $h$ is the fill distance of the set of collocation points. Usually both norms are Sobolev norms. To reduce the computational complexity, a small number of collocation points is desired which implies a large $h$. This means that a large $\tau$ is wanted such that the number of points can be reduced while the error is sufficiently close to zero.

#### Approximation Rates for Target Functions Outside the Native Space

The standard error analysis suffers from a major difficulty: The convergence can only be proven for target functions which are in the native space of the underlying radial basis function $\phi$. This means in particular that the smoother $\phi$ is, the smaller is its native space, i. e. the class of functions, where the approximation rates apply, is rather limited. This problem has been partly solved, since the target functions must still satisfy some weak smoothness conditions. First steps were done by Light and Vail in [30]. One approach has been done by Narcowich, Schaback and Ward in [36], an other ansatz was presented from Brownlee and Light in [11]. Narcowich and Ward presented an alternative approach for functions outside the native space on the sphere [39]. Other work on $\mathbb{R}^n$ followed in [28, 29, 40, 41]. An overview can be found in [35]. Recently Fuselier presented error estimates for interpolation problems with divergence-free or curl-free matrix-valued kernels, where the target function is rougher than the interpolant, see [17, 20]. Finding these error estimates is sometimes referred to as 'escaping the native space'.

Sobolev-type approximation rates for target functions outside the native space show that smooth approximating functions also provide good fits to rougher functions. The main benefit from the theoretical point of view is that there is a larger class of functions, where the error estimates apply. In practise, error estimates for a more flexible choice of

the underlying basis function are available. However, these error estimates still require a minimal smoothness of the target function depending on the space dimension.

Until now, the Sobolev-type approximation rates for target functions outside the native space were limited to interpolation problems. We will show that this concept can be extended to collocation methods for solving partial differential equations. In particular, we establish new Sobolev-type approximation rates for the discretization scheme of Darcy's problem, where the velocity and the pressure are not in the native space of the underlying function $\phi$.

The idea of the proof is to apply band-limited functions. To bound the error between the true solution and the approximating function, we add and subtract a band-limited function. This band-limited function is chosen such that it approximates and interpolates the true solution. Therefore the error between it and the true solution can be bounded. Furthermore, the difference between the approximating function and the band-limited function can be bounded via the application of standard error analysis, since both functions are sufficiently smooth and the approximating function also approximates the band-limited function.

## 1.2. Outline of the Thesis

In chapter 2 we will state the necessary definitions and introduce the notation. In particular, we will review the standard function spaces and the Fourier transform. Our method relies on positive definite kernels, therefore these are studied in more detail.

Darcy's problem will be introduced in chapter 3. Since it models flow in porous media, we provide some background in fluid dynamics before stating Darcy's law. Then we state Darcy's problem. Moreover, the most important properties of this partial differential equation will be studied.

To establish our approximation scheme, some technical background about reproducing kernel Hilbert spaces is required. The important results are provided in chapter 4. Besides the formal definition of reproducing kernel Hilbert spaces, some of their properties are established and certain examples are studied in more detail. After this, native spaces of scalar-valued and matrix-valued functions are formally introduced and their relation to Sobolev spaces is shown. Finally, the native spaces of three kernels and their most important properties will be presented.

Chapter 5 is devoted to the approximation scheme. Firstly, the application of optimal recovery to solve partial differential equations will be explained. Then combined kernels will be introduced and their native spaces built. After this, the approximation scheme will be stated. For clarification, the two-dimensional scheme will be presented explicitly.

The standard error analysis of our approximation scheme is covered in chapter 6. The proof of the error estimates relies on an extension operator and uses sampling inequalities and a smoothness result of the solution of Darcy's problem.

New Sobolev-type approximation rates for target functions outside the native space will be developed in chapter 7. They extend the error analysis to rougher target functions. Before establishing the error estimates, band-limited functions and their function spaces are introduced and band-limited interpolation and approximation is studied.

In chapter 8, we will give numerical examples to corroborate our theoretical approximation rates. Furthermore, the implementation of the method will be described and tested in several situations.

We will provide a summary of our studies in chapter 9.

In the appendix we give the important derivatives of certain Wendland functions.

## 1.3. Technical Details

We now give details about the tools used for this thesis.

All implementations have been done in the programming language C++; for the parallel implementation MPI (Message Passing Interface) was used. To avoid any negative influence from possibly ill-conditioned systems, all computations were carried out in quad-double precision as a precaution.

All simulations were undertaken on the Archimedes computing cluster at the University of Sussex, supported by funds from SRIF3.

The graphs have been built with MATLAB. All illustrations were created with Xfig.

# 2. Notation and Definitions

We will now introduce the notation and symbols used in this thesis. Furthermore, we will review the standard function spaces: The spaces of differentiable functions, the Lebesgue spaces and the Sobolev spaces. The Fourier transform is essential for the theory of reproducing kernel Hilbert spaces. We will give its definition and state its main properties. Since kernels are of particular importance, we will study them in more detail. We will therefore discuss positive definite functions and their properties. Then we will give some examples, which include Bessel and Wendland functions. Finally, we will introduce the divergence-free and curl-free matrix-valued kernels.

## 2.1. General Notation

The symbols $\mathbb{N}$, $\mathbb{R}$ and $\mathbb{C}$ indicate the sets of natural, real and complex numbers. The letter $d$ refers to the dimension of a point in a discrete set $X \subseteq \mathbb{R}^d$, while $N$ is the number of points; $n$ is often used for the dimension of the image of a function.

A vector or a vector-valued function is always bold printed, for example $\mathbf{x} \in \mathbb{R}^d$. The $j$th component of a vector $\mathbf{x}$ is denoted by $x_j$. The complex conjugate of a number $z$ is $\overline{z}$ and the absolute value is denoted by $|z|$. Throughout the whole thesis, $\mathbf{e}_i$ refers to the $i$th unit vector.

Capital Latin letters generally refer to function spaces, for instance $C$, $F$, $H$, $L$ and $W$. Exceptions are $A$, which denotes a matrix, and $I$, which is always the identity matrix. We use the standard notation for the transposed vector or matrix $A^T$ and denote by $A^*$ the transposed and complex conjugate of the matrix $A$.

The $k$-th derivative of a function $f(x)$ is denoted by $\frac{d^k}{dx^k} f(x)$, in case of a multivariate function by $\partial_j^k f(\mathbf{x})$ with respect to the $j$th component of $\mathbf{x}$. The short notation $\partial_{ij} f(\mathbf{x}) := \partial_i \partial_j f(\mathbf{x})$ is also used. Let $\boldsymbol{\alpha} \in \mathbb{N}_0^d$ be a multi-index and $|\boldsymbol{\alpha}| := \alpha_1 + \ldots + \alpha_d$. Then, $D^{\boldsymbol{\alpha}} f(\mathbf{x})$ denotes $\partial_1^{\alpha_1} \ldots \partial_d^{\alpha_d} f(\mathbf{x})$. The gradient of a function is $\nabla f(\mathbf{x}) := (\partial_1 f(\mathbf{x}), \ldots, \partial_d f(\mathbf{x}))^T$. The Laplace operator is denoted by $\Delta f(\mathbf{x}) := \sum_{j=1}^d \partial_j^2 f(\mathbf{x})$.

The closure of a set $\Omega$ is denoted by $\overline{\Omega}$. The support of a function $f : \mathbb{R}^d \to \mathbb{R}$ is the closure of the set of points where the function is not zero, i. e.

$$\operatorname{supp} f = \overline{\{\mathbf{x} \in \mathbb{R}^d \,:\, f(\mathbf{x}) \neq 0\}}.$$

A function is compactly supported, if the support is bounded.

Let $x$ be a real number. Then the truncated function $(x)_+$ is defined to be zero, if $x < 0$ and $x$ otherwise. The floor function $\lfloor x \rfloor$ gives the largest integer $i$ with $i \leq x$. The ceil function $\lceil x \rceil$ gives the smallest integer $i$ with $x \leq i$.

The Greek letters $\sigma$, $\tau$ and $\rho$ refer to real numbers. The letters $\phi$, $\mathbf{\Phi}$ and $\psi$ are used for kernels, where $\mathbf{\Phi}$ denotes a matrix-valued kernel and $\phi$ and $\psi$ are radial basis functions. These functions are usually multivariate functions.

A linear and continuous map $\lambda$ from a Hilbert space to the real numbers is called a functional, i. e. $\lambda$ is an element of the dual space $H^*$. The domain $\Omega$ is a subset of $\mathbb{R}^d$. The statement $\lambda^{\mathbf{y}}(\mathbf{f}(\mathbf{x}-\mathbf{y}))$, $\mathbf{f} : \mathbb{R}^d \to \mathbb{R}^n$, indicates that the functional $\lambda$ is applied to the $\mathbf{y}$-component of the function $\mathbf{f}(\mathbf{x}-\mathbf{y})$. We denote the point evaluation functionals by $\delta_{\mathbf{x}}$, where $\mathbf{x} \in \mathbb{R}^d$. Hence $\delta_{\mathbf{x}}(\mathbf{f}) = \mathbf{f}(\mathbf{x})$ for all functions $\mathbf{f} : \mathbb{R}^d \to \mathbb{R}^n$.

Finally, $\chi_\sigma$ denotes the characteristic function of the ball $B(\mathbf{0}, \sigma)$ with radius $\sigma$ and centre $\mathbf{0}$. Hence $\chi_\sigma(\mathbf{x})$ is equal to one if $\mathbf{x} \in B(\mathbf{0}, \sigma)$ and zero otherwise.

## 2.2. Standard Function Spaces

We now give a brief overview over the function spaces of interest. The focus is on the usual definitions of standard spaces, alternative characterisations and certain non-standard spaces will be given later.

Let $F_1(\Omega), \ldots, F_n(\Omega)$ be normed linear function spaces. Then a *tensor product function space* is defined via

$$\mathbf{F}(\Omega) := F_1(\Omega) \times \ldots \times F_n(\Omega), \qquad \mathbf{x} \mapsto \mathbf{f}(\mathbf{x}) = (f_1(\mathbf{x}), \ldots, f_n(\mathbf{x}))^T$$

and can be equipped with the norms

$$\|\mathbf{f}\|_r := \begin{cases} \left( \sum_{j=1}^n \|f_j\|_{F_j(\Omega)}^r \right)^{1/r}, & \text{if } 1 \leq r < \infty, \\ \max_{1 \leq j \leq n} \|f_j\|_{F_j(\Omega)}, & \text{if } r = \infty. \end{cases}$$

The norm $\|\cdot\|_r$ denotes the standard vector norm on $\mathbb{R}^d$, it is also referred to as $\ell_r$-norm.

In the case that the spaces $F_i(\Omega)$, $1 \leq i \leq n$, are Hilbert spaces and that $r = 2$, the space $\mathbf{F}(\Omega)$ is also a Hilbert space. If $F_1(\Omega) = \ldots = F_n(\Omega)$ we equivalently define $\mathbf{F}(\Omega) := (F_1(\Omega))^n$.

Let $k$ be an integer. The space $C^k(\Omega)$ consists of all functions $f : \Omega \to \mathbb{R}$ which are $k$-times continuously differentiable in $\Omega \subseteq \mathbb{R}^d$. The space of all infinitely many times in $\Omega$ continuously differentiable functions is denoted by $C^\infty(\Omega)$. A vector-valued function is in $\mathbf{C}^k(\Omega)$ if and only if each of its components is an element of $C^k(\Omega)$.

For a Hilbert space $H$ its dual will be denoted by $H^* = \{\lambda : H \to \mathbb{R} \mid \lambda \text{ is linear and continuous}\}$. The norm in the dual space is defined via

$$\|\lambda\|_{H^*} := \sup_{f \in H} \frac{|\lambda(\mathbf{f})|}{\|\mathbf{f}\|_H}.$$

In the case of an vector-valued Hilbert space $\mathbf{H}$, the dual is defined to be $\mathbf{H}^* = \{\boldsymbol{\alpha}^T \boldsymbol{\lambda} : \boldsymbol{\lambda} : \mathbf{H} \to \mathbb{R}^n \text{ is linear and continuous and } \boldsymbol{\alpha} \in \mathbb{R}^n\}$.

Let $\Omega$ be an open subset of $\mathbb{R}^d$, where $\overline{\Omega}$ denotes its closure, $k$ be a nonnegative integer and $0 < s \leq 1$. We denote by $C^{k,s}(\overline{\Omega})$ the space of all functions $\mathbf{f} : \overline{\Omega} \to \mathbb{R}^n$, which satisfy

(1) $D^{\boldsymbol{\alpha}}\mathbf{f}$ is continuous and bounded in $\overline{\Omega}$ for all $|\boldsymbol{\alpha}| \leq k$,

(2) for all $|\boldsymbol{\alpha}| = k$ there exists a constant $c < \infty$ such that

$$\|D^\alpha \mathbf{f}(\mathbf{x}) - D^\alpha \mathbf{f}(\mathbf{y})\| \leq c\|\mathbf{x} - \mathbf{y}\|^s,$$

where $\mathbf{x}, \mathbf{y} \in \overline{\Omega}$, i. e. $D^\alpha \mathbf{f}$ is uniformly *Hölder-continuous* with exponent $s$. In the special case that $s = 1$, the function $D^\alpha \mathbf{f}$ is also called *Lipschitz-continuous*.

A Lipschitz boundary has almost everywhere a unit normal vector $\mathbf{n}$. If $k \geq 1$ and a domain has a $C^{k,1}$ boundary, then the normal vector belongs to $\mathbf{C}^{k-1,1}(\partial\Omega)$. If $\Omega$ is also bounded, then this normal vector can be extended to function $\widetilde{\mathbf{n}} \in \mathbf{C}^{k-1,1}(\overline{\Omega})$, cf. [22]. The proof can be done with the inverse trace theorem, cf. [57].

### 2.2.1. Lebesgue Spaces

The *Lebesgue spaces* $L_r(\Omega)$ are established in the usual way. Let $\Omega$ be a subset of $\mathbb{R}^d$ and $1 \leq r < \infty$. A function $f : \Omega \to \mathbb{R}$ is said to be an element of $L_r(\Omega)$ if the integral $\int_\Omega |f(\mathbf{x})|^r d\mathbf{x}$ is finite. In the case $r = \infty$, the norm is defined by $\|f\|_{L_\infty(\Omega)} := \operatorname{ess\,sup}_{\mathbf{x} \in \Omega} |f(\mathbf{x})|$.

The vector-valued Lebesgue spaces are tensor product spaces of the scalar-valued ones, i. e. $\mathbf{L}_r(\Omega) := (L_r(\Omega))^n$. The norm is therefore defined by $\|\mathbf{f}\|_{\mathbf{L}_r(\Omega)} := \left(\int_\Omega \|\mathbf{f}(\mathbf{x})\|_r^r d\mathbf{x}\right)^{1/r}$.

The discrete $\mathbf{L}_r$-norm for a point set $X = \{\mathbf{x}_1, \ldots, \mathbf{x}_N\}$ is

$$\|\mathbf{f}\|_{\mathbf{L}_r(X)} = \left(\frac{1}{N} \sum_{j=1}^{N} \|\mathbf{f}(\mathbf{x}_j)\|_r^r\right)^{1/r}.$$

We recall the *Cauchy Schwarz inequality*. For two vectors $\mathbf{x}, \mathbf{y}$ in $\mathbb{R}^d$ we have

$$|(\mathbf{x}, \mathbf{y})| \leq \|\mathbf{x}\| \, \|\mathbf{y}\|.$$

Let $f$ and $g$ be square-integrable functions. Then,

$$\left| \int f(\mathbf{x}) g(\mathbf{x}) d\mathbf{x} \right|^2 \leq \int |f(\mathbf{x})|^2 d\mathbf{x} \int |g(\mathbf{x})|^2 d\mathbf{x}.$$

### 2.2.2. Sobolev Spaces

We will work with the usual scalar-valued Sobolev spaces. Let $\Omega \subseteq \mathbb{R}^d$, $r \geq 1$ be a real number or $r = \infty$ and $k \in \mathbb{N}_0$ an integer. Then we denote by $W_r^k(\Omega)$ the space of all functions $f \in L_r(\Omega)$ having weak derivatives $D^{\boldsymbol{\alpha}} f \in L_r(\Omega)$ for every multi-index $\boldsymbol{\alpha} \in \mathbb{N}_0^d$ with $|\boldsymbol{\alpha}| \leq k$. Let $1 \leq r < \infty$ then the semi-norm and the norm are given by

$$|u|_{W_r^k(\Omega)} = \left( \sum_{|\boldsymbol{\alpha}|=k} \|D^{\boldsymbol{\alpha}} u\|_{L_r(\Omega)}^r \right)^{1/r} \quad \text{and} \quad \|u\|_{W_r^k(\Omega)} = \left( \sum_{|\boldsymbol{\alpha}|\leq k} \|D^{\boldsymbol{\alpha}} u\|_{L_r(\Omega)}^r \right)^{1/r}$$

provided $k$ is an integer. This means in particular that $W_r^0(\Omega) = L_r(\Omega)$.

We also work with fractional order Sobolev spaces $W_r^\tau(\Omega)$. Let $\tau = k + s$, where $k \in \mathbb{N}_0$ and $0 < s < 1$, then

$$|u|_{W_r^{k+s}(\Omega)} := \left( \sum_{|\boldsymbol{\alpha}|=k} \int_\Omega \int_\Omega \frac{|D^{\boldsymbol{\alpha}} u(\mathbf{x}) - D^{\boldsymbol{\alpha}} u(\mathbf{y})|}{\|\mathbf{x} - \mathbf{y}\|_2^{d+rs}} \, d\mathbf{x} \, d\mathbf{y} \right)^{1/r},$$

$$\|u\|_{W_r^{k+s}(\Omega)} := \left( \|u\|_{W_r^k(\Omega)}^r + |u|_{W_r^{k+s}(\Omega)}^r \right)^{1/r}.$$

We set $H^\tau(\Omega) := W_2^\tau(\Omega)$. The case $r = \infty$ is dealt with in the usual way by taking the essential supremum over all derivatives. For an introduction of such fractional order Sobolev spaces we refer to [2, 9, 51].

The following result is taken from [49]. It shows that if $\tau > d/2$ then all functions in the Sobolev space are continuous.

**Corollary 2.1.** *If $\tau > d/2$ then each $f \in H^\tau(\mathbb{R}^d)$ is bounded and continuous. Moreover, if $\tau > d/2 + k$ with $k \in \mathbb{N}_0$, then*

$$H^\tau(\mathbb{R}^d) \subset C^k(\mathbb{R}^d).$$

We are interested in the relation between Sobolev spaces. The proof of the following lemma can be found, for example, in [55].

**Lemma 2.2.** *Let $\Omega \subseteq \mathbb{R}^d$ be bounded, having a Lipschitz boundary.*

*(1) Let* $1 < p \leq r < \infty$ *and* $\tau > \frac{d}{p} - \frac{d}{r}$*, then we have the continuous embedding*

$$W_p^\tau(\Omega) \subseteq W_r^{\tau - \frac{d}{p} + \frac{d}{r}}(\Omega).$$

*(2) Let* $1 \leq r \leq p$*, then we have the continuous embedding*

$$W_p^\tau(\Omega) \subseteq W_r^\tau(\Omega).$$

Since the pressure $p$ in the solution of Darcy's problem is determined only up to a constant, we will work with the quotient spaces $W_r^\tau(\Omega)/\mathbb{R}$ equipped with the norm

$$\|p\|_{W_r^\tau(\Omega)/\mathbb{R}} := \inf_{c \in \mathbb{R}} \|p + c\|_{W_r^\tau(\Omega)}. \tag{2.1}$$

The vector-valued Sobolev space $\mathbf{W}_r^\tau(\Omega) := (W_r^\tau(\Omega))^n$ consists of all vector-valued functions $\mathbf{u} = (u_1, \ldots, u_n)^T : \Omega \to \mathbb{R}^n$, where each component $u_j$ belongs to $W_r^\tau(\Omega)$. A norm on $\mathbf{W}_r^\tau(\Omega)$ can be defined by taking the discrete $\ell_r$-norm of the $W_r^\tau(\Omega)$ norms of the components, i. e. by

$$\|\mathbf{u}\|_{\mathbf{W}_r^\tau(\Omega)} = \begin{cases} \left( \sum_{j=1}^n \|u_j\|_{W_r^\tau(\Omega)}^r \right)^{1/r}, & \text{if } 1 \leq r < \infty, \\ \max_{1 \leq j \leq n} \|u_j\|_{W_\infty^\tau(\Omega)}, & \text{if } r = \infty. \end{cases}$$

Note that we do not use an index to indicate the dimension $n$ since it will become clear from the context. We only distinguish between scalar-valued function spaces and vector-valued ones. Finally, in the case $r = 2$, we also use the notation $\mathbf{H}^\tau(\Omega) := \mathbf{W}_2^\tau(\Omega)$.

## 2.3. The Fourier Transform

The Fourier transform is of particular importance in the field of mathematical analysis, it also plays a crucial role in the theory of positive definite functions. Furthermore, some Sobolev spaces can be characterised with Fourier transformations, see section 4.1.2. We now recall the definition of the Fourier transform and some of its properties. All results in this section are taken from [54, Section 5.2].

Note that there is not only one definition of the Fourier transform. The definition may have influence on the norm of a Sobolev spaces. However, this concerns only constants. We only use the following symmetric definition.

**Definition 2.3.** *For $f \in L_1(\mathbb{R}^d)$ we define its* Fourier transform *by*

$$\widehat{f}(\mathbf{x}) = (2\pi)^{-d/2} \int_{\mathbb{R}^d} f(\boldsymbol{\omega}) e^{-i\mathbf{x}^T\boldsymbol{\omega}} d\boldsymbol{\omega}$$

*and its* inverse Fourier transform *by*

$$f^\vee(\mathbf{x}) = (2\pi)^{-d/2} \int_{\mathbb{R}^d} f(\boldsymbol{\omega}) e^{i\mathbf{x}^T\boldsymbol{\omega}} d\boldsymbol{\omega}.$$

The Fourier transform extends to vector- or matrix-valued functions in the natural way, i. e. component-wise.

The following result establishes some properties of the Fourier transform.

**Theorem 2.4.** *Suppose $f, g \in L_1(\mathbb{R}^d)$; then the following is true.*

*(1)* $\int_{\mathbb{R}^d} \widehat{f}(\mathbf{x}) g(\mathbf{x}) d\mathbf{x} = \int_{\mathbb{R}^d} f(\mathbf{x}) \widehat{g}(\mathbf{x}) d\mathbf{x}$.

*(2) For* $T_\mathbf{a} f(\mathbf{x}) := f(\mathbf{x} - \mathbf{a})$, $\mathbf{a} \in \mathbb{R}^d$, *we have* $\widehat{T_\mathbf{a} f}(\mathbf{x}) = e^{-i\mathbf{x}^T\mathbf{a}} \widehat{f}(\mathbf{x})$.

*(3) If, in addition,* $\partial_j f \in L_1(\mathbb{R}^d)$ *then* $\widehat{f}$ *is differentiable with respect to* $x_j$ *and*

$$\widehat{\partial_j f}(\mathbf{x}) = -i x_j \widehat{f}(\mathbf{x}).$$

*(4) The Fourier transform of the* convolution

$$f * g(\mathbf{x}) := \int_{\mathbb{R}^d} f(\mathbf{y}) g(\mathbf{x} - \mathbf{y}) d\mathbf{y}$$

*is given by* $\widehat{f * g} = (2\pi)^{-d/2} \widehat{f}\widehat{g}$.

Due to the linearity of the integral, the Fourier transform is also linear. Furthermore, the Fourier transform of an integrable function is continuous.

The following result provides a possibility to recover a function from its Fourier transform.

**Corollary 2.5.** *If $f \in L_1(\mathbb{R}^d)$ is continuous and has a Fourier transform $\widehat{f} \in L_1(\mathbb{R}^d)$ then $f$ can be recovered from its Fourier transform:*

$$f(\mathbf{x}) = (2\pi)^{-d/2} \int_{\mathbb{R}^d} \widehat{f}(\boldsymbol{\omega}) e^{i\mathbf{x}^T\boldsymbol{\omega}} d\boldsymbol{\omega}, \qquad \mathbf{x} \in \mathbb{R}^d.$$

## 2.4. Kernels

If $\Omega = \mathbb{R}^d$, the reproducing kernel of a reproducing kernel Hilbert space is often translation invariant in the sense that it can be written as

$$\phi(\mathbf{x}, \mathbf{y}) = \varphi(\mathbf{x} - \mathbf{y})$$

with a function $\varphi : \mathbb{R}^d \to \mathbb{R}$. In this context, we will rather speak of a function than a kernel and identify $\phi$ with $\varphi$. All radial kernels are translation invariant and also the matrix-valued kernels constructed from them.

Throughout this thesis we are only interested in positive definite kernels. Besides the definition of positive definite functions, we will review some of their properties. After this we will give examples for positive definite kernels. This includes, besides three scalar-valued radial basis functions, two matrix valued kernels: The divergence-free and the curl-free matrix-valued kernels. Both matrix-valued kernels are built from scalar-valued radial basis functions. Further information can be found for example in [17, 32, 54].

### 2.4.1. Positive Definite Functions

Our main requirement on kernels is that they are positive definite. Since we are also interested in matrix-valued kernels, the following definition covers both scalar- and matrix-valued functions, cf. [54, 55].

**Definition 2.6.** *Suppose that $\phi : \mathbb{R}^d \to \mathbb{R}$ is continuous. Then $\phi$ is called* positive definite *if and only if $\phi$ is even and we have, for all $N \in \mathbb{N}$, for all $\boldsymbol{\alpha} \in \mathbb{R}^N \backslash \{\mathbf{0}\}$, and for all pair-wise distinct $\mathbf{x}_1, \dots, \mathbf{x}_N$, that*

$$\sum_{j=1}^{N} \sum_{k=1}^{N} \alpha_j \alpha_k \phi(\mathbf{x}_j - \mathbf{x}_k) > 0.$$

*More generally, a matrix-valued function $\boldsymbol{\Phi} : \mathbb{R}^d \to \mathbb{R}^{n \times n}$ is said to be* positive definite*, if it is even $\boldsymbol{\Phi}(-\mathbf{x}) = \boldsymbol{\Phi}(\mathbf{x})$, symmetric $\boldsymbol{\Phi}(\mathbf{x}) = \boldsymbol{\Phi}(\mathbf{x})^T$ and satisfies*

$$\sum_{j,k=1}^{N} \boldsymbol{\alpha}_j^T \boldsymbol{\Phi}(\mathbf{x}_j - \mathbf{x}_k) \boldsymbol{\alpha}_k > 0$$

*for all pair-wise distinct $\mathbf{x}_j \in \mathbb{R}^d$ and all $\boldsymbol{\alpha}_j \in \mathbb{R}^n$ such that $\boldsymbol{\alpha}^T = (\boldsymbol{\alpha}_1^T, \dots, \boldsymbol{\alpha}_N^T)$ is not vanishing.*

A positive definite matrix-valued kernel $\boldsymbol{\Phi}$ is not necessarily positive definite in the usual matrix sense. Therefore the eigenvalues of $\boldsymbol{\Phi}$ need not be positive. For instance, the

kernel

$$\mathbf{\Phi}_{\mathrm{div}}(\mathbf{x}) = \begin{pmatrix} -\partial_{22}\phi & \partial_{12}\phi \\ \partial_{12}\phi & -\partial_{11}\phi \end{pmatrix}(\mathbf{x}), \tag{2.2}$$

where $\phi(\mathbf{x}) := (1 - \|\mathbf{x}\|_2)_+^4(4\|\mathbf{x}\|_2 + 1)$, is positive definite in the sense of definition 2.6 as we will see later. If $\mathbf{x} = \mathbf{0}$, then

$$\mathbf{\Phi}_{\mathrm{div}}(\mathbf{0}) = \begin{pmatrix} -20 & 0 \\ 0 & -20 \end{pmatrix},$$

i. e. the kernel is not positive definite in the usual matrix sense, cf. the appendix for the derivatives of $\phi$. However, the block matrix $(A_{\mathbf{\Phi},X})_{ij} = \mathbf{\Phi}(\mathbf{x}_i - \mathbf{x}_j)$ is indeed positive definite if $\mathbf{\Phi}$ is a positive definite kernel. We will clarify this later.

The matrix-valued kernels are in general not radial in the usual sense. Even if $\phi$ is radial, we can not find a $\widetilde{\mathbf{\Phi}}_{\mathrm{div}}$ such that for the kernel $\mathbf{\Phi}_{\mathrm{div}}$ defined in (2.2) yields $\mathbf{\Phi}_{\mathrm{div}}(\mathbf{x}) = \widetilde{\mathbf{\Phi}}_{\mathrm{div}}(\|\mathbf{x}\|)$ for all $\mathbf{x} \in \mathbb{R}^2$. Nevertheless, matrix-valued kernels are called radial since they are built from radial basis functions.

The following result gives a criterion for positive definiteness. It is taken from [54, Corollary 6.9].

**Corollary 2.7.** *Suppose that $f \in L_1(\mathbb{R}^d)$ is continuous, nonnegative and non-vanishing then*

$$\phi(\mathbf{x}) := \int_{\mathbb{R}^d} f(\boldsymbol{\omega}) e^{-i\mathbf{x}^T\boldsymbol{\omega}} d\boldsymbol{\omega}, \qquad \mathbf{x} \in \mathbb{R}^d,$$

*is positive definite.*

This means in particular, that if the function $\phi$ in the corollary above is continuous and integrable we can apply corollary 2.5 to recover $f = \widehat{\phi}$.

We now state another important result for positive definite functions. Its proof can be found in [54, Corollary 6.12].

**Corollary 2.8.** *If $\phi \in C(\mathbb{R}^d) \cap L_1(\mathbb{R}^d)$ is positive definite then its Fourier transform is nonnegative and in $L_1(\mathbb{R}^d)$.*

The following kernel will play an important role later.

**Proposition 2.9.** *Suppose $\phi \in C^2(\mathbb{R}^d) \cap W_1^2(\mathbb{R}^d)$ is a positive definite function. Then the kernel defined by*

$$\psi := -\Delta\phi$$

*is integrable and positive definite, provided that its Fourier transform $\widehat{\psi} = \|\boldsymbol{\omega}\|_2^2\widehat{\phi}(\boldsymbol{\omega})$ is integrable and non-vanishing.*

*Proof.* One can see that with $\phi \in C^2(\mathbb{R}^d) \cap W_1^2(\mathbb{R}^d)$, $\psi$ is indeed integrable and continuous. Furthermore, its Fourier transform $\widehat{\psi}(\boldsymbol{\omega}) = \widehat{-\Delta\phi}(\boldsymbol{\omega}) = \|\boldsymbol{\omega}\|_2^2 \widehat{\phi}(\boldsymbol{\omega})$ is nonnegative, since $\widehat{\phi}$ is nonnegative according to corollary 2.8.

We can now apply corollaries 2.5 and 2.7 to conclude that

$$\psi(\mathbf{x}) = \int_{\mathbb{R}^d} \widehat{\psi}(\boldsymbol{\omega}) e^{-i\mathbf{x}^T\boldsymbol{\omega}} d\boldsymbol{\omega}, \qquad \mathbf{x} \in \mathbb{R}^d,$$

is indeed positive definite. □

### 2.4.2. Wendland Functions

In 1995, Wendland developed piece-wise polynomial compactly supported functions, see [53]. These functions are called *Wendland functions*. We discuss them, due to the fact that they satisfy all requirements necessary to a kernel in this thesis, i. e. they are an example for the basis functions in this thesis. All numerical examples have been computed with a kernel constructed from Wendland functions.

**Definition 2.10.** *Let $d \in \mathbb{N}$ and $k \in \mathbb{N}_0$. We define* Wendland functions *by*

$$\phi_{d,k} := \mathcal{I}^k \phi_{\lfloor \frac{d}{2} \rfloor + k + 1},$$

*where $\phi_\ell := (1-r)_+^\ell$ and $(\mathcal{I}\phi)(r) = \int_r^\infty t\phi(t)dt$ for all $r \in \mathbb{R}_0^+$.*

The Wendland functions are positive definite radial basis functions with support $[0, 1]$. On their support, the Wendland functions are polynomials. A detailed construction of these functions can be found in [53, 54].

Table 2.1 contains examples of the Wendland functions depending on the space dimension. The table is taken from [54]. The notation $\doteq$ indicates equality up to constant. Here, $r$ is the $\ell_2$-norm of the argument, i. e. we have $\phi(\mathbf{x}, \mathbf{y}) = \phi_{d,\ell}(\|\mathbf{x} - \mathbf{y}\|_2) = \phi_{d,\ell}(r)$.

| Space dimension | Function | Smoothness |
|---|---|---|
| $d = 1$ | $\phi_{1,0}(r) = (1-r)_+$ | $C^0$ |
| | $\phi_{1,1}(r) \doteq (1-r)_+^3(3r+1)$ | $C^2$ |
| | $\phi_{1,2}(r) \doteq (1-r)_+^5(8r^2+5r+1)$ | $C^4$ |
| $d \leq 3$ | $\phi_{3,1}(r) \doteq (1-r)_+^4(4r+1)$ | $C^2$ |
| | $\phi_{3,2}(r) \doteq (1-r)_+^6(35r^2+18r+3)$ | $C^4$ |
| | $\phi_{3,3}(r) \doteq (1-r)_+^8(32r^3+25r^2+8r+1)$ | $C^6$ |
| | $\phi_{3,4}(r) \doteq (1-r)_+^{10}(429r^4+450r^3+210r^2+50r+5)$ | $C^8$ |

Table 2.1: The Wendland functions.

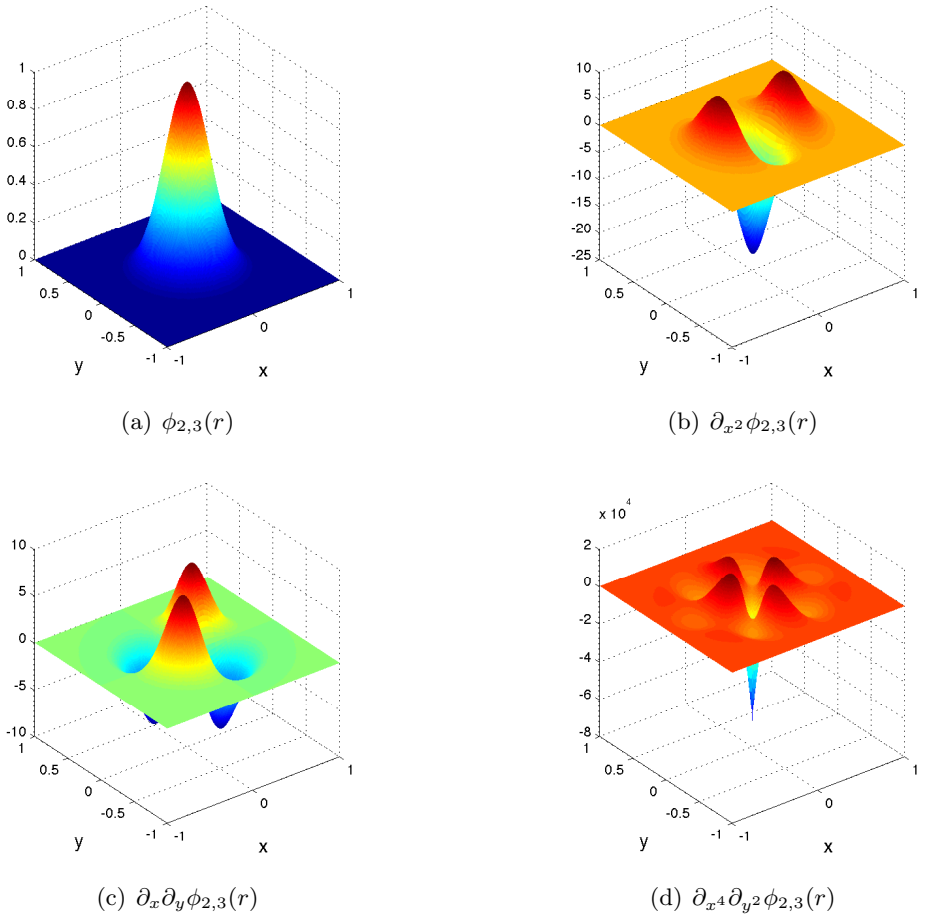


(a) $\phi_{2,3}(r)$

(b) $\partial_{x^2}\phi_{2,3}(r)$

(c) $\partial_x\partial_y\phi_{2,3}(r)$

(d) $\partial_{x^4}\partial_{y^2}\phi_{2,3}(r)$

Figure 2.1: The Wendland function $\phi_{2,3}(r)$ with $r = \sqrt{x^2 + y^2}$.

The derivatives of certain Wendland functions can be found in the appendix. Figure 2.1 illustrates the $C^6$-Wendland function and some of its derivatives.

### 2.4.3. Modified Bessel Functions

In chapter 4 we will see that some Sobolev spaces are reproducing kernel Hilbert spaces. However, in this case the reproducing kernels of the Sobolev spaces are built from modified Bessel functions of the second kind.

We give the definition of the function and a few results here. Further information about Bessel functions can be found, for example, in [1, 52, 54].

**Definition 2.11.** *The* modified Bessel function of the second kind of order $\nu$ *is defined by*

$$K_\nu(z) = \int_0^\infty e^{-z\cosh(t)}\cosh(\nu t)\,dt$$

*for* $z \in \mathbb{C}$ *with* $|\arg(z)| < \pi/2$*;* $\cosh(t) = (e^t + e^{-t})/2$.

For these Bessel functions, the following recursive formulae apply

$$K_\nu(r) = K_{-\nu}(r), \tag{2.3}$$

$$\frac{d}{dr}\left(r^\nu K_\nu(r)\right) = -r^\nu K_{\nu-1}(r). \tag{2.4}$$

From (2.4) and

$$\partial_i\left(\|\mathbf{x}\|_2^\nu K_\nu(\|\mathbf{x}\|_2)\right) = -\|\mathbf{x}\|_2^\nu K_{\nu-1}(\|\mathbf{x}\|_2)\frac{x_i}{\|\mathbf{x}\|_2} = -x_i\|\mathbf{x}\|_2^{\nu-1}K_{\nu-1}(\|\mathbf{x}\|_2), \quad 1 \le i \le d,$$

we have the second derivatives

$$\partial_{ii}\left(\|\mathbf{x}\|_2^\nu K_\nu(\|\mathbf{x}\|_2)\right) = -\|\mathbf{x}\|_2^{\nu-1}K_{\nu-1}(\|\mathbf{x}\|_2) + x_i^2\|\mathbf{x}\|_2^{\nu-2}K_{\nu-2}(\|\mathbf{x}\|_2), \qquad 1 \le i \le d, \tag{2.5}$$

$$\partial_{ij}\left(\|\mathbf{x}\|_2^\nu K_\nu(\|\mathbf{x}\|_2)\right) = x_i x_j\|\mathbf{x}\|_2^{\nu-2}K_{\nu-2}(\|\mathbf{x}\|_2), \qquad 1 \le i, j \le d,\ i \ne j. \tag{2.6}$$

The following result gives an upper bound for the modified Bessel function. It can be proved by combining corollary 5.12 and lemma 5.13 from [54].

**Lemma 2.12.** *For every* $\nu \in \mathbb{R}$ *the function* $r \mapsto r^\nu K_\nu(r)$ *is non-increasing on* $(0, \infty)$ *and*

$$r^\nu |K_\nu(r)| \le r^{\nu-1/2}\sqrt{2\pi}e^{-r}e^{\nu^2/(2r)}$$

*for every* $r > 0$ *and* $\nu \in \mathbb{R}$.

### 2.4.4. Divergence-free Matrix-valued Kernels

The *divergence* of a function $\mathbf{f} : \mathbb{R}^d \to \mathbb{R}^d$ is given by

$$\operatorname{div}\mathbf{f} := \nabla \cdot \mathbf{f} = \sum_{j=1}^{d} \partial_j f_j(\mathbf{x}).$$

A function is *divergence-free* if and only if

$$\operatorname{div}\mathbf{f} = 0.$$

Narcowich and Ward were the first to introduce matrix-valued divergence-free kernels in [38]. Then Lowitzsch introduced compactly supported divergence-free kernels in [32].

The divergence-free kernel of a positive definite kernel $\phi \in C^2(\mathbb{R}^d) \cap W_1^2(\mathbb{R}^d)$ is

$$\mathbf{\Phi}_{\text{div}} := (-\Delta I + \nabla\nabla^T)\phi = \begin{pmatrix} -\sum_{i=2}^n \partial_{ii}\phi & \partial_{12}\phi & \dots & \partial_{1n}\phi \\ \partial_{12}\phi & -\sum_{i=1,\, i\neq 2}^n \partial_{ii}\phi & \dots & \partial_{2n}\phi \\ \vdots & \vdots & \ddots & \vdots \\ \partial_{1n}\phi & \partial_{2n}\phi & \dots & -\sum_{i=1}^{n-1} \partial_{ii}\phi \end{pmatrix}. \quad (2.7)$$

Every column or row of the kernel $\mathbf{\Phi}_{\text{div}}$ is obviously divergence-free since

$$\operatorname{div}\left((\mathbf{\Phi}_{\text{div}})_j\right) = \sum_{k=1}^n \partial_k (\mathbf{\Phi}_{\text{div}})_{kj} = \sum_{k=1,\, k\neq j} \partial_k \partial_{kj}\phi - \partial_j \sum_{i=1,\, i\neq j}^n \partial_{ii}\phi = 0.$$

It is well-known that the matrix-valued kernel defined by (2.7) is positive definite, cf. [17, 38, 55]. The proof of the following lemma can be found in [32].

**Lemma 2.13.** *Suppose $\phi \in C^2(\mathbb{R}^d) \cap W_1^2(\mathbb{R}^d)$ is a positive definite function. For the kernel defined by (2.7) we have that $\mathbf{\Phi}_{\text{div}}\boldsymbol{\alpha}$ and its Fourier transform $\widehat{\mathbf{\Phi}_{\text{div}}}(\boldsymbol{\omega})\boldsymbol{\alpha} = (\|\boldsymbol{\omega}\|_2^2 - \boldsymbol{\omega}\boldsymbol{\omega}^T)\widehat{\phi}(\boldsymbol{\omega})\boldsymbol{\alpha}$ are in $\mathbf{L}_1(\mathbb{R}^d)$ for every $\boldsymbol{\alpha} \in \mathbb{R}^d$. Furthermore, $\mathbf{\Phi}_{\text{div}}$ is positive definite in the sense of definition 2.6.*

The kernel $\mathbf{\Phi}_{\text{div}}$ enables us to construct analytically divergence-free approximating functions for Darcy's problem.

### 2.4.5. Curl-free Matrix-valued Kernels

The *rotation* or *curl* of a function $\mathbf{f} = (f_1, f_2, f_3)^T \in \mathbf{H}^1(\mathbb{R}^3)$ is

$$\operatorname{curl}\mathbf{f} := \nabla \times \mathbf{f} = \begin{pmatrix} \partial_2 f_3 - \partial_3 f_2 \\ \partial_3 f_1 - \partial_1 f_3 \\ \partial_1 f_2 - \partial_2 f_1 \end{pmatrix}.$$

This definition can be used to state the curl for two dimensional functions. The curl of $\mathbf{f} \in \mathbf{H}^1(\mathbb{R}^2)$ is defined by taking the cross-product of the gradient and the function $\mathbf{f}(x_1, x_2) = (f_1(x_1, x_2), f_2(x_1, x_2), 0)^T$, it follows that $\operatorname{curl}\mathbf{f} = \partial_1 f_2 - \partial_2 f_1$.

Let $d = 2, 3$. A function $\mathbf{f} \in \mathbf{H}^1(\mathbb{R}^d)$ is called *curl-free* if and only if

$$\operatorname{curl}\mathbf{f} = \mathbf{0}.$$

An alternative definition states that a function $\mathbf{f} \in \mathbf{H}^\tau(\mathbb{R}^d)$ is *curl-free* on $\mathbb{R}^d$ if and only if there exists a function $g \in H^{\tau+1}(\mathbb{R}^d)/\mathbb{R}$ such that $\nabla g = \mathbf{f}$. This means in particular that if the Fourier transform exists, then $\widehat{\mathbf{f}}(\boldsymbol{\omega}) = -i\boldsymbol{\omega}\widehat{g}(\boldsymbol{\omega})$.

**Proposition 2.14.** *Let $d = 2, 3$ and $\tau \geq 1$. Then, both definitions of curl-free are equivalent for all $\mathbf{f} \in \mathbf{H}^\tau(\mathbb{R}^d)$.*

*Proof.* We will show the equivalence for the three-dimensional case. The two dimensional case can be shown similarly.

Suppose that $\operatorname{curl} \mathbf{f}(\mathbf{x}) = \mathbf{0}$ for all $\mathbf{x} \in \mathbb{R}^3$, then we have the following three equalities:

$$\partial_3 f_1(\mathbf{x}) = \partial_1 f_3(\mathbf{x}), \tag{2.8}$$

$$\partial_1 f_2(\mathbf{x}) = \partial_2 f_1(\mathbf{x}), \tag{2.9}$$

$$\partial_2 f_3(\mathbf{x}) = \partial_3 f_2(\mathbf{x}). \tag{2.10}$$

We now integrate both sides of (2.8) and receive the equivalent equality

$$\int_{-\infty}^{x_3} \partial_3 f_1(x_1, x_2, t)\, dt = f_1(\mathbf{x}) = \int_{-\infty}^{x_3} \partial_1 f_3(x_1, x_2, t)\, dt. \tag{2.11}$$

Similarly, we derive

$$f_2(\mathbf{x}) = \int_{-\infty}^{x_1} \partial_2 f_1(t, x_2, x_3)\, dt, \tag{2.12}$$

$$f_3(\mathbf{x}) = \int_{-\infty}^{x_2} \partial_3 f_2(x_1, t, x_3)\, dt. \tag{2.13}$$

Substituting the right hand side of (2.13) for $f_3$ in (2.11) gives

$$\begin{aligned} f_1(\mathbf{x}) &= \partial_1 \int_{-\infty}^{x_3} f_3(x_1, x_2, t)\, dt = \partial_1 \int_{-\infty}^{x_3} \left( \int_{-\infty}^{x_2} \partial_3 f_2(x_1, s, t)\, ds \right) dt \\ &= \partial_1 \int_{-\infty}^{x_2} f_2(x_1, s, x_3)\, ds, \end{aligned}$$

i. e. $\int_{-\infty}^{x_3} f_3(x_1, x_2, t)\, dt + c_3 = \int_{-\infty}^{x_2} f_2(x_1, t, x_3)\, dt + c_2$. Analogues, substituting (2.11) for $f_1$ in (2.12) leads to $\int_{-\infty}^{x_1} f_1(t, x_2, x_3)\, dt + c_1 = \int_{-\infty}^{x_3} f_3(x_1, x_2, t)\, dt + c_3$. Therefore

$$g(\mathbf{x}) := \int_{-\infty}^{x_1} f_1(t, x_2, x_3)\, dt + c_1 = \int_{-\infty}^{x_2} f_2(x_1, t, x_3)\, dt + c_2 = \int_{-\infty}^{x_3} f_3(x_1, x_2, t)\, dt + c_3$$

satisfies $\mathbf{f} = \nabla g$.

Suppose now that there exists a function $g \in H^{\tau+1}(\mathbb{R}^d)/\mathbb{R}$ with $\nabla g = \mathbf{f}$. Then substituting $\partial_k g$ for $f_k$, $1 \leq k \leq 3$, and evaluating the cross-product gives $\operatorname{curl} \mathbf{f} = \mathbf{0}$, since $\partial_i \partial_j g = \partial_j \partial_i g$ for all $1 \leq i, j \leq 3$. □

The second definition also gives a criterion when vector-valued function $\mathbf{f} : \mathbb{R}^d \to \mathbb{R}^d$ of dimension $d \in \mathbb{N}$ is curl-free. Due to the equivalence in the cases $d = 2, 3$ and the fact

that we wish to establish an approximation scheme and its error analysis for arbitrary dimensions, we will only use the second definition.

The following curl-free kernel was introduced by FUSELIER in [17]. It is defined by

$$\mathbf{\Phi}_{\text{curl}} := -\nabla\nabla^T\phi, \tag{2.14}$$

where $\phi$ is a sufficiently smooth, positive definite function. We give the proof of the positive definiteness for the convenience of the reader. Before proving the main result, we will prove the following lemma. Both proofs have been given by FUSELIER in [17]. The first proof follows from [54, Lemma 6.7].

**Proposition 2.15.** *Suppose that $U \subseteq \mathbb{R}^d$ is open. Suppose, further, that $\mathbf{x}_1, \dots, \mathbf{x}_N \in \mathbb{R}^d$ are pair-wise distinct and that $\mathbf{c}_j \in \mathbb{C}^d$, $1 \leq j \leq N$. If $f(\boldsymbol{\omega}) = \sum_{j=1}^N \boldsymbol{\omega}^T \mathbf{c}_j e^{-i\mathbf{x}_j^T\boldsymbol{\omega}} = 0$ for all $\boldsymbol{\omega} \in U$ then $\mathbf{c}_j = 0$ for all $1 \leq j \leq N$.*

*Proof.* One can easily see that $f$ is analytic in $U$. It is indeed analytic in all of $\mathbb{C}^d$. Hence we can extend it to $f : \mathbb{R}^d \to \mathbb{C}$, $f(\boldsymbol{\omega}) = \sum_{j=1}^N \boldsymbol{\omega}^T \mathbf{c}_j e^{-i\mathbf{x}_j^T\boldsymbol{\omega}}$, by successive analytic continuation in every component. The set of zeros of $f$ in $U$ has a limiting point. Therefore we can apply the identity theorem component-wise to conclude that $f$ is identically zero in $U$, cf. [44, Theorem 15.8].

Now we take a test function $g \in W_1^2(\mathbb{R}^d)$ and can conclude from $\sum_{j=1}^N \boldsymbol{\omega}^T \mathbf{c}_j e^{-i\mathbf{x}_j^T\boldsymbol{\omega}} = 0$, $\boldsymbol{\omega} \in \mathbb{R}^d$, that

$$\begin{aligned}
0 &= \sum_{j=1}^N \boldsymbol{\omega}^T \mathbf{c}_j e^{-i\mathbf{x}_j^T\boldsymbol{\omega}} \widehat{g}(\boldsymbol{\omega}) \\
&= \sum_{j=1}^N \mathbf{c}_j^T \boldsymbol{\omega} \widehat{g}(\boldsymbol{\omega} - \mathbf{x}_j) \\
&= -i \sum_{j=1}^N \mathbf{c}_j^T \widehat{\nabla g}(\boldsymbol{\omega} - \mathbf{x}_j) \\
&= \left( -i \sum_{j=1}^N \mathbf{c}_j^T \nabla g(\cdot - \mathbf{x}_j) \right)^\wedge (\boldsymbol{\omega})
\end{aligned}$$

for all $\boldsymbol{\omega} \in \mathbb{R}^d$. This implies

$$\sum_{j=1}^N \mathbf{c}_j^T \nabla g(\mathbf{x} - \mathbf{x}_j) = \sum_{j=1}^N \sum_{k=1}^d (\mathbf{c}_j)_k \partial_k g(\mathbf{x} - \mathbf{x}_j) = 0$$

for all $\mathbf{x} \in \mathbb{R}^d$ and every test function $g$.

We now show that $(\mathbf{c}_i)_l = 0$ for every fixed $i$ and $l$. Hence $\mathbf{c}_i = 0$ for all $i$. To see this, we choose $g$ such that $\operatorname{supp} g \subseteq B(\mathbf{0}, \epsilon)$, where $\epsilon < \min_{j \neq i} \|\mathbf{x}_j - \mathbf{x}_i\|_2$, $\partial_l g(0) = 1$ and $\partial_k g(0) = 0$ for all $k \neq l$. Since the support is less than $\min_{j \neq i} \|\mathbf{x}_j - \mathbf{x}_i\|_2$, we have that $\partial_k g(\mathbf{x}_i - \mathbf{x}_j) = 0$ for all $j \neq i$ and all $k$. Therefore

$$0 = \sum_{j=1}^{N} \sum_{k=1}^{d} (\mathbf{c}_j)_k \partial_k g(\mathbf{x}_i - \mathbf{x}_j) = \sum_{k=1}^{d} (\mathbf{c}_i)_k \partial_k g(\mathbf{x}_i - \mathbf{x}_i) = (\mathbf{c}_i)_l \partial_l g(0) = (\mathbf{c}_i)_l,$$

which finishes the proof. □

**Lemma 2.16.** *Suppose $\phi \in C^2(\mathbb{R}^d) \cap W_1^2(\mathbb{R}^d)$ is a positive definite function. The kernel defined by (2.14) is curl-free for every column. The kernel is also positive definite in the sense of definition 2.6. Furthermore, $\mathbf{\Phi}_{\text{curl}}\boldsymbol{\alpha}$ and its Fourier-transform $\widehat{\mathbf{\Phi}_{\text{curl}}}(\boldsymbol{\omega})\boldsymbol{\alpha} = \boldsymbol{\omega}\boldsymbol{\omega}^T \widehat{\phi}(\boldsymbol{\omega})\boldsymbol{\alpha}$ are in $\mathbf{L}_1(\mathbb{R}^d)$ for every $\boldsymbol{\alpha} \in \mathbb{R}^d$.*

*Proof.* The $j$th column is given by $\mathbf{\Phi}_{\text{curl}}\mathbf{e}_j$, i. e.

$$\mathbf{\Phi}_{\text{curl}}\mathbf{e}_j = -\nabla\nabla^T \phi \mathbf{e}_j = \nabla(-\nabla^T(\phi \mathbf{e}_j)) = \nabla g,$$

where $g = -\partial_j \phi$ is a scalar-valued function. By the symmetry of $\mathbf{\Phi}_{\text{curl}}$, its columns are also curl-free.

The kernel $\mathbf{\Phi}_{\text{curl}}$ is continuous, since $\phi \in C^2(\mathbb{R}^d)$. Moreover, we have

$$\begin{aligned}
\|\mathbf{\Phi}_{\text{curl}}\boldsymbol{\alpha}\|_{\mathbf{L}_1(\mathbb{R}^d)} &= \int_{\mathbb{R}^d} \sum_{i=1}^{d} \left| \sum_{j=1}^{d} (\mathbf{\Phi}_{\text{curl}}(\mathbf{x}))_{ij} \alpha_j \right| d\mathbf{x} \\
&\leq \int_{\mathbb{R}^d} \sum_{i,j=1}^{d} |-\partial_{ij}\phi(\mathbf{x})\alpha_j| \, d\mathbf{x} \\
&= \sum_{i,j=1}^{d} |\alpha_j| \int_{\mathbb{R}^d} |\partial_{ij}\phi(\mathbf{x})| \, d\mathbf{x} < \infty,
\end{aligned}$$

due to the fact that $\phi \in W_1^2(\mathbb{R}^d)$. Hence $\mathbf{\Phi}_{\text{curl}}\boldsymbol{\alpha}$ is integrable, therefore the Fourier transform exists. Applying theorem 2.4 gives

$$(\widehat{\mathbf{\Phi}_{\text{curl}}}(\boldsymbol{\omega})\mathbf{e}_k)_j = (\widehat{-\nabla\nabla^T}\phi(\boldsymbol{\omega})\mathbf{e}_k)_j = \widehat{\partial_k \partial_j \phi}(\boldsymbol{\omega}) = \omega_k \omega_j \widehat{\phi}(\boldsymbol{\omega}),$$

thus $\widehat{\mathbf{\Phi}_{\text{curl}}}(\boldsymbol{\omega}) = \boldsymbol{\omega}\boldsymbol{\omega}^T\widehat{\phi}(\boldsymbol{\omega})$. Keeping this in mind, we have

$$\begin{aligned}
\|\widehat{\mathbf{\Phi}_{\text{curl}}}\boldsymbol{\alpha}\|_{\mathbf{L}_1(\mathbb{R}^d)} &= \int_{\mathbb{R}^d} \sum_{k=1}^{d} \left| \sum_{j=1}^{d} (\widehat{\mathbf{\Phi}_{\text{curl}}})_{jk}(\boldsymbol{\omega})\alpha_j \right| d\boldsymbol{\omega} \\
&\leq \sum_{k,j=1}^{d} |\alpha_j| \int_{\mathbb{R}^d} \left| \omega_j\omega_k\widehat{\phi}(\boldsymbol{\omega}) \right| d\boldsymbol{\omega} \\
&= \sum_{k,j=1}^{d} |\alpha_j| \int_{\mathbb{R}^d} \left| \widehat{\partial_k\partial_j\phi}(\boldsymbol{\omega}) \right| d\boldsymbol{\omega} < \infty
\end{aligned}$$

since $\phi \in C^2(\mathbb{R}^d) \cap W_1^2(\mathbb{R}^d)$.

The kernel $\mathbf{\Phi}_{\text{curl}}$ is even and symmetric since $\phi$ is even and radial.

Let all $\mathbf{x}_j \in \mathbb{R}^d$ be pair-wise distinct and $\boldsymbol{\alpha}_j \in \mathbb{R}^d$ such that not all $\boldsymbol{\alpha}_j$ are vanishing. Applying corollary 2.5 and the Fourier transform of the kernel leads us to

$$\begin{aligned}
\sum_{j,k=1}^{N} \boldsymbol{\alpha}_j^T \mathbf{\Phi}_{\text{curl}}(\mathbf{x}_j - \mathbf{x}_k)\boldsymbol{\alpha}_k &= (2\pi)^{-d/2} \sum_{j,k=1}^{N} \boldsymbol{\alpha}_j^T \int_{\mathbb{R}^d} \widehat{\mathbf{\Phi}_{\text{curl}}}(\boldsymbol{\omega}) e^{i(\mathbf{x}_j - \mathbf{x}_k)^T\boldsymbol{\omega}} d\boldsymbol{\omega}\boldsymbol{\alpha}_k \\
&= (2\pi)^{-d/2} \int_{\mathbb{R}^d} \sum_{j,k=1}^{N} \boldsymbol{\alpha}_j^T \boldsymbol{\omega}\boldsymbol{\omega}^T \widehat{\phi}(\boldsymbol{\omega})\boldsymbol{\alpha}_k e^{i(\mathbf{x}_j - \mathbf{x}_k)^T\boldsymbol{\omega}} d\boldsymbol{\omega} \\
&= (2\pi)^{-d/2} \int_{\mathbb{R}^d} \left\| \sum_{j=1}^{N} \boldsymbol{\omega}^T\boldsymbol{\alpha}_j e^{-i\mathbf{x}_j^T\boldsymbol{\omega}} \right\|_2^2 \widehat{\phi}(\boldsymbol{\omega}) d\boldsymbol{\omega}.
\end{aligned}$$

Note that the integral in the first two steps is applied component-wise. Since $\phi$ is positive definite and $\phi \in C(\mathbb{R}^d) \cap L_1(\mathbb{R}^d)$ and with corollary 2.8, $\widehat{\phi}$ is nonnegative. Furthermore, a norm is always nonnegative. Together with proposition 2.15 we have that $\mathbf{\Phi}_{\text{curl}}$ is indeed positive definite. □

# 3. Darcy's Problem

We now establish Darcy's problem. Since it models flow in porous media, we will start with a brief introduction to porous media flow. Besides the definition of porous material, we will give some real-life examples and establish the main properties. After this we will introduce fluid flow and explain how it can be measured.

Before stating Darcy's problem, we will establish Darcy's law. Then we will look at the existence, uniqueness and regularity of the partial differential equation. Finally, we will give examples for the application of Darcy's problem.

## 3.1. Fluid Dynamics in Porous Media

Porous media flow is a topic in engineering and science. It is of particular importance in ground water hydrology, reservoir engineering, soil science, soil mechanics and chemical engineering.

Usually the goal in fluid dynamics is to recover the *velocity* $\mathbf{u}$ of the fluid and the *pressure* $p$. In the case of porous media flow $\nabla p$ is called the *hydraulic gradient*.

There are two kinds of properties, which we want to distinguish; the properties of the media and the properties of the fluid. Both are important for the mathematical modelling of a particular experimental set-up.

The material in the present section is taken from [6, 24].

### 3.1.1. Porous Media

*Porous media* are materials with interconnected pores with at least several continuous paths from one side of the medium to the other. That portion of material, for example rock, not occupied by solid matter is the *void space* or *pore space*. It contains fluids or gases. Only connected pores can act as elementary conduits within the formation. The *porosity* is the ratio of volume of the void space to the bulk volume of a porous medium. An example for porous media is given in figure 3.1.

Oil or gas reservoirs are instances of porous media. They are porous geological formations filled with oil or gas respectively. Ground water flow is another example which is of particular importance since 30.1% of the freshwater on Earth is found below the Earth's

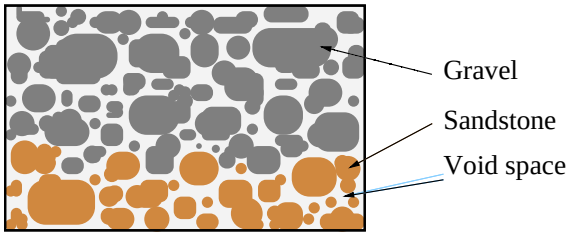


Figure 3.1: An example of porous media.

surface while more than two-thirds are frozen in glaciers, [24]. In some parts of the world, ground water is the only freshwater source. Therefore the study of ground water flow is essential for the water supply in those areas. Darcy's problem is often applied in ground water hydrology.

All water found beneath the ground surface are referred to *ground water*. The ground is partitioned into four different types of layers: Aquifer, aquiclude, aquitard and aquifuge.

An *aquifer* is a geological formation or stratum that contains water and permits significant amounts of water to move through it under ordinary field conditions. Often it consists of unconsolidated or partly consolidated gravel or sand. Sandstone and conglomerate are the consolidated equivalent to sand and gravel. In many parts of the world, limestone formations are important aquifers. Volcanic rock may form permeable aquifers. The main properties of an aquifer are to transmit, store and yield water.

In contrast to an aquifer, an *aquiclude* is a formation that may contain water, but is incapable of letting significant amounts pass through it. An example is clay, which has high porosity, but is relatively impervious due to small pores. Aquicludes are here considered impervious formations.

A semi-pervious geologic formation transmitting water at a very slow rate is called an *aquitard*. This layer often separates aquifers from each other, it allows water to leak through. Impervious formations neither contain nor transmit fluid. They are referred to as *aquifuges*.

If the porosity does not depend on the direction, then the material is *isotropic*, otherwise the medium would be *anisotropic*. Consider fractured rock with mainly horizontal fractures. The permeability in the horizontal direction is higher than in the vertical direction. Hence the rock is anisotropic, while sandstones are an example of isotropic material. Figure 3.1 displays an anisotropic medium.

We distinguish between homogeneous and inhomogeneous porous media. *Homogeneous* means that the porosity is the same at all points, i. e. independent from the position. For example pure fine sand is homogeneous. If the medium consists of more than one kind of material or has varying porosity, it is called *inhomogeneous*. Therefore virtually all natural

materials are inhomogeneous; for instance the porous medium displayed in figure 3.1.

### 3.1.2. Flow in Porous Media

All fluids considered in this thesis are *Newtonian fluids*, i. e. the viscosity $\nu$ is independent of the velocity $\mathbf{u}$. This is true for all gases and the most common liquids. The *dynamic viscosity* or *absolute viscosity* $\mu$ determines the dynamics of an incompressible Newtonian fluid. Moreover, the *kinematic viscosity* $\nu$ of a Newtonian fluid is the dynamic viscosity divided by the density, i. e. the kinematic viscosity combines the two relevant fluid properties.

A flow is said to be *incompressible*, if the density of a fluid element does not change during its motion. This means in particular that the *fluid density*, which is the mass of the fluid per unit volume, is constant.

*Newton's second principle* states that matter can neither be created nor destroyed. This means that any increase or decrease in mass must be due to the flux of matter through the surface bounding the volume. This principle is also referred to as *conservation of mass*. In the case of an incompressible flow, it is given by

$$\operatorname{div} \mathbf{u} = 0.$$

The *hydraulic conductivity* indicates the ability of aquifer material to conduct water through it under hydraulic gradients. More generally, it is the ease of fluid transportation though the porous matrix. It is therefore a combination of the properties of the fluid, i. e. the density and the viscosity, and of the porous medium which are the grain/pore size and shape, tortuosity, specific surface and porosity.

An *observation well* or *piezometer* is a tool to measure porous media flow. Usually it is a vertical pipe with a small diameter. The elevation of the fluid in the piezometer is referred to as the *piezometric* or *hydraulic head*.

An important measure in fluid dynamics is the *Reynolds number*. In porous media flow, it is given by

$$Re = \frac{uD}{\nu},$$

where $\nu$ is the kinematic viscosity, and $D$ is some length dimension. In porous media flow, $D$ is usually the mean diameter of the grains. The Reynolds number gives a criterion of the type of flow - laminar or turbulent flow. The flow is *laminar* if the fluid flows in parallel layers and the layers do not interfere. However, in *turbulent* flow there are no such layers.

## 3.2. The Experimental Law of Darcy

In 1856, Darcy's law has been published by the French engineer *Henry Darcy*. He ran a sequence of experiments to develop design parameters for sand filters. Figure 3.2 gives a sketch of his experimental set-up. The figure is inspired by [6]. In his apparatus Darcy

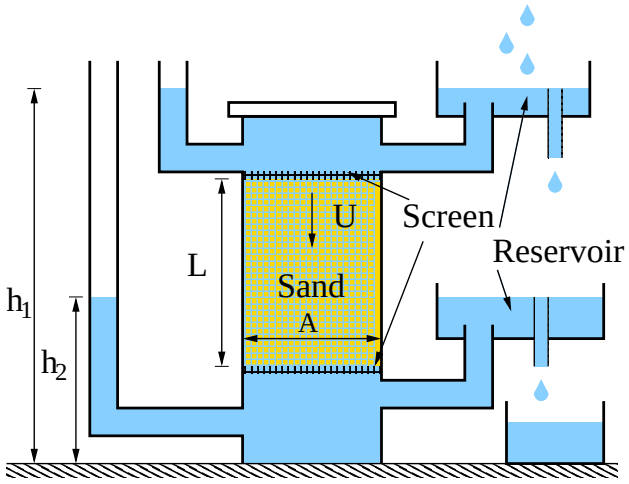


Figure 3.2: A sketch of Darcy's experimental set-up.

varied the length $L$ and cross-sectional area $A$ of a sand-packed column and also the elevations of constant-level water reservoirs connected to the upper $h_1$ and lower $h_2$ boundaries of the column. Combining his observations, Darcy obtained the following relationship

$$U = KA\frac{(h_1 - h_2)}{L}, \tag{3.1}$$

where $U$ is the rate of flow, which is the volume per unit time, $K$ is the *hydraulic conductivity*, and $(h_1 - h_2)/L$ is called the *hydraulic gradient*. In figure 3.2 the piezometric head is the level of the water in the pipes left of the filter marked by $h_1$ and $h_2$. Dividing both sides of (3.1) by the cross-sectional area $A$ gives the experimental version of Darcy's law

$$u = KJ, \qquad \text{where } J := \frac{(h_1 - h_2)}{L}.$$

The experiment of Darcy can be extended to flow through an inclined porous medium column. Further information about Darcy's experiment can be found in [6, 24].

## 3.3. The Generalised Darcy's Law

The experimental law of Darcy is limited to homogeneous, incompressible, one-dimensional flow. We now give the formal generalisation to obtain Darcy's law for $d$-dimensional flow in various kinds of porous material. A detailed description and further approaches can be found in [6].

The most obvious formal generalisation of Darcy's law is

$$\mathbf{u} = -\frac{K}{\nu}\nabla p, \tag{3.2}$$

where the kinematic viscosity $\nu > 0$ and the permeability tensor $K$ are given and the velocity $\mathbf{u}$ and the pressure $p$ have to be determined. This version of Darcy's law can be obtained from the experimental version, cf. [6]. For homogeneous media, it can also be obtained from the Navier-Stokes equations [43].

In the case of isotropic and homogeneous media, the permeability is a scalar constant, i. e. the vectors $\mathbf{u}$ and $\nabla p$ are collinear. If we have inhomogeneous media, equation (3.2) remains valid, but $K := K(\mathbf{x})$ depends on the porosity of the domain.

The case of isotropic media does not appear very often in nature. Soils are for example usually stratified, i. e. anisotropic. To model anisotropic porous media we only need to change the permeability to a matrix-valued function $K$ in (3.2).

## 3.4. Darcy's Problem

We will incorporate the viscosity into the permeability tensor. Furthermore, we will assume that the velocity field is incompressible. Then we combine Darcy's law with the conservation of mass. Appropriate boundary conditions are Neumann-boundary conditions, which ensure that the partial differential equation is well-posed [5]. Then *Darcy's problem* or the *div-grad problem* can be stated in the following way

$$\mathbf{u} + K\nabla p = \mathbf{f} \qquad \text{in } \Omega, \tag{3.3}$$

$$\nabla \cdot \mathbf{u} = 0 \qquad \text{in } \Omega, \tag{3.4}$$

$$\mathbf{u} \cdot \mathbf{n} = \mathbf{g} \cdot \mathbf{n} \qquad \text{on } \partial\Omega. \tag{3.5}$$

Here, $\mathbf{n}$ denotes the outer unit normal vector of the boundary $\partial\Omega \subseteq \mathbb{R}^d$. The right hand sides $\mathbf{f}$ and $\mathbf{g} \cdot \mathbf{n}$ and the tensor $K$ are given. For technical reasons, the tensor $K$ is supposed to be symmetric, thus $K = K^T$, and strongly elliptic in the sense that there is

a constant $\alpha > 0$ such that

$$\boldsymbol{\xi}^T K(\mathbf{x})\boldsymbol{\xi} \geq \alpha \|\boldsymbol{\xi}\|_2^2, \qquad \boldsymbol{\xi} \in \mathbb{R}^d, \mathbf{x} \in \Omega. \tag{3.6}$$

The velocity $\mathbf{u} : \Omega \to \mathbb{R}^d$ and the pressure $p : \Omega \to \mathbb{R}$ are sought.

Darcy's problem is equivalent to an elliptic second-order problem with Neumann boundary data. This immediately follows from taking the divergence of (3.3) and incorporating (3.4). The boundary conditions follow by taking the inner product of (3.3) with the unit outer normal vector $\mathbf{n}$ of $\partial\Omega$ and to use also (3.5). In doing so, we see that (3.3)-(3.5) is equivalent to solving

$$\nabla \cdot (K\nabla p) = \widetilde{f} := \nabla \cdot \mathbf{f} \qquad \text{in } \Omega, \tag{3.7}$$

$$(K\nabla p) \cdot \mathbf{n} = \widetilde{g} := (\mathbf{f} - \mathbf{g}) \cdot \mathbf{n} \qquad \text{on } \partial\Omega \tag{3.8}$$

and defining

$$\mathbf{u} := \mathbf{f} - K\nabla p. \tag{3.9}$$

We have with the divergence theorem, cf. [14, Chapter 15], and (3.4) that

$$\begin{aligned}
\int_{\partial\Omega} \widetilde{\mathbf{g}}\, dS - \int_{\Omega} \widetilde{\mathbf{f}} d\mathbf{x} &= \int_{\partial\Omega} (\mathbf{f} - \mathbf{g}) \cdot \mathbf{n}\, dS - \int_{\Omega} \nabla \cdot \mathbf{f}\, d\mathbf{x} \\
&= \int_{\partial\Omega} \mathbf{g} \cdot \mathbf{n}\, dS \\
&= \int_{\partial\Omega} \mathbf{u} \cdot \mathbf{n}\, dS \\
&= \int_{\Omega} \operatorname{div} \mathbf{u}\, d\mathbf{x} \\
&= 0,
\end{aligned}$$

i. e. the compatibility conditions of the Neumann problem are satisfied.

The other direction of the equivalence follows from rearranging (3.7) and (3.8) such that $\mathbf{f} - K\nabla p$ can be replaced by $\mathbf{u}$ and from rearranging (3.9) for $\mathbf{f}$.

## 3.5. Existence and Regularity

For the elliptic Neumann problem (3.7) and (3.8) the following existence and smoothness result is well-known. For integer order $\tau$ and $K = I$, its proof can be found in [22, Theorem 1.10], the general integer case follows from [23] and the general fractional order case follows by interpolation theory in Sobolev spaces. Though the result was originally derived for weak solutions, the higher regularity assumption on the given data implies that it also

holds for classical solutions.

**Proposition 3.1.** *Let $\Omega$ be a bounded open subset of $\mathbb{R}^d$ with a $C^{\lceil\tau\rceil+1,1}$ boundary $\partial\Omega$ and $\tau \geq 0$. Assume that the permeability tensor $K = (K_{ij})$ satisfies (3.6), $K = K^T$ and $K_{ij} \in W_r^{\tau+1}(\overline{\Omega})$. Assume further for the data that $\widetilde{f} \in W_r^{\tau}(\Omega)$ and $\widetilde{g} \in W_r^{\tau+1-1/r}(\partial\Omega)$ for $1 < r < \infty$ and $\int_{\partial\Omega} \widetilde{\mathbf{g}}\, dS = \int_\Omega \widetilde{\mathbf{f}} d\mathbf{x}$. Then there exists a function $p \in W_r^{\tau+2}(\Omega)/\mathbb{R}$ solving (3.7) and (3.8), which satisfies*

$$\|p\|_{W_r^{\tau+2}(\Omega)/\mathbb{R}} \leq c \left\{ \|\widetilde{f}\|_{W_r^{\tau}(\Omega)} + \|\widetilde{g}\|_{W_r^{\tau+1-1/r}(\partial\Omega)} \right\}$$

*with a constant $c = c(\tau, r, \Omega)$.*

Applying this to our special situation, the existence and smoothness of the solutions of Darcy's problem follow.

**Theorem 3.2.** *Let $\Omega$ be a bounded open subset of $\mathbb{R}^d$ with a $C^{\lceil\tau\rceil+1,1}$ boundary $\partial\Omega$. Assume that the data satisfies $\mathbf{f} \in \mathbf{W}_r^{\tau+1}(\Omega)$ and $\mathbf{g} \in \mathbf{W}_r^{\tau+1-1/r}(\partial\Omega)$ for $1 < r < \infty$. Assume further, that the permeability tensor $K = (K_{ij})$ satisfies (3.6), $K = K^T$ and $K_{ij} \in W_r^{\tau+1}(\overline{\Omega})$. Then there exist a velocity $\mathbf{u} \in \mathbf{W}_r^{\tau+1}(\Omega)$ and a pressure $p \in W_r^{\tau+2}(\Omega)/\mathbb{R}$, solutions to (3.3)–(3.5), which satisfy*

$$\|\mathbf{u}\|_{\mathbf{W}_r^{\tau+1}(\Omega)} + \|p\|_{W_r^{\tau+2}(\Omega)/\mathbb{R}} \leq c \left( \|\mathbf{f}\|_{\mathbf{W}_r^{\tau+1}(\Omega)} + \|\mathbf{g}\cdot\mathbf{n}\|_{W_r^{\tau+1-1/r}(\partial\Omega)} \right).$$

*Proof.* Our assumptions on the given data immediately yield $\widetilde{f} = \nabla\cdot\mathbf{f} \in W_r^{\tau}(\Omega)$. Since the boundary is also assumed to be smooth enough, we have $\widetilde{g} = (\mathbf{f}-\mathbf{g})\cdot\mathbf{n} \in W_r^{\tau+1-1/r}(\partial\Omega)$. Furthermore, we have the obvious estimates $\|\widetilde{f}\|_{W_r^{\tau}(\Omega)} \leq \|\mathbf{f}\|_{\mathbf{W}_r^{\tau+1}(\Omega)}$ and

$$\begin{aligned} \|\widetilde{g}\|_{W_r^{\tau+1-1/r}(\partial\Omega)} &= \|(\mathbf{f}-\mathbf{g})\cdot\mathbf{n}\|_{W_r^{\tau+1-1/r}(\partial\Omega)} \\ &\leq \|\mathbf{f}\|_{\mathbf{W}_r^{\tau+1-1/r}(\partial\Omega)} + \|\mathbf{g}\cdot\mathbf{n}\|_{W_r^{\tau+1-1/r}(\partial\Omega)}, \end{aligned}$$

where we have used the standard trace theorem for Sobolev spaces, see [57, Theorem 8.7]. From (3.9), we see that

$$\begin{aligned} \|\mathbf{u}\|_{\mathbf{W}_r^{\tau+1}(\Omega)} &\leq \|\mathbf{f}\|_{\mathbf{W}_r^{\tau+1}(\Omega)} + \|K\nabla p\|_{\mathbf{W}_r^{\tau+1}(\Omega)} \\ &\leq \|\mathbf{f}\|_{\mathbf{W}_r^{\tau+1}(\Omega)} + c\|p\|_{W_r^{\tau+2}(\Omega)/\mathbb{R}}. \end{aligned}$$

This all, together with proposition 3.1, gives

$$\begin{aligned} \|\mathbf{u}\|_{\mathbf{W}_r^{\tau+1}(\Omega)} + \|p\|_{W_r^{\tau+2}(\Omega)/\mathbb{R}} &\leq \|\mathbf{f}\|_{\mathbf{W}_r^{\tau+1}(\Omega)} + c\|p\|_{W_r^{\tau+2}(\Omega)/\mathbb{R}} \\ &\leq c \left( \|\mathbf{f}\|_{\mathbf{W}_r^{\tau+1}(\Omega)} + \|\mathbf{g}\cdot\mathbf{n}\|_{W_r^{\tau+1-1/r}(\partial\Omega)} \right), \end{aligned}$$

which is the desired estimate. □

Darcy's problem is well-posed, if only the normal velocity is prescribed at the boundary $\partial\Omega$. This can be concluded from the equivalence to the elliptic Neumann problem (3.7) and (3.8) which is well-posed. Therefore a unique solution of Darcy's problem exists. However, the pressure can only be unique up to an additive constant.

## 3.6. Applications and Restrictions

Darcy's law is widely used for almost all situations involving motion of fluid through soil or rock in the natural environment [24]. It can also be applied to describe the creeping flow of a Newtonian fluid in porous media [6]. In ground water hydrology Darcy's problem is used to model and predict the ground water flow in aquifers. Unfortunately there are some restrictions when Darcy's law models the reality.

Firstly, Darcy's law fails for turbulent flow. It can only be applied if the Reynolds number for porous media, based on the average grain diameter, does not exceed 1-10, cf. [6]. Moreover, for very high flow in very permeable material, Darcy's law has been found to be invalid. Darcy's law may also fail if other forces have significant influence; for instance acceleration can cause invalid results.

In a granular material, for instance sand, Darcy's law is very reliable. It also models flow in non-granular materials like clay, limestone, sandstone, and fractured crystalline well. However, there are some restrictions on the material. Darcy's law implies that even a very small hydraulic gradient causes motion of the fluid. In some clays it has been observed that below some threshold value, a small hydraulic gradient does not lead to fluid motion. Nevertheless, in the case of unsaturated soils, Darcy's law has been found to be valid.

To find the permeability of a medium, gas flow at low pressure is often used. This can be modelled with Darcy's law. Note that in this case the flow of gas is faster than one can predict by using Darcy's law. However, this is a well-known phenomenon in fluid mechanics.

In the particular form of $K = const \cdot I$, which refers to isotropic and homogeneous material, Darcy's law also plays an important role in projection methods for discretizing the Navier-Stokes equations for incompressible Newtonian fluids [45]. For the projection method, the Navier-Stokes equations are split into two problems. Darcy's problem with $\mathbf{f} = \mathbf{0}$ and $\mathbf{g} = 0$ is one of them. Both problems are solved in an iterative alternating scheme to approximate the solution.

Furthermore, coupled free-flow and porous media flow is an important application of Darcy's problem since they appear often in the nature [50]. For example river beds are usually porous media and the flow in the river and in the ground interact.

# 4. Reproducing Kernel Hilbert Spaces

Before we can establish the approximation scheme for Darcy's problem, we need to discuss reproducing kernel Hilbert spaces in detail. These spaces provide the technical tools required to establish the approximation scheme. Furthermore, these spaces and their properties are essential in the error analysis.

We will start with the definition of matrix-valued reproducing kernel Hilbert spaces and prove some general properties. After this, we introduce specific reproducing kernel Hilbert spaces. Those spaces are Sobolev or Sobolev-like spaces, which are equipped with a reproducing kernel.

Native spaces are reproducing kernel Hilbert spaces, which are constructed from a kernel. Besides their definition, we study the relation between them and certain Sobolev spaces. This includes in particular the native spaces of the divergence-free and the curl-free matrix-valued kernels.

## 4.1. Hilbert Spaces with Matrix-valued Reproducing Kernels

We now give a partial survey of reproducing kernel Hilbert spaces. First of all, we will give their definition and main properties. Then we have a look at certain examples.

### 4.1.1. Definition and Properties

Let $\Omega \subseteq \mathbb{R}^d$ be non-empty. The following definition is taken from [20]. It is a generalisation of the usual scalar-valued version, cf. [54, Definition 10.1].

**Definition 4.1.** *Let* $\mathbf{H}$ *be a Hilbert space of vector-valued functions* $\mathbf{f} : \Omega \to \mathbb{R}^n$. *A continuous* $n \times n$ *matrix-valued kernel* $\mathbf{\Phi}$ *is called a* reproducing kernel *for* $\mathbf{H}$ *if for all* $\mathbf{x} \in \Omega$ *and* $\boldsymbol{\alpha} \in \mathbb{R}^n$ *we have*

*(1)* $\mathbf{\Phi}(\cdot, \mathbf{x})\boldsymbol{\alpha} \in \mathbf{H}$,

*(2)* $\boldsymbol{\alpha}^T \mathbf{f}(\mathbf{x}) = (\mathbf{f}, \mathbf{\Phi}(\cdot, \mathbf{x})\boldsymbol{\alpha})_{\mathbf{H}}$.

The following result is a vector-valued version of theorem 10.2 in [54]. The proof follows from the proof of the scalar-valued case.

**Theorem 4.2.** *Suppose that* $\mathbf{H}$ *is a Hilbert space of vector-valued functions* $\mathbf{f} : \Omega \to \mathbb{R}^n$. *Then the following statements are equivalent:*

*(1) the point evaluation functionals are continuous, i. e.* $\boldsymbol{\alpha}^T \delta_{\mathbf{x}} \in \mathbf{H}^*$ *for all* $\mathbf{x} \in \Omega$ *and* $\boldsymbol{\alpha} \in \mathbb{R}^n$*;*

*(2)* $\mathbf{H}$ *has a reproducing kernel.*

*Proof.* Suppose that the point evaluation functionals $\boldsymbol{\alpha}^T \delta_{\mathbf{x}}$ are continuous. Then $\lambda_j := \mathbf{e}_j^T \delta_{\mathbf{x}}$, $1 \leq j \leq n$, is an element of $\mathbf{H}^*$. Riesz' representation theorem gives that we can find for every $\mathbf{x} \in \Omega$, a $\boldsymbol{\Phi}_j(\cdot, \mathbf{x}) : \Omega \to \mathbb{R}^n$ such that $\mathbf{e}_j^T \delta_{\mathbf{x}}(\mathbf{f}) = (\mathbf{f}, \boldsymbol{\Phi}_j(\cdot, \mathbf{x}))_{\mathbf{H}}$ for all $\mathbf{f} \in \mathbf{H}$, cf. theorem 1.12 in [2].

Let $\boldsymbol{\alpha} \in \mathbb{R}^n$ and $\lambda = \boldsymbol{\alpha}^T \delta_{\mathbf{x}}$. With $\boldsymbol{\alpha} = \sum_{j=1}^n \alpha_j \mathbf{e}_j$ we have $\lambda = \sum_{j=1}^n \alpha_j \lambda_j$. Then,

$$\lambda(\mathbf{f}) = \sum_{j=1}^n \alpha_j \lambda_j(\mathbf{f}) = \sum_{j=1}^n \alpha_j (\mathbf{f}, \boldsymbol{\Phi}_j(\cdot, \mathbf{x}))_{\mathbf{H}} = \left( \mathbf{f}, \sum_{j=1}^n \alpha_j \boldsymbol{\Phi}_j(\cdot, \mathbf{x}) \right)_{\mathbf{H}},$$

but also $\lambda(\mathbf{f}) = (\mathbf{f}, \mathbf{g}_\lambda)_{\mathbf{H}}$. Due to the uniqueness of the Riesz representer we can conclude $\mathbf{g}_\lambda = \sum_{j=1}^n \alpha_j \boldsymbol{\Phi}_j(\cdot, \mathbf{x})$, thus $\mathbf{g}_\lambda = \boldsymbol{\Phi}(\cdot, \mathbf{x})\boldsymbol{\alpha}$. Therefore the conditions of definition 4.1 are satisfied and $\boldsymbol{\Phi}$ is the reproducing kernel.

Now, suppose that $\mathbf{H}$ has a reproducing kernel $\boldsymbol{\Phi}$. This means that

$$\boldsymbol{\alpha}^T \delta_{\mathbf{x}}(\mathbf{f}) = \boldsymbol{\alpha}^T \mathbf{f}(\mathbf{x}) = (\mathbf{f}, \boldsymbol{\Phi}(\cdot, \mathbf{x})\boldsymbol{\alpha})_{\mathbf{H}}$$

for all $\mathbf{x} \in \Omega$. Cauchy-Schwarz and the continuity of $\boldsymbol{\Phi}$ yield that

$$\begin{aligned}
|\boldsymbol{\alpha}^T \delta_{\mathbf{x}} - \boldsymbol{\alpha}^T \delta_{\mathbf{y}}| &= \sup_{\|\mathbf{f}\|_{\mathbf{H}}=1} |(\boldsymbol{\alpha}^T \delta_{\mathbf{x}} - \boldsymbol{\alpha}^T \delta_{\mathbf{y}})(\mathbf{f})| \\
&= \sup_{\|\mathbf{f}\|_{\mathbf{H}}=1} |(\mathbf{f}, \boldsymbol{\Phi}(\cdot, \mathbf{x})\boldsymbol{\alpha})_{\mathbf{H}} - (\mathbf{f}, \boldsymbol{\Phi}(\cdot, \mathbf{y})\boldsymbol{\alpha})_{\mathbf{H}}| \\
&= \sup_{\|\mathbf{f}\|_{\mathbf{H}}=1} |(\mathbf{f}, \boldsymbol{\Phi}(\cdot, \mathbf{x})\boldsymbol{\alpha} - \boldsymbol{\Phi}(\cdot, \mathbf{y})\boldsymbol{\alpha})_{\mathbf{H}}| \\
&\leq \|\boldsymbol{\Phi}(\cdot, \mathbf{x})\boldsymbol{\alpha} - \boldsymbol{\Phi}(\cdot, \mathbf{y})\boldsymbol{\alpha}\|_{\mathbf{H}} \\
&= \left( \|\boldsymbol{\Phi}(\cdot, \mathbf{x})\boldsymbol{\alpha}\|_{\mathbf{H}}^2 - 2(\boldsymbol{\Phi}(\cdot, \mathbf{x})\boldsymbol{\alpha}, \boldsymbol{\Phi}(\cdot, \mathbf{y})\boldsymbol{\alpha})_{\mathbf{H}} + \|\boldsymbol{\Phi}(\cdot, \mathbf{y})\boldsymbol{\alpha}\|_{\mathbf{H}}^2 \right)^{1/2} \\
&= \left( \boldsymbol{\alpha}^T \boldsymbol{\Phi}(\mathbf{x}, \mathbf{x})\boldsymbol{\alpha} - 2\boldsymbol{\alpha}^T \boldsymbol{\Phi}(\mathbf{x}, \mathbf{y})\boldsymbol{\alpha} + \boldsymbol{\alpha}^T \boldsymbol{\Phi}(\mathbf{y}, \mathbf{y})\boldsymbol{\alpha} \right)^{1/2}
\end{aligned}$$

goes to zero if $\mathbf{x}$ goes to $\mathbf{y}$. Hence $\boldsymbol{\alpha}^T \delta_{\mathbf{x}}$ is continuous in $\mathbf{x}$. □

The following theorem gives the Riesz representer of a functional $\lambda \in \mathbf{H}^*$, where $\mathbf{H}$ is a vector-valued reproducing kernel Hilbert space of functions. It is the extension of theorem

16.7 in [54] to vector-valued spaces. The scalar case can be recovered if one chooses $\alpha := 1$ and thinks about the kernel as a $1 \times 1$-matrix.

**Theorem 4.3.** *Suppose that* $\mathbf{H}$ *is a real, vector-valued Hilbert space of functions with reproducing matrix-valued kernel* $\mathbf{\Phi} : \Omega \times \Omega \to \mathbb{R}^{n \times n}$*, where* $\Omega \subseteq \mathbb{R}^d$ *is non empty. Let* $\lambda$ *be an element of the dual space* $\mathbf{H}^*$*. Then* $\lambda^{\mathbf{y}}(\mathbf{\Phi}(\cdot, \mathbf{y})\boldsymbol{\alpha}) \in \mathbf{H}$ *and*

$$\lambda(\mathbf{f}) = (\mathbf{f}, \lambda^{\mathbf{y}}(\mathbf{\Phi}(\cdot, \mathbf{y})\boldsymbol{\alpha}))_{\mathbf{H}} \tag{4.1}$$

*for all* $\mathbf{f} \in \mathbf{H}$ *and all* $\boldsymbol{\alpha} \in \mathbb{R}^n$*. Moreover,*

$$\|\lambda\|_{\mathbf{H}^*} = \|\lambda^{\mathbf{y}}(\mathbf{\Phi}(\cdot, \mathbf{y})\boldsymbol{\alpha})\|_{\mathbf{H}}. \tag{4.2}$$

*Proof.* Riesz' representation theorem guarantees the existence of a $\mathbf{g}_\lambda \in \mathbf{H}$ such that $(\mathbf{f}, \mathbf{g}_\lambda)_{\mathbf{H}} = \lambda(\mathbf{f})$ for all $\mathbf{f} \in \mathbf{H}$. Since $\mathbf{f}_{\mathbf{x}} := \mathbf{\Phi}(\cdot, \mathbf{x})\boldsymbol{\alpha}$ is an element of $\mathbf{H}$, using the reproducing property of the kernel, we see that

$$\lambda(\mathbf{f}_{\mathbf{x}}) = (\mathbf{f}_{\mathbf{x}}, \mathbf{g}_\lambda)_{\mathbf{H}} = (\mathbf{g}_\lambda, \mathbf{f}_{\mathbf{x}})_{\mathbf{H}} = (\mathbf{g}_\lambda, \mathbf{\Phi}(\cdot, \mathbf{x})\boldsymbol{\alpha})_{\mathbf{H}} = \boldsymbol{\alpha}^T \mathbf{g}_\lambda(\mathbf{x}).$$

Since $\mathbf{x}$ is arbitrary and $\lambda^{\mathbf{y}}(\mathbf{\Phi}(\cdot, \mathbf{y})\boldsymbol{\alpha}) = \boldsymbol{\alpha}^T \mathbf{g}_\lambda$, we obtain $\lambda^{\mathbf{y}}(\mathbf{\Phi}(\cdot, \mathbf{y})\boldsymbol{\alpha}) \in \mathbf{H}$, i. e. (4.1) holds.

We define $\mathbf{g}_\lambda(\mathbf{x})$ such that its $i$th component is $\lambda^{\mathbf{y}}(\mathbf{\Phi}(\cdot, \mathbf{y})\mathbf{e}_i)$, where $\mathbf{e}_i$ is the $i$th unit vector.

Note that (4.2) can be directly concluded from Riesz' representation theorem. However, we will show it for the convenience of the reader.

The definition of the norm in the dual space in combination with the first property and the Cauchy Schwarz inequality gives

$$\|\lambda\|_{\mathbf{H}^*} = \sup_{\mathbf{f} \in \mathbf{H}} \frac{|\lambda(\mathbf{f})|}{\|\mathbf{f}\|_{\mathbf{H}}} = \sup_{\mathbf{f} \in \mathbf{H}} \frac{|(\mathbf{f}, \mathbf{g}_\lambda)_{\mathbf{H}}|}{\|\mathbf{f}\|_{\mathbf{H}}} \leq \sup_{\mathbf{f} \in \mathbf{H}} \frac{\|\mathbf{f}\|_{\mathbf{H}} \|\mathbf{g}_\lambda\|_{\mathbf{H}}}{\|\mathbf{f}\|_{\mathbf{H}}} = \|\mathbf{g}_\lambda\|_{\mathbf{H}},$$

but also

$$\sup_{\mathbf{f} \in \mathbf{H}} \frac{|\lambda(\mathbf{f})|}{\|\mathbf{f}\|_{\mathbf{H}}} \geq \frac{|\lambda(\mathbf{g}_\lambda)|}{\|\mathbf{g}_\lambda\|_{\mathbf{H}}} = \|\mathbf{g}_\lambda\|_{\mathbf{H}}.$$

Thus $\|\lambda\|_{\mathbf{H}^*} = \|\mathbf{g}_\lambda\|_{\mathbf{H}}$ and the Riesz representer for the functional $\lambda$ is given by $\mathbf{g}_\lambda(\mathbf{x})$. □

We will denote the reproducing kernel Hilbert space with reproducing kernel $\phi$ or $\mathbf{\Phi}$ also by $H_\phi(\mathbb{R}^d)$ or $\mathbf{H}_{\mathbf{\Phi}}(\mathbb{R}^d)$ respectively.

### 4.1.2. Examples

Some Sobolev spaces can be interpreted as reproducing kernel Hilbert spaces. We will present these characterisations and introduce the related Sobolev-like space $\widetilde{\mathbf{H}}^\tau(\mathbb{R}^d)$ and its divergence-free and curl-free subspaces. Furthermore, we will study the properties of the introduced spaces. Note that all kernels in this section are translation invariant.

#### The Space $H^s(\mathbb{R}^d)$

An alternative definition to the one in section 2.2.2 of Sobolev spaces on $\mathbb{R}^d$ uses the Fourier transform. It can be shown that

$$H^s(\mathbb{R}^d) = \left\{ f \in L_2(\mathbb{R}^d) \ : \ \widehat{f}(\cdot)(1 + \|\cdot\|_2^2)^{s/2} \in L_2(\mathbb{R}^d) \right\},$$

with the inner product

$$(f, g)_{H^s(\mathbb{R}^d)} = (2\pi)^{-d/2} \int_{\mathbb{R}^d} \widehat{f}(\boldsymbol{\omega}) \overline{\widehat{g}(\boldsymbol{\omega})} (1 + \|\boldsymbol{\omega}\|_2^2)^s d\boldsymbol{\omega}.$$

Let $s > d/2$, then this space is a subset of $C(\mathbb{R}^d)$, cf. corollary 2.1. Furthermore, it can be interpreted as the space

$$H_{\mathcal{K}^s}(\mathbb{R}^d) := \left\{ f \in L_2(\mathbb{R}^d) : \int_{\mathbb{R}^d} \frac{|\widehat{f}(\boldsymbol{\omega})|^2}{\widehat{\mathcal{K}^s}(\boldsymbol{\omega})} d\boldsymbol{\omega} < \infty \right\},$$

where $\mathcal{K}^s$ is defined by its Fourier transform $\widehat{\mathcal{K}^s}(\boldsymbol{\omega}) := (1 + \|\boldsymbol{\omega}\|_2^2)^{-s}$.

**Proposition 4.4.** *Let $s > d/2$. Then $\widehat{\mathcal{K}^s}$ is integrable.*

*Proof.* If $f$ is radial, continuous and integrable, then

$$\int_{\mathbb{R}^d} f(\mathbf{x}) d\mathbf{x} = \int_0^\infty \left( \int_{\partial B(\mathbf{0}, r)} \widetilde{f}(r) dS \right) dr = c_d \int_0^\infty r^{d-1} \widetilde{f}(r) dr,$$

cf. theorem 4 in [12, Appendix C3]. The integral of $(1+r^2)^{-s} r^{d-1}$ over a bounded domain is finite. Since $s > d/2$ we have

$$\int_1^\infty (1 + r^2)^{-s} r^{d-1} dr \leq c \int_1^\infty r^{-2s} r^{d-1} dr = c \int_1^\infty r^{d-2s-1} = c \left[ r^{-2s+d} \right]_1^\infty < \infty.$$

Therefore we can deduce that

$$\|\widehat{\mathcal{K}^s}\|_{L_1(\mathbb{R}^d)} = \int_{\mathbb{R}^d} |(1 + \|\boldsymbol{\omega}\|_2^2)^{-s}| d\boldsymbol{\omega} = c_d \int_0^\infty (1 + r^2)^{-s} r^{d-1} dr < \infty,$$

i. e. the Fourier transform of $\widehat{\mathcal{K}^s}$ exists. □

In [54, Theorem 6.13] it has been proven that $\widehat{\mathcal{K}^s}$ is positive definite and the inverse Fourier transform is given by

$$\mathcal{K}^s(\mathbf{x}) := c_s \|\mathbf{x}\|_2^{s-d/2} K_{d/2-s}(\|\mathbf{x}\|_2), \tag{4.3}$$

where $c_s = \frac{2^{1-s}}{\Gamma(s)}$ is a positive constant and $K_\nu$ is the modified Bessel function, see section 2.4.3. The function $\widehat{\mathcal{K}^s}$ is positive, radial and continuous, i. e. $\widehat{\widehat{\mathcal{K}^s}} = \mathcal{K}^s$ is integrable, cf. corollary 2.8. Therefore we can apply [54, Theorem 10.12] to conclude that $H_{\mathcal{K}^s}(\mathbb{R}^d) = H^s(\mathbb{R}^d)$ is indeed a reproducing kernel Hilbert space with reproducing function $\mathcal{K}^s(\cdot - \mathbf{x})$.

### The Spaces $\mathbf{H}^\tau(\mathbb{R}^d)$, $\mathbf{H}^\tau(\mathbb{R}^d; \mathrm{div})$ and $\mathbf{H}^\tau(\mathbb{R}^d; \mathrm{curl})$

Let $\tau > d/2$. With the definition of $H^\tau(\mathbb{R}^d)$, we can define the vector-valued Sobolev space $\mathbf{H}^\tau(\mathbb{R}^d)$ as the tensor-product space $(H^\tau(\mathbb{R}^d))^d$ equipped with the inner product

$$(\mathbf{f}, \mathbf{g})_{\mathbf{H}^\tau(\mathbb{R}^d)} := \sum_{j=1}^{d} (f_j, g_j)_{H^\tau(\mathbb{R}^d)} = (2\pi)^{-d/2} \int_{\mathbb{R}^d} \widehat{\mathbf{g}}(\boldsymbol{\omega})^* \widehat{\mathbf{f}}(\boldsymbol{\omega}) (1 + \|\boldsymbol{\omega}\|_2^2)^\tau d\boldsymbol{\omega}.$$

This means that this space is a Hilbert space with reproducing kernel $\mathcal{K}^\tau I$, and we can denote it by

$$\mathbf{H}^\tau(\mathbb{R}^d) = \left\{ \mathbf{f} \in \mathbf{L}_2(\mathbb{R}^d) : \int_{\mathbb{R}^d} \|\widehat{\mathbf{f}}(\boldsymbol{\omega})\|_2^2 (1 + \|\boldsymbol{\omega}\|_2^2)^\tau d\boldsymbol{\omega} < \infty \right\}.$$

We are interested in two subspaces of $\mathbf{H}^\tau(\mathbb{R}^d)$: The subspace of the divergence-free functions and the subspace of the curl-free functions. They are defined via

$$\begin{aligned}
\mathbf{H}^\tau(\mathbb{R}^d; \mathrm{div}) &:= \left\{ \mathbf{f} \in \mathbf{H}^\tau(\mathbb{R}^d) : \nabla \cdot \mathbf{f} = 0 \right\}, \\
\mathbf{H}^\tau(\mathbb{R}^d; \mathrm{curl}) &:= \left\{ \mathbf{f} \in \mathbf{H}^\tau(\mathbb{R}^d) : \text{ There exists } g \in \mathbf{H}^{\tau+1}(\mathbb{R}^d)/\mathbb{R} \text{ such that } \mathbf{f} = \nabla g \right\}.
\end{aligned}$$

Both spaces are equipped with the inner product of the space $\mathbf{H}^\tau(\mathbb{R}^d)$, so we will denote the norm in both spaces by $\|\mathbf{f}\|_{\mathbf{H}^\tau(\mathbb{R}^d)}$, where $\mathbf{f}$ is divergence-free or curl-free respectively. This should cause no confusion.

### The Space $\widetilde{\mathbf{H}}^\tau(\mathbb{R}^d)$

Let $\tau > d/2$. Then we define the space

$$\widetilde{\mathbf{H}}^\tau(\mathbb{R}^d) := \left\{ \mathbf{f} \in \mathbf{L}_2(\mathbb{R}^d) : \int_{\mathbb{R}^d} \frac{\|\widehat{\mathbf{f}}(\boldsymbol{\omega})\|_2^2}{\|\boldsymbol{\omega}\|_2^2} (1 + \|\boldsymbol{\omega}\|_2^2)^{\tau+1} d\boldsymbol{\omega} < \infty \right\}$$

equipped with the inner product

$$(\mathbf{f}, \mathbf{g})_{\widetilde{\mathbf{H}}^\tau(\mathbb{R}^d)} = (2\pi)^{-d/2} \int_{\mathbb{R}^d} \frac{\widehat{\mathbf{g}}(\boldsymbol{\omega})^* \widehat{\mathbf{f}}(\boldsymbol{\omega})}{\|\boldsymbol{\omega}\|_2^2} (1 + \|\boldsymbol{\omega}\|_2^2)^{\tau+1} d\boldsymbol{\omega}.$$

**Proposition 4.5.** *Let $\tau > d/2$. Then the Sobolev-like space $\widetilde{\mathbf{H}}^\tau(\mathbb{R}^d)$ is a Hilbert space with reproducing function $\psi = -\Delta \mathcal{K}^{\tau+1}$. Furthermore, the space $\widetilde{\mathbf{H}}^\tau(\mathbb{R}^d)$ is a subset of $\mathbf{H}^\tau(\mathbb{R}^d)$.*

*Proof.* The space $\widetilde{\mathbf{H}}^\tau(\mathbb{R}^d)$ is identical to the space $\mathbf{H}_\psi(\mathbb{R}^d) = (H_\psi(\mathbb{R}^d))^n$, where $\psi = -\Delta \mathcal{K}^{\tau+1}$ and

$$H_\psi(\mathbb{R}^d) := \left\{ f \in L_2(\mathbb{R}^d) \, : \, \frac{\widehat{f}}{\sqrt{\widehat{\psi}}} \in L_2(\mathbb{R}^d) \right\}.$$

Therefore it is a reproducing kernel Hilbert space if $\psi$ is positive definite and if all functions $\mathbf{f} \in \mathbf{H}_\psi(\mathbb{R}^d)$ are continuous, cf. [54, Theorem 10.12].

The kernel $\mathcal{K}^{\tau+1}$ is two times differentiable, since the Bessel function $K_{d/2-(\tau+1)}$ is. We have with proposition 2.9 that $\psi$ is indeed positive definite provided its Fourier transform $\widehat{\psi}(\boldsymbol{\omega}) = \|\boldsymbol{\omega}\|_2^2 (1 + \|\boldsymbol{\omega}\|_2^2)^{-(\tau+1)}$ is integrable. Since $\tau > d/2$, this can be shown with a similar argumentation as in the proof of proposition 4.4.

For every element $\mathbf{f} \in \widetilde{\mathbf{H}}^\tau(\mathbb{R}^d)$ we have that $\mathbf{f} \in \mathbf{H}^\tau(\mathbb{R}^d)$, since $\mathbf{f} \in \mathbf{L}_2(\mathbb{R}^d)$ and

$$\begin{aligned}
\|\mathbf{f}\|_{\mathbf{H}^\tau(\mathbb{R}^d)}^2 &= (2\pi)^{-d/2} \int_{\mathbb{R}^d} \|\widehat{\mathbf{f}}(\boldsymbol{\omega})\|_2^2 (1 + \|\boldsymbol{\omega}\|_2^2)^\tau d\boldsymbol{\omega} \\
&\leq (2\pi)^{-d/2} \int_{\mathbb{R}^d} \left(1 + \frac{1}{\|\boldsymbol{\omega}\|_2^2}\right) \|\widehat{\mathbf{f}}(\boldsymbol{\omega})\|_2^2 (1 + \|\boldsymbol{\omega}\|_2^2)^\tau d\boldsymbol{\omega} \\
&= (2\pi)^{-d/2} \int_{\mathbb{R}^d} \frac{1 + \|\boldsymbol{\omega}\|_2^2}{\|\boldsymbol{\omega}\|_2^2} \|\widehat{\mathbf{f}}(\boldsymbol{\omega})\|_2^2 (1 + \|\boldsymbol{\omega}\|_2^2)^\tau d\boldsymbol{\omega} \\
&= (2\pi)^{-d/2} \int_{\mathbb{R}^d} \frac{\|\widehat{\mathbf{f}}(\boldsymbol{\omega})\|_2^2}{\|\boldsymbol{\omega}\|_2^2} (1 + \|\boldsymbol{\omega}\|_2^2)^{\tau+1} d\boldsymbol{\omega} \\
&= \|\mathbf{f}\|_{\widetilde{\mathbf{H}}^\tau(\mathbb{R}^d)}^2 < \infty.
\end{aligned}$$

Thus $\widetilde{\mathbf{H}}^\tau(\mathbb{R}^d)$ is a subset of $\mathbf{H}^\tau(\mathbb{R}^d)$ and therefore all $\mathbf{f} \in \widetilde{\mathbf{H}}^\tau(\mathbb{R}^d)$ are also continuous. □

**The Space $\widetilde{\mathbf{H}}^\tau(\mathbb{R}^d;\mathrm{div})$**

The space $\widetilde{\mathbf{H}}^\tau(\mathbb{R}^d;\mathrm{div})$ is the subspace of the divergence-free functions of $\widetilde{\mathbf{H}}^\tau(\mathbb{R}^d)$, i. e.

$$\widetilde{\mathbf{H}}^\tau(\mathbb{R}^d;\mathrm{div}) := \left\{\mathbf{f}\in\widetilde{\mathbf{H}}^\tau(\mathbb{R}^d) : \nabla\cdot\mathbf{f}=0\right\}\subseteq\mathbf{H}^\tau(\mathbb{R}^d;\mathrm{div})$$

equipped with the inner product $(\mathbf{f},\mathbf{g})_{\widetilde{\mathbf{H}}^\tau(\mathbb{R}^d;\mathrm{div})} := (\mathbf{f},\mathbf{g})_{\widetilde{\mathbf{H}}^\tau(\mathbb{R}^d)}$. Like $\widetilde{\mathbf{H}}^\tau(\mathbb{R}^d)$ it can be characterised as a reproducing kernel Hilbert space if $\tau > d/2$. The kernel $\widetilde{\mathcal{K}}^\tau_{\mathrm{div}}$ is then defined by its Fourier transform

$$\widehat{\widetilde{\mathcal{K}}^\tau_{\mathrm{div}}}(\boldsymbol{\omega}) = \left(\|\boldsymbol{\omega}\|_2^2 I - \boldsymbol{\omega}\boldsymbol{\omega}^T\right)(1+\|\boldsymbol{\omega}\|_2^2)^{-(\tau+1)}.$$

The inverse Fourier transform of $(1+\|\boldsymbol{\omega}\|_2^2)^{-(\tau+1)}$ is given by $\mathcal{K}^{\tau+1}$, see above. Lemma 2.13 establishes that the kernel is positive definite and integrable, since $\mathcal{K}^{\tau+1}\in C^2(\mathbb{R}^d)\cap W_1^2(\mathbb{R}^d)$. We can rewrite the kernel with (4.3) such that it becomes

$$\begin{aligned}\widetilde{\mathcal{K}}^\tau_{\mathrm{div}}(\mathbf{x}) &= c_{\tau+1}\left(-\Delta I+\nabla\nabla^T\right)\|\mathbf{x}\|_2^{\tau+1-d/2}K_{\tau+1-d/2}(\|\mathbf{x}\|_2)\\ &= \left(-\Delta I+\nabla\nabla^T\right)\mathcal{K}^{\tau+1}(\|\mathbf{x}\|_2).\end{aligned}$$

We now study the properties of the kernel $\widetilde{\mathcal{K}}^\tau_{\mathrm{div}}$ and the matrix $(A_{X,\widetilde{\mathcal{K}}^\tau_{\mathrm{div}}})_{ij} := \widetilde{\mathcal{K}}^\tau_{\mathrm{div}}(\mathbf{x}_i-\mathbf{x}_j)$. These properties are of importance for the error analysis for target functions outside the native space.

**Stability of $A_{X,\widetilde{\mathcal{K}}^\tau_{\mathrm{div}}}$** The following result gives a bound for the smallest eigenvalue, it is taken from [18]. It generalises [54, Theorem 12.3] to the matrix-valued kernel $\boldsymbol{\Phi}_{\mathrm{div}}$.

**Theorem 4.6.** *Let $X\subseteq\mathbb{R}^d$ be a discrete set of pair-wise distinct points. Let $\phi$ be an even and positive definite function, which possesses a positive Fourier transform $\widehat{\phi}\in C(\mathbb{R}^d\backslash\mathbf{0})$. A lower bound for the smallest eigenvalue $\lambda_{\min}$ of the matrix $A_{X,\boldsymbol{\Phi}_{\mathrm{div}}}$ is given by*

$$\lambda_{\min}(A_{X,\boldsymbol{\Phi}_{\mathrm{div}}}) \geq \left(\frac{\sigma^2}{16\pi}\right)^{(d+2)/2}\frac{M(\sigma)\pi}{(4\pi)^d\Gamma((d+2)/2)} \tag{4.4}$$

*for any $\sigma>0$ satisfying*

$$\sigma\geq\frac{\widetilde{C}}{q_X},\qquad \widetilde{C} := 24\left(\frac{\pi(d+2)(d+3)d}{4(d-1)}\Gamma^2\left(\frac{d+2}{2}\right)\right)^{1/(d+1)}, \tag{4.5}$$

*where $M(\sigma) := \inf_{\|\boldsymbol{\omega}\|_2\leq\sigma}\widehat{\phi}(\boldsymbol{\omega})$, $q_X$ is the separation radius and $\Gamma$ is the Gamma function.*

We now look at the specific case that the kernel is $\widetilde{\mathcal{K}}^\tau_{\mathrm{div}}$.

**Proposition 4.7.** *Let $X \subseteq \mathbb{R}^d$ be a discrete set of pair-wise distinct points. The lower bound of the smallest eigenvalue of $A_{X,\widetilde{\mathcal{K}}^\tau_{\mathrm{div}}}$ is given by*

$$\lambda_{\min}(A_{X,\widetilde{\mathcal{K}}^\tau_{\mathrm{div}}}) \geq c_d q_X^{d-2\tau},$$

*where $c_d$ is a constant depending on $d$ and $q_X$ is the separation radius.*

*Proof.* We can find a constant $c$ such that

$$\widehat{\mathcal{K}^{\tau+1}}(\boldsymbol{\omega}) = (1 + \|\boldsymbol{\omega}\|_2^2)^{-(\tau+1)} \geq c\|\boldsymbol{\omega}\|_2^{-2(\tau+1)},$$

for a sufficiently large $\|\boldsymbol{\omega}\|_2$, i. e.

$$M(\sigma) = \inf_{\|\boldsymbol{\omega}\|_2 \leq \sigma} \widehat{\mathcal{K}^{\tau+1}}(\boldsymbol{\omega}) \geq c \inf_{\|\boldsymbol{\omega}\|_2 \leq \sigma} \|\boldsymbol{\omega}\|_2^{-2(\tau+1)} \geq c\sigma^{-2(\tau+1)}.$$

Therefore we can simplify (4.4) as follows

$$\begin{aligned}
\lambda_{\min}(A_{X,\widetilde{\mathcal{K}}^\tau_{\mathrm{curl}}}) &\geq \left(\frac{\sigma^2}{16\pi}\right)^{(d+2)/2} \frac{M(\sigma)\pi}{(4\pi)^d \Gamma(d+2)/2} \\
&\geq \left(\frac{\sigma^2}{16\pi}\right)^{(d+2)/2} \frac{c\sigma^{-2(\tau+1)}\pi}{(4\pi)^d \Gamma(d+2)/2} \\
&= \left(\frac{1}{16\pi}\right)^{(d+2)/2} \frac{c\sigma^{d-2\tau}\pi}{(4\pi)^d \Gamma(d+2)/2} \\
&= c_d \sigma^{d-2\tau} \\
&\geq c_d q_X^{2\tau-d}.
\end{aligned}$$

□

Due to their algebraic decay, this result also holds for Wendland functions, cf. [18].

**Eigenvalues of $\widetilde{\mathcal{K}}^\tau_{\mathrm{div}}$** We now rewrite the kernel to enable us to find the eigenvalues. Let $\nu := \tau + 1 - d/2$. For the matrix-valued kernel $\widetilde{\mathcal{K}}^\tau_{\mathrm{div}}(\mathbf{x})$ and with (2.5) and (2.6) we have

$$\begin{aligned}
\left(\widetilde{\mathcal{K}}^\tau_{\mathrm{div}}(\mathbf{x})\right)_{ii} &= -c_{\tau+1} \sum_{k=1,k\neq i}^{d} \partial_{kk} \|\mathbf{x}\|_2^\nu K_\nu(\|\mathbf{x}\|_2) \\
&= -c_{\tau+1} \sum_{k=1,k\neq i}^{d} \left[-\|\mathbf{x}\|_2^{\nu-1} K_{\nu-1}(\|\mathbf{x}\|_2) + x_k^2 \|\mathbf{x}\|_2^{\nu-2} K_{\nu-2}(\|\mathbf{x}\|_2)\right] \\
&= c_{\tau+1}(d-1)\|\mathbf{x}\|_2^{\nu-1} K_{\nu-1}(\|\mathbf{x}\|_2) - c_{\tau+1}\|\mathbf{x}\|_2^{\nu-2} K_{\nu-2}(\|\mathbf{x}\|_2) \sum_{k=1,k\neq i}^{d} x_k^2
\end{aligned}$$

and

$$\left(\widetilde{\mathcal{K}}^{\tau}_{\mathrm{div}}(\mathbf{x})\right)_{ij} = c_{\tau+1}\partial_{ij}\|\mathbf{x}\|_2^{\nu}K_{\nu}(\|\mathbf{x}\|_2) = c_{\tau+1}x_ix_j\|\mathbf{x}\|_2^{\nu-2}K_{\nu-2}(\|\mathbf{x}\|_2).$$

Hence we can write $\widetilde{\mathcal{K}}^{\tau}_{\mathrm{div}}$ as

$$\widetilde{\mathcal{K}}^{\tau}_{\mathrm{div}}(\mathbf{x}) = a(\mathbf{x})I + b(\mathbf{x})(-\|\mathbf{x}\|_2^2 I + \mathbf{x}\mathbf{x}^T)$$

with

$$\begin{aligned} a(\mathbf{x}) &:= c_{\tau+1}(d-1)\|\mathbf{x}\|_2^{\nu-1}K_{\nu-1}(\|\mathbf{x}\|_2), \\ b(\mathbf{x}) &:= c_{\tau+1}\|\mathbf{x}\|_2^{\nu-2}K_{\nu-2}(\|\mathbf{x}\|_2). \end{aligned}$$

The eigenvalues of a matrix $A$ are the roots of the polynomial $\det(A - \lambda I)$. Assume that $\lambda_1 = a(\mathbf{x}) - b(\mathbf{x})\|\mathbf{x}\|_2^2$, then

$$\det(\widetilde{\mathcal{K}}^{\tau}_{\mathrm{div}}(\mathbf{x}) - \lambda_1 I) = \det(-b(\mathbf{x})\mathbf{x}^T\mathbf{x}) = 0,$$

since $\mathbf{x}^T\mathbf{x}$ is a matrix of rank one. Thus $\lambda_1$ is indeed an eigenvalue. Similarly we can see that $\lambda_2 = a(\mathbf{x})$ is an eigenvalue; if $\mathbf{x} = \mathbf{0}$, then

$$\det(\widetilde{\mathcal{K}}^{\tau}_{\mathrm{div}}(\mathbf{0}) - \lambda_2 I) = \det(0 \cdot I) = 0.$$

If $\mathbf{x} \in \mathbb{R}^d \backslash \mathbf{0}$, then

$$\det(\widetilde{\mathcal{K}}^{\tau}_{\mathrm{div}}(\mathbf{x}) - \lambda_2 I) = \det(b(\mathbf{x})(\mathbf{x}^T\mathbf{x} - \|\mathbf{x}\|_2^2 I)) = \det\left(-b(\mathbf{x})\|\mathbf{x}\|_2^2\left(I - \frac{\mathbf{x}^T\mathbf{x}}{\|\mathbf{x}\|_2^2}\right)\right) = 0,$$

because a matrix $I + \mathbf{w}\mathbf{v}^T$ is singular if and only if $1 + \mathbf{v}^T\mathbf{w} = 0$, cf. [56, Lemma 2.14]. Therefore $\lambda_2$ is also an eigenvalue.

The eigenvalues are therefore $\lambda_1 = a(\mathbf{x}) - b(\mathbf{x})\|\mathbf{x}\|_2^2$ with multiplicity $d-1$ and $\lambda_2 = a(\mathbf{x})$ with multiplicity 1.

**Upper Bound for $\lambda(\widetilde{\mathcal{K}}^{\tau}_{\mathrm{div}})$** The absolute value of each eigenvalue is bounded by

$$\Lambda_{\mathrm{div}}(\mathbf{x}) := |a(\mathbf{x})| + \|\mathbf{x}\|_2^2|b(\mathbf{x})|.$$

Applying lemma 2.12 and defining $r := \|\mathbf{x}\|_2$ leads us to

$$\begin{aligned}\Lambda_{\mathrm{div}}(\mathbf{x}) &= |c_{\tau+1}(d-1)\|\mathbf{x}\|_2^{\nu-1}K_{\nu-1}(\|\mathbf{x}\|_2)| + \|\mathbf{x}\|_2^2|c_{\tau+1}\|\mathbf{x}\|_2^{\nu-2}K_{\nu-2}(\|\mathbf{x}\|_2)| \\ &= c_{\tau+1}(d-1)r^{\nu-1}K_{\nu-1}(r) + c_{\tau+1}r^{\nu}K_{\nu-2}(r) \\ &\leq c_{\tau+1}(d-1)r^{\nu-1-1/2}\sqrt{2\pi}e^{-r}e^{(\nu-1)^2/(2r)} + c_{\tau+1}r^{\nu-1/2}\sqrt{2\pi}e^{-r}e^{(\nu-2)^2/(2r)} \\ &= \widetilde{c}_\tau r^{\nu-3/2}e^{-r}\left((d-1)e^{(\nu-1)^2/(2r)} + re^{(\nu-2)^2/(2r)}\right),\end{aligned}$$

which bounds the eigenvalues.

### The Space $\widetilde{\mathbf{H}}^\tau(\mathbb{R}^d, \mathrm{curl})$

The subspace of the curl-free functions of $\widetilde{\mathbf{H}}^\tau(\mathbb{R}^d)$ and its kernel are essential for the error analysis for target functions outside the native space. Therefore we will study this space in more detail.

The space $\widetilde{\mathbf{H}}^\tau(\mathbb{R}^d; \mathrm{curl})$ is the subspace of the curl-free functions of $\widetilde{\mathbf{H}}^\tau(\mathbb{R}^d)$. It is defined by the application of the dimension-free definition of the curl, i. e.

$$\widetilde{\mathbf{H}}^\tau(\mathbb{R}^d; \mathrm{curl}) := \left\{\mathbf{f} \in \widetilde{\mathbf{H}}^\tau(\mathbb{R}^d) : \text{ There exists } g \in H^{\tau+1}(\mathbb{R}^d)/\mathbb{R} \text{ such that } \nabla g = \mathbf{f}\right\}$$

with the inner product $(\mathbf{f}, \mathbf{g})_{\widetilde{\mathbf{H}}^\tau(\mathbb{R}^d;\mathrm{curl})} := (\mathbf{f}, \mathbf{g})_{\widetilde{\mathbf{H}}^\tau(\mathbb{R}^d)}$.

Let $\tau > d/2$. Then the space $\widetilde{\mathbf{H}}^\tau(\mathbb{R}^d; \mathrm{curl})$ can be characterised as a reproducing kernel Hilbert space with reproducing kernel $\widetilde{\mathcal{K}}^\tau_{\mathrm{curl}}$. The kernel $\widetilde{\mathcal{K}}^\tau_{\mathrm{curl}}$ is then defined via its Fourier transform

$$\widehat{\widetilde{\mathcal{K}}^\tau_{\mathrm{curl}}}(\boldsymbol{\omega}) = \boldsymbol{\omega}\boldsymbol{\omega}^T(1 + \|\boldsymbol{\omega}\|_2^2)^{-(\tau+1)}. \tag{4.6}$$

Hence, like in the divergence-free case, we obtain, with lemma 2.16 and (4.3),

$$\mathcal{K}^\tau_{\mathrm{curl}}(\mathbf{x}) = -c_{\tau+1}\nabla\nabla^T\|\mathbf{x}\|_2^{\tau+1-d/2}K_{\tau+1-d/2}(\|\mathbf{x}\|_2) = -\nabla\nabla^T\mathcal{K}^{\tau+1},$$

which is a positive definite integrable kernel.

We will now give some properties of the kernel $\widetilde{\mathcal{K}}^\tau_{\mathrm{curl}}$ and the matrix $(A_{X,\widetilde{\mathcal{K}}^\tau_{\mathrm{curl}}})_{ij} = \widetilde{\mathcal{K}}^\tau_{\mathrm{curl}}(\mathbf{x}_i - \mathbf{x}_j)$. The following results are required for the error analysis.

**Stability of $A_{X,\widetilde{\mathcal{K}}^\tau_{\mathrm{curl}}}$** The following result gives a bound for the smallest eigenvalue, it is taken from [18]. It generalises [54, Theorem 12.3] to the matrix-valued kernel $\boldsymbol{\Phi}_{\mathrm{curl}}$.

**Theorem 4.8.** *Let $X \subseteq \mathbb{R}^d$ be a discrete set of pair-wise distinct points. Let $\phi$ be an even and positive definite function, which possesses a positive Fourier transform $\widehat{\phi} \in C(\mathbb{R}^d\backslash\mathbf{0})$.*

*A lower bound for the smallest eigenvalue* $\lambda_{\min}$ *of the matrix* $A_{X,\mathbf{\Phi}_{\text{curl}}}$ *is given by*

$$\lambda_{\min}(A_{X,\mathbf{\Phi}_{\text{curl}}}) \geq \left(\frac{\sigma^2}{16\pi}\right)^{(d+2)/2} \frac{M(\sigma)\pi}{(4\pi)^d \Gamma((d+2)/2)}$$

*for any* $\sigma > 0$ *satisfying*

$$\sigma \geq \frac{\widetilde{C}}{q_X}, \qquad \widetilde{C} := 24\left(\frac{\pi(d+2)(d+3)d}{4(d-1)}\Gamma^2\left(\frac{d+2}{2}\right)\right)^{1/(d+1)}, \tag{4.7}$$

*where* $M(\sigma) := \inf_{\|\boldsymbol{\omega}\|_2 \leq \sigma} \widehat{\phi}(\boldsymbol{\omega})$*,* $q_X$ *is the separation radius and* $\Gamma$ *is the Gamma function.*

Following the same argumentation as in the proof of proposition 4.7, we see that the lower bound of the smallest eigenvalue of $A_{X,\widetilde{\mathcal{K}}^\tau_{\text{curl}}}$ is given by

$$\lambda_{\min}(A_{X,\widetilde{\mathcal{K}}^\tau_{\text{curl}}}) \geq c_d q_X^{2\tau-d}, \tag{4.8}$$

where $c_d$ is a constant depending on $d$ and $q_X$ is the separation radius. This bound can also be shown for Wendland functions, cf. corollary 3 in [18].

**Eigenvalues of** $\widetilde{\mathcal{K}}^\tau_{\text{curl}}$ Let $\nu := \tau + 1 - d/2$. For the matrix-valued kernel $\widetilde{\mathcal{K}}^\tau_{\text{curl}}(\mathbf{x})$ and with (2.5) and (2.6) we have

$$\begin{aligned}\left(\widetilde{\mathcal{K}}^\tau_{\text{curl}}(\mathbf{x})\right)_{ii} &= -c_{\tau+1}\partial_{ii}\|\mathbf{x}\|_2^\nu K_\nu(\|\mathbf{x}\|_2) \\ &= -c_{\tau+1}x_i^2\|\mathbf{x}\|_2^{\nu-2}K_{\nu-2}(\|\mathbf{x}\|_2) + c_{\tau+1}\|\mathbf{x}\|_2^{\nu-1}K_{\nu-1}(\|\mathbf{x}\|_2)\end{aligned}$$

and

$$\left(\widetilde{\mathcal{K}}^\tau_{\text{curl}}(\mathbf{x})\right)_{ij} = -c_{\tau+1}\partial_{ij}\|\mathbf{x}\|_2^\nu K_\nu(\|\mathbf{x}\|_2) = -c_{\tau+1}x_i x_j\|\mathbf{x}\|_2^{\nu-2}K_{\nu-2}(\|\mathbf{x}\|_2).$$

Hence we can write $\widetilde{\mathcal{K}}^\tau_{\text{curl}}$ as

$$\widetilde{\mathcal{K}}^\tau_{\text{curl}}(\mathbf{x}) = a(\mathbf{x})I - b(\mathbf{x})\mathbf{x}\mathbf{x}^T \tag{4.9}$$

with

$$a(\mathbf{x}) := c_{\tau+1}\|\mathbf{x}\|_2^{\nu-1}K_{\nu-1}(\|\mathbf{x}\|_2), \tag{4.10}$$

$$b(\mathbf{x}) := c_{\tau+1}\|\mathbf{x}\|_2^{\nu-2}K_{\nu-2}(\|\mathbf{x}\|_2). \tag{4.11}$$

Analogous to the case of the divergence-free kernel, we find eigenvalues $\lambda_1 = a(\mathbf{x}) - b(\mathbf{x})\|\mathbf{x}\|_2^2$ with multiplicity 1 and $\lambda_2 = a(\mathbf{x})$ with multiplicity $d-1$.

**Upper Bound for $\lambda(\widetilde{\mathcal{K}}^{\tau}_{\mathrm{curl}})$** The absolute value of each eigenvalue is bounded by

$$\Lambda_{\mathrm{curl}}(\mathbf{x}) := |a(\mathbf{x})| + \|\mathbf{x}\|_2^2 |b(\mathbf{x})|.$$

Applying lemma 2.12 and defining $r = \|\mathbf{x}\|_2$ gives

$$\begin{aligned}
\Lambda_{\mathrm{curl}}(\mathbf{x}) &= |c_{\tau+1}\|\mathbf{x}\|_2^{\nu-1} K_{\nu-1}(\|\mathbf{x}\|_2)| + \|\mathbf{x}\|_2^2 |c_{\tau+1}\|\mathbf{x}\|_2^{\nu-2} K_{\nu-2}(\|\mathbf{x}\|_2)| \\
&= c_{\tau+1} r^{\nu-1} K_{\nu-1}(r) + r^2 c_{\tau+1} r^{\nu-2} K_{\nu-2}(r) \\
&\leq c_{\tau+1} r^{\nu-1-1/2} \sqrt{2\pi} e^{-r} e^{\frac{(\nu-1)^2}{2r}} + r^2 c_{\tau+1} r^{\nu-2-1/2} \sqrt{2\pi} e^{-r} e^{\frac{(\nu-2)^2}{2r}} \\
&= c_{\tau+1} r^{\nu-3/2} \sqrt{2\pi} e^{-r} \left( e^{\frac{(\nu-1)^2}{2r}} + r e^{\frac{(\nu-2)^2}{2r}} \right) \\
&= \widetilde{c}_{\tau} r^{\nu-3/2} e^{-r} \left( e^{\frac{(\nu-1)^2}{2r}} + r e^{\frac{(\nu-2)^2}{2r}} \right) =: \widetilde{\Lambda}_{\tau,d}(r). \qquad (4.12)
\end{aligned}$$

With

$$\widetilde{\Lambda}'_{\tau,d}(r) = \widetilde{c}_{\tau} r^{\nu-5/2} e^{\frac{(\nu-1)^2}{2r} - r} \left( \nu - \frac{3}{2} - r - \frac{(\nu-1)^2}{2r^2} + r e^{\frac{-2\nu+3}{2r}} \left( \nu - \frac{1}{2} - r - \frac{(\nu-2)^2}{2r^2} \right) \right)$$

we can see that $\widetilde{\Lambda}_{\tau,d}(r)$ decreases for every $r > \nu - \frac{1}{2}$.

## 4.2. Native Spaces for Positive Definite Kernels

In the previous section, reproducing kernel Hilbert spaces for matrix-valued kernels were established. We will now introduce a similar concept: The native spaces. A native space is a reproducing kernel Hilbert space, which is constructed from a given kernel. The kernel can be either scalar-valued or matrix-valued. After introducing the native spaces, we will look at their relation to Sobolev spaces. Finally, we will present three examples.

### 4.2.1. Scalar-valued Native Spaces

The material about scalar-valued native spaces is taken from section 10.2 in [54]. Further explanations can be found there. Here, we will just give an overview.

Let $\phi : \Omega \times \Omega \to \mathbb{R}$ be a positive definite kernel and $\Omega$ be a subset of $\mathbb{R}^d$ which contains at least one point. Then we can define the $\mathbb{R}$-linear space

$$F_{\phi}(\Omega) := \left\{ \sum_{j=1}^{N} \alpha_j \phi(\cdot, \mathbf{x}_j) \,:\, \mathbf{x}_j \in \Omega,\, \alpha_j \in \mathbb{R} \right\}$$

and equip it with the bilinear form

$$\left( \sum_{j=1}^{N} \alpha_j \phi(\cdot, \mathbf{x}_j), \sum_{k=1}^{M} \beta_k \phi(\cdot, \mathbf{y}_k) \right)_{\phi} := \sum_{j=1}^{N} \sum_{k=1}^{M} \alpha_j \beta_k \phi(\mathbf{x}_j, \mathbf{y}_k).$$

Now we can define the native space.

**Definition 4.9.** *The* native space *of a positive definite kernel $\phi$ is defined to be the closure of $F_\phi(\Omega)$ with respect to the norm $\|\cdot\|_{\mathcal{N}_\phi(\Omega)} := \|\cdot\|_\phi$ and will be denoted by $\mathcal{N}_\phi(\Omega)$.*

If $\Omega = \mathbb{R}^d$ and if $\phi$ is translation invariant, we have the following result. Its proof can be found in [54, Theorem 10.12].

**Theorem 4.10.** *Suppose that $\phi \in C(\mathbb{R}^d) \cap L_1(\mathbb{R}^d)$ is a real-valued positive definite function. Define*

$$H_\phi(\mathbb{R}^d) := \left\{ f \in C(\mathbb{R}^d) \cap L_2(\mathbb{R}^d) \ : \ \frac{\widehat{f}}{\sqrt{\widehat{\phi}}} \in L_2(\mathbb{R}^d) \right\}$$

*and equip this space with the bilinear form*

$$(f, g)_{H_\phi(\mathbb{R}^d)} := (2\pi)^{-d/2} \left( \frac{\widehat{f}}{\sqrt{\widehat{\phi}}}, \frac{\widehat{g}}{\sqrt{\widehat{\phi}}} \right)_{L_2(\mathbb{R}^d)} = (2\pi)^{-d/2} \int_{\mathbb{R}^d} \frac{\widehat{f}(\boldsymbol{\omega})\overline{\widehat{g}(\boldsymbol{\omega})}}{\widehat{\phi}(\boldsymbol{\omega})} \, d\omega.$$

*Then $H_\phi(\mathbb{R}^d)$ is a real Hilbert space with inner product $(\cdot,\cdot)_{H_\phi(\mathbb{R}^d)}$ and reproducing kernel $\phi(\cdot - \cdot)$. Hence $H_\phi(\mathbb{R}^d)$ is the native space of $\phi$ on $\mathbb{R}^d$, i. e. $H_\phi(\mathbb{R}^d) = \mathcal{N}_\phi(\mathbb{R}^d)$, and both inner products coincide. In particular, every $f \in \mathcal{N}_\phi(\mathbb{R}^d)$ can be recovered from its Fourier transform $\widehat{f} \in L_1(\mathbb{R}^d) \cap L_2(\mathbb{R}^d)$.*

Therefore we have that the reproducing kernel Hilbert space with reproducing kernel $\phi$ is identical to the native space of $\phi$ with equivalent norms. Furthermore, this space may be a Sobolev space. The following result comes from [54, Corollary 10.13].

**Corollary 4.11.** *Suppose that $\phi \in C(\mathbb{R}^d) \cap L_1(\mathbb{R}^d)$ satisfies*

$$c_1(1 + \|\boldsymbol{\omega}\|_2^2)^{-s} \leq \widehat{\phi}(\boldsymbol{\omega}) \leq c_2(1 + \|\boldsymbol{\omega}\|_2^2)^{-s}, \qquad \boldsymbol{\omega} \in \mathbb{R}^d \tag{4.13}$$

*with $s > d/2$ and two positive constants $c_1 \leq c_2$. Then the native space $\mathcal{N}_\phi(\mathbb{R}^d)$ corresponding to $\phi$ coincides with the Sobolev space*

$$H^s(\mathbb{R}^d) = \left\{ f \in L_2(\mathbb{R}^d) : \widehat{f}(\cdot)(1 + \|\cdot\|_2^2)^{s/2} \in L_2(\mathbb{R}^d) \right\} \subset C(\mathbb{R}^d),$$

*and the native space norm and the Sobolev norm are equivalent.*

### 4.2.2. Matrix-valued Native Spaces

The native space for matrix-valued kernels can be defined similarly to the scalar-valued case. We follow the ideas presented in [55].

Let $\Omega \subseteq \mathbb{R}^d$ be non-empty and $\mathbf{\Phi} : \Omega \times \Omega \to \mathbb{R}^{n\times n}$ be a positive definite matrix-valued function. Then, we can introduce the space

$$\mathbf{F}_{\mathbf{\Phi}}(\Omega) := \left\{ \sum_{j=1}^{N} \mathbf{\Phi}(\cdot, \mathbf{x}_j)\boldsymbol{\alpha}_j : \mathbf{x}_j \in \Omega, \boldsymbol{\alpha}_j \in \mathbb{R}^n \right\},$$

which can be equipped with an inner product

$$\left( \sum_{j=1}^{N} \mathbf{\Phi}(\cdot, \mathbf{x}_j)\boldsymbol{\alpha}_j, \sum_{k=1}^{M} \mathbf{\Phi}(\cdot, \mathbf{y}_k)\boldsymbol{\beta}_k \right)_{\mathbf{\Phi}} := \sum_{j=1}^{N}\sum_{k=1}^{M} \boldsymbol{\alpha}_j^T \mathbf{\Phi}(\mathbf{x}_j, \mathbf{y}_k)\boldsymbol{\beta}_k.$$

**Definition 4.12.** *The* native space *(or* reproducing kernel Hilbert space*) of a positive definite, matrix-valued kernel* $\mathbf{\Phi}$ *is defined to be the closure of* $\mathbf{F}_{\mathbf{\Phi}}(\Omega)$ *with respect to* $\|\cdot\|_{\mathcal{N}_{\mathbf{\Phi}}(\Omega)} := \|\cdot\|_{\mathbf{\Phi}}$ *and will be denoted by* $\mathcal{N}_{\mathbf{\Phi}}(\Omega)$.

From now on, we will assume that the kernel $\mathbf{\Phi}$ is translation invariant. For a matrix-valued function $\mathbf{\Phi}$ with $\mathbf{\Phi}, \widehat{\mathbf{\Phi}} \in \mathbf{C}(\mathbb{R}^d) \cap \mathbf{L}_1(\mathbb{R}^d)$ we can recover the function component-wise from its Fourier transform

$$\mathbf{\Phi}_{ij}(\mathbf{x}) = (2\pi)^{-d/2} \int_{\mathbb{R}^d} \widehat{\mathbf{\Phi}_{ij}}(\boldsymbol{\omega}) e^{i\mathbf{x}^T\boldsymbol{\omega}} d\boldsymbol{\omega},$$

where $1 \le i, j \le n$, cf. corollary 2.5. Hence, for every $\mathbf{f} \in \mathbf{F}_{\mathbf{\Phi}}(\Omega)$, i. e. $\mathbf{f} = \sum_{j=1}^{N} \mathbf{\Phi}(\cdot - \mathbf{x}_j)\boldsymbol{\alpha}_j$, we can express the norm as

$$\begin{aligned}
\|\mathbf{f}\|^2_{\mathcal{N}_{\mathbf{\Phi}}} := \|\mathbf{f}\|^2_{\mathbf{\Phi}} &= \sum_{j,k=1}^{N} \boldsymbol{\alpha}_j^T \mathbf{\Phi}(\mathbf{x}_j - \mathbf{x}_k)\boldsymbol{\alpha}_k \\
&= (2\pi)^{-d/2} \sum_{j=1}^{N}\sum_{k=1}^{N} \boldsymbol{\alpha}_j^T \int_{\mathbb{R}^d} \widehat{\mathbf{\Phi}}(\boldsymbol{\omega}) e^{i(\mathbf{x}_j - \mathbf{x}_k)^T\boldsymbol{\omega}} d\boldsymbol{\omega}\ \boldsymbol{\alpha}_k \\
&= (2\pi)^{-d/2} \int_{\mathbb{R}^d} \sum_{j,k=1}^{N} \boldsymbol{\alpha}_j^T \widehat{\mathbf{\Phi}}(\boldsymbol{\omega}) e^{-i(\mathbf{x}_k - \mathbf{x}_j)^T\boldsymbol{\omega}} \boldsymbol{\alpha}_k\, d\boldsymbol{\omega}. \qquad (4.14)
\end{aligned}$$

In the special case of $\mathbf{\Phi}$ being a diagonal matrix, with the entries $\phi_1, \ldots, \phi_n$ on the diagonal, we can interpret the native space of $\mathbf{\Phi}$ as the tensor product space $\mathbf{H}_{\mathbf{\Phi}}(\Omega) := H_{\phi_1}(\Omega) \times \ldots \times H_{\phi_n}(\Omega)$. This space is a real, vector-valued Hilbert space of functions

equipped with the inner product

$$(\mathbf{f},\mathbf{g})_{\mathbf{H}_{\boldsymbol{\phi}}(\Omega)} := \left(\sum_{j=1}^{n}(f_j,g_j)^2_{H_{\phi_j}(\Omega)}\right)^{1/2}.$$

If we have $\phi_1 = \ldots = \phi_n$, i. e. $\boldsymbol{\Phi} = \phi I$, where $I$ is the identity matrix, we can write $\mathbf{H}_{\boldsymbol{\Phi}}(\Omega) = (H_\phi(\Omega))^n$ and apply the results of the scalar-valued case.

### 4.2.3. Examples

To establish the discretization scheme for Darcy's problem and for its error analysis the native spaces of the kernels $\boldsymbol{\Phi}_{\mathrm{div}}$ and $\boldsymbol{\Phi}_{\mathrm{curl}}$ are essential. For the numerical examples, the native space of Wendland functions is of importance. From now on, all kernels are translation invariant.

#### The Native Space of Wendland Functions

Wendland functions are positive definite, cf. [54, Theorem 9.13]. Furthermore, they generate Sobolev spaces. The following result is taken from [54, Theorem 10.35].

**Theorem 4.13.** *Let $\phi_{d,\ell} : \mathbb{R} \to \mathbb{R}$ denote the compactly supported radial basis function of minimal degree that is positive definite and in $C^{2\ell}$. Let $d \geq 3$ if $\ell = 0$. Then there exist constants $c_1, c_2 > 0$ depending only on $d$ and $\ell$ such that*

$$c_1(1+\|\boldsymbol{\omega}\|_2)^{-d-2\ell-1} \leq \widehat{\phi_{d,\ell}}(\boldsymbol{\omega}) \leq c_2(1+\|\boldsymbol{\omega}\|_2)^{-d-2\ell-1} \qquad \text{for all } \boldsymbol{\omega} \in \mathbb{R}^d.$$

*This means in particular that*

$$\mathcal{N}_{\phi_{d,\ell}}(\mathbb{R}^d) = H^{d/2+\ell+1/2}(\mathbb{R}^d),$$

*i. e. the native space for these basis functions is a classical Sobolev space.*

Let $\tau := d/2 + \ell + 1/2$. The Wendland functions $\phi_{d,\ell}$ are an element of all Sobolev

spaces $H^\alpha(\mathbb{R}^d)$ with $\alpha < d + 2\ell + 1 - d/2$. This can be seen from

$$\begin{aligned}\|\phi_{d,\ell}\|_{H^\alpha(\mathbb{R}^d)} &= (2\pi)^{-d/2} \int_{\mathbb{R}^d} |\widehat{\phi_{d,\ell}}(\boldsymbol{\omega})|^2 (1 + \|\boldsymbol{\omega}\|_2^2)^\alpha d\boldsymbol{\omega} \\ &\leq c \int_{\mathbb{R}^d} (1 + \|\boldsymbol{\omega}\|_2)^{-4\tau} (1 + \|\boldsymbol{\omega}\|_2^2)^\alpha d\boldsymbol{\omega} \\ &\leq c \int_0^\infty (1 + r)^{-4\tau} (1 + r^2)^\alpha r^{d-1} dr \\ &\leq c \int_0^1 r^{-4\tau+2\alpha+d-1} dr + c \int_1^\infty r^{-4\tau+2\alpha+d-1} dr,\end{aligned}$$

where we applied theorem 4.13. The first integral is bounded, since a polynomial is integrated over a bounded domain. Thus

$$\|\phi_{d,\ell}\|_{H^\alpha(\mathbb{R}^d)} \leq \tilde{c} + c \int_1^\infty r^{-4\tau+2\alpha+d-1} dr = \tilde{c} + c \left[ r^{-4\tau+2\alpha+d} \right]_1^\infty .$$

Hence the norm is less than infinity if and only if $\alpha < d + 2\ell + 1 - d/2$.

### The Space $\mathcal{N}_{\boldsymbol{\Phi}_{\text{div}}}(\mathbb{R}^d)$

We now state the two main results regarding the native space for the kernel $\mathcal{N}_{\boldsymbol{\Phi}_{\text{div}}}(\mathbb{R}^d)$. Both were proven in [17], following from ideas presented in [54]. A shorter, straightforward proof has been done by Wendland in [55, Theorem 3.4, Corollary 3.5]. The main idea for the shorter proof is to introduce the space $\mathbf{H}_\psi(\mathbb{R}^d)$ as the tensor-product space $(H_\psi(\mathbb{R}^d))^d$ and apply the results of the scalar-valued case. The space $H_\psi(\mathbb{R}^d)$ is the one defined in theorem 4.10, where $\psi = -\Delta\phi$.

Let $\mathbf{H}_\psi(\mathbb{R}^d; \text{div})$ be the subspace of the divergence-free functions of $\mathbf{H}_\psi(\mathbb{R}^d)$.

**Theorem 4.14.** *Suppose $\phi \in C^2(\mathbb{R}^d) \cap W_1^2(\mathbb{R}^d)$ is a positive definite function. Define $\psi = -\Delta\phi \in L_1(\mathbb{R}^d)$ and $\boldsymbol{\Phi}_{\text{div}} = (-\Delta I + \nabla\nabla^T)\phi$. Then, the following relation holds:*

$$\mathcal{N}_{\boldsymbol{\Phi}_{\text{div}}}(\mathbb{R}^d) = \mathbf{H}_\psi(\mathbb{R}^d; \text{div})$$

*with identical norms. In particular, the norm on $\mathcal{N}_{\boldsymbol{\Phi}_{\text{div}}}(\mathbb{R}^d)$ can be expressed as*

$$\|\mathbf{f}\|^2_{\mathcal{N}_{\boldsymbol{\Phi}_{\text{div}}}(\mathbb{R}^d)} = (2\pi)^{-d/2} \int_{\mathbb{R}^d} \frac{\|\widehat{\mathbf{f}}(\boldsymbol{\omega})\|_2^2}{\|\boldsymbol{\omega}\|_2^2 \widehat{\phi}(\boldsymbol{\omega})} d\boldsymbol{\omega}.$$

*Hence $\mathcal{N}_{\boldsymbol{\Phi}_{\text{div}}}(\mathbb{R}^d)$ consists of all functions $\mathbf{f} \in \mathbf{L}_2(\mathbb{R}^d)$ with $\|\mathbf{f}\|_{\mathcal{N}_{\boldsymbol{\Phi}_{\text{div}}}(\mathbb{R}^d)} < \infty$.*

**Corollary 4.15.** *Let $\tau > d/2$. Suppose $\phi$ satisfies (4.13) with $s = \tau + 1$. Define $\boldsymbol{\Phi}_{\text{div}} =$*

$(-\Delta I + \nabla\nabla^T)\phi$. *Then*

$$\widetilde{\mathbf{H}}^\tau(\mathbb{R}^d; \mathrm{div}) = \mathcal{N}_{\mathbf{\Phi}_{\mathrm{div}}}(\mathbb{R}^d)$$

*with equivalent norms.*

### The Space $\mathcal{N}_{\mathbf{\Phi}_{\mathrm{curl}}}(\mathbb{R}^d)$

We define the space $\mathbf{H}_\psi(\mathbb{R}^d; \mathrm{curl})$ to be the subspace of the curl-free functions of $\mathbf{H}_\psi(\mathbb{R}^d) := (H_\psi(\mathbb{R}^d))^d$. The second native space of a matrix-valued kernel we are interested in is $\mathcal{N}_{\mathbf{\Phi}_{\mathrm{curl}}}(\mathbb{R}^d)$. The proof of the next result follows ideas from the proof for the divergence-free kernel shown in [55, Theorem 3.4].

**Theorem 4.16.** *Suppose $\phi \in C^2(\mathbb{R}^d) \cap W_1^2(\mathbb{R}^d)$ is a positive definite function. Define $\psi = -\Delta\phi \in L_1(\mathbb{R}^d)$ and $\mathbf{\Phi}_{\mathrm{curl}} = -\nabla\nabla^T\phi$. Then, the following relation holds:*

$$\mathcal{N}_{\mathbf{\Phi}_{\mathrm{curl}}}(\mathbb{R}^d) = \mathbf{H}_\psi(\mathbb{R}^d; \mathrm{curl})$$

*with identical norms. In particular, the norm on $\mathcal{N}_{\mathbf{\Phi}_{\mathrm{curl}}}(\mathbb{R}^d)$ can be expressed as*

$$\|\mathbf{f}\|^2_{\mathcal{N}_{\mathbf{\Phi}_{\mathrm{curl}}}(\mathbb{R}^d)} = (2\pi)^{-d/2} \int_{\mathbb{R}^d} \frac{\|\widehat{\mathbf{f}}(\boldsymbol{\omega})\|_2^2}{\|\boldsymbol{\omega}\|_2^2 \widehat{\phi}(\boldsymbol{\omega})} d\boldsymbol{\omega}.$$

*Hence $\mathcal{N}_{\mathbf{\Phi}_{\mathrm{curl}}}(\mathbb{R}^d)$ consists of all functions $\mathbf{f} \in \mathbf{L}_2(\mathbb{R}^d)$ with $\|\mathbf{f}\|_{\mathcal{N}_{\mathbf{\Phi}_{\mathrm{curl}}}(\mathbb{R}^d)} < \infty$.*

*Proof.* Firstly we show that the norms are identical for every $\mathbf{f} \in \mathbf{F}_{\mathbf{\Phi}_{\mathrm{curl}}}(\mathbb{R}^d)$, i. e. $\mathbf{f}$ is an element of $\mathbf{H}_\psi(\mathbb{R}^d; \mathrm{curl})$.

Let $\mathbf{f} = \sum_{j=1}^N \mathbf{\Phi}_{\mathrm{curl}}(\cdot - \mathbf{x}_j)\boldsymbol{\alpha}_j$ be an arbitrary element of $\mathbf{F}_{\mathbf{\Phi}_{\mathrm{curl}}}(\mathbb{R}^d)$, then

$$\|\mathbf{f}\|^2_{\mathcal{N}_{\mathbf{\Phi}_{\mathrm{curl}}}(\mathbb{R}^d)} = (2\pi)^{-d/2} \int_{\mathbb{R}^d} \sum_{j,k=1}^N e^{-i(\mathbf{x}_k - \mathbf{x}_j)^T\boldsymbol{\omega}} \boldsymbol{\alpha}_j^T \widehat{\mathbf{\Phi}_{\mathrm{curl}}}(\boldsymbol{\omega})\boldsymbol{\alpha}_k d\boldsymbol{\omega}.$$

Using $\widehat{\psi}(\boldsymbol{\omega}) = \|\boldsymbol{\omega}\|_2^2\widehat{\phi}(\boldsymbol{\omega})$, $\widehat{\mathbf{\Phi}_{\mathrm{curl}}}(\boldsymbol{\omega})\boldsymbol{\alpha} = \boldsymbol{\omega}\boldsymbol{\omega}^T\widehat{\phi}(\omega)\boldsymbol{\alpha}$ and the Fourier representation

$$\widehat{\mathbf{f}}(\boldsymbol{\omega}) = \sum_{j=1}^N e^{-i\mathbf{x}_j^T\boldsymbol{\omega}} \widehat{\mathbf{\Phi}_{\mathrm{curl}}}(\boldsymbol{\omega})\boldsymbol{\alpha}_j = \sum_{j=1}^N e^{-i\mathbf{x}_j^T\boldsymbol{\omega}} \boldsymbol{\omega}\boldsymbol{\omega}^T\widehat{\phi}(\boldsymbol{\omega})\boldsymbol{\alpha}_j,$$

allows us to compute

$$\begin{aligned}\|\widehat{\mathbf{f}}(\boldsymbol{\omega})\|_2^2 &= \sum_{j,k=1}^{N} e^{-i(\mathbf{x}_k-\mathbf{x}_j)^T\boldsymbol{\omega}}|\widehat{\phi}(\boldsymbol{\omega})|^2 \left(\boldsymbol{\omega}\boldsymbol{\omega}^T\boldsymbol{\alpha}_j\right)^T \left(\boldsymbol{\omega}\boldsymbol{\omega}^T\boldsymbol{\alpha}_k\right) \\ &= \|\boldsymbol{\omega}\|_2^2\widehat{\phi}(\boldsymbol{\omega})\widehat{\phi}(\boldsymbol{\omega}) \sum_{j,k=1}^{N} e^{-i(\mathbf{x}_k-\mathbf{x}_j)^T\boldsymbol{\omega}}\boldsymbol{\alpha}_j^T\boldsymbol{\omega}\boldsymbol{\omega}^T\boldsymbol{\alpha}_k \\ &= \widehat{\psi}(\boldsymbol{\omega}) \sum_{j,k=1}^{N} e^{-i(\mathbf{x}_k-\mathbf{x}_j)^T\boldsymbol{\omega}}\boldsymbol{\alpha}_j^T\widehat{\boldsymbol{\Phi}_{\mathrm{curl}}}(\boldsymbol{\omega})\boldsymbol{\alpha}_k. \end{aligned} \tag{4.15}$$

The definition of the norm in $\mathbf{H}_\psi(\mathbb{R}^d)$ and (4.15) establish

$$\begin{aligned}\|\mathbf{f}\|_{\mathbf{H}_\psi(\mathbb{R}^d)}^2 &= (2\pi)^{-d/2}\int_{\mathbb{R}^d} \frac{\|\widehat{\mathbf{f}}(\boldsymbol{\omega})\|_2^2}{\widehat{\psi}(\boldsymbol{\omega})}d\boldsymbol{\omega} \\ &= (2\pi)^{-d/2}\int_{\mathbb{R}^d} \sum_{j,k=1}^{N} e^{-i(\mathbf{x}_k-\mathbf{x}_j)^T\boldsymbol{\omega}}\boldsymbol{\alpha}_j^T\widehat{\boldsymbol{\Phi}_{\mathrm{curl}}}(\boldsymbol{\omega})\boldsymbol{\alpha}_k \, d\boldsymbol{\omega} \\ &= \|\mathbf{f}\|_{\mathcal{N}_{\boldsymbol{\Phi}_{\mathrm{curl}}}(\mathbb{R}^d)}^2.\end{aligned}$$

Since $\mathbf{f}$ is a general element of $\mathbf{F}_{\boldsymbol{\Phi}_{\mathrm{curl}}}(\mathbb{R}^d)$, we see that on $\mathbf{F}_{\boldsymbol{\Phi}_{\mathrm{curl}}}(\mathbb{R}^d) \subseteq \mathbf{H}_\psi(\mathbb{R}^d;\mathrm{curl})$ both norms are equal. $\mathbf{H}_\psi(\mathbb{R}^d;\mathrm{curl})$ is complete and $\mathcal{N}_{\boldsymbol{\Phi}_{\mathrm{curl}}}(\mathbb{R}^d)$ is the closure of $\mathbf{F}_{\boldsymbol{\Phi}_{\mathrm{curl}}}(\mathbb{R}^d)$ thus this also means $\mathcal{N}_{\boldsymbol{\Phi}_{\mathrm{curl}}}(\mathbb{R}^d) \subseteq \mathbf{H}_\psi(\mathbb{R}^d;\mathrm{curl})$ with equal norms. Suppose finally, we have an $\mathbf{f} \in \mathbf{H}_\psi(\mathbb{R}^d;\mathrm{curl})$ which is orthogonal to $\mathcal{N}_{\boldsymbol{\Phi}_{\mathrm{curl}}}(\mathbb{R}^d)$, meaning in particular

$$\begin{aligned} 0 &= (\mathbf{f}, \boldsymbol{\Phi}_{\mathrm{curl}}(\cdot-\mathbf{x})\boldsymbol{\alpha})_{\mathbf{H}_\psi(\mathbb{R}^d)} \\ &= (2\pi)^{-d/2}\int_{\mathbb{R}^d} \frac{\widehat{\mathbf{f}}(\boldsymbol{\omega})^*\widehat{\boldsymbol{\Phi}_{\mathrm{curl}}}(\boldsymbol{\omega})\boldsymbol{\alpha}}{\widehat{\psi}(\boldsymbol{\omega})}e^{-i\mathbf{x}^T\boldsymbol{\omega}}d\boldsymbol{\omega} \\ &= (2\pi)^{-d/2}\int_{\mathbb{R}^d} \frac{\widehat{\mathbf{f}}(\boldsymbol{\omega})^*\boldsymbol{\omega}\boldsymbol{\omega}^T\boldsymbol{\alpha}}{\|\boldsymbol{\omega}\|_2^2}e^{-i\mathbf{x}^T\boldsymbol{\omega}}d\boldsymbol{\omega} \\ &= (2\pi)^{-d/2}\int_{\mathbb{R}^d} \frac{\overline{-i\widehat{g}(\boldsymbol{\omega})}\boldsymbol{\omega}^T\boldsymbol{\omega}\boldsymbol{\omega}^T\boldsymbol{\alpha}}{\|\boldsymbol{\omega}\|_2^2}e^{-i\mathbf{x}^T\boldsymbol{\omega}}d\boldsymbol{\omega} \\ &= (2\pi)^{-d/2}\int_{\mathbb{R}^d} (-i\boldsymbol{\omega}\widehat{g}(\boldsymbol{\omega}))^*\boldsymbol{\alpha}e^{-i\mathbf{x}^T\boldsymbol{\omega}}d\boldsymbol{\omega} \\ &= (2\pi)^{-d/2}\int_{\mathbb{R}^d} \widehat{\mathbf{f}}(\boldsymbol{\omega})^*\boldsymbol{\alpha}e^{-i\mathbf{x}^T\boldsymbol{\omega}}d\boldsymbol{\omega}. \end{aligned}$$

Here we used the fact that $\mathbf{f}$ is curl-free, i. e. for every $\mathbf{f} \in \mathbf{H}_\psi(\mathbb{R}^d;\mathrm{curl})$ we can find $g \in H^{\tau+1}(\mathbb{R}^d)/\mathbb{R}$ such that $\widehat{\mathbf{f}}(\boldsymbol{\omega}) = \widehat{\nabla}g(\boldsymbol{\omega}) = -i\boldsymbol{\omega}\widehat{g}(\boldsymbol{\omega})$.

Because of the definition of $\mathbf{H}_\psi(\mathbb{R}^d) = (H_\psi(\mathbb{R}^d))^d$, we have with theorem 4.10 that every

component of $\mathbf{f}$ is integrable and continuous. Hence we can apply corollary 2.5 to recover $\mathbf{f}$. Thus

$$0 = (2\pi)^{-d/2} \int_{\mathbb{R}^d} \widehat{\mathbf{f}}(\boldsymbol{\omega})^* \boldsymbol{\alpha} e^{-i\mathbf{x}^T\boldsymbol{\omega}} d\boldsymbol{\omega} = \mathbf{f}(-\mathbf{x})^T \boldsymbol{\alpha}.$$

This proves that $\mathbf{f}$ is identically zero and hence $\mathbf{H}_\psi(\mathbb{R}^d; \operatorname{curl}) = \mathcal{N}_{\boldsymbol{\Phi}_{\operatorname{curl}}}(\mathbb{R}^d)$. □

Finally, we now establish the relation between $\mathcal{N}_{\boldsymbol{\Phi}_{\operatorname{curl}}}(\mathbb{R}^d)$ and $\widetilde{\mathbf{H}}^\tau(\mathbb{R}^d; \operatorname{curl})$.

**Corollary 4.17.** *Let $\tau > d/2$. Suppose $\phi$ satisfies (4.13) with $s = \tau + 1$. Define $\boldsymbol{\Phi}_{\operatorname{curl}} = -\nabla\nabla^T\phi$. Then*

$$\widetilde{\mathbf{H}}^\tau(\mathbb{R}^d; \operatorname{curl}) = \mathcal{N}_{\boldsymbol{\Phi}_{\operatorname{curl}}}(\mathbb{R}^d)$$

*with equivalent norms.*

*Proof.* We have already proven that $\mathcal{N}_{\boldsymbol{\Phi}_{\operatorname{curl}}}(\mathbb{R}^d) = \mathbf{H}_\psi(\mathbb{R}^d; \operatorname{curl})$ and the norms are equal provided that $\psi = -\Delta\phi$, cf. theorem 4.16. Note that $\widehat{\psi}(\boldsymbol{\omega}) = \|\boldsymbol{\omega}\|_2^2 \widehat{\phi}(\boldsymbol{\omega})$.

For every $\mathbf{f} \in \mathbf{H}_\psi(\mathbb{R}^d; \operatorname{curl})$ we have with (4.13) that

$$\begin{aligned}
\|\mathbf{f}\|^2_{\widetilde{\mathbf{H}}^\tau(\mathbb{R}^d)} &= (2\pi)^{-d/2} \int_{\mathbb{R}^d} \frac{\|\widehat{\mathbf{f}}(\boldsymbol{\omega})\|_2^2}{\|\boldsymbol{\omega}\|_2^2} (1 + \|\boldsymbol{\omega}\|_2^2)^{\tau+1} d\boldsymbol{\omega} \\
&\leq c_2 (2\pi)^{-d/2} \int_{\mathbb{R}^d} \frac{\|\widehat{\mathbf{f}}(\boldsymbol{\omega})\|_2^2}{\|\boldsymbol{\omega}\|_2^2 \widehat{\phi}(\boldsymbol{\omega})} d\boldsymbol{\omega} \\
&= c_2 \|\mathbf{f}\|^2_{\mathbf{H}_\psi(\mathbb{R}^d)} < \infty.
\end{aligned}$$

However, for every $\mathbf{f} \in \widetilde{\mathbf{H}}^\tau(\mathbb{R}^d; \operatorname{curl})$ we see that

$$\begin{aligned}
\|\mathbf{f}\|^2_{\mathbf{H}_\psi(\mathbb{R}^d)} &= (2\pi)^{-d/2} \int_{\mathbb{R}^d} \frac{\|\mathbf{f}(\boldsymbol{\omega})\|_2^2}{\|\boldsymbol{\omega}\|_2^2 \widehat{\phi}(\boldsymbol{\omega})} d\boldsymbol{\omega} \\
&\leq (2\pi)^{-d/2} \int_{\mathbb{R}^d} \frac{\|\mathbf{f}(\boldsymbol{\omega})\|_2^2}{c_1 \|\boldsymbol{\omega}\|_2^2} (1 + \|\boldsymbol{\omega}\|_2^2)^{\tau+1} d\boldsymbol{\omega} \\
&= \frac{1}{c_1} \|\mathbf{f}\|^2_{\widetilde{\mathbf{H}}^\tau(\mathbb{R}^d)},
\end{aligned}$$

which finishes the proof. □

# 5. Analytically Divergence-free Discretization Methods for Darcy's Problem

We will now develop the approximation scheme for Darcy's problem. The idea of the method is to apply optimal recovery to solve the partial differential equation. The approximating function will be built from a combined kernel. This kernel incorporates the divergence-free kernel introduced in section 2.4.4 to model the velocity and a general scalar-valued kernel to represent the pressure. We then discretize Darcy's problem with collocation via functionals.

All in all we will derive a discretization scheme for Darcy's problem. The method works on arbitrary geometries, in arbitrary space dimension and can be of arbitrary order. Furthermore, it is mesh-free and produces an analytically divergence-free solution of the velocity part.

Our scheme will follow from the framework presented in [55], where Stokes problem has been solved. Note that parts of this chapter can also be found in [47].

## 5.1. Optimal Recovery to Solve Partial Differential Equations

Generalised interpolation can be applied to recover the solution of a partial differential equation. The ideas of interpolation with radial basis functions are extended such that not only function values are recovered, but also certain properties. For Darcy's problem the velocity and the pressure are sought, but only the right hand sides $\mathbf{f}$ and $\mathbf{g}$ are known at the collocation points.

Let $H$ be a Hilbert space and $\lambda_1, \ldots, \lambda_N$ be linear independent functionals from the dual space $H^*$ of $H$. Suppose that the values $f_1, \ldots, f_N$ are given. Then the *generalised recovery problem* is to find a function $s \in H$ such that $\lambda_j(s) = f_j$ for all $1 \leq j \leq N$. The element $s$ is called an *approximating function* or *generalised interpolant*.

The *optimal recovery problem* is to find the norm-minimal function $s$. This means that

the function $s^* \in H$ is sought such that

$$\|s^*\|_H = \min\{\|s\|_H : s \in H, \lambda_j(s) = f_j \text{ for all } 1 \leq j \leq N\}.$$

Further information about generalised interpolation and the solution of partial differential equations by collocation can be found in [54].

We now want to establish optimal recovery for vector-valued target functions, where the approximating function is built from matrix-valued kernels.

Since $\mathbf{f} = \mathbf{\Phi}(\cdot - \mathbf{y})\mathbf{e}_j$ belongs to $\mathcal{N}_{\mathbf{\Phi}}(\Omega)$, where $\mathbf{e}_j$ is the $j$th unit vector, we see that the columns of $\mathbf{\Phi}$ and, due to the symmetry of $\mathbf{\Phi}$, its rows belong to $\mathcal{N}_{\mathbf{\Phi}}(\Omega)$. Thus, we can define $\lambda^{\mathbf{y}}(\mathbf{\Phi}(\mathbf{x} - \mathbf{y}))$ as the vector-valued function, which is generated by applying $\lambda$ with respect to $\mathbf{y}$ to every column of $\mathbf{\Phi}$, i. e. $\lambda^{\mathbf{y}}(\mathbf{\Phi}(\mathbf{x} - \mathbf{y})) := (\lambda^{\mathbf{y}}(\mathbf{\Phi}(\mathbf{x} - \mathbf{y})\mathbf{e}_1), \ldots, \lambda^{\mathbf{y}}(\mathbf{\Phi}(\mathbf{x} - \mathbf{y})\mathbf{e}_n))^T$. The resulting vector-valued function is the Riesz representer of $\lambda$ in $\mathcal{N}_{\mathbf{\Phi}}(\Omega)$ in the sense of

$$\lambda(\mathbf{f}) = (\mathbf{f}, \lambda^{\mathbf{y}}(\mathbf{\Phi}(\cdot - \mathbf{y})))_{\mathbf{\Phi}}.$$

Thus the following result, which is well-known in the context of scalar-valued kernels, remains true for matrix-valued kernels [54].

**Proposition 5.1.** *Let $\Omega \subseteq \mathbb{R}^d$. Suppose $\mathbf{\Phi} : \mathbb{R}^d \to \mathbb{R}^{n \times n}$ is a positive definite, matrix-valued kernel. Suppose further that $\lambda_1, \ldots, \lambda_N \in \mathcal{N}_{\mathbf{\Phi}}(\Omega)^*$ are linearly independent and $f_1, \ldots, f_N \in \mathbb{R}$ are given. Then, the problem*

$$\min\{\|\mathbf{s}\|_{\mathcal{N}_{\mathbf{\Phi}}(\Omega)} : \lambda_j(\mathbf{s}) = f_j, 1 \leq j \leq N\} \tag{5.1}$$

*has a unique solution, which has the representation*

$$\mathbf{s}_\lambda = \sum_{j=1}^{N} \alpha_j \lambda_j^{\mathbf{y}}(\mathbf{\Phi}(\cdot - \mathbf{y})). \tag{5.2}$$

*The coefficients $\alpha_j$ are determined via the interpolation conditions $\lambda_i(\mathbf{s}_\lambda) = f_i$, $1 \leq i \leq N$.*

Finally, we state and prove two stability results.

**Corollary 5.2.** *Under the assumptions of proposition 5.1 and if $\mathbf{f}$ is the function from which the data stems, i. e. $\lambda_j(\mathbf{f}) = f_j$, we have*

$$\|\mathbf{f} - \mathbf{s}_\lambda\|_{\mathcal{N}_{\mathbf{\Phi}}(\Omega)} \leq \|\mathbf{f}\|_{\mathcal{N}_{\mathbf{\Phi}}(\Omega)}.$$

*Moreover,*

$$\|\mathbf{s}_\lambda\|_{\mathcal{N}_{\mathbf{\Phi}}(\Omega)} \leq \|\mathbf{f}\|_{\mathcal{N}_{\mathbf{\Phi}}(\Omega)}.$$

*Proof.* The first part is to show that $\mathbf{f} - \mathbf{s}_\lambda$ is orthogonal to $\mathbf{s}_\lambda$. This follows from

$$\begin{aligned}(\mathbf{f} - \mathbf{s}_\lambda, \mathbf{s}_\lambda)_{\mathcal{N}_{\mathbf{\Phi}}(\Omega)} &= \sum_{j=1}^{N} \alpha_j (\mathbf{f} - \mathbf{s}_\lambda, \lambda_j^{\mathbf{y}}(\mathbf{\Phi}(\cdot - \mathbf{y})))_{\mathcal{N}_{\mathbf{\Phi}}(\Omega)} \\ &= \sum_{j=1}^{N} \alpha_j \lambda_j (\mathbf{f} - \mathbf{s}_\lambda) \\ &= \sum_{j=1}^{N} \alpha_j \left[\lambda_j(\mathbf{f}) - \lambda_j(\mathbf{s}_\lambda)\right] \\ &= 0,\end{aligned}$$

where theorem 4.3 has been applied. Then the Pythagorean theorem gives

$$\|\mathbf{s}_\lambda\|^2_{\mathcal{N}_{\mathbf{\Phi}}(\Omega)} + \|\mathbf{f} - \mathbf{s}_\lambda\|^2_{\mathcal{N}_{\mathbf{\Phi}}(\Omega)} = \|\mathbf{f}\|^2_{\mathcal{N}_{\mathbf{\Phi}}(\Omega)},$$

which finishes the proof. □

## 5.2. Native Spaces of Combined Kernels

In the previous section we provided tools for the optimal recovery of the solution of a partial differential equation. Before we can establish the discretization method for Darcy's problem, we introduce combined kernels. These kernels are used to built the approximating function. We are also interested in their native spaces.

Instead of having $\mathbf{u}$ for the velocity and $p$ for the pressure separately, we introduce the $(d+1)$-dimensional combined vector $\mathbf{v} = (\mathbf{u}, p)$. To model the velocity, we will use a divergence-free kernel. The approximating function of the pressure is built from a general scalar-valued positive definite kernel. These two kernels are combined in one kernel to build the approximating function for $\mathbf{v}$.

Let $\Omega \subseteq \mathbb{R}^d$ and $\phi, \psi : \Omega \times \Omega \to \mathbb{R}$ be positive definite kernels, where $\phi$ is at least twice continuously differentiable. Then, we define the combined kernel

$$\widetilde{\mathbf{\Phi}} : \mathbb{R}^d \to \mathbb{R}^{(d+1)\times(d+1)}, \qquad \widetilde{\mathbf{\Phi}} := \begin{pmatrix} \mathbf{\Phi}_{\text{div}} & \mathbf{0} \\ \mathbf{0} & \psi \end{pmatrix} =: \mathbf{\Phi}_{\text{div}} \otimes \psi,$$

where $\mathbf{\Phi}_{\text{div}} := (-\Delta I + \nabla\nabla^T)\phi$ is the matrix-valued kernel introduced in section 2.4.4.

If $\Omega = \mathbb{R}^d$ and if $\phi$ and $\psi$ are translation invariant, then the following result establishes the native space of $\widetilde{\mathbf{\Phi}}$.

**Theorem 5.3.** *Suppose $\phi \in C^2(\mathbb{R}^d) \cap W_1^2(\mathbb{R}^d)$ is a positive definite function. Define*

$\mathbf{\Phi}_{\text{div}} = (-\Delta I + \nabla\nabla^T)\phi$. *Let* $\widetilde{\mathbf{\Phi}} = \mathbf{\Phi}_{\text{div}} \otimes \psi$ *with a positive definite function* $\psi \in C(\mathbb{R}^d) \cap L_1(\mathbb{R}^d)$. *Then,*

$$\mathcal{N}_{\widetilde{\mathbf{\Phi}}}(\mathbb{R}^d) = \mathcal{N}_{\mathbf{\Phi}_{\text{div}}}(\mathbb{R}^d) \times \mathcal{N}_{\psi}(\mathbb{R}^d)$$

*with norm for* $\mathbf{f} = (\mathbf{f_u}, f_p)$ *given by*

$$\begin{aligned} \|\mathbf{f}\|^2_{\mathcal{N}_{\widetilde{\mathbf{\Phi}}}(\mathbb{R}^d)} &= \|\mathbf{f_u}\|^2_{\mathcal{N}_{\mathbf{\Phi}_{\text{div}}}(\mathbb{R}^d)} + \|f_p\|^2_{\mathcal{N}_{\psi}(\mathbb{R}^d)} \\ &= (2\pi)^{-d/2} \int_{\mathbb{R}^d} \left[ \frac{\|\widehat{\mathbf{f}_{\mathbf{u}}}(\boldsymbol{\omega})\|_2^2}{\|\boldsymbol{\omega}\|_2^2 \widehat{\phi}(\boldsymbol{\omega})} + \frac{|\widehat{f_p}(\boldsymbol{\omega})|^2}{\widehat{\psi}(\boldsymbol{\omega})} \right] d\boldsymbol{\omega}. \end{aligned}$$

*Proof.* First of all we show that the matrix-valued function $\widetilde{\mathbf{\Phi}}$ is positive definite in the sense of definition 2.6. Since $\mathbf{\Phi}_{\text{div}}$ and $\psi$ are positive definite functions, the kernel $\widetilde{\mathbf{\Phi}}$ is continuous, even and symmetric in its arguments. Furthermore, $\widetilde{\mathbf{\Phi}}$ is symmetric in the usual matrix sense, due to its structure and the symmetry of $\mathbf{\Phi}_{\text{div}}$. Finally, for $\boldsymbol{\alpha}_j = (\boldsymbol{\beta}_j, \gamma_j)^T \in \mathbb{R}^{d+1}$, where not all $\boldsymbol{\alpha}_j$ are vanishing and pair-wise distinct $\mathbf{x}_j \in \mathbb{R}^d$, we have

$$\begin{aligned} \sum_{j,k=1} \boldsymbol{\alpha}_j^T \widetilde{\mathbf{\Phi}}(\mathbf{x}_j - \mathbf{x}_k)\boldsymbol{\alpha}_k &= \sum_{j,k=1} \boldsymbol{\alpha}_j^T \begin{pmatrix} \mathbf{\Phi}_{\text{div}} & \mathbf{0} \\ \mathbf{0} & \psi \end{pmatrix} (\mathbf{x}_j - \mathbf{x}_k)\boldsymbol{\alpha}_k \\ &= \sum_{j,k=1}^{N} \boldsymbol{\beta}_j^T \mathbf{\Phi}_{\text{div}}(\mathbf{x}_j - \mathbf{x}_k)\boldsymbol{\beta}_k + \sum_{j,k=1}^{N} \gamma_j \gamma_k \psi(\mathbf{x}_j - \mathbf{x}_k) > 0 \end{aligned}$$

since $\mathbf{\Phi}_{\text{div}}$ and $\psi$ are positive definite functions. Hence $\widetilde{\mathbf{\Phi}}$ is positive definite.

Let $\mathbf{f} = \sum_{j=1}^{N} \widetilde{\mathbf{\Phi}}(\cdot - \mathbf{x}_j)\boldsymbol{\alpha}_j$ be an arbitrary function in $\mathbf{F}_{\widetilde{\mathbf{\Phi}}}(\mathbb{R}^d)$, where $\mathbf{F}_{\widetilde{\mathbf{\Phi}}}(\mathbb{R}^d)$ is defined analogues to the space $\mathbf{F}_{\mathbf{\Phi}}(\mathbb{R}^d)$ for the kernel $\widetilde{\mathbf{\Phi}}$, see section 4.2.2. Following the same idea as above, we split the function $\mathbf{f}$ in $\mathbf{f} = (\mathbf{f_u}, f_p)$ and therefore

$$\|\mathbf{f}\|^2_{\mathcal{N}_{\widetilde{\mathbf{\Phi}}}(\mathbb{R}^d)} = \|\mathbf{f_u}\|^2_{\mathcal{N}_{\mathbf{\Phi}_{\text{div}}}(\mathbb{R}^d)} + \|f_p\|^2_{\mathcal{N}_{\psi}(\mathbb{R}^d)}.$$

Hence, on $\mathbf{F}_{\widetilde{\mathbf{\Phi}}}(\mathbb{R}^d) \subseteq \mathcal{N}_{\mathbf{\Phi}_{\text{div}}}(\mathbb{R}^d) \times \mathcal{N}_{\psi}(\mathbb{R}^d)$ both norms are equal. By completion this means in particular that $\mathcal{N}_{\widetilde{\mathbf{\Phi}}}(\mathbb{R}^d) \subseteq \mathcal{N}_{\mathbf{\Phi}_{\text{div}}}(\mathbb{R}^d) \times \mathcal{N}_{\psi}(\mathbb{R}^d)$ with equal norms. Now suppose that there exists an $\mathbf{f} \in \mathcal{N}_{\mathbf{\Phi}_{\text{div}}}(\mathbb{R}^d) \times \mathcal{N}_{\psi}(\mathbb{R}^d)$ which is orthogonal to $\mathcal{N}_{\widetilde{\mathbf{\Phi}}}(\mathbb{R}^d)$, that is

$$\begin{aligned} 0 &= (\mathbf{f}, \widetilde{\mathbf{\Phi}}(\cdot - \mathbf{x})\boldsymbol{\alpha})_{\mathcal{N}_{\mathbf{\Phi}_{\text{div}}}(\mathbb{R}^d) \times \mathcal{N}_{\psi}(\mathbb{R}^d)} \\ &= (\mathbf{f_u}, \mathbf{\Phi}_{\text{div}}(\cdot - \mathbf{x})\boldsymbol{\beta})_{\mathcal{N}_{\mathbf{\Phi}_{\text{div}}}(\mathbb{R}^d)} + \gamma(f_p, \psi(\cdot - \mathbf{x}))_{\mathcal{N}_{\psi}(\mathbb{R}^d)} \\ &= \beta^T \mathbf{f_u}(\mathbf{x}) + \gamma f_p(\mathbf{x}) \end{aligned}$$

for all $\boldsymbol{\alpha} = (\boldsymbol{\beta}, \gamma) \in \mathbb{R}^{d+1}$. Therefore we have that $\mathbf{f_u}$ and $f_p$ are identically zero, which finishes the proof. □

For us, it is important that for specific functions $\phi$ and $\psi$ these native spaces coincide with Sobolev-like spaces with equivalent norms.

**Corollary 5.4.** *Assume $\phi$ generates $H^{\tau+1}(\mathbb{R}^d)$ and $\psi$ generates $H^\rho(\mathbb{R}^d)$. Then,*

$$\mathcal{N}_{\widetilde{\mathbf{\Phi}}}(\mathbb{R}^d) = \widetilde{\mathbf{H}}^\tau(\mathbb{R}^d; \operatorname{div}) \times H^\rho(\mathbb{R}^d).$$

*Proof.* This follows directly from $\mathcal{N}_{\widetilde{\mathbf{\Phi}}}(\mathbb{R}^d) = \mathcal{N}_{\mathbf{\Phi}_{\operatorname{div}}}(\mathbb{R}^d) \times \mathcal{N}_\psi(\mathbb{R}^d)$ and corollary 4.15 for the velocity part and corollary 4.11 for the pressure. □

## 5.3. The Approximation Scheme

All tools necessary to establish the analytically divergence-free discretization method for Darcy's problem are now available. Thus we can apply optimal recovery to approximate the solution of Darcy's problem.

Firstly, we establish functionals to discretise Darcy's problem

$$\mathbf{u} + K\nabla p = \mathbf{f} \qquad \text{in } \Omega, \tag{5.3}$$

$$\nabla \cdot \mathbf{u} = 0 \qquad \text{in } \Omega, \tag{5.4}$$

$$\mathbf{u} \cdot \mathbf{n} = \mathbf{g} \cdot \mathbf{n} \qquad \text{on } \partial\Omega \tag{5.5}$$

by collocation. Due to the choice of the combined kernel $\widetilde{\mathbf{\Phi}}$, we have that the approximation of the velocity $\mathbf{u}$ is analytically divergence-free. Hence we only need to employ functionals for (5.3) and (5.5) while (5.4) is automatically satisfied.

We pick discretization points $X = \{\mathbf{x}_1, \dots, \mathbf{x}_N\} \subseteq \Omega$ in the interior and $Y = \{\mathbf{y}_1, \dots, \mathbf{y}_M\} \subseteq \partial\Omega$ on the boundary. For $\mathbf{v} := (\mathbf{u}, p)$ we define the functionals

$$\begin{aligned}\lambda_j^{(i)}(\mathbf{v}) &= u_i(\mathbf{x}_j) + (K\nabla p)_i(\mathbf{x}_j) \\ &= u_i(\mathbf{x}_j) + \sum_{k=1}^{d} K_{ik}(\mathbf{x}_j)\partial_k p(\mathbf{x}_j), \qquad 1 \le i \le d,\ 1 \le j \le N =: N_i \end{aligned} \tag{5.6}$$

$$\lambda_j^{(d+1)}(\mathbf{v}) = \sum_{k=1}^{d} u_k(\mathbf{y}_j) n_k(\mathbf{y}_j), \qquad 1 \le j \le M =: N_{d+1}. \tag{5.7}$$

With these functionals the approximating function according to proposition 5.1 becomes

$$\mathbf{s}_{\mathbf{v}}(\mathbf{x}) := \sum_{k=1}^{d+1} \sum_{j=1}^{N_k} \alpha_j^{(k)} \lambda_j^{(k),\mathbf{y}}(\widetilde{\mathbf{\Phi}}(\mathbf{x} - \mathbf{y})), \tag{5.8}$$

where $\mathbf{s}_{\mathbf{v}} = (\mathbf{s}_{\mathbf{u}}, s_p)$. Here, $\mathbf{s}_{\mathbf{u}}$ approximates the velocity $\mathbf{u}$ and $s_p$ the pressure $p$.

The coefficients of the approximating function are determined via the collocation conditions

$$\lambda_j^{(i)}(\mathbf{s_v}) = \lambda_j^{(i)}(\mathbf{v}) = f_i(\mathbf{x}_j) \qquad 1 \le i \le d,\ 1 \le j \le N \tag{5.9}$$

$$\lambda_j^{(d+1)}(\mathbf{s_v}) = \lambda_j^{(d+1)}(\mathbf{v}) = \mathbf{g}(\mathbf{y}_j) \cdot \mathbf{n}(\mathbf{y}_j) \qquad 1 \le j \le M. \tag{5.10}$$

The following result ensures that the so defined functionals are linearly independent which is the main assumption in lemma 5.1.

**Theorem 5.5.** *Let $\Omega \subseteq \mathbb{R}^d$, with a Lipschitz boundary and $K$ be continuous. Assume that the generating functions $\phi, \psi : \mathbb{R}^d \to \mathbb{R}$ are positive definite and chosen such that $\mathcal{N}_{\widetilde{\mathbf{\Phi}}}(\mathbb{R}^d) = \widetilde{\mathbf{H}}^\tau(\mathbb{R}^d; \mathrm{div}) \times H^{\tau+1}(\mathbb{R}^d)$ with $\tau > d/2$. Then, the approximating function $\mathbf{s_v} = (\mathbf{s_u}, s_p)^T$ from (5.8) is well-defined and uniquely determined by the collocation conditions (5.9) and (5.10). It satisfies $L\mathbf{s_v}(\mathbf{x}_j) = \mathbf{f}(\mathbf{x}_j)$ with $L\mathbf{v} := \mathbf{u} + K\nabla p$ and $\mathbf{s_u}(\mathbf{y}_j) \cdot \mathbf{n}(\mathbf{y}_j) = \mathbf{g}(\mathbf{y}_j) \cdot \mathbf{n}(\mathbf{y}_j)$. Furthermore, we have $\nabla \cdot \mathbf{s_u} = 0$ in $\mathbb{R}^d$.*

*Proof.* Since $\tau+1 > d/2+1$, we have $\phi, \psi \in C^2(\mathbb{R}^d)$ and thus $\widetilde{\mathbf{\Phi}} \in C(\mathbb{R}^d)$. Hence, the kernel is sufficiently smooth. Since $\mathcal{N}_{\widetilde{\mathbf{\Phi}}}$ is a reproducing kernel Hilbert space, the point evaluation functionals indeed belong to its dual, cf. theorem 4.2 and corollary 5.4. Furthermore, the Sobolev embedding theorem and the smoothness of the boundary guaranty that the functions $\mathbf{u}$, $p$ and $\mathbf{n}$ are sufficiently smooth. Therefore all functionals indeed belong to the dual of the native space. Thus, we only have to show that the functionals are linearly independent over $\mathcal{N}_{\widetilde{\mathbf{\Phi}}}(\mathbb{R}^d) = \widetilde{\mathbf{H}}^\tau(\mathbb{R}^d; \mathrm{div}) \times H^{\tau+1}(\mathbb{R}^d)$.

Let us assume that there are coefficients $\alpha_j^{(k)} \in \mathbb{R}$ such that

$$\sum_{k=1}^{d+1} \sum_{j=1}^{N_k} \alpha_j^{(k)} \lambda_j^{(k)}(\boldsymbol{\gamma}) = 0 \tag{5.11}$$

for all $\boldsymbol{\gamma} \in \mathcal{N}_{\widetilde{\mathbf{\Phi}}}(\mathbb{R}^d)$. We will now pick a specific test function $\boldsymbol{\gamma}$ for every index pair $(i, \ell)$. First of all we choose $\boldsymbol{\gamma}$ to have compact support such that the only data site contained in the support of this specific $\boldsymbol{\gamma}$ is $\mathbf{x}_i$, for $1 \le \ell \le d$, or $\mathbf{y}_i$, for $\ell = d+1$. Hence, in the first case, (5.11) reduces to

$$0 = \sum_{k=1}^{d} \alpha_i^{(k)} \lambda_i^{(k)}(\boldsymbol{\gamma}) = \sum_{k=1}^{d} \alpha_i^{(k)} (L\boldsymbol{\gamma})_k(\mathbf{x}_i).$$

Since we have not yet exploited the second index $\ell$, we can now modify $\boldsymbol{\gamma}$ such that $(L\boldsymbol{\gamma})_k(\mathbf{x}_i) = \delta_{k,\ell}$, which gives $\alpha_i^{(\ell)} = 0$. Since we can do the same in the case $\ell = d+1$, we see that all coefficients have to be zero, showing that the functionals are linearly independent. □

This establishes the desired approximation scheme for Darcy's problem.

## 5.4. The Two Dimensional Scheme

To clarify the approximation scheme introduced in the previous section, we now give details about the two dimensional case. Let $X = \{\mathbf{x}_1, \dots, \mathbf{x}_N\} \subseteq \Omega$ and $Y = \{\mathbf{y}_1, \dots, \mathbf{y}_M\} \subseteq \partial\Omega$ be the collocation points, where $\Omega \subseteq \mathbb{R}^2$.

First of all we need to work out the combined kernel explicitly, i. e.

$$\widetilde{\mathbf{\Phi}} = \begin{pmatrix} -\partial_{22}\phi & \partial_{12}\phi & 0 \\ \partial_{12}\phi & -\partial_{11}\phi & 0 \\ 0 & 0 & \psi \end{pmatrix}$$

for sufficiently smooth, positive definite functions $\phi$, $\psi : \mathbb{R}^d \to \mathbb{R}$. For instance, Wendland functions could be used for $\phi$ and $\psi$.

The next step is to work out the functionals defined in the previous section, here we denote the inner product by simply adding a '$\cdot$' at the end of the functional. Furthermore, the symbol $\delta_{\mathbf{x}}$ refers to the point-evaluation functional at the point $\mathbf{x}$. Then we can denote the functionals for Darcy's problem via

$$\lambda_j^{(1)} = \begin{pmatrix} \delta_{\mathbf{x}_j} \\ 0 \\ K_{11}(\mathbf{x}_j)\delta_{\mathbf{x}_j} \circ \partial_1 + K_{12}(\mathbf{x}_j)\delta_{\mathbf{x}_j} \circ \partial_2 \end{pmatrix}, \qquad 1 \le j \le N$$

$$\lambda_j^{(2)} = \begin{pmatrix} 0 \\ \delta_{\mathbf{x}_j} \\ K_{12}(\mathbf{x}_j)\delta_{\mathbf{x}_j} \circ \partial_1 + K_{22}(\mathbf{x}_j)\delta_{\mathbf{x}_j} \circ \partial_2 \end{pmatrix}, \qquad 1 \le j \le N$$

$$\lambda_j^{(3)} = \delta_{\mathbf{y}_i} \circ \begin{pmatrix} n_1 \\ n_2 \\ 0 \end{pmatrix} \cdot, \qquad 1 \le i \le M.$$

The approximating function is given by applying these functionals to $\widetilde{\mathbf{\Phi}}$. Thus

$$\begin{aligned}
\mathbf{s_v}(\mathbf{x}) &= \sum_{j=1}^{N} \left\{ \alpha_j^{(1)} \lambda_j^{(1),\mathbf{y}} \left( \widetilde{\mathbf{\Phi}}(\cdot - \mathbf{y}) \right) + \alpha_j^{(2)} \lambda_j^{(2),\mathbf{y}} \left( \widetilde{\mathbf{\Phi}}(\cdot - \mathbf{y}) \right) \right\} + \sum_{j=1}^{M} \alpha_j^{(3)} \lambda_j^{(3),\mathbf{y}} \left( \widetilde{\mathbf{\Phi}}(\cdot - \mathbf{y}) \right) \\
&= \sum_{j=1}^{N} \alpha_j^{(1)} \begin{pmatrix} -\partial_{22}\phi(\cdot - \mathbf{x}_j) \\ \partial_{12}\phi(\cdot - \mathbf{x}_j) \\ -K_{11}(\mathbf{x}_j)\partial_1\psi(\cdot - \mathbf{x}_j) - K_{12}(\mathbf{x}_j)\partial_2\psi(\cdot - \mathbf{x}_j) \end{pmatrix} \\
&\quad + \sum_{j=1}^{N} \alpha_j^{(2)} \begin{pmatrix} \partial_{12}\phi(\cdot - \mathbf{x}_j) \\ -\partial_{11}\phi(\cdot - \mathbf{x}_j) \\ -K_{12}(\mathbf{x}_j)\partial_1\psi(\cdot - \mathbf{x}_j) - K_{22}(\mathbf{x}_j)\partial_2\psi(\cdot - \mathbf{x}_j) \end{pmatrix} \\
&\quad + \sum_{j=1}^{M} \alpha_j^{(3)} \begin{pmatrix} -n_1(\mathbf{y}_j)\partial_{22}\phi(\cdot - \mathbf{y}_j) + n_2(\mathbf{y}_j)\partial_{12}\phi(\cdot - \mathbf{y}_j) \\ n_1(\mathbf{y}_j)\partial_{12}\phi(\cdot - \mathbf{y}_j) - n_2(\mathbf{y}_j)\partial_{11}\phi(\cdot - \mathbf{y}_j) \\ 0 \end{pmatrix}.
\end{aligned}$$

We have the collocation conditions $\lambda_j^{(1)}(\mathbf{s_v}) = f_1(\mathbf{x}_j)$, $\lambda_j^{(2)}(\mathbf{s_v}) = f_2(\mathbf{x}_j)$ and $\lambda_i^{(3)}(\mathbf{s_v}) = g(\mathbf{y}_i) \cdot \mathbf{n}(\mathbf{y}_i)$, where $1 \leq j \leq N$ and $1 \leq i \leq M$. To work out the $\alpha_j^{(k)}$ and with it the approximating function, we need to solve the following linear system of equations

$$A \begin{pmatrix} \boldsymbol{\alpha}^{(1)} \\ \boldsymbol{\alpha}^{(2)} \\ \boldsymbol{\alpha}^{(3)} \end{pmatrix} = \begin{pmatrix} \mathbf{f}_1 \\ \mathbf{f}_2 \\ \mathbf{g} \cdot \mathbf{n} \end{pmatrix},$$

where the symmetric $(2N + M) \times (2N + M)$-matrix

$$A = \begin{pmatrix} A^{(1,1)} & A^{(1,2)} & A^{(1,3)} \\ A^{(2,1)} & A^{(2,2)} & A^{(2,3)} \\ A^{(3,1)} & A^{(3,2)} & A^{(3,3)} \end{pmatrix}$$

consists of nine sub-matrices. The values of those sub-matrices are given by simply applying the functionals twice to the kernel in all possible combinations. Thus the sub-matrices

are given by

$$(A^{(1,1)})_{ij} = \lambda_i^{(1),\mathbf{x}}\left(\lambda_j^{(1),\mathbf{y}}(\widetilde{\mathbf{\Phi}}(\mathbf{x}-\mathbf{y}))\right) = -\partial_{22}\phi(\mathbf{x}_i-\mathbf{x}_j) - K_{11}(\mathbf{x}_i)K_{11}(\mathbf{x}_j)\partial_{11}\psi(\mathbf{x}_i-\mathbf{x}_j)$$
$$-(K_{11}(\mathbf{x}_i)K_{12}(\mathbf{x}_j)+K_{12}(\mathbf{x}_i)K_{11}(\mathbf{x}_j))\partial_{12}\psi(\mathbf{x}_i-\mathbf{x}_j) - K_{12}(\mathbf{x}_i)K_{12}(\mathbf{x}_j)\partial_{22}\psi(\mathbf{x}_i-\mathbf{x}_j)$$
$$(A^{(1,2)})_{ij} = (A^{(2,1)})_{ji} = \lambda_i^{(1),\mathbf{x}}\left(\lambda_j^{(2),\mathbf{y}}(\widetilde{\mathbf{\Phi}}(\mathbf{x}-\mathbf{y}))\right)$$
$$= \partial_{12}\phi(\mathbf{x}_i-\mathbf{x}_j) - K_{12}(\mathbf{x}_i)K_{11}(\mathbf{x}_j)\partial_{11}\psi(\mathbf{x}_i-\mathbf{x}_j) - (K_{12}(\mathbf{x}_i)K_{12}(\mathbf{x}_j)$$
$$+K_{22}(\mathbf{x}_i)K_{11}(\mathbf{x}_j))\partial_{12}\psi(\mathbf{x}_i-\mathbf{x}_j) - K_{22}(\mathbf{x}_i)K_{12}(\mathbf{x}_j)\partial_{22}\psi(\mathbf{x}_i-\mathbf{x}_j)$$
$$(A^{(2,2)})_{ij} = \lambda_i^{(2),\mathbf{x}}\left(\lambda_j^{(2),\mathbf{y}}(\widetilde{\mathbf{\Phi}}(\mathbf{x}-\mathbf{y}))\right) = -\partial_{11}\phi(\mathbf{x}_i-\mathbf{x}_j) - K_{12}(\mathbf{x}_i)K_{12}(\mathbf{x}_j)\partial_{11}\psi(\mathbf{x}_i-\mathbf{x}_j)$$
$$-(K_{12}(\mathbf{x}_i)K_{22}(\mathbf{x}_j)+K_{22}(\mathbf{x}_i)K_{12}(\mathbf{x}_j))\partial_{12}\psi(\mathbf{x}_i-\mathbf{x}_j) - K_{22}(\mathbf{x}_i)K_{22}(\mathbf{x}_j)\partial_{22}\psi(\mathbf{x}_i-\mathbf{x}_j),$$

where $1 \le i,j \le N$,

$$(A^{(1,3)})_{ij} = (A^{(3,1)})_{ji} = \lambda_i^{(1),\mathbf{x}}\left(\lambda_j^{(3),\mathbf{y}}(\widetilde{\mathbf{\Phi}}(\mathbf{x}-\mathbf{y}))\right)$$
$$= -n_1(\mathbf{y}_i)\partial_{22}\phi(\mathbf{y}_i-\mathbf{x}_j) + n_2(\mathbf{y}_i)\partial_{12}\phi(\mathbf{y}_i-\mathbf{x}_j)$$
$$(A^{(2,3)})_{ij} = (A^{(3,2)})_{ji} = \lambda_i^{(2),\mathbf{x}}\left(\lambda_j^{(3),\mathbf{y}}(\widetilde{\mathbf{\Phi}}(\mathbf{x}-\mathbf{y}))\right)$$
$$= n_1(\mathbf{y}_i)\partial_{12}\phi(\mathbf{y}_i-\mathbf{x}_j) - n_2(\mathbf{y}_i)\partial_{11}\phi(\mathbf{y}_i-\mathbf{x}_j),$$

where $1 \le i \le N$, $1 \le j \le M$ and

$$(A^{(3,3)})_{ij} = \lambda_i^{(3),\mathbf{x}}\left(\lambda_j^{(3),\mathbf{y}}(\widetilde{\mathbf{\Phi}}(\mathbf{x}-\mathbf{y}))\right) = -n_1(\mathbf{y}_i)n_1(\mathbf{y}_j)\partial_{22}\phi(\mathbf{y}_i-\mathbf{y}_j)$$
$$+n_1(\mathbf{y}_i)n_2(\mathbf{y}_j)\partial_{12}\phi(\mathbf{y}_i-\mathbf{y}_j) + n_1(\mathbf{y}_j)n_2(\mathbf{y}_i)\partial_{12}\phi(\mathbf{y}_i-\mathbf{y}_j) - n_2(\mathbf{y}_i)n_2(\mathbf{y}_j)\partial_{11}\phi(\mathbf{y}_i-\mathbf{y}_j),$$

where $1 \le i,j \le M$.

With the information above, a solver for Darcy's problem can be implemented. An efficient solver for linear systems of equations is required. Note that the matrix $A$ is symmetric positive definite, but large, fully occupied and maybe ill-conditioned. The approximated solution is given via $\mathbf{s_u}$ for the velocity and $s_p$ for the pressure.

# 6. Error Analysis

In the previous chapter the discretization scheme for Darcy's problem has been introduced. We now present and prove the error analysis, i. e. we want to investigate how close our approximation is to the true solution and how well the method converges.

We will look at the difference between the true solution and the approximating function in a Sobolev norm. We will split it into an estimate inside the domain and an estimate on the boundary. Both will be bounded separately. The main result is then obtained by combining these two results. The idea of the proof is to apply sampling inequalities to the regularity result of Darcy's problem. An extension from the domain to $\mathbb{R}^d$ is required to enable us to apply the norm equivalence between the Sobolev space and the native space. In the native space we can use the stability results.

Again, we follow the framework presented in [55]. Our error analysis can also be found in [47].

## 6.1. Extension Operator

Since we mainly work on bounded domains, but use globally defined kernels we need to extend our local functions to global ones. The extension operator enables us to apply results from the globally defined native space. The following result is taken from [55].

**Proposition 6.1.** *Let $d = 2, 3$. Let $\tau, \rho \geq 0$ and let $\Omega \subseteq \mathbb{R}^d$ be a simply-connected domain with $C^{k,1}$ boundary, where $k \geq \tau$ is an integer. Then there exists a continuous operator $\mathbf{E} = (\widetilde{\mathbf{E}}_{\mathrm{div}}, E_S) : \mathbf{H}^\tau(\Omega; \mathrm{div}) \times H^\rho(\Omega) \to \widetilde{\mathbf{H}}^\tau(\mathbb{R}^d; \mathrm{div}) \times H^\rho(\mathbb{R}^d)$ such that $\mathbf{E}\mathbf{v}|_\Omega = \mathbf{v}|_\Omega$ for all $\mathbf{v} = (\mathbf{u}, p) \in \mathbf{H}^\tau(\Omega; \mathrm{div}) \times H^\rho(\Omega)$ and*

$$\|\widetilde{\mathbf{E}}_{\mathrm{div}}\mathbf{u}\|_{\widetilde{\mathbf{H}}^\tau(\mathbb{R}^d)} + \|E_S p\|_{H^\rho(\mathbb{R}^d)} \leq c\left(\|\mathbf{u}\|_{\mathbf{H}^\tau(\Omega)} + \|p\|_{H^\rho(\Omega)}\right).$$

The extension operator for the pressure part is the standard Stein extension operator $E_S$, see [48].

## 6.2. Error Estimates

Our error analysis is mainly based on a 'shift'-type theorem for the analytical solution of Darcy's problem which is obtained from a corresponding result for elliptic problems with Neumann boundary conditions, see sections 3.4 and 3.5.

Using the notation $\mathbf{v} = (\mathbf{u}, p)$ and $L\mathbf{v} := \mathbf{u} + K\nabla p$, the estimate from theorem 3.2 can be rewritten in the form

$$\|\mathbf{u}\|_{\mathbf{W}_r^{\eta+1}(\Omega)} + \|p\|_{W_r^{\eta+2}(\Omega)/\mathbb{R}} \leq c\left(\|L\mathbf{v}\|_{\mathbf{W}_r^{\eta+1}(\Omega)} + \|\mathbf{u}\cdot\mathbf{n}\|_{W_r^{\eta+1-1/r}(\partial\Omega)}\right)$$

for all $0 \leq \eta \leq \tau$ and all $1 < r < \infty$. We will use this for $\mathbf{v} - \mathbf{s_v}$ instead of $\mathbf{v}$, i. e.

$$\begin{aligned}&\|\mathbf{u} - \mathbf{s_u}\|_{\mathbf{W}_r^{\eta+1}(\Omega)} + \|p - s_p\|_{W_r^{\eta+2}(\Omega)/\mathbb{R}} \\ &\quad\leq c\left(\|L(\mathbf{v} - \mathbf{s_v})\|_{\mathbf{W}_r^{\eta+1}(\Omega)} + \|(\mathbf{u} - \mathbf{s_u})\cdot\mathbf{n}\|_{W_r^{\eta+1-1/r}(\partial\Omega)}\right). \qquad (6.1)\end{aligned}$$

To estimate the two terms on the right hand side of the last equation, we first observe that we have

$$\begin{aligned}(L\mathbf{v} - L\mathbf{s_v})(\mathbf{x}_j) &= \mathbf{0}, \qquad 1 \leq j \leq N,\\ (\mathbf{u} - \mathbf{s_u})\cdot\mathbf{n}(\mathbf{y}_j) &= 0, \qquad 1 \leq j \leq M.\end{aligned}$$

Hence, we are dealing with smooth functions, which have a large number of zeros. In the first case we have functions defined on a bounded region of $\mathbb{R}^d$, while in the second case we are dealing with functions on a manifold. For such functions, we can apply the so called *sampling inequalities*. To state them, we have to introduce a measure for the data density on $\Omega$ and $\partial\Omega$. In the first case we shall use the *fill distance* defined by

$$h_{X,\Omega} := \sup_{\mathbf{x}\in\Omega}\min_{\mathbf{x}_j\in X}\|\mathbf{x} - \mathbf{x}_j\|_2.$$

We start by estimating the first norm on the right hand side of (6.1). After this we will give the estimate for the second norm and finish this chapter with the main result.

### 6.2.1. Error Estimates Inside the Domain

The following result is the first sampling inequality. It comes from [4, 41, 42], and in its vector-valued form for fractional order Sobolev spaces from [55].

**Lemma 6.2.** *Let $1 < r < \infty$, and $\tau, \eta \in \mathbb{R}$ with $\tau > d/2$ and $0 \leq \eta \leq \tau - d(1/2 - 1/r)_+$. Suppose $\Omega \subseteq \mathbb{R}^d$ is a bounded domain having a Lipschitz boundary. Let $X \subseteq \Omega$ be a discrete set with fill distance $h_{X,\Omega}$ sufficiently small. Assume that $\mathbf{u} \in \mathbf{H}^\tau(\Omega)$ satisfies*

$\mathbf{u}|_X = \mathbf{0}$. *Then we also have*

$$\|\mathbf{u}\|_{\mathbf{W}_r^\eta(\Omega)} \leq c h_{X,\Omega}^{\tau-\eta-d(1/2-1/r)_+} \|\mathbf{u}\|_{\mathbf{H}^\tau(\Omega)}.$$

Let $\Omega$ have a $C^{k,1}$ boundary, $k \in \mathbb{N}$. Note that the boundary is also Lipschitz, i. e. $C^{0,1}$, since the first derivative is bounded and continuous.

With lemma 2.2 (1) we have that, if $\mathbf{u} \in \mathbf{H}^\tau(\Omega)$ then we have for $2 \leq r < \infty$ that $\mathbf{u} \in \mathbf{W}_r^{\tau-d/2+d/r}(\Omega)$. Hence $\mathbf{u} \in \mathbf{W}_r^\rho(\Omega)$, where $0 \leq \rho \leq \tau - d(1/2-1/r)_+$. If $1 < r \leq 2$ we have with lemma 2.2 (2) that $\mathbf{u} \in \mathbf{W}_r^\rho(\Omega)$, where $0 \leq \rho \leq \tau$.

Now we can prove the following estimate.

**Proposition 6.3.** *Let $\Omega$ be a bounded, simply connected, open subset of $\mathbb{R}^d$ with a $C^{\lceil\tau\rceil+1,1}$ boundary $\partial\Omega$ where $d = 2, 3$. Let permeability tensor $K = K_{ij}$ satisfy (3.6), $K = K^T$ and $K_{ij} \in H^{\tau+1}(\overline{\Omega})$. Assume that the data satisfy $\mathbf{f} \in \mathbf{H}^{\tau+1}(\Omega)$ and $\mathbf{g} \in \mathbf{H}^{\tau+1/2}(\partial\Omega)$. Suppose that the kernel $\widetilde{\mathbf{\Phi}}$ is chosen such that $\mathcal{N}_{\widetilde{\mathbf{\Phi}}}(\mathbb{R}^d) = \widetilde{\mathbf{H}}^\tau(\mathbb{R}^d; \mathrm{div}) \times H^{\tau+1}(\mathbb{R}^d)$ with $\tau > d/2$. Then, for $0 \leq \eta \leq \tau - d(1/2-1/r)_+ - 1$ and for $1 < r < \infty$ we have*

$$\|L\mathbf{v} - L\mathbf{s}_\mathbf{v}\|_{\mathbf{W}_r^{\eta+1}(\Omega)} \leq c h_{X,\Omega}^{\tau-\eta-1-d(1/2-1/r)_+} \left( \|\mathbf{f}\|_{\mathbf{H}^\tau(\Omega)} + \|\mathbf{g}\cdot\mathbf{n}\|_{\mathbf{H}^{\tau-1/2}(\partial\Omega)} \right).$$

*Proof.* First of all, we have with lemma 6.2 that

$$\|L\mathbf{v} - L\mathbf{s}_\mathbf{v}\|_{\mathbf{W}_r^{\eta+1}(\Omega)} \leq c h_{X,\Omega}^{\tau-\eta-1-d(1/2-1/r)_+} \|L\mathbf{v} - L\mathbf{s}_\mathbf{v}\|_{\mathbf{H}^\tau(\Omega)}.$$

To bound the norm we first extend the function $\mathbf{v}$ to $\mathbf{E}\mathbf{v} = (\widetilde{\mathbf{E}}_{\mathrm{div}}\mathbf{u}, E_S p) \in \widetilde{\mathbf{H}}^\tau(\mathbb{R}^d; \mathrm{div})$ $\times H^{\tau+1}(\mathbb{R}^d)$ and note that the generalised interpolant $\mathbf{s}_\mathbf{v}$ coincides with $\mathbf{s}_{\mathbf{E}\mathbf{v}}$ on $\Omega$. Furthermore, if we pick the representer $p$ for the pressure such that $\|p\|_{H^{\tau+1}(\Omega)} \geq \|p\|_{H^{\tau+1}(\Omega)/\mathbb{R}}$, i. e. $c = 0$ in (2.1), and use the properties of the extension operator then we have

$$\|L\mathbf{v} - L\mathbf{s}_\mathbf{v}\|_{\mathbf{H}^\tau(\Omega)} = \|L\mathbf{E}\mathbf{v} - L\mathbf{s}_{\mathbf{E}\mathbf{v}}\|_{\mathbf{H}^\tau(\Omega)},$$

cf. proposition 6.1. Applying the triangle inequality to the definition of the operator $L$ leads to the following bound

$$\begin{aligned}\|L\mathbf{v} - L\mathbf{s}_\mathbf{v}\|_{\mathbf{H}^\tau(\Omega)} &\leq \|\widetilde{\mathbf{E}}_{\mathrm{div}}\mathbf{u} - \mathbf{s}_{\widetilde{\mathbf{E}}_{\mathrm{div}}\mathbf{u}}\|_{\mathbf{H}^\tau(\Omega)} + \|K(\nabla E_S p - \nabla s_{E_S p})\|_{\mathbf{H}^\tau(\Omega)} \\ &\leq \|\widetilde{\mathbf{E}}_{\mathrm{div}}\mathbf{u} - \mathbf{s}_{\widetilde{\mathbf{E}}_{\mathrm{div}}\mathbf{u}}\|_{\mathbf{H}^\tau(\Omega)} + c\|E_S p - s_{E_S p}\|_{H^{\tau+1}(\Omega)},\end{aligned}$$

where we used the fact that the permeability tensor is bounded in $H^{\tau+1}(\overline{\Omega})$. After applying the properties of the extension operator, we can use the norm equivalence to the native space. In the native space we can apply the stability result given in corollary 5.2. Then,

we go back to the Sobolev space. Thus

$$\begin{aligned}
\|L\mathbf{v} - L\mathbf{s}_{\mathbf{v}}\|_{\mathbf{H}^\tau(\Omega)} &\leq \|\widetilde{\mathbf{E}}_{\mathrm{div}}\mathbf{u} - \mathbf{s}_{\widetilde{\mathbf{E}}_{\mathrm{div}}\mathbf{u}}\|_{\widetilde{\mathbf{H}}^\tau(\mathbb{R}^d)} + c\|E_S p - s_{E_S p}\|_{H^{\tau+1}(\mathbb{R}^d)} \\
&\leq c\|\mathbf{E}\mathbf{v} - \mathbf{s}_{\mathbf{E}\mathbf{v}}\|_{\mathcal{N}_{\widetilde{\mathbf{\Phi}}}(\mathbb{R}^d)} \\
&\leq c\|\mathbf{E}\mathbf{v}\|_{\mathcal{N}_{\widetilde{\mathbf{\Phi}}}(\mathbb{R}^d)} \\
&\leq c\left(\|\widetilde{\mathbf{E}}_{\mathrm{div}}\mathbf{u}\|_{\widetilde{\mathbf{H}}^\tau(\mathbb{R}^d)} + \|E_S p\|_{H^{\tau+1}(\mathbb{R}^d)}\right) \\
&\leq c\left(\|\mathbf{u}\|_{\mathbf{H}^\tau(\Omega)} + \|p\|_{H^{\tau+1}(\Omega)}\right) \\
&\leq c\left(\|\mathbf{f}\|_{\mathbf{H}^\tau(\Omega)} + \|\mathbf{g}\cdot\mathbf{n}\|_{\mathbf{H}^{\tau-1/2}(\partial\Omega)}\right),
\end{aligned}$$

where theorem 3.2 has been applied in the last step. □

### 6.2.2. Error Estimates on the Boundary

To introduce a measure on the boundary, we follow ideas from [21, 55]. Let $\partial\Omega = \cup_{j=1}^{J} V_j$, where $V_j \subseteq \partial\Omega$ are relatively open sets. Furthermore,

$$\varphi_j : B \to V_j,$$

where $\varphi_j$ is a $C^{k,s}$-diffeomorphism and $B = B(\mathbf{0}, 1)$ denotes the unit ball in $\mathbb{R}^{d-1}$. We will measure the density of the points $Y$ on $\partial\Omega$ by introducing

$$h_{Y,\partial\Omega} := \max_{1\leq j\leq J} h_{T_j,B}$$

with $T_j = \varphi_j^{-1}(Y \cap V_j) \subseteq B$ analogously to the definition of the fill distance. We assume that the atlas $V_j$ is fixed, i. e. we do not have to worry about the dependence of $h_{Y,\partial\Omega}$ on the atlas.

The standard trace theorem establishes that if $u \in H^\tau(\Omega)$ then $u \in H^{\tau-1/2}(\partial\Omega)$, cf. [57, Theorem 8.7]. If $\tau > d/2$, then this guarantees, in combination with the Sobolev embedding theorem, that $u$ is continuous on the boundary $\partial\Omega$.

To find the estimate on the boundary, we need a similar result as lemma 6.2 on manifolds. This has been done in [27] for the special case of $\partial\Omega$ being the sphere in $\mathbb{R}^d$ and in a more general context in [21]. We give an extended version which also deals with non-integer orders $\eta$, its proof can be found in [55].

**Lemma 6.4.** *Let $1 < r < \infty$ and $\tau = k + s > d/2$. Let $\Omega \subseteq \mathbb{R}^d$ be a bounded domain having a $C^{k,s}$ smooth boundary. Assume that $Y \subseteq \partial\Omega$ with $h_{Y,\partial\Omega}$ sufficiently small. Then there is a constant $c > 0$ such that for all $\mathbf{u} \in \mathbf{H}^\tau(\Omega)$ with $\mathbf{u}|_Y = 0$ we have for*

$0 \leq \eta \leq \tau - 1/2 - (d-1)(1/2 - 1/r)_+$ *that*

$$\|\mathbf{u}\|_{\mathbf{W}_r^\eta(\partial\Omega)} \leq c h_{Y,\partial\Omega}^{\tau-1/2-\eta-(d-1)(1/2-1/r)_+} \|\mathbf{u}\|_{\mathbf{H}^\tau(\Omega)}.$$

Now, the same procedure as the one employed in the proof of proposition 6.3 leads to the following result.

**Proposition 6.5.** *Let $d = 2, 3$. Assume that $\Omega$, $K$ and $\mathbf{f}, \mathbf{g}$ satisfy the smoothness assumptions of proposition 6.3. Suppose that the kernel $\widetilde{\mathbf{\Phi}}$ is chosen such that $\mathcal{N}_{\widetilde{\mathbf{\Phi}}}(\mathbb{R}^d) = \widetilde{\mathbf{H}}^\tau(\mathbb{R}^d; \operatorname{div}) \times H^{\tau+1}(\mathbb{R}^d)$ with $\tau > d/2$. Then,*

$$\begin{aligned}&\|(\mathbf{u} - \mathbf{s_u}) \cdot \mathbf{n}\|_{W_r^{\eta+1-1/r}(\partial\Omega)} \\ &\quad \leq c h_{Y,\partial\Omega}^{\tau-\eta-1-1/2+1/r-(d-1)(1/2-1/r)_+} \left( \|\mathbf{f}\|_{\mathbf{H}^\tau(\Omega)} + \|\mathbf{g} \cdot \mathbf{n}\|_{H^{\tau-1/2}(\partial\Omega)} \right)\end{aligned}$$

*with $c > 0$ independent of $\mathbf{u}$ and $\mathbf{s_u}$, where $1 < r < \infty$ and $0 \leq \eta \leq \tau - 1/2 - (d-1)(1/2 - 1/r)_+ - 1 + 1/r$.*

*Proof.* First of all, since the boundary of $\Omega$ is $C^{\lceil\tau\rceil+1,1}$ we can see, with the embedding theorem for Hölder spaces, that the boundary is also $C^{k,s}$, where $k \in \mathbb{N}_0$, $0 < s \leq 1$ such that $k + s = \tau + 1$, cf. [3, Theorem 8.6].

The domain $\Omega$ has a $C^{\lceil\tau\rceil+1,1}$ boundary, therefore the normals $\mathbf{n} \in \mathbf{C}^{\lceil\tau\rceil,1}(\partial\Omega)$ exist almost everywhere and can be extended to a vector field $\widetilde{\mathbf{n}} \in \mathbf{C}^{\lceil\tau\rceil,1}(\overline{\Omega})$ with $\widetilde{\mathbf{n}}|_{\partial\Omega} = \mathbf{n}$, cf. [22, section 1.1]. This means that $\mathbf{n} \in \mathbf{H}^{\lceil\tau\rceil}(\partial\Omega)$, since its derivatives up to order $\lceil\tau\rceil$ are bounded and continuous and

$$\|\mathbf{n}\|_{\mathbf{H}^{\lceil\tau\rceil}(\partial\Omega)} = \sum_{|\boldsymbol{\alpha}| \leq \lceil\tau\rceil} \int_{\partial\Omega} \|D^{\boldsymbol{\alpha}} \mathbf{n}(\mathbf{x})\|_2^2 \, d\mathbf{x} \leq c \sum_{|\boldsymbol{\alpha}| \leq \lceil\tau\rceil} \int_{\partial\Omega} d\mathbf{x} < \infty.$$

Similarly, we can see that $\widetilde{\mathbf{n}} \in \mathbf{H}^{\lceil\tau\rceil}(\overline{\Omega})$.

This enables us to apply lemma 6.4 to see that

$$\|(\mathbf{u} - \mathbf{s_u}) \cdot \mathbf{n}\|_{W_r^{\eta+1-1/r}(\partial\Omega)} \leq c h_{Y,\partial\Omega}^{\tau-\eta-1-1/2+1/r-(d-1)(1/2-1/r)_+} \|(\mathbf{u} - \mathbf{s_u}) \cdot \widetilde{\mathbf{n}}\|_{H^\tau(\Omega)}.$$

Then

$$\|(\mathbf{u} - \mathbf{s_u}) \cdot \widetilde{\mathbf{n}}\|_{H^\tau(\Omega)} \leq \|\widetilde{\mathbf{n}}\|_{\mathbf{H}^\tau(\Omega)} \|\mathbf{u} - \mathbf{s_u}\|_{\mathbf{H}^\tau(\Omega)} \leq c \|\mathbf{u} - \mathbf{s_u}\|_{\mathbf{H}^\tau(\Omega)}$$

and, according to the proof of proposition 6.3, also

$$\|\mathbf{u} - \mathbf{s_u}\|_{\mathbf{H}^\tau(\Omega)} \leq c \left( \|\mathbf{f}\|_{\mathbf{H}^\tau(\Omega)} + \|\mathbf{g} \cdot \mathbf{n}\|_{H^{\tau-1/2}(\partial\Omega)} \right);$$

our proof is complete. □

### 6.2.3. Main Result

Combining the results of the propositions 6.3 and 6.5 enables us to bound (6.1). Thus we have proven our main result.

**Theorem 6.6.** *Let $\Omega$ be a bounded, simply connected, open subset of $\mathbb{R}^d$, $d = 2, 3$, with a $C^{\lceil\tau\rceil+1,1}$ boundary $\partial\Omega$. Suppose that $\widetilde{\mathbf{\Phi}}$ is chosen such that its native space is $\mathcal{N}_{\widetilde{\mathbf{\Phi}}}(\mathbb{R}^d) = \widetilde{\mathbf{H}}^\tau(\mathbb{R}^d; \mathrm{div}) \times H^{\tau+1}(\mathbb{R}^d)$ and the permeability tensor $K = K_{ij}$ satisfies (3.6), $K = K^T$ and $K_{ij} \in H^{\tau+1}(\overline{\Omega})$. Furthermore, assume that the data satisfy $\mathbf{f} \in \mathbf{H}^{\tau+1}(\Omega)$ and $\mathbf{g} \in \mathbf{H}^{\tau+1/2}(\partial\Omega)$, where $\tau > d/2$. Then, the error between the true solution and the collocation approximation can be bounded by*

$$\begin{aligned}
&\|\mathbf{u} - \mathbf{s_u}\|_{\mathbf{W}_r^{\eta+1}(\Omega)} + \|p - s_p\|_{W_r^{\eta+2}(\Omega)/\mathbb{R}} \\
&\quad \le c\left(h_{X,\Omega}^{\tau-\eta-1-d(1/2-1/r)_+} + h_{Y,\partial\Omega}^{\tau-\eta-1-1/2+1/r-(d-1)(1/2-1/r)_+}\right) \times \\
&\qquad \times \left(\|\mathbf{f}\|_{\mathbf{H}^\tau(\Omega)} + \|\mathbf{g}\cdot\mathbf{n}\|_{H^{\tau-1/2}(\partial\Omega)}\right)
\end{aligned}$$

*for $1 < r < \infty$ and $0 \le \eta \le \tau - d(1/2 - 1/r)_+ - 1$. If $r \ge 2$ and $h = h_{X,\Omega} \approx h_{Y,\partial\Omega}$ this reduces to*

$$\|\mathbf{u}-\mathbf{s_u}\|_{\mathbf{W}_r^{\eta+1}(\Omega)} + \|p-s_p\|_{W_r^{\eta+2}(\Omega)/\mathbb{R}} \le c h^{\tau-\eta-1-d(1/2-1/r)} \left(\|\mathbf{f}\|_{\mathbf{H}^\tau(\Omega)} + \|\mathbf{g}\cdot\mathbf{n}\|_{H^{\tau-1/2}(\partial\Omega)}\right).$$

Note that the restriction of the dimension to $d = 2, 3$ is only necessary due to the fact that the extension operator is only proven in those dimensions.

The proven convergence rates correspond to the expected rates for the solution of scalar-valued problems. Furthermore, the error estimates also hold if one of the kernels $\phi$ and $\psi$ is smoother than the other. The result always depends on the rougher kernel.

# 7. Error Estimates for Target Functions Outside the Native Space

In the last chapter the error analysis of the approximation scheme for Darcy's problem has been done. Unfortunately, these error estimates only hold for target functions within the associated native space, i. e. the target function must satisfy smoothness conditions. We will now present a new error analysis of the collocation methods to solve Darcy's problem presented in chapter 5. We will extend the results of chapter 6 to the case that the true solution is not in the native space. In practice, these error estimates allow a more flexible choice of the underlying basis functions. For given basis functions, the error estimates apply to a larger class of target functions. However, there are still some smoothness requirements on the target function depending on the space dimension $d$.

Recently Fuselier has proven error estimates for divergence-free and curl-free matrix-valued radial basis function interpolants, where the target function is rougher than the interpolant, see [17, 20]. We will follow his ideas to present new error estimates for our approximation scheme.

The main idea is to apply band-limited functions to approximate the true solution. Thus we will firstly introduce these functions, their properties and the function spaces of band-limited functions. Then we will study their interpolation and approximation properties. Finally, we will combine all results to prove the Sobolev-type approximation rates for target functions outside the native space.

## 7.1. Band-limited Functions and Function Spaces

We now introduce band-limited functions and establish some of their attributes and the associated spaces.

Let $\sigma > 0$ and $B(\mathbf{0}, \sigma)$ denote the $d$-dimensional ball with centre $\mathbf{0}$ and radius $\sigma$. A *band-limited function* is a function $f_\sigma$ in $L_2(\mathbb{R}^d)$, where the support of the Fourier transform $\operatorname{supp} \widehat{f_\sigma}$ is compact. We also require that the support of the Fourier transform is a subset of $B(\mathbf{0}, \sigma)$. Then, the space of band-limited functions with band-width $\sigma$ is

$$\mathcal{B}^\sigma := \left\{ f \in L_2(\mathbb{R}^d) : \operatorname{supp} \widehat{f} \subseteq B(\mathbf{0}, \sigma) \right\}.$$

All functions in $\mathcal{B}^\sigma$ are analytic and therefore infinitely many times differentiable.

The concept of band-limited functions can be extended to vector-valued functions. These are also analytic, since their components are analytic. We are interested in two different kinds of vector-valued functions: Divergence-free and curl-free band-limited functions. We define the following spaces:

$$\begin{aligned}
\mathcal{B}^\sigma &:= \left\{ \mathbf{f} \in \mathbf{L}_2(\mathbb{R}^d) : \operatorname{supp} \widehat{\mathbf{f}} \subseteq B(\mathbf{0}, \sigma) \right\}, \\
\widetilde{\mathcal{B}}^\sigma &:= \left\{ \mathbf{f} \in \mathcal{B}^\sigma : \int_{\mathbb{R}^d} \frac{\|\widehat{\mathbf{f}}(\boldsymbol{\omega})\|_2^2}{\|\boldsymbol{\omega}\|_2^2} d\boldsymbol{\omega} < \infty \right\}, \\
\widetilde{\mathcal{B}}^\sigma_{\mathrm{div}} &:= \left\{ \mathbf{f} \in \widetilde{\mathcal{B}}^\sigma : \boldsymbol{\omega}^T \widehat{\mathbf{f}}(\boldsymbol{\omega}) = 0 \right\}, \\
\widetilde{\mathcal{B}}^\sigma_{\mathrm{curl}} &:= \left\{ \mathbf{f} \in \widetilde{\mathcal{B}}^\sigma : \text{There exists } g \in L_2(\mathbb{R}^d) \text{ such that } \widehat{\mathbf{f}}(\boldsymbol{\omega}) = -i\boldsymbol{\omega}\widehat{g}(\boldsymbol{\omega}) \right\}.
\end{aligned}$$

Due to their smoothness, band-limited functions are in most native spaces. However, we are in particular interested in the space $\widetilde{\mathbf{H}}^\tau(\mathbb{R}^d; \mathrm{div}) \times H^\rho(\mathbb{R}^d)$.

**Corollary 7.1.** *Let $\boldsymbol{\sigma} = (\sigma_{\mathbf{u}}, \sigma_p) \geq 1$. If the norm is defined by $\|\mathbf{v}_{\boldsymbol{\sigma}}\|_{\widetilde{\mathcal{B}}^{\sigma_{\mathbf{u}}}_{\mathrm{div}} \times \mathcal{B}^{\sigma_p}} := \|\mathbf{v}_{\boldsymbol{\sigma}}\|_{\widetilde{\mathbf{H}}^\tau(\mathbb{R}^d) \times H^\rho(\mathbb{R}^d)}$ for all $\tau, \rho \geq d/2$, then the band-limited space $\widetilde{\mathcal{B}}^{\sigma_{\mathbf{u}}}_{\mathrm{div}} \times \mathcal{B}^{\sigma_p}$ is a subspace of $\widetilde{\mathbf{H}}^\tau(\mathbb{R}^d; \mathrm{div}) \times H^\rho(\mathbb{R}^d)$.*

*Proof.* Let $\mathbf{v}_{\boldsymbol{\sigma}} = (\mathbf{u}_\sigma, p_\sigma) \in \widetilde{\mathcal{B}}^{\sigma_{\mathbf{u}}}_{\mathrm{div}} \times \mathcal{B}^{\sigma_p}$. We will omit the second sub-index and write $\mathbf{u}_\sigma$ and $p_\sigma$ respectively. This should cause no confusion.

By definition, every band-limited function is in $L_2(\mathbb{R}^d)$. Moreover, they are continuous, due to the fact that they are analytic. Thus we only need to show that the norm of $\mathbf{v}_{\boldsymbol{\sigma}}$ in the space $\widetilde{\mathbf{H}}^\tau(\mathbb{R}^d; \mathrm{div}) \times H^\rho(\mathbb{R}^d)$ is finite.

Using fact that $\mathcal{N}_{\widetilde{\boldsymbol{\Phi}}}(\mathbb{R}^d) = \widetilde{\mathbf{H}}^\tau(\mathbb{R}^d; \mathrm{div}) \times H^\rho(\mathbb{R}^d)$ and the norm equivalence, see corollary 5.4, we see that

$$\begin{aligned}
\|\mathbf{v}_{\boldsymbol{\sigma}}\|^2_{\widetilde{\mathbf{H}}^\tau(\mathbb{R}^d) \times H^\rho(\mathbb{R}^d)} &= (2\pi)^{-d/2} \left[ \int_{\mathbb{R}^d} \frac{\|\widehat{\mathbf{u}}_\sigma(\boldsymbol{\omega})\|_2^2}{\|\boldsymbol{\omega}\|_2^2} (1 + \|\boldsymbol{\omega}\|_2^2)^\tau d\boldsymbol{\omega} + \int_{\mathbb{R}^d} |\widehat{p}_\sigma(\boldsymbol{\omega})|^2 (1 + \|\boldsymbol{\omega}\|_2^2)^\rho d\boldsymbol{\omega} \right] \\
&= (2\pi)^{-d/2} \left[ \int\limits_{\|\boldsymbol{\omega}\|_2 \leq \sigma_{\mathbf{u}}} \frac{\|\widehat{\mathbf{u}}_\sigma(\boldsymbol{\omega})\|_2^2}{\|\boldsymbol{\omega}\|_2^2} (1 + \|\boldsymbol{\omega}\|_2^2)^\tau d\boldsymbol{\omega} + \int\limits_{\|\boldsymbol{\omega}\|_2 \leq \sigma_p} |\widehat{p}_\sigma(\boldsymbol{\omega})|^2 (1 + \|\boldsymbol{\omega}\|_2^2)^\rho d\boldsymbol{\omega} \right],
\end{aligned}$$

where we used the fact that the Fourier transform is compactly supported. For all $\|\boldsymbol{\omega}\|_2 \leq$

$\sigma$ we have $(1+\|\boldsymbol{\omega}\|_2^2)^\beta \le (1+\sigma^2)^\beta$. Thus

$$\begin{aligned}\|\mathbf{v}_{\boldsymbol{\sigma}}\|^2_{\widetilde{\mathbf{H}}^\tau(\mathbb{R}^d)\times H^\rho(\mathbb{R}^d)} &\le c(2\pi)^{-d/2}\left[\int_{\|\boldsymbol{\omega}\|_2\le\sigma_{\mathbf{u}}}\frac{\|\widehat{\mathbf{u}}_\sigma(\boldsymbol{\omega})\|_2^2}{\|\boldsymbol{\omega}\|_2^2}d\boldsymbol{\omega}+\int_{\|\boldsymbol{\omega}\|_2\le\sigma_p}|\widehat{p}_\sigma(\boldsymbol{\omega})|^2 d\boldsymbol{\omega}\right]\\ &\le c(2\pi)^{-d/2}\left[\int_{\mathbb{R}^d}\frac{\|\widehat{\mathbf{u}}_\sigma(\boldsymbol{\omega})\|_2^2}{\|\boldsymbol{\omega}\|_2^2}d\boldsymbol{\omega}+\int_{\mathbb{R}^d}|\widehat{p}_\sigma(\boldsymbol{\omega})|^2 d\boldsymbol{\omega}\right].\end{aligned}$$

The definition of $\widetilde{\mathcal{B}}^{\sigma_{\mathbf{u}}}_{\mathrm{div}}$ gives us that

$$\int_{\mathbb{R}^d}\frac{\|\widehat{\mathbf{u}}_\sigma(\boldsymbol{\omega})\|_2^2}{\|\boldsymbol{\omega}\|_2^2}d\boldsymbol{\omega}<\infty$$

and therefore that the first integral is finite. Since $p\in L_2(\mathbb{R}^d)$ we can apply Plancharel's theorem, see [54, Corollary 5.25]. Therefore we can conclude

$$\int_{\mathbb{R}^d}|\widehat{p}_\sigma(\boldsymbol{\omega})|^2 d\boldsymbol{\omega}=(2\pi)^{d/2}\|\widehat{p}_\sigma\|^2_{L_2(\mathbb{R}^d)}=(2\pi)^{d/2}\|p_\sigma\|^2_{L_2(\mathbb{R}^d)},$$

i. e. the second integral is also finite. □

Let $\tau\ge\beta\ge 0$ and $\sigma\ge 1$. Then we have

$$(1+\|\boldsymbol{\omega}\|_2^2)^{\tau-\beta}\le(1+\sigma^2)^{\tau-\beta}\le 2^{\tau-\beta}\sigma^{2(\tau-\beta)}$$

for all $\boldsymbol{\omega}$ with $\|\boldsymbol{\omega}\|_2\le\sigma$. Hence, for every band-limited function $\mathbf{f}_\sigma\in\mathcal{B}^\sigma$ we have

$$\begin{aligned}\|\mathbf{f}_\sigma\|^2_{\mathbf{H}^\tau(\mathbb{R}^d)} &= (2\pi)^{-d/2}\int_{\|\boldsymbol{\omega}\|_2\le\sigma}\|\mathbf{f}_\sigma(\boldsymbol{\omega})\|_2^2(1+\|\boldsymbol{\omega}\|_2^2)^\tau d\boldsymbol{\omega}\\ &= (2\pi)^{-d/2}\int_{\|\boldsymbol{\omega}\|_2\le\sigma}\|\mathbf{f}_\sigma(\boldsymbol{\omega})\|_2^2(1+\|\boldsymbol{\omega}\|_2^2)^\beta(1+\|\boldsymbol{\omega}\|_2^2)^{\tau-\beta}d\boldsymbol{\omega}\\ &\le 2^{\tau-\beta}\sigma^{2(\tau-\beta)}\|\mathbf{f}_\sigma\|^2_{\mathbf{H}^\beta(\mathbb{R}^d)}.\end{aligned}\tag{7.1}$$

This inequality is called the *Bernstein inequality.*

## 7.2. Band-limited Interpolation and Approximation

We now review and establish certain interpolation and approximation results of band-limited functions.

The distance between an element $y$ of a space $\mathcal{Y}$ and a subspace $\mathcal{V}$ of $\mathcal{Y}$ is defined by

$$\mathrm{dist}_{\mathcal{Y}}(y,\mathcal{V}):=\inf_{v\in\mathcal{V}}\|y-v\|_{\mathcal{Y}}.$$

The next result is central for those following. We only state it, its proof can be found in [40].

**Proposition 7.2.** *Let $\mathcal{Y}$ be a (possibly complex) Banach space, $\mathcal{V}$ be a subspace of $\mathcal{Y}$, and $Z^*$ be a finite dimensional subspace of $\mathcal{Y}^*$, the dual of $\mathcal{Y}$. If for every $\lambda^* \in Z^*$ and some $\beta > 1$, $\beta$ independent of $\lambda^*$,*

$$\|\lambda^*\|_{\mathcal{Y}^*} \leq \beta \|\lambda^*|_{\mathcal{V}}\|_{\mathcal{V}^*},$$

*then for $y \in \mathcal{Y}$ there exists $v \in \mathcal{V}$ such that $v$ interpolates $y$ on $Z^*$; that is, $\lambda^*(y) = \lambda^*(v)$ for all $\lambda^* \in Z^*$. In addition, $v$ approximates $y$ in the sense that*

$$\|y - v\|_{\mathcal{Y}} \leq (1 + 2\beta) \operatorname{dist}_{\mathcal{Y}}(y, \mathcal{V}).$$

The following lemma was proven by Fuselier in [20, Lemma 1]. It shows that every $\mathbf{f} \in \widetilde{\mathbf{H}}^\tau(\mathbb{R}^d; \operatorname{div})$ can be approximated by a band-limited function $\mathbf{f}_\sigma \in \widetilde{\mathcal{B}}^\sigma_{\operatorname{div}}$. We give a slightly extended version, since we need it for functions in $\widetilde{\mathbf{H}}^\tau(\mathbb{R}^d; \operatorname{div}) \times H^\rho(\mathbb{R}^d)$.

**Lemma 7.3.** *Let $\tau \geq \beta \geq 0$ and $\sigma > 0$. For every $\mathbf{f} \in \widetilde{\mathbf{H}}^\tau(\mathbb{R}^d; \operatorname{div})$ exists a function $\mathbf{g}_\sigma \in \widetilde{\mathcal{B}}^\sigma_{\operatorname{div}}$ with*

$$\|\mathbf{f} - \mathbf{g}_\sigma\|_{\widetilde{\mathbf{H}}^\beta(\mathbb{R}^d)} \leq \sigma^{\beta-\tau} \|\mathbf{f}\|_{\widetilde{\mathbf{H}}^\tau(\mathbb{R}^d)}.$$

*Moreover, for every $f \in H^\tau(\mathbb{R}^d)$ exists a function $g_\sigma \in \mathcal{B}^\sigma$ with*

$$\|f - g_\sigma\|_{H^\beta(\mathbb{R}^d)} \leq \sigma^{\beta-\tau} \|f\|_{H^\tau(\mathbb{R}^d)}.$$

*Proof.* Let $\chi_\sigma$ be the characteristic function of the ball $B(\mathbf{0}, \sigma)$. We define $\mathbf{g}_\sigma$ by $\widehat{\mathbf{g}}_\sigma := \widehat{\mathbf{f}} \chi_\sigma$. Then we have that $\mathbf{g}_\sigma = \mathbf{f} * \overset{\vee}{\chi}_\sigma$, and therefore $\partial_j \mathbf{g}_\sigma = \partial_j \mathbf{f} * \overset{\vee}{\chi}_\sigma$, cf. theorem 2.4. Thus $\operatorname{div} \mathbf{g}_\sigma = 0$, since $\mathbf{f}$ is divergence-free.

The definition of $\mathbf{g}_\sigma$ implies that $\widehat{\mathbf{f}} - \widehat{\mathbf{g}}_\sigma$ is zero inside the ball $B(\mathbf{0}, \sigma)$. Therefore

$$\begin{aligned}
\|\mathbf{f} - \mathbf{g}_\sigma\|^2_{\widetilde{\mathbf{H}}^\beta(\mathbb{R}^d)} &= (2\pi)^{-d/2} \int_{\mathbb{R}^d} \frac{\|(\widehat{\mathbf{f}} - \widehat{\mathbf{g}}_\sigma)(\boldsymbol{\omega})\|_2^2}{\|\boldsymbol{\omega}\|_2^2} (1 + \|\boldsymbol{\omega}\|_2^2)^{\beta+1} d\boldsymbol{\omega} \\
&= (2\pi)^{-d/2} \int_{\|\boldsymbol{\omega}\|_2^2 \geq \sigma} \frac{\|\widehat{\mathbf{f}}(\boldsymbol{\omega})\|_2^2}{\|\boldsymbol{\omega}\|_2^2} (1 + \|\boldsymbol{\omega}\|_2^2)^{\beta+1} d\boldsymbol{\omega} \\
&= (2\pi)^{-d/2} \int_{\|\boldsymbol{\omega}\|_2^2 \geq \sigma} \frac{\|\widehat{\mathbf{f}}(\boldsymbol{\omega})\|_2^2}{\|\boldsymbol{\omega}\|_2^2} (1 + \|\boldsymbol{\omega}\|_2^2)^{\tau+1} (1 + \|\boldsymbol{\omega}\|_2^2)^{\beta-\tau} d\boldsymbol{\omega}.
\end{aligned}$$

The assumption $\tau \geq \beta$ yields

$$(1 + \|\boldsymbol{\omega}\|_2^2)^{\beta-\tau} = \frac{1}{(1 + \|\boldsymbol{\omega}\|_2^2)^{\tau-\beta}} \leq \frac{1}{(1 + \sigma^2)^{\tau-\beta}} \leq \frac{1}{(\sigma^2)^{\tau-\beta}} \leq \sigma^{2(\beta-\tau)} \tag{7.2}$$

for all $\boldsymbol{\omega} \in \mathbb{R}^d$ with $\|\boldsymbol{\omega}\|_2 \geq \sigma$. Applying the inequality above enables us to bound the norm by

$$\begin{aligned}\|\mathbf{f} - \mathbf{g}_\sigma\|^2_{\widetilde{\mathbf{H}}^\beta(\mathbb{R}^d)} &\leq \sigma^{2(\beta-\tau)}(2\pi)^{-d/2} \int_{\|\boldsymbol{\omega}\|_2^2 \geq \sigma} \frac{\|\widehat{\mathbf{f}}(\boldsymbol{\omega})\|_2^2}{\|\boldsymbol{\omega}\|_2^2}(1+\|\boldsymbol{\omega}\|_2^2)^{\tau+1} d\boldsymbol{\omega} \\ &\leq \sigma^{2(\beta-\tau)} \|\mathbf{f}\|^2_{\widetilde{\mathbf{H}}^\tau(\mathbb{R}^d)}.\end{aligned}$$

In the last step we used the fact that the integrand is positive, i. e. the integral can be bounded by an integral over all $\mathbb{R}^d$. Taking the square roots proves the first statement.

The second part can be shown with similar arguments. We define $g_\sigma$ by $\widehat{g}_\sigma := \widehat{f}\chi_\sigma$. With (7.2) we can conclude that

$$\begin{aligned}\|f - g_\sigma\|^2_{H^\beta(\mathbb{R}^d)} &= (2\pi)^{-d/2} \int_{\mathbb{R}^d} |(\widehat{f} - \widehat{g}_\sigma)(\boldsymbol{\omega})|^2 (1+\|\boldsymbol{\omega}\|_2^2)^\beta d\boldsymbol{\omega} \\ &= (2\pi)^{-d/2} \int_{\|\boldsymbol{\omega}\|_2 \geq \sigma} |\widehat{f}(\boldsymbol{\omega})|^2 (1+\|\boldsymbol{\omega}\|_2^2)^\tau (1+\|\boldsymbol{\omega}\|_2^2)^{\beta-\tau} d\boldsymbol{\omega} \\ &\leq \sigma^{2(\beta-\tau)}(2\pi)^{-d/2} \int_{\|\boldsymbol{\omega}\|_2 \geq \sigma} |\widehat{f}(\boldsymbol{\omega})|^2 (1+\|\boldsymbol{\omega}\|_2^2)^\tau d\boldsymbol{\omega} \\ &= \sigma^{2(\beta-\tau)} \|f\|^2_{H^\tau(\mathbb{R}^d)}.\end{aligned}$$

Taking the square roots finishes the proof. □

Note that the first statement of the previous lemma would also hold for curl-free functions.

The following lemma stems from lemma 2 in [20], but only the case of the divergence-free functions was proven there. We give the proof for the curl-free case, which is following the proof of the divergence-free case.

The separation radius of the discrete set $X = \{\mathbf{x}_1, \ldots, \mathbf{x}_N\}$ is

$$q_X = \frac{1}{2} \min_{j \neq k} \|\mathbf{x}_j - \mathbf{x}_k\|_2.$$

From now on, we will assume that $\sigma$ is sufficiently large, such that $\sigma \geq \frac{\widetilde{C}}{q_X}$, where $\widetilde{C}$ is as in (4.5) or (4.7).

**Lemma 7.4.** *Let $d > 1$. Let $\mathbf{g} = \sum_{j=1}^N \widetilde{\mathcal{K}}^\tau_{\mathrm{div}}(\cdot - \mathbf{x}_j)\boldsymbol{\alpha}_j$ or $\mathbf{g} = \sum_{j=1}^N \widetilde{\mathcal{K}}^\tau_{\mathrm{curl}}(\cdot - \mathbf{x}_j)\boldsymbol{\alpha}_j$, $\tau > d/2$, respectively and define $\mathbf{g}_\sigma$ by $\widehat{\mathbf{g}}_\sigma = \widehat{\mathbf{g}}\chi_\sigma$, where $\chi_\sigma$ is the characteristic function of the ball $B(\mathbf{0}, \sigma)$. Then, there exists a constant $\varsigma > 0$, which is independent of the discrete set $X = \{\mathbf{x}_1, \ldots, \mathbf{x}_N\}$ and the $\boldsymbol{\alpha}_j$'s, such that for $\sigma = \varsigma/q_X$ the following inequality holds:*

$$I_\sigma := \|\mathbf{g} - \mathbf{g}_\sigma\|_{\widetilde{\mathbf{H}}^\tau(\mathbb{R}^d)} \leq \frac{1}{2}\|\mathbf{g}\|_{\widetilde{\mathbf{H}}^\tau(\mathbb{R}^d)}.$$

*Proof.* Using the equality $\widehat{\mathbf{g}}_\sigma(\boldsymbol{\omega}) = \widehat{\mathbf{g}}(\boldsymbol{\omega})$ for all $\boldsymbol{\omega} \in B(\mathbf{0}, \sigma)$ we have that

$$\begin{aligned} I_\sigma^2 &= (2\pi)^{-d/2} \int_{\mathbb{R}^d} \frac{\|\widehat{(\mathbf{g} - \mathbf{g}_\sigma)}(\boldsymbol{\omega})\|_2^2}{\|\boldsymbol{\omega}\|_2^2} (1 + \|\boldsymbol{\omega}\|_2^2)^{\tau+1} d\boldsymbol{\omega} \\ &= (2\pi)^{-d/2} \int_{\|\boldsymbol{\omega}\|_2^2 \geq \sigma} \frac{\|\widehat{\mathbf{g}}(\boldsymbol{\omega})\|_2^2}{\|\boldsymbol{\omega}\|_2^2} (1 + \|\boldsymbol{\omega}\|_2^2)^{\tau+1} d\boldsymbol{\omega}. \end{aligned}$$

A change of variables $\boldsymbol{\omega} = \sigma\boldsymbol{\omega}$ leads to

$$I_\sigma^2 = (2\pi)^{-d/2} \sigma^d \int_{\|\boldsymbol{\omega}\|_2^2 \geq 1} \frac{\|\widehat{\mathbf{g}}(\sigma\boldsymbol{\omega})\|_2^2}{\|\sigma\boldsymbol{\omega}\|_2^2} (1 + \sigma^2\|\boldsymbol{\omega}\|_2^2)^{\tau+1} d\boldsymbol{\omega}.$$

Using the properties of the Fourier transform and the definition of the kernel $\widehat{\widetilde{\mathcal{K}}^\tau_{\mathrm{curl}}}(\boldsymbol{\omega})$, we can compute the Fourier transform of $\mathbf{g}$, see section 2.3 and (4.6). Thus

$$\widehat{\mathbf{g}}(\boldsymbol{\omega}) = \boldsymbol{\omega}\boldsymbol{\omega}^T (1 + \|\boldsymbol{\omega}\|_2^2)^{-(\tau+1)} \sum_{j=1}^N e^{-i\mathbf{x}_j^T \boldsymbol{\omega}} \boldsymbol{\alpha}_j.$$

Then the $\ell_2$-norm of the Fourier transform is

$$\|\widehat{\mathbf{g}}(\boldsymbol{\omega})\|_2^2 = \|\boldsymbol{\omega}\|_2^2 (1 + \|\boldsymbol{\omega}\|_2^2)^{-2(\tau+1)} \sum_{j,k=1}^N e^{-i(\mathbf{x}_k - \mathbf{x}_j)^T \boldsymbol{\omega}} \boldsymbol{\alpha}_j^T \boldsymbol{\omega}\boldsymbol{\omega}^T \boldsymbol{\alpha}_k. \tag{7.3}$$

Substituting $\sigma\boldsymbol{\omega}$ for $\boldsymbol{\omega}$ leads to the identity

$$I_\sigma^2 = \sigma^{d+2} (2\pi)^{-d/2} \int_{\|\boldsymbol{\omega}\|_2^2 \geq 1} \sum_{j,k=1}^N e^{-i\sigma(\mathbf{x}_k - \mathbf{x}_j)^T \boldsymbol{\omega}} \boldsymbol{\alpha}_j^T \boldsymbol{\omega}\boldsymbol{\omega}^T \boldsymbol{\alpha}_k (1 + \sigma^2\|\boldsymbol{\omega}\|_2^2)^{-(\tau+1)} d\boldsymbol{\omega}.$$

The idea is to bound $(1+\sigma^2\|\boldsymbol{\omega}\|_2^2)^{-(\tau+1)}$ such that we can reformulate the right hand side to give a bound of $I_\sigma$ in terms of $\|\mathbf{g}\|_{\widetilde{\mathbf{H}}^\tau(\mathbb{R}^d)}$ on the scaled point set $\sigma X$. Since $\|\boldsymbol{\omega}\|_2 \geq 1$, we have $\sigma^2 \leq 2 + \sigma^2\|\boldsymbol{\omega}\|_2^2$. Adding $\sigma^2\|\boldsymbol{\omega}\|_2^2$ and dividing both sides of the inequality by $\sigma^2(1 + \|\boldsymbol{\omega}\|_2^2)(1 + \sigma^2\|\boldsymbol{\omega}\|_2^2)$ leads to the equivalent inequality

$$\frac{1}{1 + \sigma^2\|\boldsymbol{\omega}\|_2^2} \leq \frac{2}{\sigma^2} \frac{1}{1 + \|\boldsymbol{\omega}\|_2^2}.$$

Raising this inequality to the $(\tau + 1)$th power leads to the bound

$$\frac{1}{(1 + \sigma^2\|\boldsymbol{\omega}\|_2^2)^{\tau+1}} \leq \frac{2^{\tau+1}}{\sigma^{2(\tau+1)}} \frac{1}{(1 + \|\boldsymbol{\omega}\|_2^2)^{\tau+1}}. \tag{7.4}$$

If we define $\boldsymbol{\gamma} := \sum_{j=1}^N \boldsymbol{\alpha}_j e^{i\mathbf{x}_j^T \boldsymbol{\omega}}$, then we can write $\boldsymbol{\gamma}^* \boldsymbol{\omega}\boldsymbol{\omega}^T \boldsymbol{\gamma} = (\boldsymbol{\gamma}^* \boldsymbol{\omega})^2 \geq 0$. Therefore the

integrand is positive and $I_\sigma^2$ is less than the integral over $\mathbb{R}^d$. We then see with (7.4) that

$$\begin{aligned} I_\sigma^2 &\leq \sigma^{d-2\tau} 2^{\tau+1} (2\pi)^{-d/2} \int_{\|\boldsymbol{\omega}\|_2^2 \geq 1} \sum_{j,k=1}^{N} e^{-i(\mathbf{x}_k - \mathbf{x}_j)^T \sigma \boldsymbol{\omega}} \boldsymbol{\alpha}_j^T \boldsymbol{\omega}\boldsymbol{\omega}^T \boldsymbol{\alpha}_k (1 + \|\boldsymbol{\omega}\|_2^2)^{-(\tau+1)} d\boldsymbol{\omega} \\ &\leq \sigma^{d-2\tau} 2^{\tau+1} (2\pi)^{-d/2} \int_{\mathbb{R}^d} \sum_{j,k=1}^{N} e^{-i(\mathbf{x}_k - \mathbf{x}_j)^T \sigma \boldsymbol{\omega}} \boldsymbol{\alpha}_j^T \boldsymbol{\omega}\boldsymbol{\omega}^T (1 + \|\boldsymbol{\omega}\|_2^2)^{-(\tau+1)} \boldsymbol{\alpha}_k d\boldsymbol{\omega}. \end{aligned}$$

Multiplying the Fourier transform $\widehat{\widetilde{\mathcal{K}}_{\mathrm{curl}}^\tau}(\boldsymbol{\omega}) = \boldsymbol{\omega}\boldsymbol{\omega}^T (1 + \|\boldsymbol{\omega}\|_2^2)^{-(\tau+1)}$ with

$$1 = \frac{\boldsymbol{\omega}^T \boldsymbol{\omega}}{\|\boldsymbol{\omega}\|_2^2} (1 + \|\boldsymbol{\omega}\|_2^2)^{\tau+1-(\tau+1)}$$

gives

$$\begin{aligned} \boldsymbol{\omega}\boldsymbol{\omega}^T (1 + \|\boldsymbol{\omega}\|_2^2)^{-(\tau+1)} &= \boldsymbol{\omega}\boldsymbol{\omega}^T \boldsymbol{\omega}\boldsymbol{\omega}^T (1 + \|\boldsymbol{\omega}\|_2^2)^{-2(\tau+1)} \frac{(1 + \|\boldsymbol{\omega}\|_2^2)^{\tau+1}}{\|\boldsymbol{\omega}\|_2^2} \\ &= \left( \boldsymbol{\omega}\boldsymbol{\omega}^T (1 + \|\boldsymbol{\omega}\|_2^2)^{-(\tau+1)} \right)^* \left( \boldsymbol{\omega}\boldsymbol{\omega}^T (1 + \|\boldsymbol{\omega}\|_2^2)^{-(\tau+1)} \right) \frac{(1 + \|\boldsymbol{\omega}\|_2^2)^{\tau+1}}{\|\boldsymbol{\omega}\|_2^2} \\ &= \widehat{\widetilde{\mathcal{K}}_{\mathrm{curl}}^\tau}^*(\boldsymbol{\omega}) \widehat{\widetilde{\mathcal{K}}_{\mathrm{curl}}^\tau}(\boldsymbol{\omega}) \frac{(1 + \|\boldsymbol{\omega}\|_2^2)^{\tau+1}}{\|\boldsymbol{\omega}\|_2^2}. \end{aligned}$$

Therefore

$$I_\sigma^2 \leq \sigma^{d-2\tau} 2^{\tau+1} (2\pi)^{-d/2} \sum_{j,k=1}^{N} \int_{\mathbb{R}^d} e^{-i(\sigma\mathbf{x}_k - \sigma\mathbf{x}_j)^T \boldsymbol{\omega}} \boldsymbol{\alpha}_j^T \widehat{\widetilde{\mathcal{K}}_{\mathrm{curl}}^\tau}^*(\boldsymbol{\omega}) \widehat{\widetilde{\mathcal{K}}_{\mathrm{curl}}^\tau}(\boldsymbol{\omega}) \boldsymbol{\alpha}_k \frac{(1 + \|\boldsymbol{\omega}\|_2^2)^{\tau+1}}{\|\boldsymbol{\omega}\|_2^2} d\boldsymbol{\omega}.$$

The properties of the Rayleigh-quotient establish that for every matrix $A$ and every vector $\mathbf{x} \neq 0$ we have that $\lambda_{\min} \leq \frac{\mathbf{x}^T A \mathbf{x}}{\mathbf{x}^T \mathbf{x}} \leq \lambda_{\max}$. Let $\Lambda_{\sigma X, A}$ be the maximal eigenvalue of the matrix $(A_{\sigma X})_{ij} = \widetilde{\mathcal{K}}_{\mathrm{curl}}^\tau(\sigma\mathbf{x}_i - \sigma\mathbf{x}_j)$, $1 \leq i, j \leq N$. Applying the definition of the inner product in $\widetilde{\mathbf{H}}^\tau(\mathbb{R}^d)$ and the reproducing property leads to

$$\begin{aligned} I_\sigma^2 &\leq \sigma^{d-2\tau} 2^{\tau+1} \sum_{j,k=1}^{N} (2\pi)^{-d/2} \int_{\mathbb{R}^d} \left( \widehat{\widetilde{\mathcal{K}}_{\mathrm{curl}}^\tau}(\boldsymbol{\omega} - \sigma\mathbf{x}_j) \boldsymbol{\alpha}_j \right)^* \widehat{\widetilde{\mathcal{K}}_{\mathrm{curl}}^\tau}(\boldsymbol{\omega} - \sigma\mathbf{x}_k) \boldsymbol{\alpha}_k \frac{(1 + \|\boldsymbol{\omega}\|_2^2)^{\tau+1}}{\|\boldsymbol{\omega}\|_2^2} d\boldsymbol{\omega} \\ &= \sigma^{d-2\tau} 2^{\tau+1} \sum_{j,k=1}^{N} \left( \widetilde{\mathcal{K}}_{\mathrm{curl}}^\tau(\cdot - \sigma\mathbf{x}_k) \boldsymbol{\alpha}_k, \widetilde{\mathcal{K}}_{\mathrm{curl}}^\tau(\cdot - \sigma\mathbf{x}_j) \boldsymbol{\alpha}_j \right)_{\widetilde{\mathbf{H}}^\tau(\mathbb{R}^d)} \\ &= \sigma^{d-2\tau} 2^{\tau+1} \sum_{j,k=1}^{N} \boldsymbol{\alpha}_j^T \widetilde{\mathcal{K}}_{\mathrm{curl}}^\tau(\sigma\mathbf{x}_j - \sigma\mathbf{x}_k) \boldsymbol{\alpha}_k \\ &\leq \sigma^{d-2\tau} 2^{\tau+1} \Lambda_{\sigma X, A} \|\boldsymbol{\alpha}\|_2^2, \end{aligned}$$

where $\boldsymbol{\alpha}^T = (\boldsymbol{\alpha}_1^T, \dots, \boldsymbol{\alpha}_N^T)$.

We now bound $\|\boldsymbol{\alpha}\|_2$ in terms of $\|\mathbf{g}\|_{\widetilde{\mathbf{H}}^\tau(\mathbb{R}^d)}$ by using a lower bound of the smallest eigenvalue of the block matrix $A_X$, where $(A_X)_{ij} = \widetilde{\mathcal{K}}^\tau_{\mathrm{curl}}(\mathbf{x}_i - \mathbf{x}_j)$ for all $1 \le i, j \le N$. After this we establish a bound for $\Lambda_{\sigma X, A}$, which will finish the proof.

The lower bound of the smallest eigenvalue of $A_X$ is given by (4.8) in the form $c_d q_X^{2\tau - d} \le \lambda_{\min}(A_X)$. With (7.3) and following the same idea as above we can conclude

$$\begin{aligned}
\|\mathbf{g}\|^2_{\widetilde{\mathbf{H}}^\tau(\mathbb{R}^d)} &= (2\pi)^{-d/2} \int_{\mathbb{R}^d} \frac{\|\widehat{\mathbf{g}}(\boldsymbol{\omega})\|_2^2}{\|\boldsymbol{\omega}\|_2^2} (1 + \|\boldsymbol{\omega}\|_2^2)^{\tau+1} d\boldsymbol{\omega} \\
&= (2\pi)^{-d/2} \int_{\mathbb{R}^d} \sum_{j,k=1}^N e^{i(\mathbf{x}_k - \mathbf{x}_j)^T \boldsymbol{\omega}} \boldsymbol{\alpha}_j^T \boldsymbol{\omega}\boldsymbol{\omega}^T \boldsymbol{\alpha}_k (1 + \|\boldsymbol{\omega}\|_2^2)^{-(\tau+1)} d\boldsymbol{\omega} \\
&= \sum_{j,k=1}^N \boldsymbol{\alpha}_j^T \widetilde{\mathcal{K}}^\tau_{\mathrm{curl}}(\mathbf{x}_j - \mathbf{x}_k) \boldsymbol{\alpha}_k \\
&= \boldsymbol{\alpha}^T A_X \boldsymbol{\alpha}.
\end{aligned}$$

We then have

$$c_d q_X^{2\tau - d} \|\boldsymbol{\alpha}\|_2^2 \le \|\mathbf{g}\|^2_{\widetilde{\mathbf{H}}^\tau(\mathbb{R}^d)}$$

and therefore

$$\|\boldsymbol{\alpha}\|_2^2 \le c_d^{-1} q_X^{d - 2\tau} \|\mathbf{g}\|^2_{\widetilde{\mathbf{H}}^\tau(\mathbb{R}^d)}.$$

All in all we obtain the bound

$$I_\sigma^2 \le \sigma^{d-2\tau} 2^{\tau+1} \Lambda_{\sigma X, A} c_d^{-1} q_X^{d-2\tau} \|\mathbf{g}\|^2_{\widetilde{\mathbf{H}}^\tau(\mathbb{R}^d)},$$

where $\Lambda_{\sigma X, A}$ denotes the maximal eigenvalue of $A_{\sigma X}$. Since the set $\sigma X$ has the separation radius $q_{\sigma X} = \sigma q_X$, we will now show that we can choose $\sigma$ such that $\Lambda_{\sigma X, A}$ is uniformly bounded.

Let $\boldsymbol{\xi}^T = (\boldsymbol{\xi}_1^T, \dots, \boldsymbol{\xi}_N^T) \in \mathbb{R}^{dN}$ be the unit eigenvector of $A_{\sigma X} \in \mathbb{R}^{dN \times dN}$ associated with $\Lambda_{\sigma X, A}$ and let $\boldsymbol{\xi}_j \in \mathbb{R}^d$ be the $j$th $d$-components of $\boldsymbol{\xi}$. We have $\widetilde{\mathcal{K}}^\tau_{\mathrm{curl}}(\mathbf{x}) = a(\mathbf{x}) I - b(\mathbf{x}) \mathbf{x}\mathbf{x}^T$, i. e. $\widetilde{\mathcal{K}}^\tau_{\mathrm{curl}}(\mathbf{0}) = \mathbf{0}$, cf. (4.9) and (4.10). In combination with the definition of $A_{\sigma X}$ and the triangle inequality we have the bound

$$\Lambda_{\sigma X, A} = \boldsymbol{\xi}^T A_{\sigma X} \boldsymbol{\xi} \le \left| \sum_{j,k=1}^N \boldsymbol{\xi}_j^T \widetilde{\mathcal{K}}^\tau_{\mathrm{curl}}(\sigma \mathbf{x}_j - \sigma \mathbf{x}_k) \boldsymbol{\xi}_k \right| \le \sum_{j \ne k} |\boldsymbol{\xi}_j^T \widetilde{\mathcal{K}}^\tau_{\mathrm{curl}}(\sigma \mathbf{x}_j - \sigma \mathbf{x}_k) \boldsymbol{\xi}_k|.$$

For every symmetric matrix $A$ and vector $\mathbf{x}$ we have

$$\|A\mathbf{x}\|_2^2 = \mathbf{x}^T A^T A \mathbf{x} \le \lambda_{\max}(A^T A) \|\mathbf{x}\|_2^2 = \lambda_{\max}(A)^2 \|\mathbf{x}\|_2^2,$$

i. e. $\|A\mathbf{x}\|_2 \leq |\lambda_{\max}(A)| \, \|\mathbf{x}\|_2$. Since $\boldsymbol{\xi}$ is a unit vector, we have $\|\boldsymbol{\xi}_j\|_2 \leq 1$. Applying this and the Cauchy-Schwarz inequality leads to

$$\begin{aligned}
\Lambda_{\sigma X,A} &\leq \sum_{j \neq k} \|\boldsymbol{\xi}_j\|_2 \|\widetilde{\mathcal{K}}^{\tau}_{\mathrm{curl}}(\sigma \mathbf{x}_j - \sigma \mathbf{x}_k)\boldsymbol{\xi}_k\|_2 \\
&\leq \sum_{j \neq k} \|\boldsymbol{\xi}_j\|_2 |\Lambda_{\widetilde{\mathcal{K}}^{\tau}_{\mathrm{curl}}}(\sigma \mathbf{x}_j - \sigma \mathbf{x}_k)| \, \|\boldsymbol{\xi}_k\|_2 \\
&\leq \sum_{j \neq k} |\Lambda_{\widetilde{\mathcal{K}}^{\tau}_{\mathrm{curl}}}(\sigma \mathbf{x}_j - \sigma \mathbf{x}_k)| \\
&\leq \sum_{j \neq k} \widetilde{\Lambda}_{\tau,d}(\sigma \mathbf{x}_j - \sigma \mathbf{x}_k),
\end{aligned}$$

where $\Lambda_{\widetilde{\mathcal{K}}^{\tau}_{\mathrm{curl}}}$ denotes the maximal eigenvalue of $\widetilde{\mathcal{K}}^{\tau}_{\mathrm{curl}}$ and $\widetilde{\Lambda}_{\tau,d}$ is the upper bound of $\Lambda_{\widetilde{\mathcal{K}}^{\tau}_{\mathrm{curl}}}$ which is defined in (4.12).

In [37, Equation 4.11], the following bound has been proven

$$\sum_{j \neq k} \widetilde{f}(\|\mathbf{x}_j - \mathbf{x}_k\|_2) \leq 3^d \sum_{m=1}^{\infty} m^{d-1} \kappa_{\widetilde{f},m},$$

where $\widetilde{f}$ is a scalar-valued function on $\mathbb{R}^d$ and

$$\kappa_{\widetilde{f},m} := \sup \left\{ |\widetilde{f}(\|\mathbf{x}\|_2)| : mq_X \leq \|\mathbf{x}\|_2 \leq (m+1)q_X \right\}.$$

For $\widetilde{f} := \widetilde{\Lambda}_{\tau,d}$ the supremum is $\kappa_{\widetilde{\Lambda}_{\tau,d},m} = \widetilde{\Lambda}_{\tau,d}(m\sigma q_X)$, since $\widetilde{\Lambda}_{\tau,d}$ is positive and decreasing for $\sigma q_X \geq \nu - 1/2$. To establish the lower bound for the eigenvalue, we had to assume that $\sigma \geq \frac{\widetilde{C}}{q_X}$, i. e. $\sigma q_X \geq \widetilde{C}$. With $\widetilde{C} > 1$ for all $d > 1$ we have $\sigma q_X \geq 1$. Since $\widetilde{\Lambda}_{\tau,d}$ is decreasing, $\widetilde{\Lambda}_{\tau,d}(m\sigma q_X) \leq \widetilde{\Lambda}_{\tau,d}(m)$. In combination we can conclude

$$\begin{aligned}
\Lambda_{\sigma X,A} &\leq 3^d \sum_{m=1}^{\infty} m^{d-1} \widetilde{\Lambda}_{\tau,d}(m\sigma q_X) \\
&\leq 3^d \sum_{m=1}^{\infty} m^{d-1} \widetilde{\Lambda}_{\tau,d}(m).
\end{aligned}$$

The ratio test gives that the series is convergent, since $\widetilde{\Lambda}_{\tau,d}$ is decreasing. Therefore it can be bounded by a constant $C_{d,\tau}$ depending on $d$ and $\tau$ only. From this bound it follows that

$$I_\sigma^2 \leq 2^{\tau+1} c_d^{-1} C_{d,\tau} (\sigma q_X)^{d-2\tau} \|\mathbf{g}\|^2_{\widetilde{\mathbf{H}}^{\tau}(\mathbb{R}^d)}.$$

Now we choose $\sigma q_X = \varsigma$ large enough that the factor in front of $\|\mathbf{g}\|^2_{\widetilde{\mathbf{H}}^{\tau}(\mathbb{R}^d)}$ is less than $1/4$. Taking the square roots finishes the proof. □

Let $\Omega \subseteq \mathbb{R}^d$ with a $C^{\lceil\tau\rceil+1,1}$ boundary and denote the normals of $\Omega$ by $\mathbf{n}$. Let $X = \{\mathbf{x}_1, \dots, \mathbf{x}_N\} \subseteq \Omega$ and $Y = \{\mathbf{y}_1, \dots, \mathbf{y}_M\} \subseteq \partial\Omega$ be discrete sets. As in the previous chapter, we combine the velocity and pressure in a vector $\mathbf{v} = (\mathbf{u}, p)$. Again, we describe Darcy's problem with the operator $L\mathbf{v} := \mathbf{u} + K\nabla p$, where $K_{ij} \in H^\rho(\mathbb{R}^d)$ for all $1 \leq i, j \leq d$.

We now state and prove the main result of this section, which is central for the proof of the error estimate. It guarantees the existence of a band-limited function, which approximates the true solution of Darcy's problem and also gives a bound for the error.

**Theorem 7.5.** *Let $\tau$, $\rho$, $t$, $r \in \mathbb{R}$ with $\tau > d/2$, $\rho > d/2 + 1$ and $t, r \geq 0$. Given $\mathbf{v} = (\mathbf{u}, p) \in \widetilde{\mathbf{H}}^\tau(\mathbb{R}^d; \mathrm{div}) \times H^\rho(\mathbb{R}^d)$ and discrete point sets $X$ and $Y$ with separation radius $q := q_{X\cup Y}$, then there exists a function $\mathbf{v}_{\boldsymbol{\sigma}} \in \widetilde{\mathcal{B}}^{\sigma_{\mathbf{u}}}_{\mathrm{div}} \times \mathcal{B}^{\sigma_p}$ such that*

$$L\mathbf{v}|_X = L\mathbf{v}_{\boldsymbol{\sigma}}|_X, \qquad \mathbf{u}\cdot\mathbf{n}|_Y = \mathbf{u}_\sigma \cdot \mathbf{n}|_Y$$

*and*

$$\begin{aligned}\|\mathbf{v} - \mathbf{v}_{\boldsymbol{\sigma}}\|_{\widetilde{\mathbf{H}}^\tau(\mathbb{R}^d)\times H^\rho(\mathbb{R}^d)} &\leq 5\,\mathrm{dist}_{\widetilde{\mathbf{H}}^\tau(\mathbb{R}^d;\mathrm{div})\times H^\rho(\mathbb{R}^d)}(\mathbf{v}, \widetilde{\mathcal{B}}^{\sigma_{\mathbf{u}}}_{\mathrm{div}} \times \mathcal{B}^{\sigma_p}) \\ &\leq 5\left(\sigma_{\mathbf{u}}^{-2t}\|\mathbf{u}\|^2_{\widetilde{\mathbf{H}}^{\tau+t}(\mathbb{R}^d)} + \sigma_p^{-2r}\|p\|^2_{H^{\rho+r}(\mathbb{R}^d)}\right)^{1/2}.\end{aligned}$$

*Proof.* The main idea for proving this statement is to apply proposition 7.2 with

$$\mathcal{Y} := \widetilde{\mathbf{H}}^\tau(\mathbb{R}^d; \mathrm{div}) \times H^\rho(\mathbb{R}^d), \qquad \mathcal{V} := \widetilde{\mathcal{B}}^{\sigma_{\mathbf{u}}}_{\mathrm{div}} \times \mathcal{B}^{\sigma_p}$$

and $Z^* := \mathrm{span}\{Z_X^* \cup Z_Y^*\}$ with

$$\begin{aligned}Z_X^* &:= \left\{\lambda(\mathbf{v}) = \boldsymbol{\alpha}^T\mathbf{u}(\mathbf{x}) + \boldsymbol{\alpha}^T K(\mathbf{x})\nabla p(\mathbf{x}) :\ \mathbf{x}\in X,\ \mathbf{v} = (\mathbf{u}, p) \in \mathcal{Y}, \boldsymbol{\alpha} \in \mathbb{R}^d\right\} \\ Z_Y^* &:= \left\{\lambda(\mathbf{v}) = \alpha\mathbf{n}(\mathbf{x})^T\mathbf{u}(\mathbf{x}) :\ \mathbf{x}\in Y,\ \mathbf{v} = (\mathbf{u}, p) \in \mathcal{Y},\ \alpha \in \mathbb{R}\right\}.\end{aligned}$$

Before applying proposition 7.2 we need to check that the assumptions are satisfied.

Corollary 5.4 shows that $\mathcal{Y}$ is a Hilbert space, therefore it is indeed a Banach space. Furthermore, $\mathcal{V}$ is a subspace of $\mathcal{Y}$, cf. corollary 7.1.

Due to the fact that $Z^*$ is generated by a finite number of elements it is indeed finite dimensional. Every $\lambda \in Z^*$ is obviously linear. Since $\mathcal{Y}$ is a reproducing kernel Hilbert space, the point evaluation functionals are in $\mathcal{Y}^*$, see theorem 4.2. Furthermore, corollary 2.1 gives that for every $\mathbf{v} \in \mathcal{Y}$, $\mathbf{u}$ is continuous and $p$ is at least once continuous differentiable since $\tau > d/2$ and $\rho > d/2 + 1$, i. e. $\nabla p$ is also continuous. The Sobolev embedding theorem guarantees that $K$ is also continuous, since $\rho > d/2 + 1$. Moreover, the normals are continuous, since the boundary is Lipschitz. Therefore we have that all functionals

$\lambda \in Z^*$ are indeed continuous.

We will now show that for every $\lambda \in Z^*$ we have

$$\|\lambda\|_{\mathcal{Y}^*} \leq 2\|\lambda|_{\mathcal{V}}\|_{\mathcal{V}^*}. \tag{7.5}$$

First of all, we will calculate the Riesz representer and express the norms of the dual space in terms of the original space. Then we can bound $\|\lambda\|_{\mathcal{Y}^*}$ and show that (7.5) holds.

Let $\mathbf{x}_{N+j} := \mathbf{y}_j$ for all $1 \leq j \leq M$. Let $\mathbf{f} = (\mathbf{f_u}, f_p) \in \mathcal{Y}$. We pick an arbitrary element $\lambda \in Z^*$, which can be written as

$$\lambda(\mathbf{f}) = \sum_{j=1}^{N} \boldsymbol{\alpha}_j^T \left[\mathbf{f_u}(\mathbf{x}_j) + K(\mathbf{x}_j)\nabla f_p(\mathbf{x}_j)\right] + \sum_{j=N+1}^{N+M} \alpha_j \mathbf{n}(\mathbf{x}_j)^T \mathbf{f_u}(\mathbf{x}_j),$$

for all $\mathbf{f} = (\mathbf{f_u}, f_p) \in \mathcal{Y}$, where $\boldsymbol{\alpha}_j \in \mathbb{R}^d$ for $1 \leq j \leq N$ and $\alpha_j \in \mathbb{R}$ for $N < j \leq N + M$. If we define

$$\boldsymbol{\gamma}_j := \begin{cases} \boldsymbol{\alpha}_j, & \text{if } 1 \leq j \leq N \\ \alpha_j \mathbf{n}(\mathbf{x}_j), & \text{if } N < j \leq N + M \end{cases}$$

and $\boldsymbol{\zeta}_j := \boldsymbol{\alpha}_j^T K(\mathbf{x}_j)$ then we can write the functional as $\lambda(\mathbf{f}) := \lambda_{\mathbf{u}}(\mathbf{f_u}) + \lambda_p(f_p)$, where $\lambda_{\mathbf{u}}(\mathbf{f_u}) := \sum_{j=1}^{N+M} \boldsymbol{\gamma}_j^T \mathbf{f_u}(\mathbf{x}_j)$ and $\lambda_p(f_p) := \sum_{j=1}^{N} \boldsymbol{\zeta}_j^T \nabla f_p(\mathbf{x}_j)$.

The reproducing function of the space $\widetilde{\mathbf{H}}^\tau(\mathbb{R}^d; \mathrm{div}) \times H^\rho(\mathbb{R}^d)$ is given by

$$\mathcal{K}_{\widetilde{\mathbf{H}}^\tau(\mathbb{R}^d;\mathrm{div})\times H^\rho(\mathbb{R}^d)}(\mathbf{x}, \mathbf{y}) := \begin{pmatrix} \widetilde{\mathcal{K}}^\tau_{\mathrm{div}}(\mathbf{x} - \mathbf{y}) & \mathbf{0} \\ \mathbf{0} & \mathcal{K}^\rho(\mathbf{x} - \mathbf{y}) \end{pmatrix},$$

with the inner product

$$(\mathbf{f}, \mathbf{g})_{\widetilde{\mathbf{H}}^\tau(\mathbb{R}^d)\times H^\rho(\mathbb{R}^d)} = (\mathbf{f_u}, \mathbf{g_u})_{\widetilde{\mathbf{H}}^\tau(\mathbb{R}^d)} + (f_p, g_p)_{H^\rho(\mathbb{R}^d)},$$

i. e. we can work out the Riesz representer $\mathbf{g_u}$ and $g_p$ separately.

The reproducing property of the kernel establishes $\boldsymbol{\gamma}_j^T \mathbf{f_u}(\mathbf{x}_j) = (\mathbf{f_u}, \widetilde{\mathcal{K}}^\tau_{\mathrm{div}}(\cdot - \mathbf{x}_j)\boldsymbol{\gamma}_j)$. Theorem 4.3 gives that $\lambda_{\mathbf{u}}(\mathbf{f_u}) = (\mathbf{f_u}, \sum_{j=1}^{N+M} \widetilde{\mathcal{K}}^\tau_{\mathrm{div}}(\cdot - \mathbf{x}_j)\boldsymbol{\gamma}_j)_{\widetilde{\mathbf{H}}^\tau(\mathbb{R}^d)}$, i. e.

$$\mathbf{g_u} := \sum_{j=1}^{N+M} \widetilde{\mathcal{K}}^\tau_{\mathrm{div}}(\cdot - \mathbf{x}_j)\boldsymbol{\gamma}_j \quad \text{with} \quad \|\lambda_{\mathbf{u}}\|^2_{\widetilde{\mathbf{H}}^\tau(\mathbb{R}^d;\mathrm{div})^*} = \sum_{j,k=1}^{N+M} \boldsymbol{\gamma}_j^T \widetilde{\mathcal{K}}^\tau_{\mathrm{div}}(\mathbf{x}_j - \mathbf{x}_k)\boldsymbol{\gamma}_k.$$

The Riesz representer for $\lambda_p(f) = \sum_{j=1}^{N} \boldsymbol{\zeta}_j^T \nabla f(\mathbf{x}_j)$ is given by $g_p = \sum_{j=1}^{N} \boldsymbol{\zeta}_j^T \nabla \mathcal{K}^\rho(\cdot - \mathbf{x}_j)$

with $\lambda_p(f) = (f, g_p)_{H^\rho(\mathbb{R}^d)}$, cf. theorem 4.3. Since $\boldsymbol{\zeta}_k^T \nabla p$ is a scalar, we have

$$\begin{aligned}\|\lambda_p\|^2_{H^\rho(\mathbb{R}^d)^*} &= \|g_p\|^2_{H^\rho(\mathbb{R}^d)} \\ &= \sum_{j,k=1}^N \boldsymbol{\zeta}_j^T \nabla_{\mathbf{x}} \left(\boldsymbol{\zeta}_k^T \nabla_{\mathbf{y}} \mathcal{K}^\rho(\mathbf{x}_j - \mathbf{x}_k)\right)^T \\ &= \sum_{j,k=1}^N \boldsymbol{\zeta}_j^T \nabla_{\mathbf{x}} \nabla_{\mathbf{y}}^T \mathcal{K}^\rho(\mathbf{x}_j - \mathbf{x}_k) \boldsymbol{\zeta}_k.\end{aligned}$$

Altogether we see that

$$\|\lambda\|^2_{\mathcal{Y}^*} = \|\mathbf{g}_\lambda\|^2_{\mathcal{Y}} = \sum_{j,k=1}^{N+M} \boldsymbol{\gamma}_j^T \widetilde{\mathcal{K}}^\tau_{\mathrm{div}}(\mathbf{x}_j - \mathbf{x}_k)\boldsymbol{\gamma}_k + \sum_{j,k=1}^N \boldsymbol{\zeta}_j^T \nabla_{\mathbf{x}} \nabla_{\mathbf{y}}^T \mathcal{K}^\rho(\mathbf{x}_j - \mathbf{x}_k)\boldsymbol{\zeta}_k.$$

The next step is to show that $\|\lambda|_{\mathcal{V}}\|_{\mathcal{V}^*} = \|\mathbf{g}_\sigma\|_{\mathcal{Y}}$, where $\mathbf{g}_\sigma = (\mathbf{g}_{\mathbf{u},\sigma}, g_{p,\sigma})$ is the Riesz representer from the band-limited space. Since $\mathcal{V}$ is a subspace of $\mathcal{Y}$ the norms are the same for every element in $\mathcal{V}$. Again let us have a look at $\lambda_{\mathbf{u}}$ first. Let $\mathbf{f} \in \widetilde{\mathcal{B}}^{\sigma_{\mathbf{u}}}_{\mathrm{div}}$ and $\mathbf{g}_{\mathbf{u},\sigma}$ be defined by $\widehat{\mathbf{g}_{\mathbf{u},\sigma}} = \widehat{\mathbf{g}_{\mathbf{u}}}\chi_{\sigma_{\mathbf{u}}}$. This gives

$$\begin{aligned}\lambda_{\mathbf{u}}(\mathbf{f}) = (\mathbf{f}, \mathbf{g}_{\mathbf{u}})_{\widetilde{\mathbf{H}}^\tau(\mathbb{R}^d)} &= (2\pi)^{-d/2} \int_{\mathbb{R}^d} \frac{\widehat{\mathbf{g}_{\mathbf{u}}}(\boldsymbol{\omega})^* \widehat{\mathbf{f}}(\boldsymbol{\omega})}{\|\boldsymbol{\omega}\|_2^2} (1 + \|\boldsymbol{\omega}\|_2^2)^{\tau+1} d\boldsymbol{\omega} \\ &= (2\pi)^{-d/2} \int_{\|\boldsymbol{\omega}\|_2^2 \le \sigma_{\mathbf{u}}} \frac{\widehat{\mathbf{g}_{\mathbf{u}}}(\boldsymbol{\omega})^* \widehat{\mathbf{f}}(\boldsymbol{\omega})}{\|\boldsymbol{\omega}\|_2^2} (1 + \|\boldsymbol{\omega}\|_2^2)^{\tau+1} d\boldsymbol{\omega} \\ &= (2\pi)^{-d/2} \int_{\|\boldsymbol{\omega}\|_2^2 \le \sigma_{\mathbf{u}}} \frac{\widehat{\mathbf{g}_{\mathbf{u},\sigma}}(\boldsymbol{\omega})^* \widehat{\mathbf{f}}(\boldsymbol{\omega})}{\|\boldsymbol{\omega}\|_2^2} (1 + \|\boldsymbol{\omega}\|_2^2)^{\tau+1} d\boldsymbol{\omega} \\ &= (2\pi)^{-d/2} \int_{\mathbb{R}^d} \frac{\widehat{\mathbf{g}_{\mathbf{u},\sigma}}(\boldsymbol{\omega})^* \widehat{\mathbf{f}}(\boldsymbol{\omega})}{\|\boldsymbol{\omega}\|_2^2} (1 + \|\boldsymbol{\omega}\|_2^2)^{\tau+1} d\boldsymbol{\omega} \\ &= (\mathbf{f}, \mathbf{g}_{\mathbf{u},\sigma})_{\widetilde{\mathbf{H}}^\tau(\mathbb{R}^d)},\end{aligned}$$

where we used the fact that $\widehat{\mathbf{f}}$ vanishes outside the ball $B(\mathbf{0}, \sigma_{\mathbf{u}})$. This equality and the same idea as in the proof of theorem 4.3 lead us to

$$\|\lambda_{\mathbf{u}}|_{\widetilde{\mathcal{B}}^{\sigma_{\mathbf{u}}}_{\mathrm{div}}}\|_{(\widetilde{\mathcal{B}}^{\sigma_{\mathbf{u}}}_{\mathrm{div}})^*} = \|\lambda_{\mathbf{u}}|_{\widetilde{\mathcal{B}}^{\sigma_{\mathbf{u}}}_{\mathrm{div}}}\|_{\widetilde{\mathbf{H}}^\tau(\mathbb{R}^d;\mathrm{div})^*} = \|\mathbf{g}_{\mathbf{u},\sigma}\|_{\widetilde{\mathbf{H}}^\tau(\mathbb{R}^d)}.$$

With a similar argumentation and $g_{p,\sigma}$ defined by $\widehat{g_{p,\sigma}} = \widehat{g_p}\chi_{\sigma_p}$ we see that

$$(f, g_p)_{H^\rho(\mathbb{R}^d)} = (f, g_{p,\sigma})_{H^\rho(\mathbb{R}^d)}$$

and

$$\|\lambda_p|_{\mathcal{B}^{\sigma_p}}\|_{\mathcal{B}^{\sigma_p}*} = \|\lambda_p|_{\mathcal{B}^{\sigma_p}}\|_{H^\rho(\mathbb{R}^d)^*} = \|g_{p,\sigma}\|_{H^\rho(\mathbb{R}^d)}.$$

Altogether we have

$$\begin{aligned}
\|\lambda|_{\mathcal{V}}\|^2_{\mathcal{V}^*} &= \|\lambda|_{\mathcal{V}}\|^2_{\mathcal{Y}^*} \\
&= \|\lambda_{\mathbf{u}}|_{\widetilde{\mathcal{B}}^{\sigma_{\mathbf{u}}}_{\mathrm{div}}}\|^2_{\widetilde{\mathbf{H}}^\tau(\mathbb{R}^d)^*} + \|\lambda_p|_{\mathcal{B}^{\sigma_p}}\|^2_{H^\rho(\mathbb{R}^d)^*} \\
&= \|\mathbf{g}_{\mathbf{u},\sigma}\|^2_{\widetilde{\mathbf{H}}^\tau(\mathbb{R}^d)} + \|g_{p,\sigma}\|^2_{H^\rho(\mathbb{R}^d)} \\
&= \|\mathbf{g}_{\lambda,\sigma}\|^2_{\mathcal{Y}}.
\end{aligned}$$

Later we want to apply lemma 7.4 to bound $\|g_p - g_{p,\sigma}\|_{H^\rho(\mathbb{R}^d)}$ by $\|g_p\|_{H^\rho(\mathbb{R}^d)}$. Before doing so, we need to show that $\|g_p\|_{H^\rho(\mathbb{R}^d)} = \|\mathbf{g}_{\mathrm{curl}}\|_{\widetilde{\mathbf{H}}^{\rho-1}(\mathbb{R}^d)}$ and $\|g_p - g_{p,\sigma}\|_{H^\rho(\mathbb{R}^d)} = \|\mathbf{g}_{\mathrm{curl}} - \mathbf{g}_{\mathrm{curl},\sigma}\|_{\widetilde{\mathbf{H}}^{\rho-1}(\mathbb{R}^d;\mathrm{curl})}$, where $\mathbf{g}_{\mathrm{curl}} = \sum_{j=1}^N \widetilde{\mathcal{K}}^{\rho-1}_{\mathrm{curl}}(\cdot - \mathbf{x}_j)\boldsymbol{\zeta}_j$ and $g_{p,\sigma}$, $\mathbf{g}_{\mathrm{curl},\sigma}$ are defined by $\widehat{g_{p,\sigma}} = \widehat{g_p}\chi_\sigma$ and $\widehat{\mathbf{g}_{\mathrm{curl},\sigma}} = \widehat{\mathbf{g}_{\mathrm{curl}}}\chi_\sigma$ respectively. Here, $\chi_\sigma$ denotes again the characteristic function of the ball $B(\mathbf{0},\sigma)$.

We have that $\widetilde{\mathcal{K}}^{\rho-1}_{\mathrm{curl}} = -\nabla\nabla^T\mathcal{K}^\rho$, where $\mathcal{K}^\rho$ is the reproducing kernel of $H^\rho(\mathbb{R}^d)$, see section 4.1.2. Therefore

$$\begin{aligned}
\mathbf{g}_{\mathrm{curl}} &= \sum_{j=1}^N \widetilde{\mathcal{K}}^{\rho-1}_{\mathrm{curl}}(\cdot - \mathbf{x}_j)\boldsymbol{\zeta}_j \\
&= -\sum_{j=1}^N \nabla\nabla^T\mathcal{K}^\rho(\cdot - \mathbf{x}_j)\boldsymbol{\zeta}_j \\
&= -\nabla\left(\sum_{j=1}^N \nabla^T\mathcal{K}^\rho(\cdot - \mathbf{x}_j)\boldsymbol{\zeta}_j\right) \\
&= -\nabla g_p.
\end{aligned}$$

We are using the identities above to show

$$\begin{aligned}
\|\mathbf{g}_{\mathrm{curl}} - \mathbf{g}_{\mathrm{curl},\sigma}\|^2_{\widetilde{\mathbf{H}}^{\rho-1}(\mathbb{R}^d)} &= (2\pi)^{-d/2} \int_{\mathbb{R}^d} \frac{\|(\widehat{\mathbf{g}_{\mathrm{curl}}} - \widehat{\mathbf{g}_{\mathrm{curl},\sigma}})(\boldsymbol{\omega})\|_2^2}{\|\boldsymbol{\omega}\|_2^2} (1 + \|\boldsymbol{\omega}\|_2^2)^\rho d\boldsymbol{\omega} \\
&= (2\pi)^{-d/2} \int_{\|\boldsymbol{\omega}\|_2 \geq \sigma_p} \frac{\|\widehat{\mathbf{g}_{\mathrm{curl}}}(\boldsymbol{\omega})\|_2^2}{\|\boldsymbol{\omega}\|_2^2} (1 + \|\boldsymbol{\omega}\|_2^2)^\rho d\boldsymbol{\omega} \\
&= (2\pi)^{-d/2} \int_{\|\boldsymbol{\omega}\|_2 \geq \sigma_p} \frac{\|\widehat{-\nabla g_p}(\boldsymbol{\omega})\|_2^2}{\|\boldsymbol{\omega}\|_2^2} (1 + \|\boldsymbol{\omega}\|_2^2)^\rho d\boldsymbol{\omega} \\
&= (2\pi)^{-d/2} \int_{\|\boldsymbol{\omega}\|_2 \geq \sigma_p} \frac{\|i\boldsymbol{\omega}\widehat{g_p}(\boldsymbol{\omega})\|_2^2}{\|\boldsymbol{\omega}\|_2^2} (1 + \|\boldsymbol{\omega}\|_2^2)^\rho d\boldsymbol{\omega} \\
&= (2\pi)^{-d/2} \int_{\|\boldsymbol{\omega}\|_2 \geq \sigma_p} |\widehat{g_p}(\boldsymbol{\omega})|^2 (1 + \|\boldsymbol{\omega}\|_2^2)^\rho d\boldsymbol{\omega} \\
&= (2\pi)^{-d/2} \int_{\mathbb{R}^d} |(\widehat{g_p} - \widehat{g_{p,\sigma}})(\boldsymbol{\omega})|^2 (1 + \|\boldsymbol{\omega}\|_2^2)^\rho d\boldsymbol{\omega} \\
&= \|g_p - g_{p,\sigma}\|^2_{H^\rho(\mathbb{R}^d)}. \qquad (7.6)
\end{aligned}$$

The second identity

$$\|\mathbf{g}_{\mathrm{curl}}\|_{\widetilde{\mathbf{H}}^{\rho-1}(\mathbb{R}^d)} = \|g_p\|_{H^\rho(\mathbb{R}^d)} \qquad (7.7)$$

can be shown similarly.

For two real numbers $x$ and $y$ we have the inverse triangle inequality $||x| - |y|| \leq |x - y|$. We add the term $\mathbf{g} - \mathbf{g}$ and apply the inverse triangle inequality to establish

$$\begin{aligned}
\|\mathbf{g}_\sigma\|_{\widetilde{\mathbf{H}}^\tau(\mathbb{R}^d) \times H^\rho(\mathbb{R}^d)} &= \|\mathbf{g} - (\mathbf{g} - \mathbf{g}_\sigma)\|_{\widetilde{\mathbf{H}}^\tau(\mathbb{R}^d) \times H^\rho(\mathbb{R}^d)} \\
&\geq \left| \|\mathbf{g}\|_{\widetilde{\mathbf{H}}^\tau(\mathbb{R}^d) \times H^\rho(\mathbb{R}^d)} - \|\mathbf{g} - \mathbf{g}_\sigma\|_{\widetilde{\mathbf{H}}^\tau(\mathbb{R}^d) \times H^\rho(\mathbb{R}^d)} \right|
\end{aligned}$$

To bound the norm above, we apply (7.6) and (7.7) together with lemma 7.4,

$$\begin{aligned}
\|\mathbf{g} - \mathbf{g}_\sigma\|_{\widetilde{\mathbf{H}}^\tau(\mathbb{R}^d) \times H^\rho(\mathbb{R}^d)} &= \left( \|\mathbf{g}_{\mathbf{u}} - \mathbf{g}_{\mathbf{u},\sigma}\|^2_{\widetilde{\mathbf{H}}^\tau(\mathbb{R}^d)} + \|g_p - g_{p,\sigma}\|^2_{H^\rho(\mathbb{R}^d)} \right)^{1/2} \\
&= \left( \|\mathbf{g}_{\mathbf{u}} - \mathbf{g}_{\mathbf{u},\sigma}\|^2_{\widetilde{\mathbf{H}}^\tau(\mathbb{R}^d)} + \|\mathbf{g}_{\mathrm{curl}} - \mathbf{g}_{\mathrm{curl},\sigma}\|^2_{\widetilde{\mathbf{H}}^{\rho-1}(\mathbb{R}^d)} \right)^{1/2} \\
&\leq \left( \frac{1}{4}\|\mathbf{g}_{\mathbf{u}}\|^2_{\widetilde{\mathbf{H}}^\tau(\mathbb{R}^d)} + \frac{1}{4}\|\mathbf{g}_{\mathrm{curl}}\|^2_{\widetilde{\mathbf{H}}^{\rho-1}(\mathbb{R}^d)} \right)^{1/2} \\
&= \left( \frac{1}{4}\|\mathbf{g}_{\mathbf{u}}\|^2_{\widetilde{\mathbf{H}}^\tau(\mathbb{R}^d)} + \frac{1}{4}\|g_p\|^2_{H^\rho(\mathbb{R}^d)} \right)^{1/2} \\
&= \frac{1}{2}\|\mathbf{g}\|_{\widetilde{\mathbf{H}}^\tau(\mathbb{R}^d) \times H^\rho(\mathbb{R}^d)}.
\end{aligned}$$

In total we get

$$\begin{aligned}\|\lambda|_{\mathcal{V}}\|_{\mathcal{V}^*} &= \|\mathbf{g}_\sigma\|_{\widetilde{\mathbf{H}}^\tau(\mathbb{R}^d)\times H^\rho(\mathbb{R}^d)} \\ &\geq \left| \|\mathbf{g}\|_{\widetilde{\mathbf{H}}^\tau(\mathbb{R}^d)\times H^\rho(\mathbb{R}^d)} - \frac{1}{2}\|\mathbf{g}\|_{\widetilde{\mathbf{H}}^\tau(\mathbb{R}^d)\times H^\rho(\mathbb{R}^d)} \right| \\ &= \frac{1}{2}\|\mathbf{g}\|_{\widetilde{\mathbf{H}}^\tau(\mathbb{R}^d)\times H^\rho(\mathbb{R}^d)} \\ &= \frac{1}{2}\|\lambda\|_{\mathcal{Y}^*}.\end{aligned}$$

Therefore

$$\|\lambda\|_{\mathcal{Y}^*} \leq 2\|\lambda|_{\mathcal{V}}\|_{\mathcal{V}^*}$$

for every $\lambda \in Z^*$, i. e. all assumptions of theorem 7.2 are satisfied with $\beta = 2$. Thus for every $\mathbf{v} \in \widetilde{\mathbf{H}}^\tau(\mathbb{R}^d;\mathrm{div}) \times H^\rho(\mathbb{R}^d)$ there exists a $\mathbf{v}_{\boldsymbol{\sigma}} \in \widetilde{\mathcal{B}}^{\sigma_{\mathbf{u}}}_{\mathrm{div}} \times \mathcal{B}^{\sigma_p}$ such that $\mathbf{v}_{\boldsymbol{\sigma}}$ interpolates $\mathbf{v}$ on $Z^*$; that is $\lambda(\mathbf{v}) = \lambda(\mathbf{v}_{\boldsymbol{\sigma}})$ for all $\lambda \in Z^*$. In addition, $\mathbf{v}_{\boldsymbol{\sigma}}$ approximates $\mathbf{v}$ in the sense that

$$\|\mathbf{v} - \mathbf{v}_{\boldsymbol{\sigma}}\|^2_{\mathcal{Y}} = \|\mathbf{u} - \mathbf{u}_\sigma\|^2_{\widetilde{\mathbf{H}}^\tau(\mathbb{R}^d)} + \|p - p_\sigma\|^2_{H^\rho(\mathbb{R}^d)} \leq 5^2\,\mathrm{dist}_{\mathcal{Y}}(\mathbf{v}, \widetilde{\mathcal{B}}^{\sigma_{\mathbf{u}}}_{\mathrm{div}} \times \mathcal{B}^{\sigma_p})^2.$$

The definition of the distance gives that

$$\begin{aligned}\mathrm{dist}_{\mathcal{Y}}(\mathbf{v}, \widetilde{\mathcal{B}}^{\sigma_{\mathbf{u}}}_{\mathrm{div}} \times \mathcal{B}^{\sigma_p})^2 &= \inf_{\widetilde{\mathbf{v}}_{\boldsymbol{\sigma}} \in \mathcal{V}} \left\{ \|\mathbf{u} - \widetilde{\mathbf{u}}_\sigma\|^2_{\widetilde{\mathbf{H}}^\tau(\mathbb{R}^d)} + \|p - \widetilde{p}_\sigma\|^2_{H^\rho(\mathbb{R}^d)} \right\} \\ &= \inf_{\widetilde{\mathbf{u}}_\sigma \in \widetilde{\mathcal{B}}^{\sigma_{\mathbf{u}}}_{\mathrm{div}}} \|\mathbf{u} - \widetilde{\mathbf{u}}_\sigma\|^2_{\widetilde{\mathbf{H}}^\tau(\mathbb{R}^d)} + \inf_{\widetilde{p}_\sigma \in \mathcal{B}^{\sigma_p}} \|p - \widetilde{p}_\sigma\|^2_{H^\rho(\mathbb{R}^d)}.\end{aligned}$$

Firstly, we have a look at $\inf_{\widetilde{\mathbf{u}}_\sigma \in \widetilde{\mathcal{B}}^{\sigma_{\mathbf{u}}}_{\mathrm{div}}} \|\mathbf{u} - \widetilde{\mathbf{u}}_\sigma\|_{\widetilde{\mathbf{H}}^\tau(\mathbb{R}^d)}$. Defining $\mathbf{u}_\sigma$ by $\widehat{\mathbf{u}_\sigma} = \widehat{\mathbf{u}}\chi_{\sigma_{\mathbf{u}}}$ shows, with lemma 7.3,

$$\inf_{\widetilde{\mathbf{u}}_\sigma \in \widetilde{\mathcal{B}}^{\sigma_{\mathbf{u}}}_{\mathrm{div}}} \|\mathbf{u} - \widetilde{\mathbf{u}}_\sigma\|^2_{\widetilde{\mathbf{H}}^\tau(\mathbb{R}^d)} \leq \|\mathbf{u} - \mathbf{u}_\sigma\|^2_{\widetilde{\mathbf{H}}^\tau(\mathbb{R}^d)} \leq \sigma_{\mathbf{u}}^{2(\tau-(\tau-t))}\|\mathbf{u}\|^2_{\widetilde{\mathbf{H}}^{\tau+t}(\mathbb{R}^d)}.$$

Analogously we have

$$\inf_{\widetilde{p}_\sigma \in \mathcal{B}^{\sigma_p}} \|p - \widetilde{p}_\sigma\|^2_{H^\rho(\mathbb{R}^d)} \leq \sigma_p^{2(\rho-(\rho+r))}\|p\|_{H^{\rho+r}(\mathbb{R}^d)}$$

and therefore

$$\begin{aligned}\mathrm{dist}_{\mathcal{Y}}(\mathbf{v}, \widetilde{\mathcal{B}}^{\sigma_{\mathbf{u}}}_{\mathrm{div}} \times \mathcal{B}^{\sigma_p})^2 &\leq \sigma_{\mathbf{u}}^{2(\tau-(\tau+t))}\|\mathbf{u}\|^2_{\widetilde{\mathbf{H}}^{\tau+t}(\mathbb{R}^d)} + \sigma_p^{2(\rho-(\rho+r))}\|p\|^2_{H^{\rho+r}(\mathbb{R}^d)} \\ &\leq \sigma_{\mathbf{u}}^{-2t}\|\mathbf{u}\|^2_{\widetilde{\mathbf{H}}^{\tau+t}(\mathbb{R}^d)} + \sigma_p^{-2r}\|p\|^2_{H^{\rho+r}(\mathbb{R}^d)}.\end{aligned}$$

which finishes the proof. □

Note that some modifications of the proof could lead to a result for other partial differential equations.

## 7.3. Error Analysis

We now state and prove the error estimates for target functions outside the native space. Besides a similar approach as in the standard error analysis, the main idea is to find a band-limited function $\mathbf{v}_{\boldsymbol{\sigma}}$, which approximates the true solution. Then we can add the term $\mathbf{v}_{\boldsymbol{\sigma}} - \mathbf{v}_{\boldsymbol{\sigma}}$ to the difference between the true solution $\mathbf{v}$ and our approximating function $\mathbf{s}_{\mathbf{v}}$. With the triangle inequality the norm can be split into two. The difference between the true solution and the band-limited function can be bounded with theorem 7.5. The difference between the band-limited function and the approximating function can be bounded with standard error analysis, since $\mathbf{s}_{\mathbf{v}}$ also approximates $\mathbf{v}_{\boldsymbol{\sigma}}$ and both functions are sufficiently smooth.

**Theorem 7.6.** *Let $\Omega$ be a bounded, simply connected, open subset of $\mathbb{R}^d$, $d = 2, 3$, with a $C^{\lceil\beta\rceil+1,1}$ boundary $\partial\Omega$. Suppose that $\widetilde{\mathbf{\Phi}}$ is chosen such that its native space is $\mathcal{N}_{\widetilde{\mathbf{\Phi}}}(\mathbb{R}^d) = \widetilde{\mathbf{H}}^{\tau}(\mathbb{R}^d; \operatorname{div}) \times H^{\tau+1}(\mathbb{R}^d)$ and the permeability tensor $K = K_{ij}$ satisfies (3.6), $K = K^T$ and $K_{ij} \in H^{\beta+1}(\overline{\Omega})$. Furthermore, assume that the data satisfy $\mathbf{f} \in \mathbf{H}^{\beta+1}(\Omega)$ and $\mathbf{g} \in \mathbf{H}^{\beta+1/2}(\partial\Omega)$, where $d/2 < \beta \leq \tau$. Then, the error between the true solution and the collocation approximation can be bounded by*

$$\begin{aligned}
&\|\mathbf{u} - \mathbf{s}_{\mathbf{u}}\|_{\mathbf{W}_r^{\eta+1}(\Omega)} + \|p - s_p\|_{W_r^{\eta+2}(\Omega)/\mathbb{R}} \\
&\quad \leq c \frac{h_{X,\Omega}^{\tau-\beta} + h_{Y,\partial\Omega}^{\tau-\beta}}{q^{\tau-\beta}} \left( h_{X,\Omega}^{\beta-\eta-1-d(1/2-1/r)_+} + h_{Y,\partial\Omega}^{\beta-\eta-1-1/2+1/r-(d-1)(1/2-1/r)_+} \right) \times \\
&\qquad \times \left( \|\mathbf{f}\|_{\mathbf{H}^{\beta}(\Omega)} + \|\mathbf{g} \cdot \mathbf{n}\|_{H^{\beta-1/2}(\partial\Omega)} \right)
\end{aligned}$$

*for every $1 < r < \infty$ and $0 \leq \eta \leq \beta - d(1/2 - 1/r)_+ - 1$ and separation radius $q := q_{X \cup Y}$. If $r \geq 2$ and $h = h_{X,\Omega} \approx h_{Y,\partial\Omega}$ this reduces to*

$$\begin{aligned}
&\|\mathbf{u} - \mathbf{s}_{\mathbf{u}}\|_{\mathbf{W}_r^{\eta+1}(\Omega)} + \|p - \mathbf{s}_p\|_{W_r^{\eta+2}(\Omega)/\mathbb{R}} \\
&\qquad \leq c h^{\beta-\eta-1-d(1/2-1/r)} \left( \frac{h}{q} \right)^{\tau-\beta} \left( \|\mathbf{f}\|_{\mathbf{H}^{\beta}(\Omega)} + \|\mathbf{g} \cdot \mathbf{n}\|_{H^{\beta-1/2}(\partial\Omega)} \right).
\end{aligned}$$

*Proof.* First of all, we pick a representer $p$ of the pressure such that $\|p\|_{W_r^{\beta+2}(\Omega)} \geq \|p\|_{W_r^{\beta+2}(\Omega)/\mathbb{R}}$, i. e. $c = 0$ in (2.1).

Let $\mathbf{v} = (\mathbf{u}, p)$. Since all norms on $\mathbb{R}^d$ are equivalent, we have that $\|\mathbf{u} - \mathbf{s_u}\|_{\mathbf{W}_r^{\eta+1}(\Omega)} + \|p - s_p\|_{W_r^{\eta+2}(\Omega)}$is equivalent to $\|\mathbf{v} - \mathbf{s_v}\|_{\mathbf{W}_r^{\eta+1}(\Omega)\times W_r^{\eta+2}(\Omega)/\mathbb{R}}$.

We now apply theorem 3.2 to the difference $\mathbf{v} - \mathbf{s_v}$ instead of $\mathbf{v}$, i. e. we see that

$$\|\mathbf{u}-\mathbf{s_u}\|_{\mathbf{W}_r^{\eta+1}(\Omega)}+\|p-s_p\|_{W_r^{\eta+2}(\Omega)} \leq c\left(\|L\mathbf{v} - L\mathbf{s_v}\|_{\mathbf{W}_r^{\eta+1}(\Omega)} + \|(\mathbf{u} - \mathbf{s_u})\cdot\mathbf{n}\|_{W_r^{\eta+1-1/r}(\partial\Omega)}\right),$$

for all $0 \leq \eta \leq \beta$. We will bound $\|L\mathbf{v} - L\mathbf{s_v}\|_{\mathbf{W}_r^{\eta+1}(\Omega)}$ and $\|(\mathbf{u} - \mathbf{s_u})\cdot\mathbf{n}\|_{W_r^{\eta+1-1/r}(\partial\Omega)}$ separately.

We will start with the estimate in the interior. The function $L\mathbf{v} - L\mathbf{s_v}$ has many zeros, i. e. we can apply the sampling inequality lemma 6.2, such that

$$\|L\mathbf{v} - L\mathbf{s_v}\|_{\mathbf{W}_r^{\eta+1}(\Omega)} \leq c h_{X,\Omega}^{\beta-\eta-1-d(1/2-1/r)_+}\|L\mathbf{v} - L\mathbf{s_v}\|_{\mathbf{H}^\beta(\Omega)}.$$

From the proof of proposition 6.3 we can see that

$$\begin{aligned}\|L\mathbf{v} - L\mathbf{s_v}\|_{\mathbf{H}^\beta(\Omega)} &\leq c\left(\|\mathbf{u} - \mathbf{s_u}\|_{\mathbf{H}^\beta(\Omega)} + \|p - s_p\|_{H^{\beta+1}(\Omega)}\right)\\ &\leq c\|\mathbf{v} - \mathbf{s_v}\|_{\mathbf{H}^\beta(\Omega)\times H^{\beta+1}(\Omega)}. \end{aligned} \tag{7.8}$$

To bound (7.8), we apply the extension operator $\mathbf{E}$ to $\mathbf{v}$ and extend $K$ component-wise with Stein's extension operator $E_S$, see proposition 6.1. Then there exists a band-limited function $\mathbf{v_\sigma}$ which approximates the extension of $\mathbf{v}$, see theorem 7.5. Adding $\mathbf{v_\sigma} - \mathbf{v_\sigma}$ and using the triangle inequality leads to

$$\begin{aligned}\|\mathbf{v} - \mathbf{s_v}\|_{\mathbf{H}^\beta(\Omega)\times H^{\beta+1}(\Omega)} &= \|\mathbf{E}\mathbf{v} - \mathbf{s_{Ev}}\|_{\mathbf{H}^\beta(\Omega)\times H^{\beta+1}(\Omega)}\\ &\leq \|\mathbf{E}\mathbf{v} - \mathbf{v_\sigma}\|_{\mathbf{H}^\beta(\Omega)\times H^{\beta+1}(\Omega)} + \|\mathbf{v_\sigma} - \mathbf{s_{Ev}}\|_{\mathbf{H}^\beta(\Omega)\times H^{\beta+1}(\Omega)}. \end{aligned} \tag{7.9}$$

The first part of (7.9) can be bounded by theorem 7.5 with $t, r = 0$ and the properties of the extension operator:

$$\begin{aligned}\|\mathbf{E}\mathbf{v} - \mathbf{v_\sigma}\|_{\mathbf{H}^\beta(\Omega)\times H^{\beta+1}(\Omega)} &\leq \|\mathbf{E}\mathbf{v} - \mathbf{v_\sigma}\|_{\widetilde{\mathbf{H}}^\beta(\mathbb{R}^d)\times H^{\beta+1}(\mathbb{R}^d)}\\ &\leq c\left(\|\widetilde{\mathbf{E}}_{\mathrm{div}}\mathbf{u}\|_{\widetilde{\mathbf{H}}^\beta(\mathbb{R}^d)} + \|E_S p\|_{H^{\beta+1}(\mathbb{R}^d)}\right)\\ &\leq c\left(\|\mathbf{u}\|_{\mathbf{H}^\beta(\Omega)} + \|p\|_{H^{\beta+1}(\Omega)}\right)\\ &\leq c\|\mathbf{v}\|_{\mathbf{H}^\beta(\Omega)\times H^{\beta+1}(\Omega)}. \end{aligned} \tag{7.10}$$

To bound the second part of (7.9) we can apply theorem 6.6 with $\mathbf{f} := L\mathbf{v_\sigma}$, $\mathbf{g} := \mathbf{u}_\sigma$, $r := 2$ and $\eta := \beta - 1$, since all functions are sufficiently smooth. The definition of $\mathbf{v_\sigma}$ provides that $L\mathbf{v_\sigma} = L\mathbf{v}$ on $X$ and $\mathbf{v_\sigma}\cdot\mathbf{n} = \mathbf{v}\cdot\mathbf{n}$ on $Y$. Furthermore, Darcy's problem is

well defined, therefore $\mathbf{s}_{\mathbf{Ev}}$ approximates $\mathbf{v}_{\boldsymbol{\sigma}}$ and we can define $\mathbf{s}_{\mathbf{v}_{\boldsymbol{\sigma}}} := \mathbf{s}_{\mathbf{Ev}}$. In addition, we use the trace theorem and $\|L\mathbf{v}_{\boldsymbol{\sigma}}\|_{\mathbf{H}^\tau(\Omega)} \leq c\|\mathbf{v}_{\boldsymbol{\sigma}}\|_{\mathbf{H}^\tau(\Omega)\times H^{\tau+1}(\Omega)}$, cf. the proof of proposition 6.3. All in all we get

$$\begin{aligned}\|\mathbf{v}_{\boldsymbol{\sigma}} - \mathbf{s}_{\mathbf{Ev}}\|_{\mathbf{H}^\beta(\Omega)\times H^{\beta+1}(\Omega)} &\leq c\left(h_{X,\Omega}^{\tau-\beta} + h_{Y,\partial\Omega}^{\tau-\beta}\right)\left(\|L\mathbf{v}_{\boldsymbol{\sigma}}\|_{\mathbf{H}^\tau(\Omega)} + \|\mathbf{u}_\sigma \cdot \mathbf{n}\|_{H^{\tau-1/2}(\partial\Omega)}\right)\\ &\leq c\left(h_{X,\Omega}^{\tau-\beta} + h_{Y,\partial\Omega}^{\tau-\beta}\right)\left(\|\mathbf{u}_\sigma\|_{\mathbf{H}^\tau(\Omega)} + \|p_\sigma\|_{H^{\tau+1}(\Omega)} + \|\mathbf{u}_\sigma\|_{\mathbf{H}^\tau(\Omega)}\right)\\ &\leq c\left(h_{X,\Omega}^{\tau-\beta} + h_{Y,\partial\Omega}^{\tau-\beta}\right)\|\mathbf{v}_{\boldsymbol{\sigma}}\|_{\mathbf{H}^\tau(\Omega)\times H^{\tau+1}(\Omega)}.\end{aligned}$$

There exists constants $\varsigma$ and $\widetilde{\varsigma}$ such that $\sigma_{\mathbf{u}} = \varsigma/q_{X\cup Y}$ and $\sigma_p = \widetilde{\varsigma}/q_X$, cf. lemma 7.4 and theorem 7.5. Without loss of generality we define $\sigma := \max\{\sigma_{\mathbf{u}}, \sigma_p\}$, since every band-limited function $f \in \mathcal{B}^\mu$ is also in $\mathcal{B}^\nu$ for all $\nu \geq \mu$. Following the ideas of (7.1) establishes the Bernstein inequality

$$\|\mathbf{v}_{\boldsymbol{\sigma}}\|_{\widetilde{\mathbf{H}}^\tau(\mathbb{R}^d)\times H^{\tau+1}(\mathbb{R}^d)} \leq cq^{\beta-\tau}\|\mathbf{v}_{\boldsymbol{\sigma}}\|_{\widetilde{\mathbf{H}}^\beta(\mathbb{R}^d)\times H^{\beta+1}(\mathbb{R}^d)}.$$

Adding and subtracting $\mathbf{Ev}$ and applying the triangle inequality gives in combination with (7.10) and the properties of the extension operator that

$$\begin{aligned}\|\mathbf{v}_{\boldsymbol{\sigma}}\|_{\widetilde{\mathbf{H}}^\beta(\mathbb{R}^d)\times H^{\beta+1}(\mathbb{R}^d)} &\leq \|\mathbf{Ev} - \mathbf{v}_{\boldsymbol{\sigma}}\|_{\widetilde{\mathbf{H}}^\beta(\mathbb{R}^d)\times H^{\beta+1}(\mathbb{R}^d)} + \|\mathbf{Ev}\|_{\widetilde{\mathbf{H}}^\beta(\mathbb{R}^d)\times H^{\beta+1}(\mathbb{R}^d)}\\ &\leq c\|\mathbf{v}\|_{\mathbf{H}^\beta(\Omega)\times H^{\beta+1}(\Omega)}. \qquad (7.11)\end{aligned}$$

With (7.11), we can bound the second part of (7.9) by

$$\|\mathbf{v}_{\boldsymbol{\sigma}} - \mathbf{s}_{\mathbf{Ev}}\|_{\mathbf{H}^\beta(\Omega)\times H^{\beta+1}(\Omega)} \leq cq^{\beta-\tau}\left(h_{X,\Omega}^{\tau-\beta} + h_{Y,\partial\Omega}^{\tau-\beta}\right)\|\mathbf{v}\|_{\mathbf{H}^\beta(\Omega)\times H^{\beta+1}(\Omega)}.$$

Since $q \leq q_X \leq h_{X,\Omega}$ and $\beta \leq \tau$, we have that $\frac{h_{X,\Omega}^{\tau-\beta}+h_{Y,\partial\Omega}^{\tau-\beta}}{q^{\tau-\beta}}$ is greater than or equal to one. Combining the above inequalities and applying theorem 3.2 gives

$$\begin{aligned}\|L\mathbf{v} - L\mathbf{s}_{\mathbf{v}}\|_{\mathbf{H}^\beta(\Omega)} &\leq c\|\mathbf{v} - \mathbf{s}_{\mathbf{v}}\|_{\mathbf{H}^\beta(\Omega)\times H^{\beta+1}(\Omega)}\\ &\leq c\frac{h_{X,\Omega}^{\tau-\beta} + h_{Y,\partial\Omega}^{\tau-\beta}}{q^{\tau-\beta}}\left(\|\mathbf{u}\|_{\mathbf{H}^\beta(\Omega)} + \|p\|_{H^{\beta+1}(\Omega)/\mathbb{R}}\right)\\ &\leq c\frac{h_{X,\Omega}^{\tau-\beta} + h_{Y,\partial\Omega}^{\tau-\beta}}{q^{\tau-\beta}}\left(\|\mathbf{f}\|_{\mathbf{H}^\beta(\Omega)} + \|\mathbf{g}\cdot\mathbf{n}\|_{H^{\beta-1/2}(\Omega)}\right). \qquad (7.12)\end{aligned}$$

We now bound the boundary part. The proof of proposition 6.5 establishes that there exists an extension $\widetilde{\mathbf{n}} \in \mathbf{H}^{\lceil\beta\rceil}(\overline{\Omega})$ of the normals $\mathbf{n}$ to the interior of $\Omega$ with $\widetilde{\mathbf{n}}|_{\partial\Omega} = \mathbf{n}|_{\partial\Omega}$.

The function $\mathbf{u} - \mathbf{s}_{\mathbf{u}}$ has many zeros, i. e. we can apply the sampling inequality lemma

6.4. Therefore

$$\|(\mathbf{u}-\mathbf{s_u})\cdot\mathbf{n}\|_{W_r^{\eta+1-1/r}(\partial\Omega)} \le c h_{Y,\partial\Omega}^{\beta-1-1/2-\eta+1/r-(d-1)(1/2-1/r)_+} \|(\mathbf{u}-\mathbf{s_u})\cdot\widetilde{\mathbf{n}}\|_{H^\beta(\Omega)}.$$

The proof of proposition 6.5 also establishes

$$\|(\mathbf{u}-\mathbf{s_u})\cdot\widetilde{\mathbf{n}}\|_{H^\beta(\Omega)} \le \|\widetilde{\mathbf{n}}\|_{\mathbf{H}^\beta(\Omega)}\|\mathbf{u}-\mathbf{s_u}\|_{\mathbf{H}^\beta(\Omega)} \le c\|\mathbf{u}-\mathbf{s_u}\|_{\mathbf{H}^\beta(\Omega)}.$$

With (7.12) we have

$$\|\mathbf{u}-\mathbf{s_u}\|_{\mathbf{H}^\beta(\Omega)} \le c\frac{h_{X,\Omega}^{\tau-\beta}+h_{Y,\partial\Omega}^{\tau-\beta}}{q^{\tau-\beta}}\left(\|\mathbf{f}\|_{\mathbf{H}^\beta(\Omega)}+\|\mathbf{g}\cdot\mathbf{n}\|_{H^{\beta-1/2}(\Omega)}\right),$$

which finishes the proof. □

The main difference between the result above and the one for smooth target functions is the factor $(h/q)^{\tau-\beta}$. In the case that $\beta=\tau$, the new result is identical to the one in theorem 6.6 with a constant $c$. If $\tau>\beta$ then this factor is of importance. Since $q$ is always less or equals to $h$, this factor can make the error significantly larger. However, on an equidistant grid or on relatively well spread collocation points, it will have only minor influence.

Note that the limitation of this result to the dimensions $d=2,3$ is again only due to the fact that the extension operator is not yet proven for a general $d>3$.

# 8. Numerical Examples

The numerical validation of the method to solve Darcy's problem and its error estimates is the subject of this chapter. First of all we will give information about the implementation of the computer program used. Then we give two examples to check the error estimates of theorem 6.6. In both cases isotropic material is used. However, in the first example the material is homogeneous and in the second a more realistic inhomogeneous experimental set-up is modelled. After this we will check the error estimates for target functions, which are not in the native space. Furthermore, we look into the dependency of the solution on the given parameters which includes the choice of the basis function, the porosity and the point distribution.

In all computations, the compactly supported Wendland functions $\phi_{d,\ell}$ are chosen for the underlying functions $\phi$ and $\psi$ of

$$\widetilde{\mathbf{\Phi}} = \begin{pmatrix} \mathbf{\Phi}_{\text{div}} & \mathbf{0} \\ \mathbf{0} & \psi \end{pmatrix},$$

where $\mathbf{\Phi}_{\text{div}} = (-\Delta I + \nabla\nabla^T)\phi$.

To ensure that a sufficient amount of collocation points is in the support of the basis functions, we scale them with $\delta := 10$. Moreover, since the error estimates only exists for the case $\phi = \psi$, we choose $\phi = \psi = \phi_{d,\ell}(\frac{\cdot}{\delta})$ for all numerical examples.

## 8.1. Implementation of the Method

The implementation of the mesh-free collocation method presented in chapter 5 requires a numerically stable, efficient solver for large linear systems of equations. We chose the generalised minimal residual (GMRES) method with Householder orthogonalization. The pseudo-code can be found in algorithm 8.1, cf. [46]. The GMRES method gives a numerical solution for the linear system $A\boldsymbol{\alpha} = \mathbf{b}$ with a $\widetilde{N} \times \widetilde{N}$ matrix $A$ and a vector $\mathbf{b} \in \mathbb{R}^{\widetilde{N}}$. An initial guess $\boldsymbol{\alpha}_0 \in \mathbb{R}^{\widetilde{N}}$ for the solution $\boldsymbol{\alpha}$ is required. The solution depends on the computational accuracy given by $\epsilon \geq 0$. In all simulations $\epsilon := 10^{-13}$ is used. The main advantage over the standard GMRES method or the method of conjugate gradients is, that it remains numerically stable for data sets with a small fill distance. Unfortunately,

there is no easy way to implement a parallel version of algorithm 8.1.

Let $\widetilde{N} = dN + M$, where $d$ is the dimension, $N$ is the number of points inside the domain and $M$ gives the number of points on the boundary. To solve Darcy's problem the linear system $A\boldsymbol{\alpha} = \mathbf{b}$ has to be solved, where

$$A := \begin{pmatrix} \left(\lambda_i^{1,\mathbf{x}}\left(\lambda_j^{1,\mathbf{y}}\left(\widetilde{\mathbf{\Phi}}(\mathbf{x}-\mathbf{y})\right)\right)\right) & \dots & \left(\lambda_i^{1,\mathbf{x}}\left(\lambda_\ell^{d+1,\mathbf{y}}\left(\widetilde{\mathbf{\Phi}}(\mathbf{x}-\mathbf{y})\right)\right)\right) \\ \vdots & \ddots & \vdots \\ \left(\lambda_k^{d+1,\mathbf{x}}\left(\lambda_j^{1,\mathbf{y}}\left(\widetilde{\mathbf{\Phi}}(\mathbf{x}-\mathbf{y})\right)\right)\right) & \dots & \left(\lambda_k^{d+1,\mathbf{x}}\left(\lambda_\ell^{d+1,\mathbf{y}}\left(\widetilde{\mathbf{\Phi}}(\mathbf{x}-\mathbf{y})\right)\right)\right) \end{pmatrix} \in \mathbb{R}^{\widetilde{N}\times\widetilde{N}},$$

$1 \le i, j \le N$ and $1 \le k, \ell \le M$, with the functionals defined in (5.6) and (5.7). The initial guess is $\boldsymbol{\alpha}_0 := \mathbf{b}$, where $\mathbf{b} = \begin{pmatrix} \mathbf{f}^T & \mathbf{g}\cdot\mathbf{n} \end{pmatrix}^T \in \mathbb{R}^{dN+M}$ is the right hand side of Darcy's problem. Formula (5.8) gives the approximating function $\mathbf{s_v}$, which depends on the computed solution $\boldsymbol{\alpha}$ of the linear system of equations.

Besides computing the approximating function, its evaluation is the other important part of the computer program. This can be done by a simple `for`-loop over all collocation points. To attain valid results for the error estimates, the approximating function is evaluated on a fine grid. In all simulations, a $\widetilde{M} = 300 \times 300$ grid has been used. The implementation is a `for`-loop over all grid points. For each grid or evaluation point, the approximating function is evaluated and the difference to the true solution computed. The combination of these differences gives the approximation error. However, this can easily be parallelized. Initially the evaluation grid needs to be divided into $n_p$ partitions, where $n_p$ is the number of processors used. For a total of $\widetilde{M}$ evaluation points, every processor evaluates only $\widetilde{M}/n_p$ of them. The partitioning is demonstrated in figure 8.1 for four processors and 196 points. Every colour or symbol refers to the data of a single processor. After evaluating the approximating function at the local set of points, the results from all processors are gathered to compute the final result.

For $n_p$ processors the *speedup* $S_{n_p}$ of a parallel algorithm is given by

$$S_{n_p} = T_1/T_{n_p},$$

where $T_i$ is the runtime for $i$ processors. In the case that $S_{n_p} = n_p$, the speedup is linear. If $S_{n_p} < n_p$ then the code does not scale well. Due to cache effects super linear scaling, i. e. $S_{n_p} > n_p$, is possible. Figure 8.2 shows that the scaling of our parallel implementation of the evaluation step is indeed linear. The computation of the runtime has been done by using the example which will be introduced in section 8.2.1 on a $32 \times 32$ input grid. To reduce the possible influence of other computations running at the time, all time measurements were done twice and the mean value is displayed.

Due to the matrix-vector product and the number of iterations, the computational

**Algorithm 8.1 (GMRES):** GMRES with Householder orthogonalization

**Require:** $A \in \mathbb{R}^{\widetilde{N}\times\widetilde{N}}$, $\mathbf{b}, \boldsymbol{\alpha}_0 \in \mathbb{R}^{\widetilde{N}}$ and $\epsilon \geq 0$
**Ensure:** $\boldsymbol{\alpha}_m$ is the solution of $A\boldsymbol{\alpha} = \mathbf{b}$ with the accuracy $\epsilon$.
Calculate the residual and define $z \leftarrow b - Ax_0$.
**for** $j = 1, \ldots, m+1$ **do**
Compute the Householder unit vector $\mathbf{w}_j$ such that

$$(\mathbf{w}_j)_i = \begin{cases} 0 & 1 \leq i < j \\ z_j + \operatorname{sign}(z_j)\|\mathbf{z}\|_2 & i = j \\ z_i & j < i \leq \widetilde{N} \end{cases}$$

and set $\mathbf{w}_j \leftarrow \mathbf{w}_j/\|\mathbf{w}_j\|_2$, $\mathbf{h}_{j-1} \leftarrow \mathbf{z} - \sigma\mathbf{w}_j$ with $\sigma \leftarrow 2\mathbf{w}_j^T\mathbf{z}$.
**if** $(\mathbf{h}_{j-1})_j < \epsilon$ **then**
Set $m \leftarrow j$ and **stop the loop**.
**end if**
**if** $j = 1$ **then**
Set $\gamma_j \leftarrow (\mathbf{h}_0)_1$.
**end if**
**if** $j \leq m$ **then**
Compute $\mathbf{v} \leftarrow (I - 2\mathbf{w}_1\mathbf{w}_1^T)\ldots(I - 2\mathbf{w}_j\mathbf{w}_j^T)\mathbf{e}_j$ and
$\mathbf{z} \leftarrow (I - 2\mathbf{w}_j\mathbf{w}_j^T)\ldots(I - 2\mathbf{w}_1\mathbf{w}_1^T)A\mathbf{v}$.
**end if**
**for** $i = 1, \ldots, j-1$ **do**
Set $\tilde{h} \leftarrow h_{ij}$ and multiply new column with the calculated Givens rotation $G_{i,i+1}$:
$h_{ij} \leftarrow c_i\tilde{h} + s_i h_{i+1,j}$ and $h_{i+1,j} \leftarrow -s_i\tilde{h} + c_i h_{i+1,j}$.
**end for**
Calculate the new Givens rotation: $\beta \leftarrow \sqrt{h_{jj}^2 + h_{j+1,j}^2}$, $c_j \leftarrow h_{jj}/\beta$, $s_j \leftarrow h_{j+1,j}/\beta$ and update $H$ and $\boldsymbol{\gamma}$, i. e. $h_{jj} \leftarrow \beta$, $h_{j+1,j} \leftarrow 0$, $\gamma_{j+1} \leftarrow -s_j\gamma_j$ and $\gamma_j \leftarrow c_j\gamma_j$.
**if** $|\gamma_{j+1}| < \epsilon$ **then**
Set $m \leftarrow j$ and **stop the loop**.
**end if**
**end for**
Compute the minimiser $\mathbf{y}$ of $\|\boldsymbol{\gamma} - H_m\mathbf{y}\|_2$, $H_m := (\mathbf{h}_1, \ldots, \mathbf{h}_m)$, via back substitution:
**for** $i = m, \ldots, 1$ **do**
$y_i \leftarrow \frac{1}{h_{ii}}\left(\gamma_i - \sum_{k=i+1}^{m} h_{ik}y_k\right)$
**end for**
$\mathbf{z} \leftarrow \mathbf{0}$
**for** $j = m, \ldots, 1$ **do**
Set $\mathbf{z} \leftarrow y_j e_j + \mathbf{z} - \sigma\mathbf{w}_j$ with $\sigma \leftarrow 2\mathbf{w}_j^T\mathbf{z}$.
**end for**
Compute the solution $\boldsymbol{\alpha}_m \leftarrow \boldsymbol{\alpha}_0 + \mathbf{z}$.

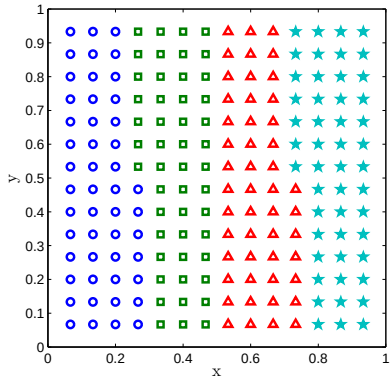


Figure 8.1: Partitioning of 196 evaluation points for the parallel implementation with four processors.

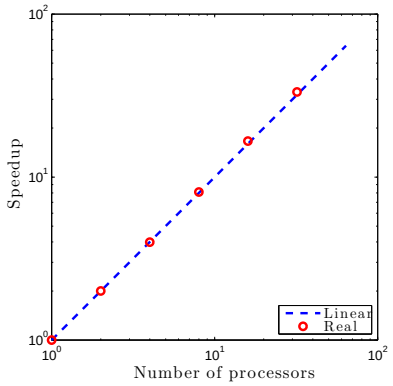


Figure 8.2: The speedup of the evaluation step.

complexity of the GMRES method is $O(m\widetilde{N}^2)$. Here $\widetilde{N} \times \widetilde{N}$ is the dimension of the collocation matrix $A$ and $m$ is the number of iterations. Usually the number of iterations is significantly smaller than the dimension of the problem. Evaluating the approximating function at a single point has complexity $O(\widetilde{N})$. Since the evaluation is done for $\widetilde{M}$ evaluation points the complexity of the evaluation step is $O(\widetilde{M}\widetilde{N})$. In total the computational complexity of our implementation is $O(m\widetilde{N}^2 + \widetilde{M}\widetilde{N})$.

Our computer program could be improved such that the runtime is reduced. For example, a more efficient solver for the system of equations could be applied, or some preconditioning algorithm used. A parallel implementation of the matrix-vector products in the GMRES method is also possible. Further improvement could be achieved by a far-field expansion for the evaluation of the approximating function.

## 8.2. Numerical Error Estimates

We will now test the theoretical error estimates of chapter 6 on two numerical examples. Our first example deals with homogeneous and isotropic permeability, where $K$ reduces to a constant times the identity matrix. Our second example deals with inhomogeneous material. However, it is still isotropic.

We will employ Wendland functions $\phi_{2,\ell} \in C^{2\ell}(\mathbb{R}^2)$ for both $\phi$ and $\psi$, which generate Sobolev spaces $H^{\ell+3/2}(\mathbb{R}^2)$, see theorem 4.13. Thus by picking $\phi = \psi = \phi_{2,\ell}$, we have

$$\mathcal{N}_{\widetilde{\mathbf{\Phi}}}(\mathbb{R}^2) = \mathbf{H}^{\ell+1/2}(\mathbb{R}^2; \mathrm{div}) \times H^{\ell+3/2}(\mathbb{R}^2), \tag{8.1}$$

which means $\tau = \ell + 1/2$. This follows from corollary 4.15, which shows that if $\phi$ generates the space $H^{\tau+1}(\mathbb{R}^d)$ then $\mathbf{\Phi}_{\mathrm{div}}$ generates $\widetilde{\mathbf{H}}^{\tau}(\mathbb{R}^d)$. We will concentrate on the $L_\infty$ and $L_2$ error only, i. e. we want to verify the estimates

$$\begin{aligned} \|\mathbf{u} - \mathbf{s_u}\|_{\mathbf{H}^\eta(\Omega)} + \|p - s_p\|_{H^{\eta+1}(\Omega)/\mathbb{R}} &\leq c_{\mathbf{f},\mathbf{g}} h^{\tau-\eta} &&= c_{\mathbf{f},\mathbf{g}} h^{\ell+\frac{1}{2}-\eta}, \\ \|\mathbf{u} - \mathbf{s_u}\|_{\mathbf{W}^\eta_\infty(\Omega)} + \|p - s_p\|_{W^{\eta+1}_\infty(\Omega)/\mathbb{R}} &\leq c_{\mathbf{f},\mathbf{g}} h^{\tau-\eta-d/2} &&= c_{\mathbf{f},\mathbf{g}} h^{\ell-\frac{1}{2}-\eta}. \end{aligned}$$

Note that the first estimate was only shown for $\eta \geq 1$ in theorem 6.6. The second estimate is also not justified by our theoretical analysis.

In all cases the notation $\mathbf{e_u} = \mathbf{u} - \mathbf{s_u}$ and $e_p = p - s_p$ is used. The numerical tests were run on a sequence of equidistant grids. The computational approximation orders are given by

$$\frac{\log(e_n/e_{2n})}{\log(1/2)},$$

where $e_n$ is the error on an $n \times n = N + M$ input grid. Therefore we have $N = (n-2)^2$ collocation points in the interior and $M = 4n - 4$ on the boundary, for an example see figure 8.8 (a).

### 8.2.1. Homogeneous Permeability

In our first example, we choose $\Omega = [0,1]^2$ and $K = I$ and $\mathbf{f}$ and $\mathbf{g}$ such that the true solution is given by

$$\mathbf{u}(x,y) = (-2x^3y,\, 3x^2y^2)^T, \qquad p(x,y) = x^3y^2.$$

The velocity and pressure are illustrated in figure 8.3. The velocity field is displayed with unit vectors. In figure 8.3 (b), the contour lines of the pressure are visualised. Therefore

the boundary function $\mathbf{g}$ is defined by $\mathbf{u}$ on $\partial\Omega$, while

$$\mathbf{f}(x,y) = \mathbf{u}(x,y) + K\nabla p(x,y) = \begin{pmatrix} -2x^3y + 3x^2y^2 \\ 2x^3y + 3x^2y^2 \end{pmatrix}.$$

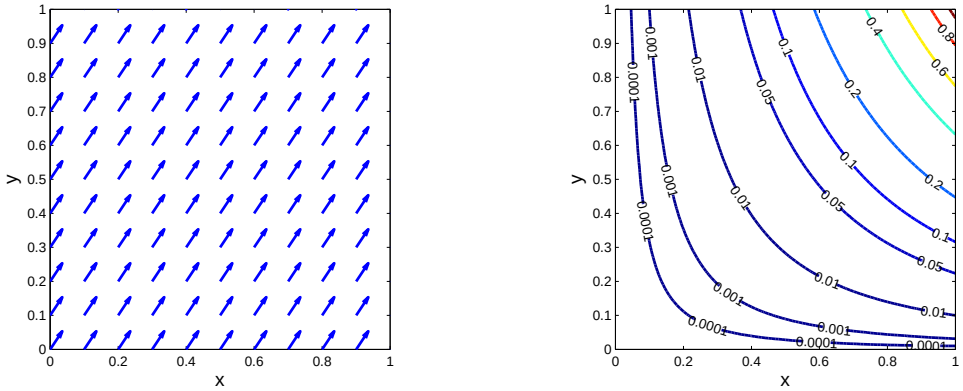


(a) The velocity field for the homogeneous example visualised with unit vectors.

(b) The contour lines of the pressure field.

Figure 8.3: The true solution of the homogeneous example.

We tested this for a variety of basis functions as explained above. The error has been computed using discretized versions of the various norms on a fine $300 \times 300$ grid. The results are presented in tables 8.1 to 8.6 and in figure 8.4. They indicate that the numerical approximation orders more than match the theoretical ones.

| n | $\|\mathbf{e_u}\|_{\mathbf{L}_2}$ | $\|\mathbf{e_u}\|_{\mathbf{L}_\infty}$ | $\|\mathbf{e_u}\|_{\mathbf{H}^1}$ | $\|\mathbf{e_u}\|_{\mathbf{H}^2}$ | $\|\nabla e_p\|_{\mathbf{L}_2}$ | $\|\nabla e_p\|_{\mathbf{L}_\infty}$ |
|---|---|---|---|---|---|---|
| 4 | 1.6335e-01 | 7.7583e-01 | 1.1289e+00 | 6.8905e+00 | 2.9920e-01 | 2.1715e+00 |
| 8 | 2.9333e-02 | 2.1230e-01 | 4.6740e-01 | 5.3876e+00 | 4.9407e-02 | 6.9474e-01 |
| 16 | 4.7724e-03 | 5.5458e-02 | 1.6321e-01 | 3.7585e+00 | 6.9639e-03 | 1.8473e-01 |
| 32 | 6.5486e-04 | 1.3832e-02 | 4.7138e-02 | 2.2668e+00 | 8.8743e-04 | 4.4247e-02 |
| 64 | 7.9729e-05 | 3.0498e-03 | 1.2110e-02 | 1.2395e+00 | 1.0140e-04 | 9.2248e-03 |

Table 8.1: Approximation errors for the homogeneous example with $\phi = \psi = \phi_{2,2}$.

### 8.2.2. Inhomogeneous Permeability

Our second example deals with inhomogeneous and isotropic material, meaning that $K = \kappa I$ with a non-constant function $\kappa$. Our example is motivated by a similar example from [50] and describes the flow through a two dimensional cylinder with varying permeability.

| | $\|\mathbf{e_u}\|_{\mathbf{L}_2}$ | $\|\mathbf{e_u}\|_{\mathbf{L}_\infty}$ | $\|\mathbf{e_u}\|_{\mathbf{H}^1}$ | $\|\mathbf{e_u}\|_{\mathbf{H}^2}$ | $\|\nabla e_p\|_{\mathbf{L}_2}$ | $\|\nabla e_p\|_{\mathbf{L}_\infty}$ |
|---|---|---|---|---|---|---|
| computed | 2.4774 | 1.8697 | 1.2722 | 0.3550 | 2.5983 | 1.6442 |
| | 2.6197 | 1.9366 | 1.5179 | 0.5195 | 2.8267 | 1.9111 |
| | 2.8655 | 2.0033 | 1.7918 | 0.7295 | 2.9722 | 2.0618 |
| | 3.0380 | 2.1813 | 1.9606 | 0.8710 | 3.1296 | 2.2620 |
| estimated | 2.5 | 1.5 | 1.5 | 0.5 | 2.5 | 1.5 |

Table 8.2: Approximation orders for the homogeneous example with $\phi = \psi = \phi_{2,2}$.

| n | $\|\mathbf{e_u}\|_{\mathbf{L}_2}$ | $\|\mathbf{e_u}\|_{\mathbf{L}_\infty}$ | $\|\mathbf{e_u}\|_{\mathbf{H}^1}$ | $\|\mathbf{e_u}\|_{\mathbf{H}^2}$ | $\|\nabla e_p\|_{\mathbf{L}_2}$ | $\|\nabla e_p\|_{\mathbf{L}_\infty}$ |
|---|---|---|---|---|---|---|
| 4 | 1.0127e-01 | 3.6764e-01 | 7.0026e-01 | 4.1830e+00 | 2.1525e-01 | 1.4904e+00 |
| 8 | 8.6886e-03 | 4.3353e-02 | 1.4323e-01 | 1.7673e+00 | 1.2082e-02 | 1.8352e-01 |
| 16 | 6.6247e-04 | 5.3868e-03 | 2.4002e-02 | 6.3930e-01 | 7.6629e-04 | 2.0568e-02 |
| 32 | 4.0582e-05 | 5.8268e-04 | 3.0337e-03 | 1.7604e-01 | 4.1610e-05 | 1.7658e-03 |
| 64 | 2.2916e-06 | 5.6109e-05 | 3.3587e-04 | 4.0901e-02 | 2.1316e-06 | 8.3619e-05 |

Table 8.3: Approximation errors for the homogeneous example with $\phi = \psi = \phi_{2,3}$.

| | $\|\mathbf{e_u}\|_{\mathbf{L}_2}$ | $\|\mathbf{e_u}\|_{\mathbf{L}_\infty}$ | $\|\mathbf{e_u}\|_{\mathbf{H}^1}$ | $\|\mathbf{e_u}\|_{\mathbf{H}^2}$ | $\|\nabla e_p\|_{\mathbf{L}_2}$ | $\|\nabla e_p\|_{\mathbf{L}_\infty}$ |
|---|---|---|---|---|---|---|
| computed | 3.5430 | 3.0841 | 2.2896 | 1.2430 | 4.1550 | 3.0217 |
| | 3.7132 | 3.0086 | 2.5771 | 1.4670 | 3.9788 | 3.1575 |
| | 4.0289 | 3.2087 | 2.9840 | 1.8606 | 4.2029 | 3.5420 |
| | 4.1464 | 3.3764 | 3.1751 | 2.1057 | 4.2869 | 4.4003 |
| estimated | 3.5 | 2.5 | 2.5 | 1.5 | 3.5 | 2.5 |

Table 8.4: Approximation orders for the homogeneous example with $\phi = \psi = \phi_{2,3}$.

| n | $\|\mathbf{e_u}\|_{\mathbf{L}_2}$ | $\|\mathbf{e_u}\|_{\mathbf{L}_\infty}$ | $\|\mathbf{e_u}\|_{\mathbf{H}^1}$ | $\|\mathbf{e_u}\|_{\mathbf{H}^2}$ | $\|\nabla e_p\|_{\mathbf{L}_2}$ | $\|\nabla e_p\|_{\mathbf{L}_\infty}$ |
|---|---|---|---|---|---|---|
| 4 | 6.1153e-02 | 2.0845e-01 | 4.3615e-01 | 2.8112e+00 | 2.0304e-01 | 1.2941e+00 |
| 8 | 2.3251e-03 | 1.1990e-02 | 4.1046e-02 | 5.5070e-01 | 3.2751e-03 | 5.0862e-02 |
| 16 | 7.9533e-05 | 7.1673e-04 | 3.0418e-03 | 9.1047e-02 | 9.5225e-05 | 2.7176e-03 |
| 32 | 2.3199e-06 | 3.8217e-05 | 1.7927e-04 | 1.1659e-02 | 2.4788e-06 | 1.0642e-04 |
| 64 | 7.4599e-08 | 1.1181e-06 | 1.2205e-05 | 1.6011e-03 | 1.0738e-07 | 3.4691e-06 |

Table 8.5: Approximation errors for the homogeneous example with $\phi = \psi = \phi_{2,4}$.

| | $\|\mathbf{e_u}\|_{\mathbf{L}_2}$ | $\|\mathbf{e_u}\|_{\mathbf{L}_\infty}$ | $\|\mathbf{e_u}\|_{\mathbf{H}^1}$ | $\|\mathbf{e_u}\|_{\mathbf{H}^2}$ | $\|\nabla e_p\|_{\mathbf{L}_2}$ | $\|\nabla e_p\|_{\mathbf{L}_\infty}$ |
|---|---|---|---|---|---|---|
| computed | 4.7171 | 4.1198 | 3.4095 | 2.3518 | 5.9541 | 4.6693 |
| | 4.8696 | 4.0643 | 3.7543 | 2.5966 | 5.1040 | 4.2262 |
| | 5.0994 | 4.2291 | 4.0847 | 2.9652 | 5.2636 | 4.6745 |
| | 4.9588 | 5.0951 | 3.8765 | 2.8643 | 4.5289 | 4.9390 |
| estimated | 4.5 | 3.5 | 3.5 | 2.5 | 4.5 | 3.5 |

Table 8.6: Approximation orders for the homogeneous example with $\phi = \psi = \phi_{2,4}$.

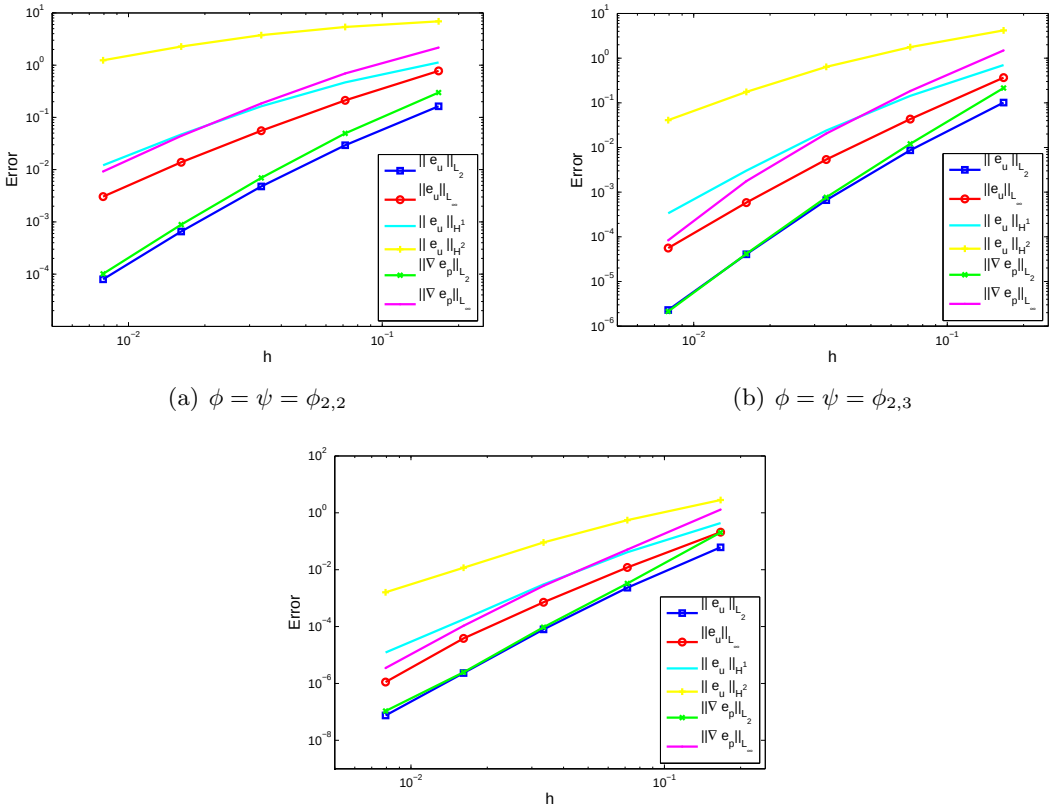


(a) $\phi = \psi = \phi_{2,2}$

(b) $\phi = \psi = \phi_{2,3}$

(c) $\phi = \psi = \phi_{2,4}$

Figure 8.4: Approximation errors of the homogeneous example.

| n | $\|\mathbf{e_u}\|_{\mathbf{L}_2}$ | $\|\mathbf{e_u}\|_{\mathbf{L}_\infty}$ | $\|\mathbf{e_u}\|_{\mathbf{H}^1}$ | $\|\mathbf{e_u}\|_{\mathbf{H}^2}$ | $\|\nabla e_p\|_{\mathbf{L}_2}$ | $\|\nabla e_p\|_{\mathbf{L}_\infty}$ |
|---|---|---|---|---|---|---|
| 4 | 6.2920e-03 | 2.3987e-02 | 5.2479e-02 | 5.1676e-01 | 4.9587e-02 | 1.2463e-01 |
| 8 | 5.3211e-04 | 4.6569e-03 | 8.8350e-03 | 1.3797e-01 | 2.2983e-03 | 9.9190e-03 |
| 16 | 4.0233e-05 | 5.5241e-04 | 1.4920e-03 | 4.5095e-02 | 1.8430e-04 | 1.4879e-03 |
| 32 | 2.9049e-06 | 5.3613e-05 | 2.3020e-04 | 1.3925e-02 | 1.7299e-05 | 2.4952e-04 |
| 64 | 1.8260e-07 | 4.1769e-06 | 3.0837e-05 | 3.8451e-03 | 1.5696e-06 | 3.8521e-05 |

Table 8.7: Approximation errors for the inhomogeneous example with $\phi = \psi = \phi_{2,3}$.

To be more precise, pressure, velocity and permeability are given by

$$\begin{aligned} p(x,y) &= \frac{p_1 - p_0}{L}x + p_0, \\ \mathbf{u}(x,y) &= \left(\frac{p_0 - p_1}{L\mu}(y-y_a)(y-y_b), 0\right)^T, \\ \kappa(x,y) &= (y-y_a)(y-y_b), \end{aligned}$$

where $\mu$ is the viscosity and $L$ the length of the cylinder. Thus $\mathbf{f} = \mathbf{0}$ and $\mathbf{g} = (\frac{p_0-p_1}{L\mu}(y-y_a)(y-y_b), 0)$. Obviously, these quantities satisfy (3.2) and $\nabla \cdot \mathbf{u} = 0$. The permeability is constant along horizontal lines and is zero at the top and bottom boundary of the cylinder. The flow is also horizontal, see figure 8.5.

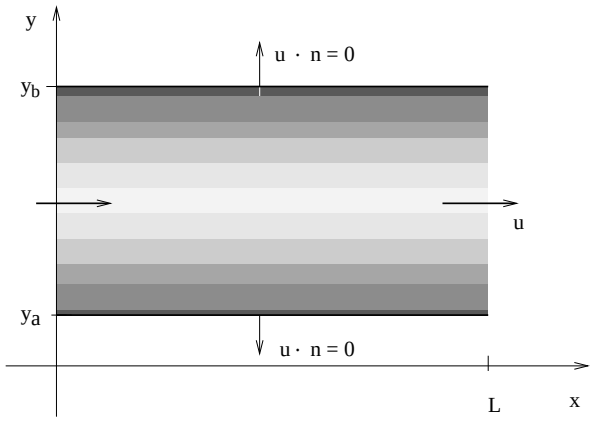


Figure 8.5: The schematic set up for the inhomogeneous example.

For our computations, we set $L = 1$, $y_a = 0$, $y_b = 1$, $\mu = 1$, $p_1 = 2$ and $p_0 = 1$. For $\phi = \psi$ we have chosen the $C^6$ compactly supported function.

The results are represented in tables 8.7 and 8.8 and in figure 8.6.

| | $\|\mathbf{e_u}\|_{\mathbf{L}_2}$ | $\|\mathbf{e_u}\|_{\mathbf{L}_\infty}$ | $\|\mathbf{e_u}\|_{\mathbf{H}^1}$ | $\|\mathbf{e_u}\|_{\mathbf{H}^2}$ | $\|\nabla e_p\|_{\mathbf{L}_2}$ | $\|\nabla e_p\|_{\mathbf{L}_\infty}$ |
|---|---|---|---|---|---|---|
| computed | 3.5637 | 2.3648 | 2.5705 | 1.9052 | 4.4313 | 3.6513 |
| | 3.7253 | 3.0756 | 2.5660 | 1.6133 | 3.6404 | 2.7370 |
| | 3.7918 | 3.3651 | 2.6963 | 1.6953 | 3.4133 | 2.5760 |
| | 3.9917 | 3.6821 | 2.9001 | 1.8566 | 3.4623 | 2.6954 |
| estimated | 3.5 | 2.5 | 2.5 | 1.5 | 3.5 | 2.5 |

Table 8.8: Approximation orders for the inhomogeneous example with $\phi = \psi = \phi_{2,3}$.

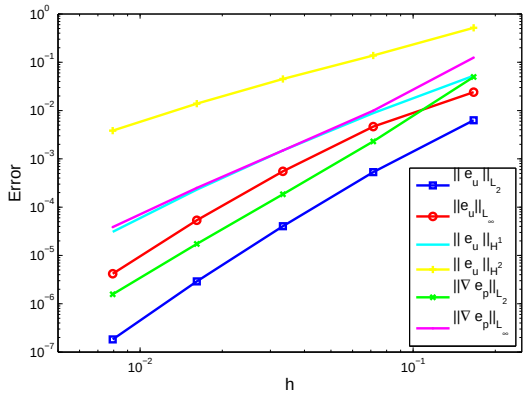


Figure 8.6: Approximation errors of the inhomogeneous example with $\phi = \psi = \phi_{2,3}$.

## 8.3. Numerical Error Estimates for Target Functions Outside the Native Space

We will now give an example for target functions which are not in the native space. Again we employ Wendland functions and pick $\phi = \psi = \phi_{2,\ell}$, i. e. they generate the native spaces given in (8.1). As in the previous examples we will focus on the $L_2$ and $L_\infty$ errors. Let $\mathbf{f} \in \mathbf{H}^{\beta+1}(\Omega)$ and $\mathbf{g} \in \mathbf{H}^{\beta+1/2}(\partial\Omega)$, where $d/2 < \beta \leq \tau := d/2 + \ell + 1/2$. Theorem 7.6 gives the following error estimates

$$\|\mathbf{u} - \mathbf{s_u}\|_{\mathbf{H}^\eta(\Omega)} + \|p - s_p\|_{H^{\eta+1}(\Omega)} \leq c_{\mathbf{f},\mathbf{g}} \left(\frac{h}{q}\right)^{\tau-\beta} h^{\beta-\eta},$$
$$\|\mathbf{u} - \mathbf{s_u}\|_{\mathbf{W}^\eta_\infty(\Omega)} + \|p - s_p\|_{W^{\eta+1}_\infty(\Omega)} \leq c_{\mathbf{f},\mathbf{g}} \left(\frac{h}{q}\right)^{\tau-\beta} h^{\beta-\eta-d/2}.$$

Note that the first estimate was proven for $\eta \geq 1$ only. Moreover, the second estimate is actually not verified by theorem 7.6. Note further that the convergence order does not depend on the smoothness $\tau$ of the native space if the separation radius equals the fill distance, i. e. on equidistant grids.

We choose $\mathbf{f}$ and $\mathbf{g}$ such that the true solution of the velocity and the pressure are

$$\mathbf{u}(x,y) = \begin{pmatrix} -\partial_y \\ \partial_x \end{pmatrix} \phi_{2,1}(r), \qquad p(x,y) = x^3 y^2,$$

where $r := \sqrt{(x-x_0)^2 + (y-y_0)^2}/\gamma$ with $x_0 = y_0 = \gamma = 0.5$. Furthermore, we pick $K = I$, where $I$ is the identity matrix. The remaining setting is identical to the one in the previous examples. Figure 8.7 illustrates the velocity field. The pressure is identical to the pressure in the homogeneous example, see figure 8.3 (b).

The Wendland functions $\phi_{d,\ell}$ are an element of all Sobolev spaces $H^\alpha(\mathbb{R}^d)$ with $\alpha < 2\tau - d/2 = d + 2\ell + 1 - d/2$, cf. section 4.2.3. Therefore the function $\phi_{2,1}$ is in $H^\alpha(\Omega)$ with $\alpha < 4$. Due to our choice of the velocity, we have $\mathbf{u} \in H^{\beta+1}(\Omega)$ for all $\beta < 2$. Thus $\mathbf{u}$ is not an element of the native spaces of $\phi_{2,3}$ and $\phi_{2,4}$, where $\tau = 3.5$ and $\tau = 4.5$ respectively. We chose $\beta = 2$ which is the supremum of the smoothness', to work out the theoretical approximation orders.

To investigate the dependency of the error on the fill distance $h$ and the separation radius $q$, all calculations were done twice. First on an equidistant grid, then on an equidistant grid, where the $y$-components of some collocation points are moved by $s/2$ up, see figure 8.8. Here, $s = 1/(n-1)$ is the spacing of the grid. Hence, in the first case we have $q = h = s/2$ and in the second case $q < h$, i. e. $q = s/4$ and $h = 3s/4$.

All results are displayed in tables 8.9–8.16. Here, the values in the brackets give the

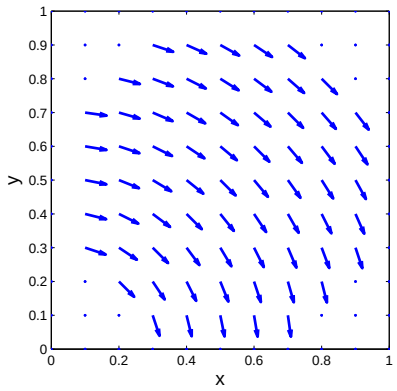


Figure 8.7: The velocity field for the example with target functions outside the native space visualised with unit vectors.

approximation orders if the target functions were in the native space. The figures 8.9 and 8.9 illustrate the numerical approximation errors. From tables 8.10, 8.12, 8.14 and 8.16 it can be seen that the numerical approximation orders again more than match the theoretical ones. Moreover, some of them even match the approximation orders for smoother target functions.

According to the theoretical error estimates, the error in table 8.12 should be $(q/h)^{\tau-\beta} = 5.1962$ times larger than in table 8.10. Analogously, the values in table 8.16 should be 15.588 times larger than the values in table 8.14. In practise, the influence of the factor $(q/h)^{\tau-\beta}$ seems to be less than expected, since the calculated values are in about the same range.

| n | $\|\mathbf{e_u}\|_{\mathbf{L}_2}$ | $\|\mathbf{e_u}\|_{\mathbf{L}_\infty}$ | $\|\mathbf{e_u}\|_{\mathbf{H}^1}$ | $\|\nabla e_p\|_{\mathbf{L}_2}$ | $\|\nabla e_p\|_{\mathbf{L}_\infty}$ |
|---|---|---|---|---|---|
| 4 | 1.2836e+00 | 2.2024e+00 | 9.8131e+00 | 2.0342e-01 | 1.5629e+00 |
| 8 | 7.9192e-02 | 3.8168e-01 | 1.6632e+00 | 3.4692e-02 | 2.1824e-01 |
| 16 | 8.7058e-03 | 5.1376e-02 | 3.9872e-01 | 2.9099e-03 | 3.0136e-02 |
| 32 | 7.4455e-04 | 1.1950e-02 | 7.9047e-02 | 2.7432e-04 | 3.0789e-03 |
| 64 | 6.5388e-05 | 2.8183e-03 | 1.6406e-02 | 2.8833e-05 | 7.2737e-04 |

Table 8.9: Approximation errors for the example with target functions outside the native space with $\phi = \psi = \phi_{2,3}$, where $q = h$.

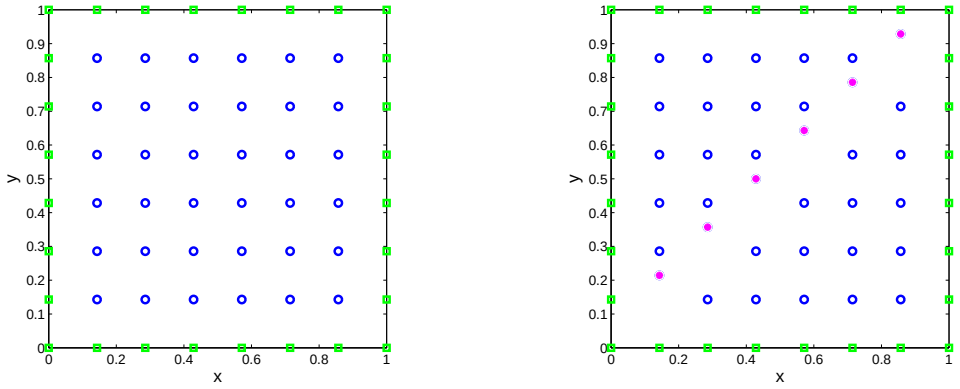


(a) $q = h$ (b) $q < h$

Figure 8.8: The $n \times n$-grid for the example with target functions outside the native space, where $n = 8$. The collocation points in the interior are maked with blue circles, the ones on the boundary with green squares and the moved points with a magenta dots.

| | $\|\mathbf{e_u}\|_{\mathbf{L}_2}$ | $\|\mathbf{e_u}\|_{\mathbf{L}_\infty}$ | $\|\mathbf{e_u}\|_{\mathbf{H}^1}$ | $\|\nabla e_p\|_{\mathbf{L}_2}$ | $\|\nabla e_p\|_{\mathbf{L}_\infty}$ |
|---|---|---|---|---|---|
| computed | 4.0187 | 2.5286 | 2.5607 | 2.5518 | 2.8403 |
| | 3.1853 | 2.8932 | 2.0605 | 3.5756 | 2.8564 |
| | 3.5475 | 2.1041 | 2.3346 | 3.4070 | 3.2910 |
| | 3.5093 | 2.0841 | 2.2685 | 3.2501 | 2.0817 |
| estimated | 2 (3.5) | 1 (2.5) | 1 (2.5) | 2 (3.5) | 1 (2.5) |

Table 8.10: Approximation orders for the example with target functions outside the native space with $\phi = \psi = \phi_{2,3}$, where the values in the brackets give the approximation orders if the target function would be in the native space and $q = h$.

| n | $\|\mathbf{e_u}\|_{\mathbf{L}_2}$ | $\|\mathbf{e_u}\|_{\mathbf{L}_\infty}$ | $\|\mathbf{e_u}\|_{\mathbf{H}^1}$ | $\|\nabla e_p\|_{\mathbf{L}_2}$ | $\|\nabla e_p\|_{\mathbf{L}_\infty}$ |
|---|---|---|---|---|---|
| 4 | 9.6580e-01 | 1.6182e+00 | 9.0492e+00 | 2.0209e+00 | 6.3613e+00 |
| 8 | 8.0852e-02 | 3.7836e-01 | 1.7364e+00 | 1.0950e-01 | 4.5009e-01 |
| 16 | 9.2390e-03 | 7.9565e-02 | 4.1916e-01 | 4.7343e-03 | 4.0854e-02 |
| 32 | 8.3544e-04 | 1.8466e-02 | 8.5372e-02 | 5.0651e-04 | 9.6855e-03 |
| 64 | 7.9497e-05 | 4.3506e-03 | 1.8161e-02 | 5.8489e-05 | 2.3040e-03 |

Table 8.11: Approximation errors for the example with target functions outside the native space with $\phi = \psi = \phi_{2,3}$, where $q < h$.

| | $\|\mathbf{e_u}\|_{\mathbf{L}_2}$ | $\|\mathbf{e_u}\|_{\mathbf{L}_\infty}$ | $\|\mathbf{e_u}\|_{\mathbf{H}^1}$ | $\|\nabla e_p\|_{\mathbf{L}_2}$ | $\|\nabla e_p\|_{\mathbf{L}_\infty}$ |
|---|---|---|---|---|---|
| computed | 3.5784 | 2.0965 | 2.3817 | 4.2060 | 3.8210 |
| | 3.1295 | 2.2495 | 2.0505 | 4.5316 | 3.4616 |
| | 3.4671 | 2.1073 | 2.2957 | 3.2245 | 2.0766 |
| | 3.3936 | 2.0856 | 2.2329 | 3.1143 | 2.0717 |
| estimated | 2 (3.5) | 1 (2.5) | 1 (2.5) | 2 (3.5) | 1 (2.5) |

Table 8.12: Approximation orders for the example with target functions outside the native space with $\phi = \psi = \phi_{2,3}$, where the values in the brackets give the approximation orders if the target function would be in the native space and $q < h$.

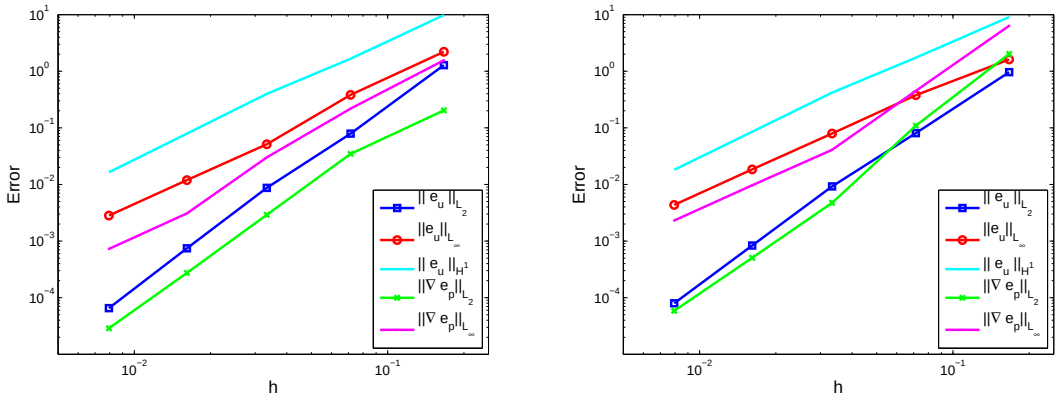


(a) $q = h$ (b) $q \leq h$

Figure 8.9: Approximation errors of example with target functions outside the native space, where $\phi = \psi = \phi_{2,3}$.

| n | $\|\mathbf{e_u}\|_{\mathbf{L}_2}$ | $\|\mathbf{e_u}\|_{\mathbf{L}_\infty}$ | $\|\mathbf{e_u}\|_{\mathbf{H}^1}$ | $\|\nabla e_p\|_{\mathbf{L}_2}$ | $\|\nabla e_p\|_{\mathbf{L}_\infty}$ |
|---|---|---|---|---|---|
| 4 | 1.5065e+00 | 2.9039e+00 | 1.1038e+01 | 1.8339e-01 | 1.3481e+00 |
| 8 | 5.3121e-01 | 2.4564e+00 | 8.7189e+00 | 9.7268e-02 | 2.0440e-01 |
| 16 | 1.2688e-02 | 6.9891e-02 | 5.3229e-01 | 3.1878e-03 | 1.1819e-02 |
| 32 | 5.8579e-04 | 1.1669e-02 | 7.1774e-02 | 2.6409e-04 | 2.7596e-03 |
| 64 | 6.3984e-05 | 2.7337e-03 | 1.6597e-02 | 2.7801e-05 | 6.5679e-04 |

Table 8.13: Approximation errors for the example with target functions outside the native space with $\phi = \psi = \phi_{2,4}$, where $q = h$.

| | $\|\mathbf{e_u}\|_{\mathbf{L}_2}$ | $\|\mathbf{e_u}\|_{\mathbf{L}_\infty}$ | $\|\mathbf{e_u}\|_{\mathbf{H}^1}$ | $\|\nabla e_p\|_{\mathbf{L}_2}$ | $\|\nabla e_p\|_{\mathbf{L}_\infty}$ |
|---|---|---|---|---|---|
| computed | 1.5038 | 0.2415 | 0.3403 | 0.9149 | 2.7214 |
| | 5.3877 | 5.1353 | 4.0339 | 4.9313 | 4.1122 |
| | 4.4369 | 2.5825 | 2.8907 | 3.5935 | 2.0986 |
| | 3.1946 | 2.0937 | 2.1126 | 3.2478 | 2.0709 |
| estimated | 2 (4.5) | 1 (3.5) | 1 (3.5) | 2 (4.5) | 1 (3.5) |

Table 8.14: Approximation orders for the example with target functions outside the native space with $\phi = \psi = \phi_{2,4}$, where the values in the brackets give the approximation orders if the target function would be in the native space and $q = h$.

| n | $\|\mathbf{e_u}\|_{\mathbf{L}_2}$ | $\|\mathbf{e_u}\|_{\mathbf{L}_\infty}$ | $\|\mathbf{e_u}\|_{\mathbf{H}^1}$ | $\|\nabla e_p\|_{\mathbf{L}_2}$ | $\|\nabla e_p\|_{\mathbf{L}_\infty}$ |
|---|---|---|---|---|---|
| 4 | 9.9594e-01 | 1.8031e+00 | 9.5157e+00 | 2.6038e+00 | 9.0934e+00 |
| 8 | 4.9692e-01 | 2.4419e+00 | 8.2523e+00 | 2.0109e-01 | 7.5860e-01 |
| 16 | 1.2221e-02 | 7.1743e-02 | 5.1902e-01 | 5.3100e-03 | 3.6592e-02 |
| 32 | 6.3966e-04 | 1.6423e-02 | 7.4964e-02 | 4.6787e-04 | 8.6301e-03 |
| 64 | 7.0954e-05 | 3.8505e-03 | 1.7397e-02 | 5.3756e-05 | 2.0566e-03 |

Table 8.15: Approximation errors for the example with target functions outside the native space with $\phi = \psi = \phi_{2,4}$, where $q < h$.

| | $\|\mathbf{e_u}\|_{\mathbf{L}_2}$ | $\|\mathbf{e_u}\|_{\mathbf{L}_\infty}$ | $\|\mathbf{e_u}\|_{\mathbf{H}^1}$ | $\|\nabla e_p\|_{\mathbf{L}_2}$ | $\|\nabla e_p\|_{\mathbf{L}_\infty}$ |
|---|---|---|---|---|---|
| computed | 1.0030 | -0.4375 | 0.2055 | 3.6947 | 3.5834 |
| | 5.3456 | 5.0890 | 3.9909 | 5.2430 | 4.3737 |
| | 4.2559 | 2.1271 | 2.7915 | 3.5045 | 2.0841 |
| | 3.1724 | 2.0926 | 2.1073 | 3.1216 | 2.0691 |
| estimated | 2 (4.5) | 1 (3.5) | 1 (3.5) | 2 (4.5) | 1 (3.5) |

Table 8.16: Approximation orders for the example with target functions outside the native space with $\phi = \psi = \phi_{2,4}$, where the values in the brackets give the approximation orders if the target function would be in the native space and $q < h$.

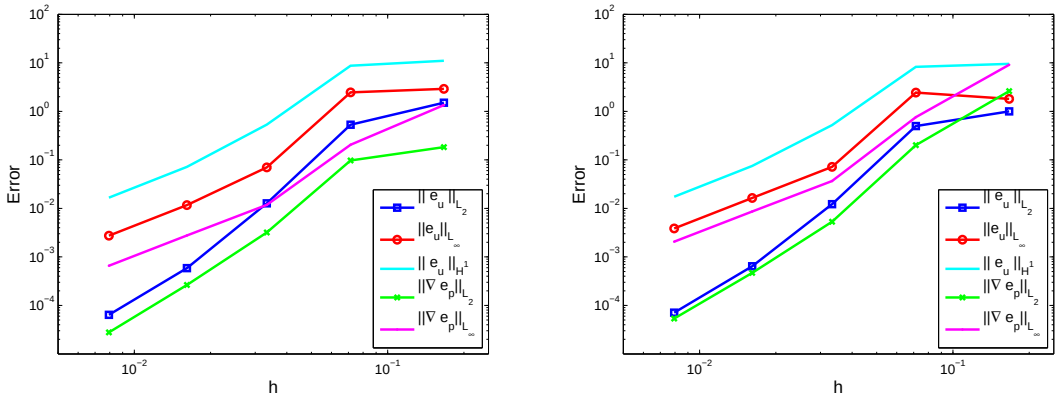


(a) $q = h$ (b) $q \leq h$

Figure 8.10: Approximation errors of example with target functions outside the native space, where $\phi = \psi = \phi_{2,4}$.

## 8.4. Dependency on the Parameters

In the previous sections we have shown that the error estimates for different right hand sides hold. We now wish to examine the dependency of the method on the choice of the parameters. All tests were done by using the setting presented in section 8.2.1 with $32^2$ data points in the unit cube $[0, 1]^2$. Also, if not stated otherwise, the $\phi_{2,3} \in C^6$ Wendland function with support radius $\delta = 10$ is applied. In all tables, the column marked by '$m$' gives the number of iterations required by the GMRES method.

### 8.4.1. Dependency on the Basis Function

Comparing the results of different basis functions showed that a smoother function leads to a smaller error. This can be seen from theory as well as from table 8.17. However, since the matrix becomes ill-conditioned, more iterations are required. Hence the runtime increases. Therefore we chose the $C^6$ compactly supported function for $\phi$ and $\psi$ for the following examples.

| $\phi = \psi$ | $\|\mathbf{e_u}\|_{\mathbf{L}_2}$ | $\|\mathbf{e_u}\|_{\mathbf{L}_\infty}$ | $\|\mathbf{e_u}\|_{\mathbf{H}^1}$ | $\|\mathbf{e_u}\|_{\mathbf{H}^2}$ | $\|\nabla e_p\|_{\mathbf{L}_2}$ | $\|\nabla e_p\|_{\mathbf{L}_\infty}$ | $m$ |
|---|---|---|---|---|---|---|---|
| $\phi_{2,2}$ | 5.4045e-04 | 8.9660e-03 | 3.5235e-02 | 1.6621e+00 | 4.4943e-04 | 6.5394e-03 | 402 |
| $\phi_{2,3}$ | 3.8164e-05 | 5.8268e-04 | 2.6256e-03 | 1.4199e-01 | 3.5269e-05 | 8.2462e-04 | 598 |
| $\phi_{2,4}$ | 2.1488e-06 | 3.8134e-05 | 1.5244e-04 | 9.3344e-03 | 2.1664e-06 | 7.2435e-05 | 784 |

Table 8.17: Approximation errors depending on the basis function.

| $\delta$ | $\|\mathbf{e_u}\|_{\mathbf{L}_2}$ | $\|\mathbf{e_u}\|_{\mathbf{L}_\infty}$ | $\|\mathbf{e_u}\|_{\mathbf{H}^1}$ | $\|\mathbf{e_u}\|_{\mathbf{H}^2}$ | $\|\nabla e_p\|_{\mathbf{L}_2}$ | $\|\nabla e_p\|_{\mathbf{L}_\infty}$ | $m$ |
|---|---|---|---|---|---|---|---|
| 0.001 | 6.7667e-01 | 3.2628e+00 | 6.1466e+01 | 4.1039e+05 | 6.7283e-01 | 3.2628e+00 | 2 |
| 0.01 | 6.7899e-01 | 3.7183e+00 | 4.5176e+01 | 3.9309e+04 | 6.7477e-01 | 3.4481e+00 | 2 |
| 0.1 | 6.1248e-01 | 3.4393e+00 | 3.8858e+01 | 7.2132e+03 | 7.0797e-01 | 6.3891e+00 | 138 |
| 1 | 1.8052e-03 | 3.2753e-02 | 1.0180e-01 | 5.3527e+00 | 1.9106e-03 | 6.5062e-02 | 630 |
| 10 | 3.8164e-05 | 5.8268e-04 | 2.6256e-03 | 1.4199e-01 | 3.5269e-05 | 8.2462e-04 | 598 |
| 100 | 2.8177e-05 | 4.1931e-04 | 2.0651e-03 | 1.1579e-01 | 3.1795e-05 | 6.5283e-04 | 592 |
| 1000 | 2.7763e-05 | 4.1629e-04 | 2.0440e-03 | 1.1483e-01 | 3.1675e-05 | 6.3968e-04 | 591 |

Table 8.18: Approximation errors depending on the support of the basis function with $\phi = \psi = \phi_{2,3}$.

The size of the support radius $\delta$ of the basis function has a major influence on the solution. If the support radius is less than the fill distance of the set, there are no other points in the support of the basis function. Then the collocation matrix becomes independent from the points and therefore the solution too. Our $32 \times 32$ grid has fill distance $h \approx 0.016$, i. e. the solution will be the same for all $\delta < h$. An increasing support leads to a shrinking error, see table 8.18. However, the number of iterations also increases, since the system becomes ill-conditioned. This leads to longer runtimes. Therefore the support radius in all simulations is chosen to be $\delta = 10$ which ensures a balance between a small error and a low runtime.

We did not consider the case $\phi \neq \psi$, since the error estimate always depends on the rougher function. However, our computer program provides the option.

### 8.4.2. Dependency on the Permeability

We set the permeability of the example to be $K = \kappa I$, where $\kappa$ is a constant which models the specific media. If $\kappa$ is a very small number it models a pervious material, which is a good aquifer such as clean gravel. For a slightly bigger $\kappa$ it is material which is still pervious as for example clean sand or a mix of sand and gravel. A medium figure models semi-pervious material like very fine sand, silt, loam or stratified clay. Moreover, a high value for $\kappa$ describes impervious material such as sandstone or granite, i. e. there is almost no transport of fluids. Darcy's law does not model the reality in this case, but we can still solve Darcy's problem. Further information about the permeability can be found in [6].

The table 8.19 gives the numerical error for different values of $\kappa$. The error for the velocity is only slightly increasing with $\kappa$, it basically remains constant. However, the error for the pressure is high for a small $\kappa$. This is due to the fact that if $\kappa$ is very small, then the pressure part of (3.3) has only little influence and the problem is mainly solved for the velocity. Therefore there exists a minimal value for $\kappa$ such that the equation

| $\kappa$ | $\|\mathbf{e_u}\|_{\mathbf{L}_2}$ | $\|\mathbf{e_u}\|_{\mathbf{L}_\infty}$ | $\|\mathbf{e_u}\|_{\mathbf{H}^1}$ | $\|\mathbf{e_u}\|_{\mathbf{H}^2}$ | $\|\nabla e_p\|_{\mathbf{L}_2}$ | $\|\nabla e_p\|_{\mathbf{L}_\infty}$ | $m$ |
|---|---|---|---|---|---|---|---|
| 0.001 | 3.8423e-05 | 5.8719e-04 | 2.7881e-03 | 1.4714e-01 | 2.1266e-02 | 1.2881e-01 | 681 |
| 0.01 | 3.1941e-05 | 5.0460e-04 | 2.3218e-03 | 1.2756e-01 | 1.5515e-03 | 1.2863e-02 | 696 |
| 0.1 | 3.4404e-05 | 4.9713e-04 | 2.4140e-03 | 1.3248e-01 | 1.6417e-04 | 1.7867e-03 | 664 |
| 1 | 4.0582e-05 | 5.8268e-04 | 3.0337e-03 | 1.7604e-01 | 4.1610e-05 | 1.7658e-03 | 598 |
| 10 | 4.5555e-05 | 7.1693e-04 | 3.3261e-03 | 1.8593e-01 | 3.6071e-05 | 1.6006e-03 | 852 |
| 100 | 1.2115e-04 | 1.6915e-03 | 7.0860e-03 | 2.9158e-01 | 3.4959e-05 | 1.5909e-03 | 1409 |
| 1000 | 7.8590e-04 | 6.5696e-03 | 2.9012e-02 | 6.9103e-01 | 3.3929e-05 | 1.5906e-03 | 1831 |

Table 8.19: Approximation errors depending on the permeability with $\phi = \psi = \phi_{2,3}$.

for the pressure can be solved satisfactorily. However, a value too large can lead to an unsatisfactory solution of the velocity part.

We now wish to check how the error behaves if we choose a fixed right hand side

$$\mathbf{f}(x, y) = (3x^2y^2 - 2x^3y, 3x^2y^2 + 2x^3y)^T$$

and vary the pressure with the permeability. Therefore we choose

$$\mathbf{u}(x, y) = (-2x^3y, 3x^2y^2)^T \quad \text{and} \quad p(x, y) = \frac{x^3y^2}{\kappa},$$

where the permeability is given by $K = \kappa I$. The results are presented in table 8.20. It shows that the error is low when $\mathbf{u}$ and $p$ are in the same range, i. e. if $\kappa \approx 1$. If one function is a significantly larger than the other, then the number of iterations increases and also the error.

| $\kappa$ | $\|\mathbf{e_u}\|_{\mathbf{L}_2}$ | $\|\mathbf{e_u}\|_{\mathbf{L}_\infty}$ | $\|\mathbf{e_u}\|_{\mathbf{H}^1}$ | $\|\mathbf{e_u}\|_{\mathbf{H}^2}$ | $\|\nabla e_p\|_{\mathbf{L}_2}$ | $\|\nabla e_p\|_{\mathbf{L}_\infty}$ | $m$ |
|---|---|---|---|---|---|---|---|
| 0.001 | 3.1111e-02 | 3.4893e-01 | 2.0528e+00 | 9.8502e+01 | 2.0270e+01 | 1.5448e+02 | 748 |
| 0.01 | 1.4253e-03 | 1.9740e-02 | 8.5725e-02 | 4.2610e+00 | 1.0901e-01 | 1.6525e+00 | 741 |
| 0.1 | 5.4448e-05 | 8.1086e-04 | 3.8001e-03 | 2.2358e-01 | 6.0992e-04 | 1.6145e-02 | 683 |
| 1 | 3.8164e-05 | 5.8268e-04 | 2.6256e-03 | 1.4199e-01 | 3.5269e-05 | 8.2462e-04 | 598 |
| 10 | 4.4193e-05 | 7.8505e-04 | 2.9651e-03 | 1.5274e-01 | 4.6534e-06 | 1.1126e-04 | 852 |
| 100 | 1.1584e-04 | 1.9172e-03 | 6.1878e-03 | 2.4153e-01 | 6.0809e-06 | 2.1434e-04 | 1408 |
| 1000 | 6.9794e-04 | 7.1977e-03 | 2.4130e-02 | 5.9180e-01 | 7.6250e-06 | 2.1776e-04 | 1831 |

Table 8.20: Approximation errors depending on the permeability for a fixed right hand side with $\phi = \psi = \phi_{2,3}$.

Note that the viscosity has also influence on $K$. The error and the runtime react similarly to changes in viscosity as for the permeability.

### 8.4.3. Dependency on the Data Set

We now wish to check how the error depends on the data set. We compute the errors for three different types of point sets. First on an equidistant grid, then on Halton points and finally on a set of random data. All simulations are done on $32^2$ input points in the unit cube. Hence, we have $N = 900$ collocation points in the interior and $M = 124$ on the boundary in all examples. Figure 8.11 illustrates the used data sets.

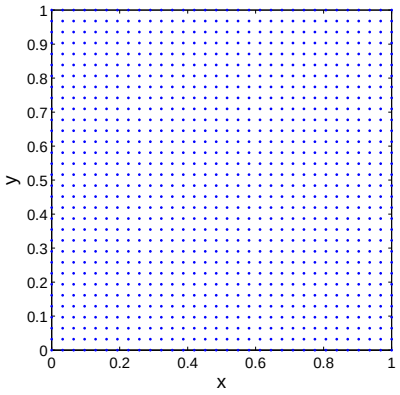


(a) Grid points

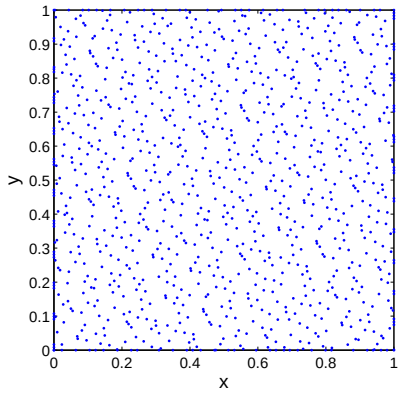


(b) Halton points

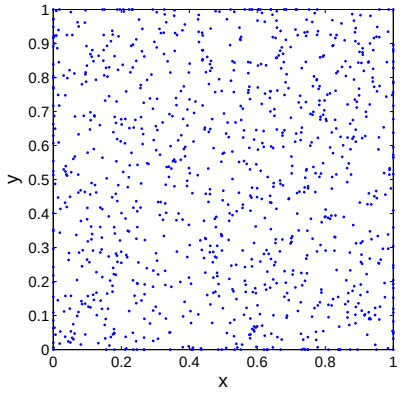


(c) Random points

Figure 8.11: The different point sets.

The grid data is a set of equidistant distributed points, which is generated by two nested `for`-loops. For the random data the C++ - function `rand()` is used, and the result is shifted in the unit cube. The Halton points are generated by algorithm 8.2. They are quasi-random, but well distributed over the domain and unlikely to cluster. Furthermore, they are indeed unique for different values of $k \in \mathbb{N}_0$ and $r \in \mathbb{N}$ prime. Information about Halton points can be found for example in [58]. We used $r = 7$ for the $x$ component inside

the domain and $r = 11$ for the $y$ component respectively. On the boundary we chose $r = 3$ for $x$ and $r = 5$ for $y$.

**Algorithm 8.2 (Halton):** Generating Halton points

**Require:** A prime number $r$ and an integer $k$.
**Ensure:** $x$ is the $k$-th Halton point of base $r$

```
x ← 0
if k = 0 then
  return
end if
f ← 1/r
while k > 0 do
  h ← k modulo r
  x ← x + hf
  k ← k/r
  f ← f/r
end while
```

From table 8.21 we can see that the errors are in the same range. Only the number of iterations is changing. The stability of the linear system of equations depends on the data set, but Darcy's problem can be satisfactorily solved in all tested cases.

| | $\|\mathbf{e_u}\|_{\mathbf{L}_2}$ | $\|\mathbf{e_u}\|_{\mathbf{L}_\infty}$ | $\|\mathbf{e_u}\|_{\mathbf{H}^1}$ | $\|\mathbf{e_u}\|_{\mathbf{H}^2}$ | $\|\nabla e_p\|_{\mathbf{L}_2}$ | $\|\nabla e_p\|_{\mathbf{L}_\infty}$ | $m$ |
|---|---|---|---|---|---|---|---|
| grid | 3.8164e-05 | 5.8268e-04 | 2.6256e-03 | 1.4199e-01 | 3.5269e-05 | 8.2462e-04 | 598 |
| Halton | 2.3039e-05 | 4.4810e-04 | 7.0380e-04 | 5.6247e-02 | 2.2809e-05 | 2.1013e-04 | 965 |
| rand | 4.8118e-05 | 3.5398e-04 | 9.2909e-04 | 6.0463e-02 | 4.9007e-05 | 1.0417e-03 | 1782 |

Table 8.21: Approximation errors depending on the data set with $\phi = \psi = \phi_{2,3}$.

# 9. Conclusions

After introducing Darcy's problem and discussing reproducing kernel Hilbert spaces, a new discretization scheme to solve Darcy's problem has been presented. The scheme is based on a collocation method and implements optimal recovery to solve the partial differential equation. Besides producing analytically incompressible flow fields, our method can be of arbitrary order, works in arbitrary space dimension and for arbitrary geometries. Furthermore, our method is mesh-free.

The error analysis of the presented scheme has been carried out and the expected approximation orders were obtained. The error estimates were only shown for the two and three dimensional cases, since the extension operator is not yet proven for arbitrary dimensions. However, our estimates would hold for arbitrary dimensions if the extension operator exists.

New error estimates for the case that the target function does not belong to native space have been developed. These new error estimates extend the former to a larger class of target functions. The roughness of the target function is only limited by the Sobolev embedding theorem, i. e. a constant depending on the space dimension.

An implementation of the scheme has been done and tested in various numerical simulations. Overall it was shown that the theoretical error estimates hold for target functions in and outside the native space.

The implementation of the scheme has been tested to find optimal parameters. A smoother basis function leads to a smaller error, however it increases the runtime. Furthermore, the runtime is reduced for a small support radius while the error increases. The permeability has minor influence on the numerical solution. Only a particular low or high permeability leads to a unsatisfactory solution. However, Darcy's problem might not model the reality in those cases. Different point sets have been tested and a satisfactory solution computed in either case. Nevertheless, the numerics do not hold if two points are too close together. Then the matrix becomes numerically non-invertible.

# Bibliography


[1] Milton Abramowitz and Irene Stegun. *Handbook of mathematical functions*. Dover Publications inc., 1965.

[2] Robert A. Adams. *Sobolev spaces*. New York : Academic P., 1975.

[3] Hans W. Alt. *Lineare Funktionalanalysis*. Springer, 2006.

[4] Rémi Arcangéli, María Cruz López de Silanes, and Juan José Torrens. An extension of a bound for functions in Sobolev spaces, with applications to (m, s)-spline interpolation and smoothing. *Numerische Mathematik*, 107(2):181–211, 2007.

[5] Mejdi Azaiez, Christine Bernardi, and Miloslav Grundmann. Spectral methods applied to porous media equations. *East West Journal of Numerical Mathematics*, 2(2):91–105, 1994.

[6] Jacob Bear. *Dynamics of fluids in porous media*. American Elsevier Publishing Company, inc., 1972.

[7] Jörn Behrens and Armin Iske. Grid-free adaptive semi-Lagrangian advection using radial basis functions. *Computers & Mathematics with Applications*, 43(3-5):319–327, 2002.

[8] Jean-Marie Bernard. Conforming and nonconforming finite element methods for solving the Darcy's equations. *Nonlinear Analysis. Real World Applications.*, 7(4):789–812, 2006.

[9] Susanne C. Brenner and L. Ridgway Scott. *The mathematical theory of finite element methods*. Springer, 1994.

[10] Franco Brezzi, Thomas J. R. Hughes, Luisa D. Marini, and Arif Masud. Mixed discontinuous Galerkin methods for Darcy flow. *SIAM Journal of Scientific Computing*, 22/23:119–145, 2005.

[11] Robert A. Brownlee and Will Light. Approximation orders for interpolation by surface splines to rough functions. *IMA Journal of Numerical Analysis*, 24(2):179–192, 2004.

[12] Lawrence C. Evans. *Partial differential equations.* American Mathematical Society, 1991.

[13] Gregory E. Fasshauer. Solving partial differential equations by collocation with radial basis functions. In *Surface Fitting and Multiresolution Methods A. Le Mèhautè, C. Rabut and L.L. Schumaker (eds.), Vanderbilt*, pages 131–138. University Press, 1997.

[14] Otto Forster. *Analysis 3.* Vieweg, 1999.

[15] Carsten Franke and Robert Schaback. Convergence order estimates of meshless collocation methods using radial basis functions. In *Adv. Comput. Math*, pages 381–399, 1997.

[16] Carsten Franke and Robert Schaback. Solving partial differential equations by collocation using radial basis functions. *Applied Mathematics and Computation*, 93(1):73–82, 1998.

[17] Edward J. Fuselier. *Refined error estimates for matrix-valued radial basis functions.* PhD thesis, Texas A & M University, 2006.

[18] Edward J. Fuselier. Improved stability estimates and a characterization of the native space for matrix-valued rbf's. *Advances in Computational Mathematics*, 29(3):269–290, 2007.

[19] Edward J. Fuselier. Erratum: Improved stability estimates and a characterization of the native space for matrix-valued rbfs. *Advances in Computational Mathematics*, 29(3):311–313, 2008.

[20] Edward J. Fuselier. Sobolev-type approximation rates for divergence-free and curl-free rbf interpolants. *Mathematics of Computation*, 77(263):1407–1423, 2008.

[21] Peter Giesl and Holger Wendland. Meshless collocation: Error estimates with application to dynamical systems. *SIAM Journal on Numerical Analysis*, 45(4):1723–1741, 2007.

[22] Vivette Girault and Pierre-Arnaud Raviart. *Finite element methods for Navier-Stokes equations.* Springer, 1986.

[23] Pierre Grisvard. *Elliptic problems in nonsmooth domains.* Pitman, 1985.

[24] Georg M. Hornberger, Jeffrey P. Raffensperger, Patricia L. Wilberg, and Keith N. Eshleman. *Elements of physical hydrology.* John Hopkins University Press, 1998.

[25] Edward J. Kansa. Multiquadrics - A scattered data approximation scheme with applications to computational fluid dynamics: I. Surface approximations and partial derivative estimates. *Computers & Mathematics with Applications*, 19(6-8):127–145, 1990.

[26] Edward J. Kansa. Multiquadrics - A scattered data approximation scheme with applications to computational fluid dynamics: II. solutions to parabolic, hyperbolic, and elliptic partial differential equations. *Computers & Mathematics with Applications*, 19(6-8):147–161, 1990.

[27] Quoc T. Le Gia, Francis J. Narcowich, Joseph D. Ward, and Holger Wendland. Continuous and discrete least-squares approximation by radial basis functions on spheres. *Journal of Approximation Theory*, 143(1):124–133, 2006.

[28] Jeremy Levesley and Xingping Sun. Approximation in rough native spaces by shifts of smooth kernels on spheres. *Journal of Approximation Theory*, 133(2):269–283, 2005.

[29] Jeremy Levesley and Xingping Sun. Corrigendum to and two open questions arising from the article: "Approximation in rough native spaces by shifts of smooth kernels on spheres" [*J. Approx. Theory*, 133(2):269–283, 2005]. *Journal of Approximation Theory*, 138(1):124–127, 2006.

[30] Will Light and Michelle Vail. Extension theorems for spaces arising from approximation by translates of a basic function. *Journal of Approximation Theory*, 114(2):164–200, 2002.

[31] R. A. Lorentz, Francis J. Narcowich, and Joseph D. Ward. Collocation discretizations of the transport equation with radial basis functions. *Applied Mathematics and Computation*, 145(1):97–116, 2003.

[32] Svenja Lowitzsch. *Approximation and interpolation employing divergence-free radial basis functions with applications*. PhD thesis, Texas A & M University, 2002.

[33] Svenja Lowitzsch. Error estimates for matrix-valued radial basis function interpolation. *Journal of Approximation Theory*, 137(2):238–249, 2005.

[34] Svenja Lowitzsch. Matrix-valued radial basis functions: Stability estimates and applications. *Advances in Computational Mathematics*, 23(3):299–315, 2005.

[35] Francis J. Narcowich. Recent developments in error estimates for scattered-data interpolation via radial basis functions. *Numerical Algorithms*, 39(1-3):307–315, 2005.

[36] Francis J. Narcowich, Robert Schaback, and Joseph D. Ward. Approximations in Sobolev spaces by kernel expansions. *Journal of Approximation Theory*, 114(1):70–83, 2002.

[37] Francis J. Narcowich and Joseph D. Ward. Norms of inverses and condition numbers for matrices associated with scattered data. *Journal of Approximation Theory*, 64(1):69–94, 1991.

[38] Francis J. Narcowich and Joseph D. Ward. Generalized Hermite interpolation via matrix-valued conditionally positive definite functions. *Mathematics of Computation*, 63(208):661–687, 1994.

[39] Francis J. Narcowich and Joseph D. Ward. Scattered data interpolation on spheres: Error estimates and locally supported basis functions. *SIAM Journal on Mathematical Analysis*, 33(6):1393–1410, 2002.

[40] Francis J. Narcowich and Joseph D. Ward. Scattered-data interpolation on $\mathbb{R}^n$: Error estimates for radial basis and band-limited functions. *SIAM Journal on Mathematical Analysis*, 36(1):284–300, 2004.

[41] Francis J. Narcowich, Joseph D. Ward, and Holger Wendland. Sobolev bounds on functions with scattered zeros, with applications to radial basis function surface fitting. *Mathematics of Computation*, 74(250):743–763, 2005.

[42] Francis J. Narcowich, Joseph D. Ward, and Holger Wendland. Sobolev error estimates and a Bernstein inequality for scattered data interpolation via radial basis functions. *Constructive Approximation*, 24(2):175–186, 2006.

[43] Shlomo P. Neuman. Theoretical derivation of Darcy's law. *Acta Mechanica*, 25(3-4):153–170, 1975.

[44] Hilary A. Priestley. *Introduction to complex analysis*. Oxford University Press, 2004.

[45] Alfio Quarteroni, Fausto Salari, and Alesandro Veneziani. Factorisation methods for the numerical approximation of Navier-Stokes equations. *Computer Methods in Applied Mechanics and Engineering*, 188(1-3):505–526, 1998.

[46] Yousef Saad. *Iterative methods for sparse linear systems*. Philadelphia, Pa. : SIAM, 2003.

[47] Daniela Schräder and Holger Wendland. *A high-order, analytically divergence-free discretization method for Darcy's problem*. Preprint Sussex, 2008.

[48] Elias M. Stein. *Singular integrals and differentiability properties of functions*. Princeton University Press, 1971.

[49] Michael E. Taylor. *Partial differential equations 1 - Basic theory*. Springer, 1996.

[50] Svetlana Tlupova and Ricardo Cortez. Boundary integral solutions of coupled Stokes and Darcy flows. *Journal of Computational Physics*, 228(1):158–179, 2009.

[51] Hans Triebel. *Interpolation theory, function spaces, differential operators*. North-Holland Publishing Company, 1978.

[52] George N. Watson. *A treatise on the theory of Bessel functions*. Cambridge University Press, 1966.

[53] Holger Wendland. Piecewise polynomial, positive definite and compactly supported radial functions of minimal degree. *Advances in Computational Mathematics*, 4(1):389–396, 1995.

[54] Holger Wendland. *Scattered data approximation*. Cambridge Monographs on Applied and Computational Mathematics. Cambridge University Press, 2005.

[55] Holger Wendland. *Divergence-free kernel methods for approximating Stoke's problem*. Preprint Sussex, 2008.

[56] Jochen Werner. *Numerische Mathematik 1*. Vieweg, 1992.

[57] Joseph Wloka. *Partial differential equations*. Cambridge University Press, 1987.

[58] Tien-Tsin Wong, Wai-Shing Luk, and Pheng-Ann Heng. Sampling with Hammersley and Halton points. *Journal of Graphics Tools*, 2(2):9–24, 1997.

# A. Appendix

For the implementation of the discretization scheme we need the derivatives of certain Wendland functions. Since all examples are two dimensional, we will give the derivatives of $\phi_{2,\ell}(x,y)$, where $x$ and $y$ are real numbers. For the implementation the derivatives up to the fourth degree are needed. However, for completeness reasons we give all derivatives.

To ensure that the evaluation is numerically stable and efficient, a Horner scheme has been applied in the implementation of the scheme.

Let $\alpha \in \mathbb{N}_0^2$ and define $r := \sqrt{x^2+y^2}$. We sort the derivatives $\partial_{x^{\alpha_1}y^{\alpha_2}}\phi_{2,\ell}$ in groups of order $|\alpha| = \alpha_1 + \alpha_2$.

The compactly supported function $\phi_{2,1}(x,y) = (1-r)_+^4(4r+1)$, has the derivatives:

- $|\alpha| = 1$

$$\begin{aligned}\partial_x\phi_{2,1}(x,y) &= -20\,x\,(1-r)_+^3\\ \partial_y\phi_{2,1}(x,y) &= -20\,y\,(1-r)_+^3\end{aligned}$$

- $|\alpha| = 2$

$$\begin{aligned}\partial_{x^2}\phi_{2,1}(x,y) &= 20\,(1-r)_+^2\left(\frac{3x^2}{r}-1+r\right)\\ \partial_{y^2}\phi_{2,1}(x,y) &= 20\,(1-r)_+^2\left(\frac{3y^2}{r}-1+r\right)\\ \partial_{xy}\phi_{2,1}(x,y) &= \frac{60\,x\,y}{r}(1-r)_+^2\end{aligned}$$

The derivatives of function $\phi_{2,2}(x,y) = (1-r)_+^6(35r^2+18r+3)$ are:

- $|\alpha| = 1$

$$\begin{aligned}\partial_x\phi_{2,2}(x,y) &= -56\,x\,(1-r)_+^5\,(5r+1)\\ \partial_y\phi_{2,1}(x,y) &= -56\,y\,(1-r)_+^5\,(5r+1)\end{aligned}$$

- $|\alpha| = 2$

$$\partial_{x^2}\phi_{2,2}(x,y) = 56\,(1-r)_+^4\left(5r^2-4r-1+30x^2\right)$$
$$\partial_{y^2}\phi_{2,2}(x,y) = 56\,(1-r)_+^4\left(5r^2-4r-1+30y^2\right)$$
$$\partial_{xy}\phi_{2,2}(x,y) = 1680\,x\,y\,(1-r)_+^4$$

- $|\alpha| = 3$

$$\partial_{x^3}\phi_{2,2}(x,y) = 1680\,x\,(1-r)_+^3\left(-3r+3-\frac{4x^2}{r}\right)$$
$$\partial_{y^3}\phi_{2,2}(x,y) = 1680\,y\,(1-r)_+^3\left(-3r+3-\frac{4y^2}{r}\right)$$
$$\partial_{x^2y}\phi_{2,2}(x,y) = 1680\,y\,(1-r)_+^3\left(-r+1\frac{4x^2}{r}\right)$$
$$\partial_{xy^2}\phi_{2,2}(x,y) = 1680\,x\,(1-r)_+^3\left(-r+1\frac{4y^2}{r}\right)$$

- $|\alpha| = 4$

$$\partial_{x^4}\phi_{2,2}(x,y) = 1680\,(1-r)_+^2\left(-6r+3+30x^2-\frac{20x^2}{r}+\frac{5x^4+3y^4}{r^2}-\frac{4x^2y^2}{r^3}\right)$$
$$\partial_{y^4}\phi_{2,2}(x,y) = 1680\,(1-r)_+^2\left(-6r+3+30y^2-\frac{20y^2}{r}+\frac{5y^4+3x^4}{r^2}-\frac{4x^2y^2}{r^3}\right)$$
$$\partial_{x^3y}\phi_{2,2}(x,y) = -6720\,x\,y\,(1-r)_+^2\left(-3+\frac{2}{r}-\frac{2x^2}{r^2}+\frac{y^2}{r^3}\right)$$
$$\partial_{xy^3}\phi_{2,2}(x,y) = -6720\,x\,y\,(1-r)_+^2\left(-3+\frac{2}{r}-\frac{2y^2}{r^2}+\frac{x^2}{r^3}\right)$$
$$\partial_{x^2y^2}\phi_{2,2}(x,y) = 1680\,(1-r)_+^2\left(5r^2-6r+1+\frac{8x^2y^2}{r^2}+\frac{4x^2y^2}{r^3}\right)$$

The derivatives of function $\phi_{2,3}(x,y) = (1-r)_+^8\left(32r^3+25r^2+8r+1\right)$ are:

- $|\alpha| = 1$

$$\partial_x\phi_{2,3}(x,y) = -22\,x\,(1-r)_+^7\left(16r^2+7r+1\right)$$
$$\partial_y\phi_{2,3}(x,y) = -22\,y\,(1-r)_+^7\left(16r^2+7r+1\right)$$

- $|\alpha| = 2$

$$\begin{aligned}
\partial_{x^2}\phi_{2,3}(x,y) &= 22\,(1-r)_+^6\left(16r^3-9r^2+144x^2r-6r+24x^2-1\right)\\
\partial_{y^2}\phi_{2,3}(x,y) &= 22\,(1-r)_+^6\left(16r^3-9r^2+144y^2r-6r+24y^2-1\right)\\
\partial_{xy}\phi_{2,3}(x,y) &= 528\,x\,y\,(1-r)_+^6\,(6r+1)
\end{aligned}$$

- $|\alpha| = 3$

$$\begin{aligned}
\partial_{x^3}\phi_{2,3}(x,y) &= 1584\,x\,(1-r)_+^5\left(-6r^2+5r-14x^2+1\right)\\
\partial_{y^3}\phi_{2,3}(x,y) &= 1584\,y\,(1-r)_+^5\left(-6r^2+5r-14y^2+1\right)\\
\partial_{x^2y}\phi_{2,3}(x,y) &= 528\,y\,(1-r)_+^5\left(-6r^2+5r+1-42x^2\right)\\
\partial_{xy^2}\phi_{2,3}(x,y) &= 528\,x\,(1-r)_+^5\left(-6r^2+5r+1-42y^2\right)
\end{aligned}$$

- $|\alpha| = 4$

$$\begin{aligned}
\partial_{x^4}\phi_{2,3}(x,y) &= 1584\,(1-r)_+^4\left(6r^3-11r^2+4r+84x^2r-84x^2+\frac{70x^4}{r}+1\right)\\
\partial_{y^4}\phi_{2,3}(x,y) &= 1584\,(1-r)_+^4\left(6r^3-11r^2+4r+84y^2r-84y^2+\frac{70y^4}{r}+1\right)\\
\partial_{x^3y}\phi_{2,3}(x,y) &= 22176\,x\,y\,(1-r)_+^4\left(3r-3+\frac{5x^2}{r}\right)\\
\partial_{xy^3}\phi_{2,3}(x,y) &= 22176\,x\,y\,(1-r)_+^4\left(3r-3+\frac{5x^2}{r}\right)\\
\partial_{x^2y^2}\phi_{2,3}(x,y) &= 528\,(1-r)_+^4\left(48r^3-53r^2+4r+1+\frac{210x^2y^2}{r}\right)
\end{aligned}$$

- $|\alpha| = 5$

$$\begin{aligned}
\partial_{x^5}\phi_{2,3}(x,y) &= 110880\,x\,(1-r)_+^3\left(-3r^2+6r-3-10x^2+\frac{9x^2}{r}+\frac{x^2y^2-3x^4}{r^2}\right)\\
\partial_{y^5}\phi_{2,3}(x,y) &= 110880\,y\,(1-r)_+^3\left(-3r^2+6r-3-10y^2+\frac{9y^2}{r}+\frac{x^2y^2-3y^4}{r^2}\right)\\
\partial_{x^4y}\phi_{2,3}(x,y) &= 22176\,y\,(1-r)_+^3\left(-3r^2+6r-30x^2-3+\frac{25x^2}{r}-\frac{15x^4}{r^2}+\frac{5x^2y^2}{r^3}\right)\\
\partial_{xy^4}\phi_{2,3}(x,y) &= 22176\,x\,(1-r)_+^3\left(-3r^2+6r-30y^2-3+\frac{25y^2}{r}-\frac{15y^4}{r^2}+\frac{5x^2y^2}{r^3}\right)\\
\partial_{x^3y^2}\phi_{2,3}(x,y) &= 22176\,x\,(1-r)_+^3\left(-8r^2+11r-10y^2-3+\frac{5y^2}{r}-\frac{15x^2y^2}{r^2}+\frac{5y^4}{r^3}\right)
\end{aligned}$$

$$\partial_{x^2y^3}\phi_{2,3}(x,y) = 22176\, y\,(1-r)_+^3\left(-8r^2+11r-10x^2-3+\frac{5x^2}{r}-\frac{15x^2y^2}{r^2}+\frac{5x^4}{r^3}\right)$$

- $|\alpha| = 6$

$$\begin{aligned}
\partial_{x^6}\phi_{2,3}(x,y) &= 332640\,(1-r)_+^2\Bigg(r^3-3r^2+15x^2r+3r-1-30x^2+\frac{15x^2+15x^4}{r}\\
&\quad-\frac{8x^4}{r^2}+\frac{x^6-4x^4}{r^3}-\frac{2x^4y^2}{r^4}-\frac{x^4y^2}{r^5}\Bigg)\\
\partial_{y^6}\phi_{2,3}(x,y) &= 332640\,(1-r)_+^2\Bigg(r^3-3r^2+15y^2r+3r-1-30y^2+\frac{15y^2+15y^4}{r}\\
&\quad-\frac{8y^4}{r^2}+\frac{y^6-4y^4}{r^3}-\frac{2x^2y^4}{r^4}-\frac{x^2y^4}{r^5}\Bigg)\\
\partial_{x^5y}\phi_{2,3}(x,y) &= 110880\,x\,y\,(1-r)_+^2\Bigg(15r-30+\frac{30x^2+8}{r}-\frac{14x^2}{r^2}+\frac{3x^4+4y^2}{r^3}\\
&\quad-\frac{6x^2y^2}{r^4}+\frac{3y^4}{r^5}\Bigg)\\
\partial_{xy^5}\phi_{2,3}(x,y) &= 110880\,x\,y\,(1-r)_+^2\Bigg(15r-30+\frac{30y^2+8}{r}-\frac{14y^2}{r^2}+\frac{3y^4+4x^2}{r^3}\\
&\quad-\frac{6x^2y^2}{r^4}+\frac{3x^4}{r^5}\Bigg)\\
\partial_{x^4y^2}\phi_{2,3}(x,y) &= 22176\,(1-r)_+^2\Bigg(18r^3-39r^2+30x^2r+24r-40x^2-3\\
&\quad+\frac{10x^2+75x^2y^2}{r}-\frac{20x^2}{r^2}+\frac{15x^4-10x^2}{r^3}-\frac{30x^2y^2}{r^4}-\frac{15x^2y^2}{r^5}\Bigg)\\
\partial_{x^2y^4}\phi_{2,3}(x,y) &= 22176\,(1-r)_+^2\Bigg(18r^3-39r^2+30y^2r+24r-40y^2-3\\
&\quad+\frac{10y^2+75x^2y^2}{r}-\frac{20y^2}{r^2}+\frac{15y^4-10y^2}{r^3}-\frac{30x^2y^2}{r^4}-\frac{15x^2y^2}{r^5}\Bigg)\\
\partial_{x^3y^3}\phi_{2,3}(x,y) &= 332640\,x\,y\,(1-r)_+^2\Bigg(6r^3-20r^2+24r-12+\frac{2+x^2y^2}{r}-\frac{2x^2y^2}{r^3}\\
&\quad+\frac{x^2y^2}{r^5}\Bigg)
\end{aligned}$$

The derivatives of function $\phi_{2,4}(x,y) = (1-r)_+^{10}\left(429r^4+450r^3+210r^2+50r+5\right)$ are:

- $|\alpha| = 1$

$$\begin{aligned}
\partial_x\phi_{2,4}(x,y) &= -26\,x\,(1-r)_+^9\left(231r^3+159r^2+45r+5\right)\\
\partial_y\phi_{2,4}(x,y) &= -26\,y\,(1-r)_+^9\left(231r^3+159r^2+45r+5\right)
\end{aligned}$$

- $|\alpha| = 2$

$$\begin{aligned}
\partial_{x^2}\phi_{2,4}(x,y) &= 26\,(1-r)_+^8(231r^4 - 72r^3 + 2772x^2r^2 - 114r^2 + 1056x^2r - 40r \\
&\quad + 132x^2 - 5) \\
\partial_{y^2}\phi_{2,4}(x,y) &= 26\,(1-r)_+^8(231r^4 - 72r^3 + 2772y^2r^2 - 114r^2 + 1056y^2r - 40r \\
&\quad + 132y^2 - 5) \\
\partial_{xy}\phi_{2,4}(x,y) &= 3432\,x\,y\,(1-r)_+^8\left(21r^2 + 8r + 1\right)
\end{aligned}$$

- $|\alpha| = 3$

$$\begin{aligned}
\partial_{x^3}\phi_{2,4} &= -10296\,x\,(1-r)_+^7\left(21r^3 - 13r^2 + 70x^2r - 7r + 10x^2 - 1\right) \\
\partial_{y^3}\phi_{2,4} &= -10296\,y\,(1-r)_+^7\left(21r^3 - 13r^2 + 70y^2r - 7r + 10y^2 - 1\right) \\
\partial_{x^2y}\phi_{2,4} &= 3432\,y\,(1-r)_+^7\left(-21r^3 + 13r^2 - 210x^2r + 7r - 30x^2 + 1\right) \\
\partial_{xy^2}\phi_{2,4} &= 3432\,x\,(1-r)_+^7\left(-21r^3 + 13r^2 - 210y^2r + 7r - 30y^2 + 1\right)
\end{aligned}$$

- $|\alpha| = 4$

$$\begin{aligned}
\partial_{x^4}\phi_{2,4}(x,y) &= 10296\,(1-r)_+^6\Bigg(462x^2r^2 - 394x^2r - 34y^2r + 6r + 1 + 539x^4 \\
&\quad - 48x^2 + 21y^4 + \frac{6y^4 - 6x^4}{r^2}\Bigg) \\
\partial_{y^4}\phi_{2,4}(x,y) &= 10296\,(1-r)_+^6\Bigg(462y^2r^2 - 394y^2r - 34x^2r + 6r + 1 + 539y^4 \\
&\quad - 48y^2 + 21x^4 + \frac{6x^4 - 6y^4}{r^2}\Bigg) \\
\partial_{x^3y}\phi_{2,4}(x,y) &= 102960\,x\,y\,(1-r)_+^6\left(21r^2 - 18r + 56x^2 - 3\right) \\
\partial_{xy^3}\phi_{2,4}(x,y) &= 102960\,x\,y\,(1-r)_+^6\left(21r^2 - 18r + 56y^2 - 3\right) \\
\partial_{x^2y^2}\phi_{2,4}(x,y) &= 3432\,(1-r)_+^6\left(231r^4 - 214r^3 - 24r^2 + 6r + 1680x^2y^2 + 1\right)
\end{aligned}$$

- $|\alpha| = 5$

$$\begin{aligned}
\partial_{x^5}\phi_{2,4}(x,y) &= 102960\,x\,(1-r)_+^5\Bigg(-15r^3 + 195r^2 - 560x^2r - 75r + 560x^2 - 15 \\
&\quad - \frac{336x^4}{r}\Bigg)
\end{aligned}$$

$$\partial_{y^5}\phi_{2,4}(x,y) = 102960\,y\,(1-r)_+^5\Big( -15r^3+195r^2-560y^2r-75r+560y^2-15 - \frac{336y^4}{r}\Big)$$

$$\partial_{x^4y}\phi_{2,4}(x,y) = 308880\,y\,(1-r)_+^5\Big( -7r^3+13r^2-112x^2r-5r+112x^2-1 - \frac{112x^4}{r}\Big)$$

$$\partial_{xy^4}\phi_{2,4}(x,y) = 308880\,x\,(1-r)_+^5\Big( -7r^3+13r^2-112y^2r-5r+112y^2-1 - \frac{112y^4}{r}\Big)$$

$$\partial_{x^3y^2}\phi_{2,4}(x,y) = 102960\,x\,(1-r)_+^5\left(-77r^3+95r^2-112y^2-3-\frac{336x^2y^2}{r}\right)$$

$$\partial_{x^2y^3}\phi_{2,4}(x,y) = 102960\,y\,(1-r)_+^5\left(-77r^3+95r^2-112x^2-3-\frac{336x^2y^2}{r}\right)$$

- $|\alpha| = 6$

$$\partial_{x^6}\phi_{2,4}(x,y) = 308880\,(1-r)_+^4\Big(35r^4-100r^3+840x^2r^2+90r^2-1680x^2r-20r + 1680x^4+840x^2-5-\frac{1568x^4}{r}+\frac{448x^6}{r^2}-\frac{112x^4y^2}{r^3}\Big)$$

$$\partial_{x^6}\phi_{2,4}(x,y) = 308880\,(1-r)_+^4\Big(35r^4-100r^3+840y^2r^2+90r^2-1680y^2r-20r + 1680y^4+840y^2-5-\frac{1568y^4}{r}+\frac{448y^6}{r^2}-\frac{112x^2y^4}{r^3}\Big)$$

$$\partial_{x^5y}\phi_{2,4}(x,y) = 17297280\,x\,y\,(1-r)_+^4\Big(5r^2-10r+20x^2+5-\frac{18x^2}{r}+\frac{8x^4}{r^2} - \frac{2x^2y^2}{r^3}\Big)$$

$$\partial_{xy^5}\phi_{2,4}(x,y) = 17297280\,x\,y\,(1-r)_+^4\Big(5r^2-10r+20y^2+5-\frac{18y^2}{r}+\frac{8y^4}{r^2} - \frac{2x^2y^2}{r^3}\Big)$$

$$\partial_{x^4y^2}\phi_{2,4}(x,y) = 308880\,(1-r)_+^4\Big(63r^4-132r^3+168x^2r^2+74r^2-224x^2r-4r + 560x^2y^2+56x^2-1-\frac{448x^2y^2}{r}+\frac{448x^4y^2}{r^2}-\frac{112x^2y^4}{r^3}\Big)$$

$$\partial_{x^2y^4}\phi_{2,4}(x,y) = 308880\,(1-r)_+^4\Big(63r^4 - 132r^3 + 168y^2r^2 + 74r^2 - 224y^2r - 4r + 560x^2y^2 + 56y^2 - 1 - \frac{448x^2y^2}{r} + \frac{448x^2y^4}{r^2} - \frac{112x^4y^2}{r^3}\Big)$$

$$\partial_{x^3y^3}\phi_{2,4}(x,y) = 17297280\,x\,y\,(1-r)_+^4\left(9r^2 - 12r + 3 + \frac{8x^2y^2}{r^2} + \frac{2x^2y^2}{r^3}\right)$$

- $|\alpha| = 7$

$$\partial_{x^7}\phi_{2,4}(x,y) = 17297280\,x\,(1-r)_+^3\Big(-35r^3 + 105r^2 - 210x^2r - 105r + 420x^2 + 35 - \frac{168x^4 + 174x^2}{r} + \frac{108x^4}{r^2} - \frac{16x^6 + 30x^2y^2}{r^3} + \frac{18x^4y^2}{r^4} - \frac{6x^2y^4}{r^5}\Big)$$

$$\partial_{y^7}\phi_{2,4}(x,y) = 17297280\,y\,(1-r)_+^3\Big(-35r^3 + 105r^2 - 210y^2r - 105r + 420y^2 - 35 - \frac{168y^4 + 174y^2}{r} + \frac{108y^4}{r^2} - \frac{16y^6 + 30x^2y^2}{r^3} + \frac{18x^2y^4}{r^4} - \frac{6x^4y^2}{r^5}\Big)$$

$$\partial_{x^6y}\phi_{2,4}(x,y) = 17297280\,y\,(1-r)_+^3\Big(-5r^3 + 15r^2 - 90x^2r - 15r + 180x^2 + 5 - \frac{120x^4}{r} + \frac{72x^4}{r^2} - \frac{16x^6 + 66x^4}{r^3} + \frac{18x^4y^2}{r^4} - \frac{84x^4y^2 + 90x^2y^4}{r^5}\Big)$$

$$\partial_{xy^6}\phi_{2,4}(x,y) = 17297280\,y\,(1-r)_+^3\Big(-5r^3 + 15r^2 - 90y^2r - 15r + 180y^2 + 5 - \frac{120y^4}{r} + \frac{72y^4}{r^2} - \frac{16y^6 + 66y^4}{r^3} + \frac{18x^2y^4}{r^4} - \frac{84x^2y^4 + 90x^4y^2}{r^5}\Big)$$

$$\partial_{x^5y^2}\phi_{2,4}(x,y) = 17297280\,x\,(1-r)_+^3\Big(-33r^3 + 61r^2 - 2y^2r - 33r + 14y^2 + 5 - \frac{72x^2y^2}{r} + \frac{36x^2y^2}{r^2} - \frac{6x^2y^2 + 16x^4y^2}{r^3} + \frac{18x^2y^4}{r^4} + \frac{6x^4y^2 - 12y^6}{r^5}\Big)$$

$$\partial_{x^2y^5}\phi_{2,4}(x,y) = 17297280\,y\,(1-r)_+^3\Big(-33r^3 + 61r^2 - 2x^2r - 33r + 14x^2 + 5 - \frac{72x^2y^2}{r} + \frac{36x^2y^2}{r^2} - \frac{6x^2y^2 + 16x^2y^4}{r^3} + \frac{18x^4y^2}{r^4} + \frac{6x^2y^4 - 12x^6}{r^5}\Big)$$

$$\partial_{x^4y^3}\phi_{2,4}(x,y) = 17297280\,y\,(1-r)_+^3\Big(-9r^3 + 21r^2 - 54x^2r - 15r + 78x^2 + 3 - \frac{18x^2 + 24x^2y^2}{r} - \frac{16x^4y^2}{r^3} + \frac{18x^2y^4}{r^4} - \frac{12x^4y^2 + 6x^6}{r^5}\Big)$$

$$\partial_{x^3y^4}\phi_{2,4}(x,y) = 17297280\,x\,(1-r)_+^3\Big(-9r^3 + 21r^2 - 54y^2r - 15r + 78y^2 + 3 - \frac{18y^2 + 24x^2y^2}{r} - \frac{16x^2y^4}{r^3} + \frac{18x^4y^2}{r^4} - \frac{12x^2y^4 + 6y^6}{r^5}\Big)$$

- $|\alpha| = 8$

$$\partial_{x^8}\phi_{2,4}(x,y) = 17297280\,(1-r)_+^2\Bigg(35r^4 - 140r^3 + 840x^2r^2 + 210r^2 - 2520x^2r - 140r + 1680x^4 + 2520x^2 + 35 - \frac{2540x^4 + 840x^2}{r} + \frac{448x^6 + 840x^4}{r^2} + \frac{56x^6 + 420x^4}{r^3} - \frac{336x^6}{r^4} + \frac{30x^8 - 168x^6}{r^5} + \frac{60x^8}{r^6} + \frac{30x^8}{r^7}\Bigg)$$

$$\partial_{y^8}\phi_{2,4}(x,y) = 17297280\,(1-r)_+^2\Bigg(35r^4 - 140r^3 + 840y^2r^2 + 210r^2 - 2520y^2r - 140r + 1680y^4 + 2520y^2 + 35 - \frac{2540y^4 + 840y^2}{r} + \frac{448y^6 + 840y^4}{r^2} + \frac{56y^6 + 420y^4}{r^3} - \frac{336y^6}{r^4} + \frac{30y^8 - 168y^6}{r^5} + \frac{60y^8}{r^6} + \frac{30y^8}{r^7}\Bigg)$$

$$\partial_{x^7y}\phi_{2,4}(x,y) = 103783680\,x\,y\,(1-r)_+^2\Bigg(35r^2 - 105r + 140x^2 + 105 - \frac{245x^2 + 35}{r} + \frac{56x^2 + 35}{r^2} + \frac{7x^4 + 35x^2}{r^3} - \frac{42x^4}{r^4} + \frac{5x^6 - 21x^4}{r^5} + \frac{10x^6}{r^6} + \frac{5x^6}{r^7}\Bigg)$$

$$\partial_{xy^7}\phi_{2,4}(x,y) = 103783680\,x\,y\,(1-r)_+^2\Bigg(35r^2 - 105r + 140y^2 + 105 - \frac{245y^2 + 35}{r} + \frac{56y^2 + 35}{r^2} + \frac{7y^4 + 35y^2}{r^3} - \frac{42y^4}{r^4} + \frac{5y^6 - 21y^4}{r^5} + \frac{10y^6}{r^6} + \frac{5y^6}{r^7}\Bigg)$$

$$\partial_{x^6y^2}\phi_{2,4}(x,y) = 17297280\,(1-r)_+^2\Bigg(35r^4 - 110r^3 + 420x^2r^2 + 120r^2 - 810x^2r - 50r + 360x^2 + 5 + \frac{30x^2 + 450x^4}{r} - \frac{224x^6 + 300x^4}{r^2} + \frac{2x^6 - 150x^4}{r^3} + \frac{228x^6}{r^4} + \frac{114x^6 - 30x^8}{r^5} - \frac{60x^8}{r^6} - \frac{30x^8}{r^7}\Bigg)$$

$$\partial_{x^2y^6}\phi_{2,4}(x,y) = 17297280\,(1-r)_+^2\Bigg(35r^4 - 110r^3 + 420y^2r^2 + 120r^2 - 810y^2r - 50r + 360y^2 + 5 + \frac{30y^2 + 450y^4}{r} - \frac{224y^6 + 300y^4}{r^2} + \frac{2y^6 - 150y^4}{r^3} + \frac{228y^6}{r^4} + \frac{114y^6 - 30y^8}{r^5} - \frac{60y^8}{r^6} - \frac{30y^8}{r^7}\Bigg)$$

$$\partial_{x^5y^3}\phi_{2,4}(x,y) = 34594560\,x\,y\,(1-r)_+^2\Bigg(105r^2 - 240r + 140x^2 + 165 - \frac{95x^2 + 30}{r} - \frac{56x^4 + 30x^2}{r^2} + \frac{8x^4 - 15x^2}{r^3} + \frac{72x^4}{r^4} + \frac{36x^4 - 15x^6}{r^5} - \frac{30x^6}{r^6} - \frac{15x^6}{r^7}\Bigg)$$

$$\partial_{x^3y^5}\phi_{2,4}(x,y) = 34594560\,x\,y\,(1-r)_+^2\Bigg(105r^2 - 240r + 140y^2 + 165 - \frac{95y^2 + 30}{r} - \frac{56y^4 + 30y^2}{r^2} + \frac{8y^4 - 15y^2}{r^3} + \frac{72y^4}{r^4} + \frac{36y^4 - 15y^6}{r^5} - \frac{30y^6}{r^6} - \frac{15y^6}{r^7}\Bigg)$$

$$\partial_{x^4y^4}\phi_{2,4}(x,y) = 17297280\,(1-r)_+^2\Bigg(63r^4 - 162r^3 + 138r^2 - 42r + 336x^2y^2 + 3 - \frac{408x^2y^2}{r} + \frac{48x^2y^2}{r^2} + \frac{24x^2y^2}{r^3} + \frac{30x^4y^4}{r^5} + \frac{60x^4y^4}{r^6} + \frac{30x^4y^4}{r^7}\Bigg)$$